Investigating the role of GWAS-identified *NCX3* and *Gas7* in pain



Teodora Trendafilova

Supervisor: Prof David Bennett

A/Prof Annina Schmid

Nuffield Department of Clinical Neurosciences

The Queen's College, University of Oxford

This thesis is submitted for the degree of

Doctor of Philosophy

Hilary Term 2021

Declaration

I declare that the work within this thesis is my own unless otherwise stated. Acknowledgements are found in the Methods and Results sections of each chapter.

Key contributions were made by:

Dr Ryan Patel from University College London, UK who performed the *in vivo* electrophysiology experiments in Chapter 3 and 4.

Dr Andrew Bell and Dr Allen Dickie from the University of Glasgow, UK who performed the multiplex *in situ* hybridisation, confocal imaging and spinal cord surgeries in Chapter 4.

Teodora Trendafilova

Hilary Term 2021

Abstract

This thesis reports the results of a genome-wide association study (GWAS) of experimental pain in healthy volunteers and focuses on the validation of the identified genes as targets for pain research. We found a significant association between *SLC8A3* encoding the sodium-calcium exchanger type-3 (NCX3) and wind-up ratio; as well as an association between *Gas7* (growth arrest specific protein 7) and secondary punctate hyperalgesia after mustard oil. We were able to validate the role of both of these genes in pain processing through behavioural tests in mice lacking either NCX3 or Gas7. We found increased response to the second phase of the formalin test in mice with an NCX3 genetic deletion. Using *in vitro* calcium imaging and *in vivo* electrophysiology in the same mouse line, we observed increased intracellular calcium following stimulation, slowed calcium clearance and increased wind-up which could be evoked at lower frequencies. On the other hand, mice with a Gas7 genetic ablation showed decreased pain behaviour after capsaicin treatment. We also performed *in vivo* electrophysiology and dorsal horn dendritic spine analysis, searching for functional and structural mechanisms linked to our behavioural results. While this work is still on-going, our attempt to back-translate GWAS results, has revealed and validated two important and novel pain genes, one of which, NCX3, showed a distinct mechanism of action in the spinal dorsal horn.

Acknowledgements

When I started my DPhil, I had the dream of making a meaningful contribution to a scientific topic. Looking back, I know I met the exact people I needed to guide me and make my journey exciting and enjoyable.

I would like to thank Professor David Bennett for his continuous encouragement and the inspiration of having an amazing scientist and leader as a mentor. Thank you for guiding me through all the ups and downs of this work and for creating a laboratory environment of mutual support and motivation.

I would also like to express my gratitude to Associate Professor Annina Schmid who helped me put the biology of this project into clinical context. Thank you for the encouragement and optimism, and for being such an amazing role model.

My DPhil experience would not have been possible without the support of all the members of the Bennett group, as well as all external contributors. Thank you for the professional and personal help, for accepting me and nurturing me as a scientist and for answering my never-ending questions.

Finally, my biggest gratitude goes to my family who always loved me and supported me, especially during the last year of my DPhil. I am forever grateful to my grandfather who instilled a deep sense of curiosity in me. Also, to my parents who taught me to put all my love in everything I do.

Table of contents

List of figures xvii

List of tables xxi

1 General Introduction 1

1.1 The study of acute and chronic pain 1

1.2 Anatomy of the peripheral pain circuitry 3

1.2.1 Historical classification of sensory neurons and their cutaneous nerve endings 4

1.2.2 Classification of LTMRS in glabrous and hairy skin 4

1.2.3 Classification of HTMRS 7

1.3 Anatomical organisation of the spinal cord 8

1.3.1 Primary afferent input into the dorsal horn 10

1.3.2 Classification of interneurons and projection neurons 11

1.3.3 Further neurochemical sub-divisions of inhibitory interneurons . 12

1.3.4 Further neurochemical sub-divisions of excitatory interneurons . 13

1.3.5 RNA-sequencing-based sub-divisions 13
1.3.6 Sub-divisions based on morphological classification 14
1.3.7 Synaptic circuits – function depends on neuronal interplay . . . 14
1.3.8 Projection neurons – ascending pathways 17
1.4 Short anatomy of brain regions associated with pain – descending pathways 19
1.5 Pathological pain and sensitisation 20
1.5.1 Central sensitisation - lost in translation 21
1.5.2 Top-down - Bottom-up sensitisation 24
1.5.3 The role of the periphery and potential for reversibility 25
1.6 GWAS - the search for novel genes associated with pain 26
1.6.1 What is a GWAS? 26
1.6.2 A brief history of GWA studies 29
1.6.3 Heritability of human pain sensitivity 31
1.6.4 GWAS identifies two novel gene targets linked to sensitised pain 32
1.7 NCX3 – a novel target in spinal cord sensitisation and chronic pain . . 33
1.7.1 The domain structure of the NCX family of proteins 34
1.7.2 Regulatory pathways affecting the function of the NCX family of proteins 35
1.8 Gas7 – a novel target in spinal cord sensitisation and chronic pain . . . 38
1.8.1 The Gas family of proteins 38
1.9 Summary and aims 39

2 *Slc8a3* - anatomy and modulation of pain behaviour in the mouse 41

2.1 Introduction . . . 42

2.1.1 Anatomy overview – approaches for studying *Slc8a3* expression in the DRG and dorsal horn of the spinal cord . . . 42

2.1.2 NCX3 - functional characteristics . . . 45

2.1.3 Aims and hypotheses . . . 46

2.2 Materials and Methods . . . 46

2.2.1 Histology - Tissue preparation . . . 46

2.2.2 Immunohistochemistry and *in-situ* hybridisation . . . 47

2.2.3 Western blot . . . 49

2.2.4 Mouse line and animal housing . . . 50

2.2.5 Behavioural procedures . . . 50

2.2.6 Materials . . . 55

2.3 Results . . . 56

2.3.1 Anatomical studies showed expression of NCX3 (*Slc8a3* mRNA) in the dorsal root ganglia and the spinal cord . . . 56

2.3.2 *Slc8a3* mRNA expressed in all tested interneuronal populations and found in projection neurons . . . 58

2.3.3 NCX3 knock-out mice show normal motor and acute pain-related behaviour but hypersensitivity to the second phase of the formalin test . . . 61

2.4 Discussion . . . 64

2.4.1 Distribution of NCX3 in the DRG according to functional, molecular and anatomical studies 64

2.4.2 Motor, tactile and acute pain phenotypes of the NCX KO mouse line 67

2.4.3 Sensitised pain phenotypes of the NCX KO mouse line 68

3 *Slc8a3* - abnormalities in calcium handling and wind-up at the dorsal horn level 71

3.1 Introduction 72

3.1.1 The role of temporal summation in pain conditions 72

3.1.2 Wind-up and central sensitisation 73

3.1.3 Phases and maintenance of central sensitisation 74

3.1.4 The importance of calcium as a second messenger 75

3.1.5 Reorganisation of dorsal horn circuitry 76

3.1.6 Aims and hypotheses 80

3.2 Materials and Methods 80

3.2.1 Calcium imaging 80

3.2.2 *In vivo* electrophysiology 84

3.2.3 RNA extraction and Quantitative Real Time PCR 86

3.2.4 Cloning 87

3.2.5 Histology and Immunocytochemistry 88

3.3 Results 88

3.3.1 *In vitro* calcium imaging of dorsal horn neurons shows significant differences in calcium handling of HOM vs WT neurons 88

3.3.2 Loss of NCX3 produces enhanced wind-up of deep dorsal horn neurons 98

3.3.3 Generation of NCX3 AAV 99

3.4 Discussion 101

3.4.1 Abnormal calcium handling in cultured dorsal horn neurons . . 101

3.4.2 Loss of NCX3 produces exacerbated wind-up of deep dorsal horn neurons 108

3.4.3 Generation of NCX3 AAV for overexpression in the mouse spinal cord 110

3.5 Conclusion 111

4 *Gas7* - anatomy and modulation of pain behaviour in the mouse 113

4.1 Introduction 114

4.1.1 Mustard oil as an irritant 114

4.1.2 Overview of Gas7 115

4.1.3 Dendritic spine formation in the spinal cord – implication in chronic pain 118

4.1.4 Aims and hypotheses 119

4.2 Materials and Methods 120

4.2.1 Histology 120

4.2.2 Behavioural studies 122

4.2.3 Electrophysiology 124

4.2.4 Assessment of dendritic spine morphology in *Gas7*-KO mice . . 125

4.3 Results 129

4.3.1 Anatomical studies show expression of *Gas7* mRNA in the dorsal root ganglia and the spinal cord 129

4.3.2 Anatomical studies show all interneuronal populations express *Gas7* mRNA. 129

4.3.3 Behavioural assays in a Gas7 knock-out mouse line show hyposensitivity to hot plate, capsaicin and the second phase of formalin. 131

4.3.4 Loss of Gas7 does not change sensory coding properties or wind-up of dorsal horn neurons. 136

4.3.5 Loss of Gas7 does not affect dendritic morphology of *Tac1* excitatory interneurons in the dorsal horn. 137

4.4 Discussion 141

4.5 Conclusion 147

5 General Discussion **149**

5.1 From Human to Mouse and back 149

5.2 Central sensitisation - physiology meets anatomy 151

5.2.1 Calcium signalling and *NCX3* 151

5.2.2 Structural changes and *Gas7* 154

5.2.3 Central sensitisation - translational potential and challenges . . 155

Bibliography 159

List of figures

1.1 The circuit of pain – focus on the periphery 2

1.2 Labelling and classification of sensory neurons 9

1.3 Spinal cord anatomy 11

1.4 Spinal cord anatomy - sub-divisions based on RNA sequencing and morphology 15

1.5 Homosynaptic and heterosynapstic mechanisms in central sensitisation 22

1.6 The main neurobiological changes implicated in central sensitisation at the spinal cord level 27

1.7 GWAS in healthy participants - main findings 33

1.8 Domain structure of NCX3 36

2.1 *Slc8a3* is expressed in DRG neurons and the spinal cord 57

2.2 *Slc8a3* mRNA co-localises with both excitatory and inhibitory spinal cord interneuron markers 59

2.3 *Slc8a3* mRNA co-localises with projection neuron marker *Lypd1* 60

2.4 NCX3 KO line – design and behavioural results. 63

D.3.1The main neurobiological changes implicated in central sensitisation at the spinal cord level. 77

D.3.2Calcium entry and exit mechanisms in dorsal horn neurons of the spinal cord 79

3.1 Sorting of cultured dorsal horn neurons based on calcium imaging response reliability 91

3.2 Ca^{2+} maging properties of dorsal horn neurons from NCX3 HOM mice show significant differences to neurons from control NCX3 WT mice . . 94

3.3 Sorting of cultured DRG neurons based on calcium imaging response reliability 95

3.4 Ca^{2+} maging properties of DRG neurons from NCX3 HOM mice show no significant differences to neurons from control NCX3 WT mice . . . 97

3.5 Representative traces of single exponential decay fit of single cells from each of the four groups of neurons 100

3.6 Normal sensory coding of deep dorsal horn neurons in NCX3 WT, HET and HOM mice. 102

3.7 Increased wind-up of deep dorsal horn neurons in NCX3 HET and NCX3 HOM mice vs NCX3 WT controls. 103

3.8 Design of an adeno-associated virus (AAV) carrying the *Slc8a3*-isoform B104

D.4.1Schematic describing the possible role of Gas7 in neurite outgrowth . . 117

4.1 *Gas7* is likely expressed in DRG glia and co-localises with NeuN in the spinal dorsal horn. 130

4.2 *Gas7* mRNA co-localises with both excitatory and inhibitory spinal cord interneuron markers. 132

4.3 Gas7 KO line – behavioural results. 134

4.4 No change in wind-up of deep dorsal horn neurons in Gas7 HET, Gas7 HOM mice and Gas7 WT controls. 138

4.5 Expression of *Gas7* in the *Tac1* population in the spinal dorsal horn. . 140

4.6 Dendritic spine properties in Gas7 WT vs mutant HOM neurons in the *Tac1* population of excitatory interneurons. 142

List of tables

2.1 Reagents used in Chapter 2 55

3.1 Reagents used in Chapter 3 89

4.1 Reagents used in Chapter 4 128

Chapter 1

General Introduction

1.1 The study of acute and chronic pain

In his book "The Man Who Mistook his Wife for a Hat" Oliver Sacks describes a woman, Christine, who strangely woke up in a state not allowing her to move without looking at her feet. She could still sense touch, but she had no proprioception - the ability to feel the location of different body parts in the surrounding world. She never recovered from the sensory neuropathy she developed, which meant that she had to adapt to a type of 'body blindness' and learn to follow her limbs with her eyes in order to move them.

The somatosensory system is often overlooked as we rarely suffer from obvious abnormalities. However, without the ability to perceive touch, pressure, pain, temperature or proprioception, our world would be deprived of essential characteristics. In the context of pain, insensitivity is rare and extremely debilitating. The opposite pathology - chronic pain, however, is a major source of suffering, lacking safe and efficacious treatment (Breivik et al., 2006). This chapter will discuss the somatosensory

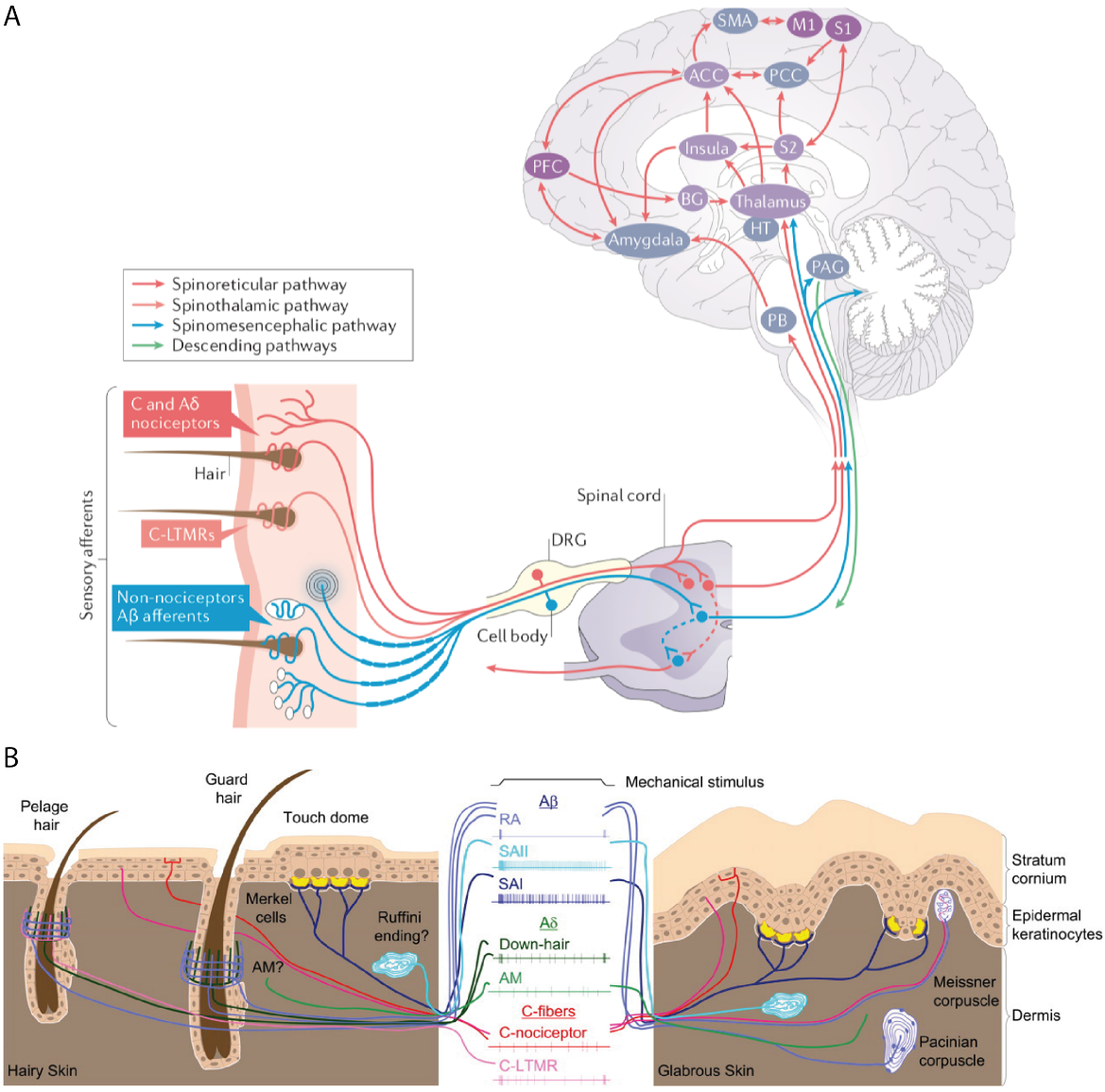


Fig. 1.1 The circuit of pain – focus on the periphery .
A. Nociceptive pathways from skin to brain – peripheral information about noxious and innocuous stimulation travels from cutaneous nerve endings, through their cell bodies in the dorsal root and trigeminal ganglia, and then projects to the spinal cord and brain stem. The brain processes the final signal and then relays it back to the spinal cord through descending pathways. **B**. Cutaneous receptors – the anatomical and functional diversity of skin nerve endings in hairy and glabrous skin. Adapted from (Kuner and Flor, 2017a; Bautista and Lumpkin, 2011).

system - its anatomy and physiology, starting at the peripheral end organs, moving through the spinal cord and finally reaching the brain (Figure 1.1A). It will also focus on pain and two novel targets involved in the processing of this sensation which provide further details about the mechanisms that turn normal acute pain into a debilitating and long-lasting condition.

1.2 Anatomy of the peripheral pain circuitry

Historically, pain was first described as a protective feeling in the 1900s by Sir Charles Sherrington. In 1906, he was the first to suggest that although pain is caused by different stimuli (mechanical, thermal, chemical), the threat of tissue damage collects them into a common experience. He used the term "nociceptor" to highlight the existence of a cutaneous end organ, detecting pain. In 1965, Melzack and Wall (1965) published the Gate-Control Theory which suggested that pain is the result of two effects occurring in the spinal cord: 1) the modulation coming from either large or small non-functionally specific skin fibres that could reduce or increase the signals reaching the brain; 2) the descending control that the brain exerts on the spinal cord (discussed by (Mendell, 2014)). In 1967, Burgess and Perl (1967) challenged the first point of the Gate-Control Theory by describing the existence of thinly myelinated afferents in the cat skin that were excited only by strong, tissue-damaging stimuli. This and other work defined the existence of specific nociceptor categories in the skin – the slow-conducting, unmyelinated C fibres and the thinly-myelinated, faster Aδ fibres (Bessou and Perl, 1969; Lynn and Carpenter, 1982).

Since then, much research has been done in order to identify and classify the different fibers residing in the skin and projecting to the dorsal root ganglia (DRG) or the trigeminal ganglia. As sensory neurons are pseudo-unipolar, they have one axonal

branch coming from the skin and one – projecting to the spinal cord and/or hind brain. Their main function is to turn mechanical, thermal and chemical stimulation into action potentials. Being able to classify the different skin nerve endings as well as the DRG neurons that they belong to, is of extreme importance as it allows us to decipher the code of the peripheral somatosensory information, fed into the central nervous system (CNS). The complexity of this question means that it is still heavily debated, and the classification listed below, is under constant revision.

1.2.1 Historical classification of sensory neurons and their cutaneous nerve endings

The noxious stimuli are broadly identified by high-threshold mechanoreceptors (HTMRs), whereas innocuous touch sensations are linked to low-threshold mechanoreceptors (LTMRs). All cutaneous sensory neurons are also classified as either Aβ, Aδ or C fibers based on cell size, axonal diameter, myelination and conduction velocity. Aβ and Aδ fibers have large and medium cell body size (respectively), their axons are highly and lightly myelinated (respectively) and their conduction velocities vary from fast to medium. C fibers are small in size, unmyelinated and have slow conduction velocity (Abraira and Ginty, 2013) for detailed, species-dependent information about conduction velocity).

1.2.2 Classification of LTMRS in glabrous and hairy skin

Classification of LTMRS in glabrous skin

Aβ fibers are light-touch mechanoreceptors and belong to the group of LTMRs. Importantly, there are Aδ and C fiber subpopulations which also belong to this group as they exhibit low activation thresholds – Aδ LTMRs (also known as D-hairs) as well as

C-LTMRs. Aβ fibers in the glabrous skin can be roughly separated into four groups: SA (slowly adapting) which are subdivided into SAI and SAII and RA (rapidly adapting) subdivided into RAI and RAII. The slowly adapting afferents fire action potentials throughout the duration of the touch stimuli, whereas the rapidly adapting ones exhibit fast action potentials only at the start and the end of the stimulus (Figure 1.1B). The first group - SAI fibers - are very sensitive and detect even shallow skin displacement (less than 15µm in humans)(Willis W.D, 1991). They provide good spatial resolution, allowing high sensitivity to the location of the stimulus. They form contacts with epidermal dome-like structures known as Merkel clusters (Merkel, 1875; Iggo and Muir, 1969)(Figure 1.1B). The anatomical density of Merkel cell clusters as well as the complexity of their innervation allows for the extremely detailed tactile discrimination and special resolution in both humans and rodents. For example, in humans the SAI fiber activation is linked to the ability to read Braille-like patterns (Johnson et al., 2000), whereas in mice ablation of these cell populations in the feet leads to inability to detect textured surfaces (Maricich et al., 2012) (reviewed by (Haeberle and Lumpkin, 2008).

While SAI fibers respond with irregular spiking, SAII fibers show much more uniform action potential pattern (Iggo and Muir, 1969). They are sensitive to skin stretch as well as object movement. For example, microstimulation of SAII fibers specifically leads to a pulling-like sensation in the skin (Vallbo et al., 1984). The receptor organs thought to associate with SAII fibers are known as Ruffini endings (Ruffini, 1894). These are spindle-shaped structures, located in the dermis (Figure 1.1B).

As mentioned previously, RAI-LTMR respond with fast action potentials only at the beginning and ending of mechanical stimuli. They are highly sensitive but not spatially accurate. This can be explained by their proximity to the surface of the skin and large density but also relatively large receptive fields (Berntson, 2009). RAI-LTMRs are

associated with cutaneous receptor organs known as Meissner corpuscles (Iggo and Ogawa, 1977) (Figure 1.1B), whose role was recently shown to involve gentle touch perception and fine sensorimotor control (Neubarth et al., 2020). Mechanistically, it is thought that the indentation of glabrous skin deforms the corpuscle and triggers the first action potential firing of RAI-LTMRs (Cauna, 1956; Ide, 1976; Pare et al., 2002). When the corpuscle regains its shape, the nerve fiber is activated again, firing a second action potential. It is also known that nociceptive C-fibers innervate Meissner corpuscles as well, linking their function to pain detection (Abraira and Ginty, 2013).

The fourth group, RAII-LTMRs, are associated with the detection of high frequency vibration but are not sensitive to spatial localisation. This can be explained by their large receptive fields with poorly defined borders and central region of maximal sensitivity (Johnson, 2001). These fibers innervate structures known as Pacinian corpuscles, which are large receptor organs located deep in the dermis linked to movement and vibration of objects held in our hands (Figure 1.1B).

Classification of LTMRS in hairy skin

The cutaneous afferents residing in hairy skin are similar to the ones mentioned above but several differences are also observed. These are mainly associated with RA fibers. In hairy skin, they detect the movement of single hair follicles and are associated with longitudinal lanceolate endings. RA fibers in hairy skin end with circumferential endings around each hair follicle. They are sensitive to hair movement but have much higher activation thresholds for punctate stimuli (Horch et al., 1977; Bai et al., 2015).

While the paragraphs above concentrated mainly on Aβ fibers, the hairy skin is also populated by Aδ LTMRs. They have intermediate conduction velocity and axon myelination. Although their role in human hairy skin is not well known, in mice and cats they exhibit very low mechanical thresholds and high dynamic sensitivity, making

them the most sensitive mechanoreceptors in the skin (Brown and Iggo, 1967; Burgess and Perl, 1967). Genetic labelling has shown that these fibers are also associated with lanceolate endings and also respond to hair movement (Rutlin et al., 2014).

The last type of touch receptors are the C-LTMRs. Unlike the above-mentioned LTMRs, C-LTMRs are unmyelinated. They are also very sensitive to skin indentation but are mostly activated by slow motion across their receptive field and are therefore linked to pleasant touch and stroking (Liu et al., 2007; Vrontou et al., 2013).

Interestingly, each LTMR class possesses a unique molecular signature. For example, C-LTMRs express tyrosine hydroxylase (TH), while Aδ-LTMRs express tropomysine receptor kinase B (TrkB) (Li et al., 2011; Rutlin et al., 2014). Other commonly used markers are illustrated in (Figure 1.2A).

It is also important to note that although the LTMR classes described above all have unique roles, most touch stimuli activate multiple subtypes and therefore the final touch perception is the integrated result of varying LTMR signals.

1.2.3 Classification of HTMRS

HTMRs include Aδ and C-fibers. They are evolutionary adapted for detecting noxious, damaging stimuli. Therefore they are optimally activated by strong, threatening stimulation. Nociceptors are also classified as peptidergic (expressing calcitonin gene-related peptide CGRP, subtastnace P and the tyrosine kinase receptor A (TrkA)) and non-peptidergic (expressing isolectin-B4, IB4) (Willis W.D, 1991; Gascon and Moqrich, 2010). The former are linked to mechanical and thermal sensations some of which are lost after specific cell ablation (Cavanaugh et al., 2009), while the latter are mainly mechanical nociceptors and no lack of thermal sensation is observed in knock-out mice (Cavanaugh et al., 2009; Zylka et al., 2005). The exact functions

of each neuron would depend on the subset of ion channels and G-protein coupled receptors it expresses. For example, the members of the TRP family of cation channels (TRPV1 – 4) are associated with detecting heat stimuli, while TRPM8 is linked to cold sensations. TRPA1 on the other hand, is activated by chemical substances (such as AITC, found in mustard, and cinnamaldehyde, found in cinnamon) and so is TRPV1 (capsaicin, found in chilli peppers) (Ramsey et al., 2006; Caterina, 2007; Woolf and Ma, 2007; Gascon and Moqrich, 2010; Bandell et al., 2004). Interestingly, HTMRs form free nerve endings in the dermis and epidermis and are located throughout the skin (Zylka et al., 2005; Dubin and Patapoutian, 2010).

As mentioned above (Figure 1.2A) lists markers that can be used to visualise and experimentally interrogate the different classes of sensory neurons. However, with the development of RNA sequencing, we are noticing that the classic, well-known populations can be sub-divided even further (Figure 1.2B for details) (Zeisel et al., 2018; Usoskin et al., 2015). This knowledge is frequently updated and can be used for the better understanding of the functions of the respective primary afferents as well as for the development of better methods to visualise them or create ablation-based mouse lines.

1.3 Anatomical organisation of the spinal cord

While the Gate Control Theory was largely disproved in its idea that primary afferents are non-functionally specific, the hypothesis that the spinal cord modulates and gates the incoming peripheral signals is still accepted. Primary afferent axons, coming from the DRG, terminate in the spinal dorsal horn. The neurons residing there can be classified in many different ways. For example, they can be largely divided into excitatory and inhibitory interneurons; and projection neurons (excitatory spinal

A

Marker	Sensory cell type
Parvalbumin	Proprioceptors and Aβ fibers
CGRP	Peptidergic C fibers, sub-population of Aδ fibers
Substance P	Peptidergic C fibers
NF200	Myelinated Aδ fibers, Aβ fibers, and proprioceptors
IB4	Non-peptidergic C fibers
Trpv1	Small diameter C fibers (heat and pain)
Trpm8	Small diameter C fibers (cold and pain)
MrgprD	Small diameter C fibers (noxious mechanical, pain)
MrgprA3	Small diameter C fibers (itch)
MrgprB4	Small diameter C fibers (innocuous mechanical)
VGlut3	Non-peptidergic C fibers (innocuous mechanical, cooling)
TH	Non-peptidergic C fibers (innocuous mechanical, cooling)
TrkB	Aδ fibers (innocuous mechanical, cooling)
Npy2r	Aβ fibers (innocuous mechanical)
Chondrolectin	Aβ fibers (innocuous mechanical)

B

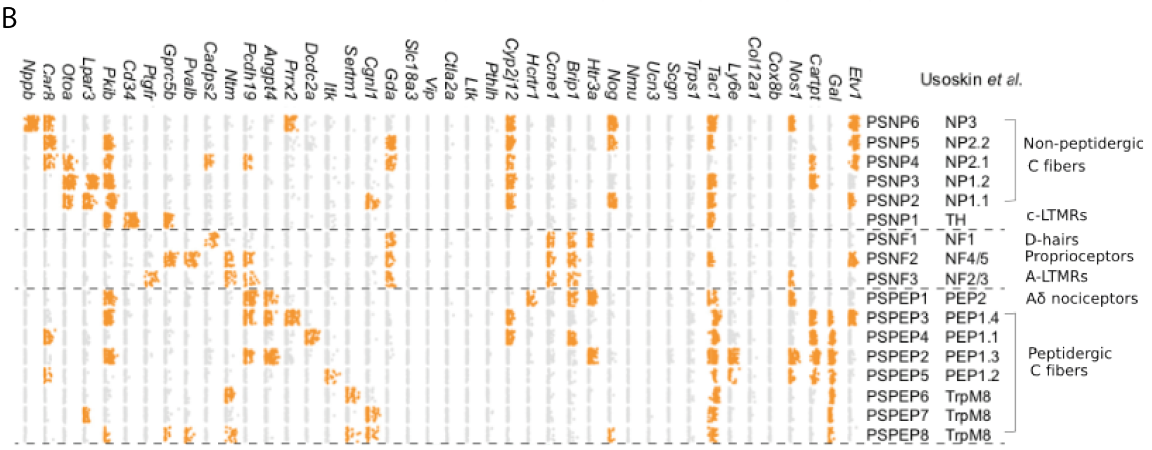


Fig. 1.2 Labelling and classification of sensory neurons.
A. Common sensory cell type markers - Abbreviations: CGRP, calcitonin gene-related peptide; NF200, neurofilament heavy chain 200; IB4, isolectin B4; Trpv1, transient receptor potential cation channel subfamily V member 1; Trpm8, transient receptor potential cation channel subfamily M member 8; MrgprD, Mas-related G-protein-coupled receptor D; MrgprA3, Mas-related G-protein-coupled receptor A3; MrgprB4, Mas-related G-protein-coupled receptor B4; VGluT3, vesicular glutamate transporter type 3; TH, tyrosine hydroxylase; TrkB, tyrosine receptor kinase B; Npy2r, neuropeptide Y receptor type 2. **B**. Marker genes (shown in orange) serving to classify novel primary afferent sub-populations. Adapted from (Le Pichon and Chesler, 2014; Usoskin et al., 2015; Zeisel et al., 2018).

cord neurons form ascending tracts which travel rostrally to the brain). The pain circuit is then completed by descending pathways which modulate spinal cord signalling (Figure 1.1A), as hypothesised by (Melzack and Wall, 1965).

1.3.1 Primary afferent input into the dorsal horn

One of the first steps in studying the anatomy of the spinal dorsal horn came from Rexed (1952) who divided the grey matter into 6 parallel laminae. In the 1970s-1980s a series of studies showed the projection patterns of primary afferents in the spinal dorsal horn. The afferents, responsible for innocuous touch, usually terminate in the deep dorsal horn (Aβ fibers project to laminae III-VI with some of them extending to lamina IIinner) while Aδ hair-follicle afferents arborise around the border between laminae II and III(Brown et al., 1981; Light and Perl, 1979). One of the first studies investigating this matter was done by Light and Perl (1979) who functionally identified primary afferents terminating in the dorsal horn and labelled them with horseradish peroxidase (HRP). This reagent, after a subsequent chemical reaction, labelled all terminations of the selected neurons and showed the above-mentioned pattern.

Similar methods have been used to label C-fibers – for example wheat germ agglutinin (WGA-HRP) or plant lectin known as PHA-L (Ma and Tian, 2002; Sugiura et al., 1986; LaMotte et al., 1991). These and other methods have shown that nociceptors usually project to the superficial laminae with Aδ nociceptors terminating in lamina I while most of the non-peptidergic C fibers project to an IB4-positive band in the centre of lamina II (Light and Perl, 1979; Lorenzo et al., 2008), (Reviewed by Todd (2010); Battaglia (2016) (Figure 1.3)). Conveniently, there are neurochemical markers that can be used to recognise functional populations such as CGRP, labelling peptidergic nociceptors and MRGD, used for non-peptidergic fibers (Zylka et al., 2005).

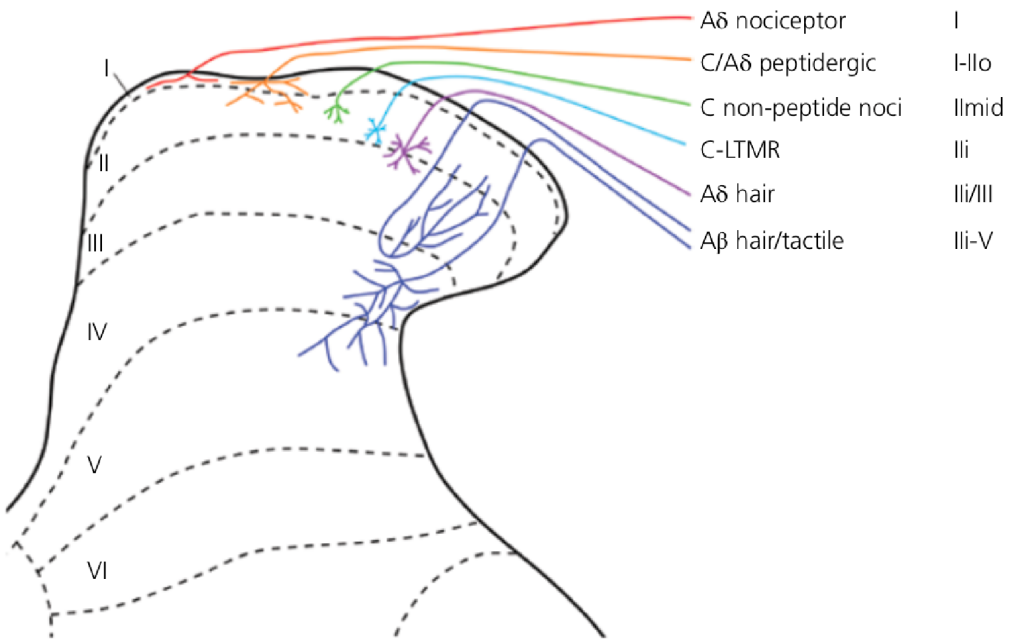


Fig. 1.3 Spinal cord anatomy.
Location of primary afferent central arbors in the Rexed's laminae of the spinal dorsal horn (Todd, 2010).

1.3.2 Classification of interneurons and projection neurons

Interneurons in the spinal cord form contacts locally, usually within the lamina they reside in. Sometimes they also project to neighbouring laminae or even further (Battaglia, 2016). Interneurons are the most common population in the spinal cord, making up 95% of all neurons in lamina I, almost 100% in lamina II and unknown, but high percentage in the deeper laminae (Todd, 2010). This would mean that there are many sub-groups of interneurons, which are different neurochemically, morphologically and functionally. The most parsimonious distinction so far is between inhibitory and excitatory interneurons. The former use GABA and/or Glycine as their major neurotransmitter(s) which can be revealed by expression of GAD or the GlyT2 transporter. These neurons are mainly seen in laminae I-III, with GlyT2 expression largely in lamina III (Zeilhofer et al., 2012). Polgar et al. (2013a) have recently reported that

the inhibitory interneurons account for 26% of the neurones in laminae I-II and 38% of those in lamina III. It is likely that all of the remaining neurons are excitatory including interneurons and 5-10% projection neurons (reviewed by Todd (2017)). Excitatory interneurons use glutamate as their major neurotransmitter and express mainly VGLUT2, with some cells in lamina III expressing low levels of VGLUT3 (Battaglia, 2016; Todd et al., 2003).

1.3.3 Further neurochemical sub-divisions of inhibitory interneurons

Subdividing the different interneuronal populations based on various neurochemicals is challenging as it leads to overlapping subgroups. Efforts by Polgar et al. (2013b) have identified 4 different non-overlapping inhibitory populations expressing neuropeptide Y (NPY), neuronal nitric oxide synthase (nNos), galanin or parvalbumin. Interestingly, functional differences between these sub-groups were also observed using the expression of the transcription factor c-Fos or the phosphorylated extracellular signal-regulated kinase (pERK). Galanin- and NPY-positive populations responded to noxious heat as well as intradermal capsaicin and formalin. nNOS-containing cells, on the other hand, responded only to noxious heat and formalin, while parvalbumin-positive neurons remained inactive to all three stimuli. These results suggest that the first three populations are important for reducing pain but likely receive inputs from different primary afferent populations. In addition, Hughes et al. (2012) have shown that the parvalbumin population forms axoaxonic synapses with the central terminals of myelinated LTMRs, pointing to a feedback loop associated with touch sensitivity (Hughes et al., 2012; Boyle et al., 2019) (discussed in more detail in Sub-section 1.3.7).

As mentioned previously, these data should be interpreted cautiously as nNOS, for example, has been found in some excitatory interneurons.

1.3.4 Further neurochemical sub-divisions of excitatory interneurons

The difficulty in finding specific neurochemical markers exists in the excitatory population as well. For example, somatostatin (SST) has been well-studied as a protein expressed by excitatory interneurons, mainly in lamina II (Yasaka et al., 2010; Proudlock et al., 1993). This marker, however, is expressed in several other populations as well. Work by Gutierrez-Mecinas et al. (2016) has shown that the population it marks is functionally heterogenous. In contrast, there are six neurochemical proteins, which are largely restricted to excitatory interneurons and which form mostly non-overlapping sub-populations - neurokinin B (NKB), neurotensin, gastrin-releasing peptide (GRP),substance P, cholecystokinin (CCK) and neuropeptide FF (NPFF) (Gutierrez-Mecinas et al., 2016, 2019a,b; Dickie et al., 2019) Little is known about the distinct function of these neuronal groups but GRP, for example, has been implicated in itch (Mishra and Hoon, 2013).

1.3.5 RNA-sequencing-based sub-divisions

As with dorsal root ganglion neurons, the dorsal horn neurons have been subjected to RNA sequencing and separated into distinct groups based on mRNA expression at the single cell level (Haring et al., 2018) (Figure 1.4A). This resulted in 15 GABA-ergic, inhibitory sub-populations and 15 glutamatergic, excitatory groups. As expected, the defining features and branching points of each cluster corresponded with neuropeptides, which were already known to mark sub-populations of neurons. These were then used

to annotate the different branches of the created hierarchical tree (Figure 1.4A). One such example is Gal, the gene that encodes galanin, which was used to define a cluster of three GABA-ergic populations.

1.3.6 Sub-divisions based on morphological classification

The most cited study about the morphological classification of DH neurons is the one by Grudt and Perl (2002) where the authors identified four main types of lamina II neurons – islets, vertical, radial and central. As seen in (Figure 1.4B), islet cells have long dendritic trees, orientated in the rostrocaudal axis; vertical cells are cone-shaped, with their dendritic trees located ventrally from their soma; radial cells have radiating dendrites; and central cells are similar to islet cells but have restricted dendritic trees. The main limitations of this classification strategies are that 1) around 30% of the neurons cannot be assigned to any of these four groups; and 2) in many cases these four populations are very heterogeneous in function and neurochemical make-up. Interestingly Yasaka et al. (2010), found that all islets cells are inhibitory and expressed GABA, while radial cells and most vertical cells were excitatory. Therefore, although not very specific, these data taken together show that morphology does provide a level of knowledge about the function of the respective population.

1.3.7 Synaptic circuits – function depends on neuronal interplay

As mentioned at the start of this chapter, one of the main, still-existing theories about the integration of information at the level of the spinal cord is the Gate-Control Theory by Melzack and Wall. In 1965 they proposed that inhibitory interneurons function as a gate, reducing the input of LTMR afferents and preventing the interpre-

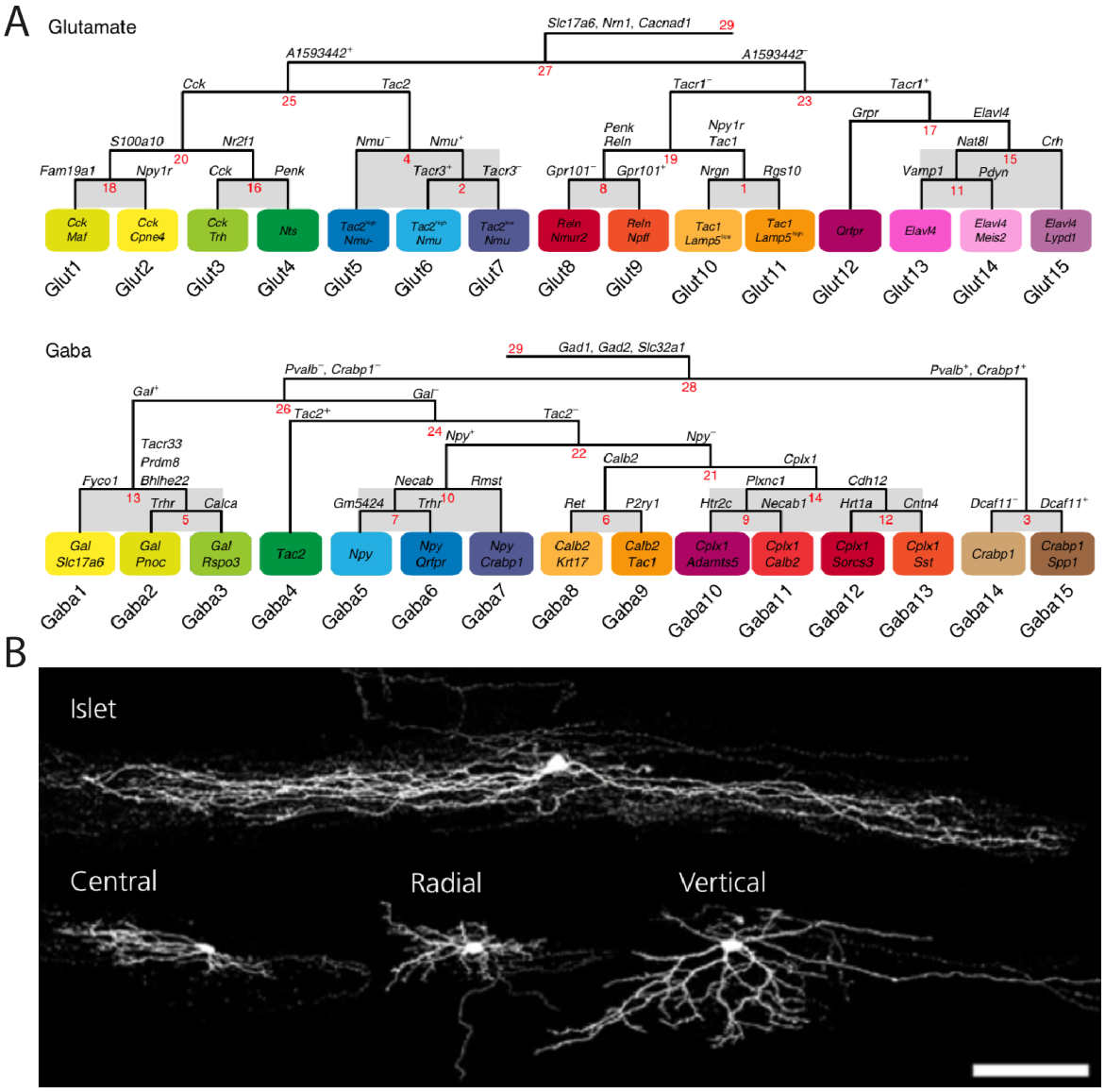


Fig. 1.4 Spinal cord anatomy - sub-divisions based on RNA sequencing and morphology.

A. Hierarchical representation of the 15 GABA-ergic and 15 Glutamate-ergic sub-populations found in the spinal dorsal horn, based on single cell RNA sequencing (Haring et al., 2018). **B**. Confocal images of lamina II neurons corresponding to the morphological classification of Grudt and Perl (2002)(reviewed by (Battaglia, 2016).

tation of touch stimuli as pain. This effect could be pre-synaptic – at the level of the primary afferents, or post-synaptic – acting on local circuit excitation. This theory is especially logical in pathological pain states, when the reduction of inhibition in the spinal cord opens "the gate" and allows innocuous sensations to be interpreted as pain. This phenomenon is known as *tactile allodynia*.

An example of such a circuit was recently published by (Boyle et al., 2019) who demonstrated that parvalbumin positive interneurons are likely to mediate pre-synaptic inhibition of LTMR afferents, as well as post-synaptic inhibition of excitatory vertical cells. This then creates a circuit which reduces the amount of excitatory input reaching the projection neurons in Lamina I. The authors also showed that parvalbumin interneurons have reduced function in response to spared nerve injury, giving evidence for their physiological function as a "gate" between innocuous touch and injury-driven tactile allodynia. Uncovering this circuit, however, is the result of a number of previous studies. For example, the morphology, location, firing patterns and the ability of parvalbumin interneurons to form inhibitory axoaxonic presynaptic connections with primary afferent central terminals was reported by (Abraira et al., 2017; Hughes et al., 2012; Petitjean et al., 2015). This signifies the difficulty in uncovering synaptic circuits and understanding how peripheral signalling is integrated and decoded by the spinal cord.

Apart from the Gate-Control Theory, there have been other models about the coding of nociceptive information in the spinal cord. These include: *the labelled line theory*, *the intensity theory*, *the pattern theory* and *the combinatorial theory* (Ma, 2010; Prescott et al., 2014; Koch et al., 2018). In short, the labelled line theory suggests that information about a certain modality is carried by a specific line of neurons dedicated to this function; the intensity theory proposes that pain is a result of a series of sub-threshold stimulations which, under certain summation conditions, can be

unmasked due to reduced thresholds. The pattern theory focuses on firing patterns which are specific for certain modalities and therefore serve as a code, deciphered by the spinal cord. Finally, the combinatorial theory relies on the combination between the activity of low- and high-threshold neurons in the spinal cord and their interaction. Interestingly, both the pattern and the combinatorial theory propose levels of plasticity within the local circuits.

These theories provide a variety of possibilities which are not mutually exclusive and highlight the complexity of the spinal cord. However, it is clear that the final result of this processing mechanism is the signal which eventually reaches the projection neurons and gets transmitted to the brain (Torsney and MacDermott, 2006). The excitability of these neurons is critical to which stimuli are perceived as pain and which remain innocuous.

1.3.8 Projection neurons – ascending pathways

Spinal projection neurons carry the output signal from the dorsal horn to the brain. These neurons are found mainly superficially in lamina I, as well as in deeper laminae III-VI. It has been estimated that roughly 80% of the projection neurons express the neurokinin 1 receptor – NK1R, which is activated by substance P (Todd, 2002). The fact that this neuropeptide is released by a large proportion of the nociceptive afferents consolidates the notion that projection neurons carry noxious information (Doyle and Hunt, 1999; Mantyh et al., 1997). Lamina I NK1R+ neurons have been shown to receive monosynaptic inputs from C and Aδ fibers. They also receive polysynaptic signals from Aβ LTMRS, which are likely to be unmasked and interpreted as pain under injury conditions (Torsney and MacDermott, 2006). Another piece of evidence, showing the importance of projection neurons in pain processing, comes from studies that have

selectively ablated lamina I NK1R+ neurons with saporin-conjugated substance P which led to a decrease in heat and mechanical hyperalgesia after intradermal capsaicin (Mantyh et al., 1997). In addition, electrophysiological studies have demonstrated that all lamina I projection neurons in the rat are activated by noxious stimuli and some of them - by innocuous mechanical and thermal stimulation (Bester et al., 2000; Andrew, 2009).

Lamina I projection neurons send signals into the brainstem, in areas such as the rostral ventromedial medulla (RVM), which in turn sends descending signals back to the spinal cord, creating a feedback loop. In addition, superficial NK1R+ neurons project to higher brain centres in the thalamus, the periaqueductal grey (PAG) and the parabrachial area (PB) (Todd, 2002; Dickenson et al., 1997).

The projection neurons residing in deeper laminae send information predominantly to the thalamus, thereby forming a large part of the spinothalamic tract. The signals from the thalamus are then transmitted to the cortical centres of pain which include the insular, anterior cingulate and prefrontal cortices (Tracey and Mantyh, 2007).

The major ascending tract for pain and temperature, where the axons of superficial and deep projection neurons join together and ascend to the brainstem and thalamus, is known as the spinothalamic tract (also known as the anterolateral system, ALT). The ALT is not the only ascending pathway to start in the dorsal horn. Other tracts include the spinocervical (ascending to the sensory cortex) and the postsynaptic dorsal column pathway (ascending to the medulla). Much less is known about those two tracts (Brown, 1983; Abraira and Ginty, 2013).

1.4 Short anatomy of brain regions associated with pain – descending pathways

As mentioned previously, the brain does not simply accept information from the spinal cord but also forms feedback loops, which further modulate the spinal processing. The network of supraspinal structures that mediate descending pathways includes the following structures: prefrontal cortex, anterior cingulate cortex, insula, amygdala, hypothalamus, periaqueductal grey, rostral ventromedial medulla, and dorsolateral pons/tegmentum (Tracey and Mantyh, 2007). Such descending influences can be both pro- and anti-nociceptive. For example, descending facilitation has been shown to have a role in the maintenance of nerve injury-induced pain (Burgess et al., 2002). The authors used a lidocaine injection into the RVM and reported that it blocked spinal-nerve-ligation-induced tactile and thermal hypersensitivity 6-12 days after injury, but not on day 3. This distinguished the mechanism which led to neuropathic pain from the descending supraspinal influences that contribute to its maintenance. Another early study showed that electrical stimulation of the PAG produced dramatic analgesic effects which allowed for animals to undergo surgery without pain (Reynolds, 1969)(reviewed by (Garland, 2012)).

The role of the brain in pain processing adds extreme complexity to the understanding of chronic pain. This is partly due to the emotional aspect, added to the experience of pain. For example, shock can temporarily suppress pain, whereas depression and anxiety can amplify and prolong it (Garland, 2012). This is why the interplay between the different mechanisms in the PNS and CNS needs to be studied in a holistic manner.

1.5 Pathological pain and sensitisation

The ability to sense pain is essential for our survival. After tissue damage, an inflammatory process is triggered which sensitises the pain circuit and creates a protection area of hypersensitivity which promotes healing. Hypersensitivity in the area of tissue damage is known as *primary hyperalgesia*, while hypersensitivity in the area surrounding the damage is referred to as *secondary hyperalgesia*. The former can be caused by sensitisation of peripheral and/or central neurons, whereas the latter is linked to diffusion of pro-nociceptive molecules from the inflamed to the adjacent, non-inflamed areas, as well as increased responsiveness in the CNS. In addition, stimulation of touch-sensitive fibers can also begin to elicit pain. As mentioned previously, this phenomenon is known as tactile allodynia.

Both the PNS and CNS play important roles in pain signalling. The sensitisation of peripheral nociceptors is called *peripheral sensitisation* (Gold and Gebhart, 2010; Basbaum et al., 2009). As mentioned previously, injuries lead to local inflammation and the release of pro-inflammatory factors such as NGF, serotonin (5-HT), prostaglandins, bradykinin, histamine, ATP and protons (collectively known as "the inflammatory soup") (Kessler et al., 1992), which creates periphery-driven sensitivity(Woolf and Ma, 2007). Long-lasting stimulation, however, can cause a CNS phenomenon, which is specific to the spinal cord and is known as *central sensitisation*. If prolonged, such sensitisation can become maladaptive and lead to the long-term functional and structural changes, contributing to chronic pain. This phenomenon will be thoroughly discussed in the paragraphs below.

CS was first reported in 1983, when Woolf (1983) observed that thermal injury to the foot of decerebrated rats led to a heightened flexor reflex. This involved enlarged receptive fields of the motor efferents, which now included more inputs from

contralateral areas and the tail. Although some of this facilitation could be explained by increased sensitisation of adjacent peripheral nociceptors (peripheral sensitisation), the expansion of the receptive fields to contralateral areas and the tail pointed to a central component.

1.5.1 Central sensitisation - lost in translation

Today CS is known as the "enhanced responsiveness of nociceptive neurons in the CNS to their normal afferent input" (IASP). The terminology used to explain this phenomenon and the processes it involves is somewhat dependent on the authors that write about it. This thesis will use the terminology adopted by Woolf and colleagues, but it is important to mention the debate that exists in the field as alternative terms have been used in book chapters (for example (Zeilhofer and Ganley, 2019) and reviews, for example (Kuner and Flor, 2017b).

Latremoliere and Woolf (2009) used the term *long-term potentiation (LTP)* as a homosynaptic mechanism (Figure 1.5) but longer lasting and usually caused by high frequency stimulation (100Hz). The authors considered LTP a cortical mechanism, linked to memory, which strengthens single synapses (without affecting neighbouring ones) and lasts a long time or even permanently. As C-fibers do not naturally fire at a frequency of 100Hz, the existence of LTP in the spinal cord is debated by Woolf and colleagues.

On the other side of the argument, Sandkuhler and colleagues (Sandkuhler, 2007) describe LTP as an increase in monosynaptically-evoked post-synaptic currents. The authors highlighted the fact that central sensitisation is used as an umbrella term to include all forms of changes within the CNS which lead to enhanced pain perception. This can easily become vague and include mechanisms which are hypothetical and

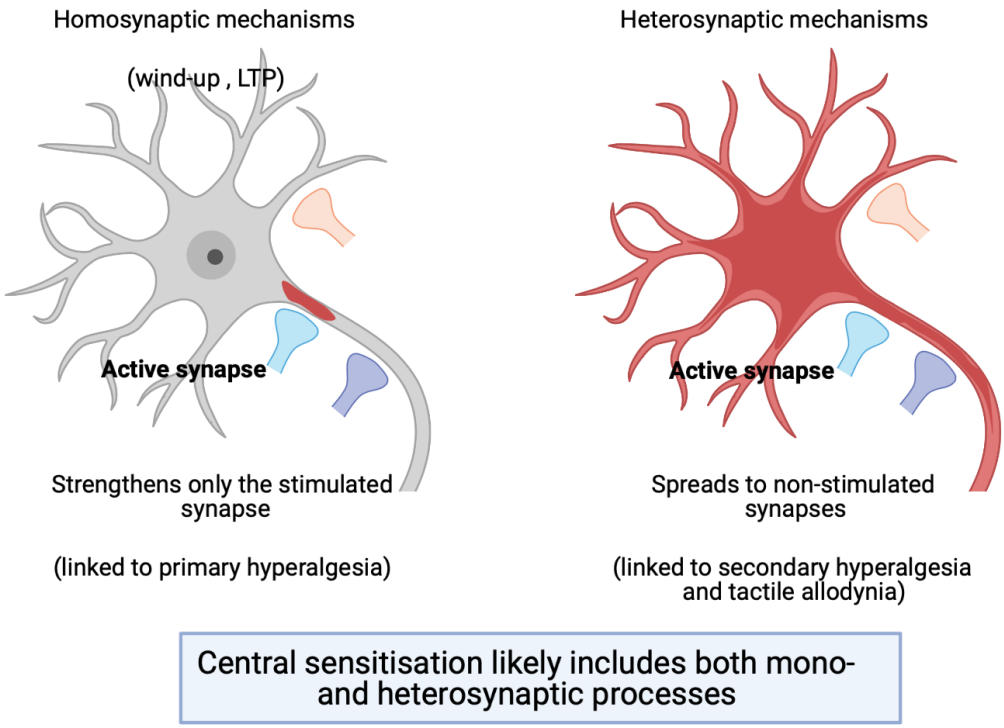


Fig. 1.5 Homosynaptic and heterosynapstic mechanisms in central sensitisation.
Homosynaptic **(left panel)** mechanisms involve activity-dependent potentiation of a single synapse, caused by continuous signalling through that same synapse. Heterosynaptic potentiation **(right panel)** develops when one set of synapses (conditioning input) are sensitised and this leads to stimulation of other, non-activated groups of synapses. Adapted from Latremoliere and Woolf (2009) .

unclear. Sandkuhler also pointed that if we consider the above-mentioned definition by IASP, we should bear in mind that enhanced responsiveness of inhibitory interneurons is also possible, and it can lead to less pain. As LTP and long-term depression can be measured, the authors discuss them as well-studied cellular mechanisms to explain synaptic plasticity in the spinal cord. They refer to studies by Randic et al. (1993) showing high frequency stimulation leading to LTP between C/Aδ fibers and dorsal horn neurons. More importantly, work by (Ikeda et al., 2006) demonstrated long lasting synaptic potentiation (at least 60minutes) elicited by C-fibers at natural frequencies (2Hz) and also in response to capsaicin and formalin. Latremoliere and Woolf (2009) disagree with the terminology proposed by Ikeda et al. (2006) and suggest that formalin and capsaicin injections can cause a large variety of effects in the dorsal horn, including heterosynaptic and circuit-dependent ones. Latremoliere and Woolf (2009), however, did not deny the result from Ikeda et al. (2006) showing low frequency-induced LTP in the spinal cord, but rather suggested that this was only seen in the less common spino-PAG neurons and not the spinoparabrachial neurons (which represent 80% of lamina I projection neurons)(Hylden et al., 1989a; Spike et al., 2003).

The existence of LTP in the spinal cord is not the only debate. The terminology used by Sandkuhler and colleagues also includes a type of LTP which is not homosynaptic but rather *lacks synapse specificity*. According to (Kronschlager et al., 2016) LTP does not explain secondary hyperalgesia and widespread hyperalgesia. The group points that LTP can be accompanied by LTP in adjacent inactive synapses due to a spread of molecular signals in the cytoplasm of the post-synaptic neuron. This definition is similar to the one given by Woolf and colleagues for heterosynaptic sensitisation (Figure 1.5), albeit heterosynaptic mechanisms can be many and varied. The phenomenon Kronschlager et al. (2016) demonstrated, was termed *gliogenic LTP*. They showed that LTP can spread potentiation from one conditioned neuron to another

non-conditioned one, making gliogenic LTP a larger phenomenon, with a potential to influence many cells and many synapses. This creates the possibility of confusion between LTP and the larger phenomenon of central sensitisation. To avoid confusion, this thesis will focus on the terminology used by Woolf and colleagues but also take into account the work of Sandkuhler and colleagues (Figure 1.5).

The clinical importance of central sensitisation, the molecular mechanisms which underlie it and the important role of Ca^{2+} will be discussed in more detail in Chapter 3 of this thesis.

1.5.2 Top-down - Bottom-up sensitisation

It is important to mention that CS is often separated into two groups of central effects. The first one, which is described in (Figure 1.6) and in Chapter 3 of this thesis, is often referred to as "bottom-up" and is likely initiated and maintained by peripheral effects. The second one, "top-down" sensitisation, is associated with supra-spinal effects (reviewed by (Staud, 2013). This can explain why psychological factors such as fear, expectation and depression are so important in the complete experience of chronic pain, sometimes even in the absence of peripheral pathology. For example, noradrenergic projections from the brainstem provide descending inhibition by activating α2-adrenergic receptors and decreasing the excitatory drive in the spinal cord D'Mello and Dickenson (2008); Arendt-Nielsen et al. (2018). Peripheral inflammation has been largely shown to decrease this and other inhibitory processes as well as increase the opposite phenomenon - descending facilitation. "Bottom-up" and "top-down" sensitisation can produce similar phenotypes and can also exist together. Differentiating between the two is challenging in a clinical setting but understanding the differences would be an important advancement in the field.

1.5.3 The role of the periphery and potential for reversibility

The importance of the periphery in "bottom-up" CS has been the subject of long debates. A recent study by Chisholm et al. (2018) used the formalin test and in-vivo calcium imaging in the DRG to address this debate. The formalin test in rodents is largely used by the pharmaceutical industry and presents an in-vivo model of acute and sensitised pain. During this test, rodents are subjected to an intraplantar injection of formalin. They respond by strong pain behaviour during the first 5 minutes which is followed by a quiet phase and a longer second phase starting at 15 minutes post formalin and lasting until the end of the test at 60 minutes. The first phase is considered acute while the second - models central sensitisation. A recent report using in-vivo Ca^{2+} imaging at the level of the DRG showed that the first phase was associated with a strong activation of many sensory neurons, explaining the acute pain behaviour in mice. This was followed by the second phase where the authors observed lower levels of intermittent firing. This result was interpreted as evidence that the DRG in the first phase sensitises the spinal cord so that the weaker firing in the second phase is enough to generate pain and create a sustained and longer-lasting pain behaviour. This highlights the role of the DRG even when pain becomes centrally mediated in the second phase of formalin Chisholm et al. (2018). Although still debated, this idea is supported by older research showing lower levels of DRG neuron firing during the second phase as well as reports that skin lidocaine was able to reduce sensitised pain post formalin (McCall et al., 1996; Taylor et al., 1995).

In conclusion, central sensitisation is a dynamic and adaptive process. "Bottom-up" sensitisation is considered to be the result of heightened spinal response to peripheral signalling. There is evidence, however, that this sensitised state is reversible (Figure 1.6) and still coupled, although more loosely, to the periphery. Therefore, treatment strategies could benefit from differentiating between "bottom-up" and "top-down"

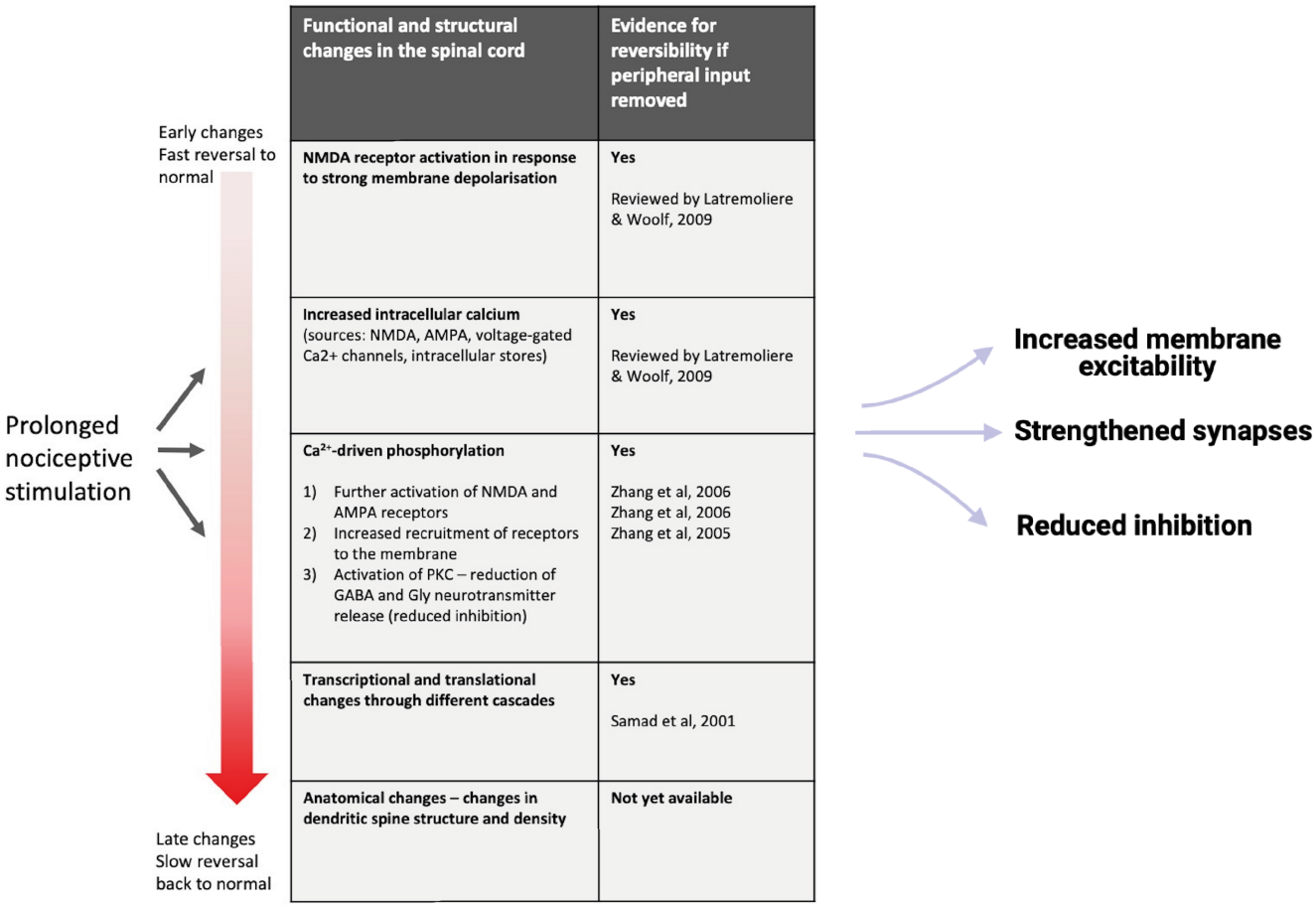
central mechanisms, and focus efforts on the DRG and spinal cord if the former is suspected and is found to dominate.

1.6 GWAS - the search for novel genes associated with pain

The treatment of complex diseases, such as chronic pain and its peripheral and central components, requires the deep understanding of the genes and processes underlying those conditions. This thesis will focus on a genome-wide association study (GWAS) which led to the discovery of two novel genes, associated with experimental pain in healthy volunteers. Therefore, the following paragraphs will discuss the advantages and disadvantages of GWAS-s, as well as the importance of validating the produced results.

1.6.1 What is a GWAS?

GWAS-s measure and analyse DNA variations, across the human genome, which are significantly linked to a disease or a trait. These variations are known as *single nucleotide polymorphisms (SNPs)* and represent single base-pair changes in the genome. They are by far the most common type of genetic variation known. The typical GWAS uses SNP arrays to compare cases (individuals who possess the respective phenotype) to controls. The identified SNPs can occur in the untranslated regions of the genome, or in exonic sequences. They can have functional consequences such as **1.** amino acid changes in a protein of interest; **2.** differences in mRNA transcript stability or **3.** variation in expression levels due to effects on transcription factors binding efficiency and interaction with enhancers. In most cases, however, the identified SNPs lead to



Functional and structural changes in the spinal cord	Evidence for reversibility if peripheral input removed
NMDA receptor activation in response to strong membrane depolarisation	**Yes** Reviewed by Latremoliere & Woolf, 2009
Increased intracellular calcium (sources: NMDA, AMPA, voltage-gated Ca2+ channels, intracellular stores)	**Yes** Reviewed by Latremoliere & Woolf, 2009
Ca^{2+}-driven phosphorylation 1) Further activation of NMDA and AMPA receptors 2) Increased recruitment of receptors to the membrane 3) Activation of PKC – reduction of GABA and Gly neurotransmitter release (reduced inhibition)	**Yes** Zhang et al, 2006 Zhang et al, 2006 Zhang et al, 2005
Transcriptional and translational changes through different cascades	**Yes** Samad et al, 2001
Anatomical changes – changes in dendritic spine structure and density	**Not yet available**

Fig. 1.6 The main neurobiological changes implicated in central sensitisation at the spinal cord level.
The intense stimulation of spinal cord neurons leads to increased intracellular Ca^{2+} through NMDA and AMPA receptor activation and recruitment. This can cause various transcriptional changes that can ultimately bring about long-term modulation of spine structure and density. Notably, there are other, rapid mechanisms for spine re-structuring, such as RHO GTPases, which modulate actin polymerisation. Legend: NMDA: N-methyl-D-aspartate, NMDAR: NMDA receptor, AMPA: α-amino-3-hydroxy-5-methyl-4-isoxazolepropionic acid, AMPAR: AMPA receptor, Ca^{2+}: calcium, PKC: protein kinase C, GABA: Gamma aminobutyric acid, Gly: glycine. Information from (Latremoliere and Woolf, 2009; Zhang et al., 2005, 2006a,b; Samad et al., 2001) Similar schematic published in (van Griensven et al., 2020a).

small effect size differences. This is because GWAS-s assess the relationship between common SNPs and physical traits/diseases, characterised by a large amount of genes and variations within them. Risk, associated with a variant, is often assessed by odds ratio (OR) – the chance of a disease in individuals with the variant, divided by the chance of disease in those without it. The OR for most genetic variants which contribute to the risk of complex diseases is likely to be around 1.3. Therefore, the statistical power of GWAS-s can greatly vary depending on the OR of genetic variants, as well as their frequency within a given population (reviewed by (Ikegawa, 2012; Manolio et al., 2008)).

Interestingly, not all SNPs, identified by GWAS-s, are directly associated with the disease or trait in question. In some cases, SNPs have no functional role, but are instead inherited together with causal SNPs. This is known as indirect association and is due to a phenomenon known as *linkage disequilibrium* (Bush and Moore, 2012). Therefore, GWAS-s identify variants which tag a region of the genome, containing causal variants. Additional studies are usually needed to narrow the region of association and locate the exact causal variant.

The term "linkage disequilibrium" is based on a phenomenon known as "chromosomal linkage". This phenomenon describes the consequences of crossover events during meiosis. During crossover, two homologous chromosomes physically exchange parts of their arms, resulting in novel chromosomes, containing mixed segments from the original two. This process creates variation during the production of gametes (Stitt et al., 1995). It also means that two SNPs can remain physically joined on a chromosome, resulting in linkage disequilibrium. However, repeated random recombination events from generation to generation, will continue to break apart segments of the novel chromosomes until eventually all alleles in the population become independent and reach "linkage equilibrium" (Bush and Moore, 2012).

The commonly unknown or relatively small functional role of the identified SNPs has led to scepticism in certain areas, regarding the significance of GWAS-s. It is important to point out, however, that SNPs are usually commonly observed genetic variations. Therefore, as mentioned previously, they have small penetrance or small contribution to the disease/trait in question. For example, if a SNP is observed in 20-30% of the population and causes a potentially deadly disease, this would mean that a high proportion of humans would develop the condition. Therefore, such SNPs(gene mutations) are maintained at extremely low frequencies by evolution. Common SNPs, on the other hand, almost always have small penetrance (effect size). This is why, in many cases, GWAS-s do not aim to discover a causal SNP but rather to use these SNPs to guide basic science research to functionally interesting DNA regions. These regions can then be studied in greater detail (Bush and Moore, 2012).

At present, GWAS-s are most commonly used for the association of common SNPs with common, genetically complex diseases (such as diabetes or chronic pain). Notably, because the identified SNPs often have relatively small penetrance, they only partially explain the heritability of common diseases. Therefore, there is a variety of SNPs and genetic regions, important for the development of a trait or disease (Ikegawa, 2012).

1.6.2 A brief history of GWA studies

The first, albeit very early-stage, GWAS was published in 2002 (Ozaki et al., 2002)and found a SNP in the lymphotoxin-alpha (LTA) gene associated with myocardial infarction. The completion of the human genome project in 2003, as well as the end of the International HapMap Project in 2005 provided a GWAS toolbox containing databases of the reference sequence of the human genome and a map of human genetic variation (International Human Genome Sequencing, 2004; International HapMap,

2005). In addition, the emergence of genetic arrays made GWAS-s more accessible and easier to conduct. Two more major GWAS-s were also published (Duerr et al., 2006; Klein et al., 2005). This encouraged the efforts for fine-tuning of the process by increasing the size of the human cohorts used, perfecting the gene arrays and paying greater attention to bias and statistics.

Over the past decade, the initial enthusiasm about GWAS studies has decreased due to the modest causal effects of the identified hits. However, they have been an invaluable source of information about common disease/trait genetics. We now see that common heritable diseases do not follow the same traits of Mendelian diseases but rather depend on thousands of common variants, which each have modest functional effects and contribution to the overall risk in each population.

There are limitations that inevitably come with GWAS-s. For example, most GWAS and sequencing studies so far have focused on individuals of European descent. This can lead to biases and missing knowledge when it comes to risk alleles and variation frequency in the different populations (Martin et al., 2019; Claussnitzer et al., 2020).

Another common limitation is that, due to the modest causality of the identified SNPs, many GWAS-s provide only a hypothesis about the expected function of the reported associations. For example, although thousands of SNPs have already been associated with traits/disease, **relatively few studies have achieved the goal of understanding the genetic, molecular and cellular mechanisms underlying the predisposition**. There have been some success articles (Smemo et al., 2014; Claussnitzer et al., 2015) but the challenges that have to be overcome make these attempts rare.

There has been an effort to map thousands of trait-associated variants to the processes that they regulate and the respective cell types. For example, the GTEx

consortium created a data resource and tissue bank to study the links between genetic variants and gene expression across multiple tissues and individuals. However, even this effort is not sufficient to explain in detail the exact causality between genes and disease association. Therefore, one of the future ambitions in the field would be the development of comprehensive inventories of genotype-phenotype relationships across populations and environments (Consortium et al., 2017; Claussnitzer et al., 2020).

1.6.3 Heritability of human pain sensitivity

The heritability of pain, in the context of GWAS work, has been an area of interest and success has been achieved, especially in high-impact variants, linked to Mendelian traits such as severe pain or congenital insensitivity to pain (Fischer and Waxman, 2010; Reimann et al., 2010; Belfer I, 2013). In the majority of cases, however, chronic pain is a complex trait and its heritability has been estimated to be between 30-57% (MacGregor et al., 2004; Battie et al., 2007; Belfer I, 2013). Understanding these complex, acquired pain phenotypes and the variants associated with them, is still in a state of relative infancy, especially compared to other fields, such as diabetes. Most of the published research has been done in twin studies which tested both experimental pain on healthy individuals and common medical conditions (such as sciatica) (Nielsen et al., 2012; Norbury et al., 2007). Twin studies offer an answer to the common question of "nature vs. nurture" as they usually compare dizygotic twins (who share 50% of their genetic material) and monozygotic twins (who are genetically identical). If we assume that both types of twins experience the same process of "nurture" in their familial environment, then any differences between the two groups in their response to pain experiments, should have a genetic origin ("nature"). Interestingly, the level of heritability has been found to depend on the sensory modality tested, due to the varying genetic components of each trait (Norbury et al., 2007). The distinct molecular

mechanisms underlying the different sensory modalities can also be seen in animal studies, where different inbred strains of mice are tested against the same behavioural paradigms. Such experiments, for example, show that inbred strains differ robustly in their behavioural sensitivity to noxious heat. This phenomenon has been linked to the expression of the Calca gene that codes of CGRPα (Mogil et al., 2005).

The pain heritability level as well as the differences seen between different pain modalities make GWAS work important, but also difficult. This is because of the high number of participants needed to power the studies and the difficulty in phenotyping a subjective perception like pain accurately (Schmid et al., 2019; Zorina-Lichtenwalter et al., 2016). There have been some published GWAS-s in the field, most of which focused on pain-related conditions (Zorina-Lichtenwalter et al., 2016). Taking the approach of using experimental pain methods and applying them on healthy individuals, gives the advantage of reduced bias coming from medication or disease severity, both of which are caveats in GWAS-s with chronic pain patients. To date, no complete GWAS studying human pain sensitivity using experimental pain has been published (Schmid et al., 2019) and this thesis will present some of the results from the first such study, and the validation of the identified significant associations.

1.6.4 GWAS identifies two novel gene targets linked to sensitised pain

As described by Schmid et al. (2019), our laboratory performed a GWAS on the genetic variation in baseline pain sensitivity and nociceptive sensitisation within a group of healthy volunteers from mixed Latin American ancestry. There were two experimental pain paradigms which yielded genome-wide-significant hits: **1.** Wind-up ratio and **2.** Secondary punctate hyperalgesia after mustard oil application. A

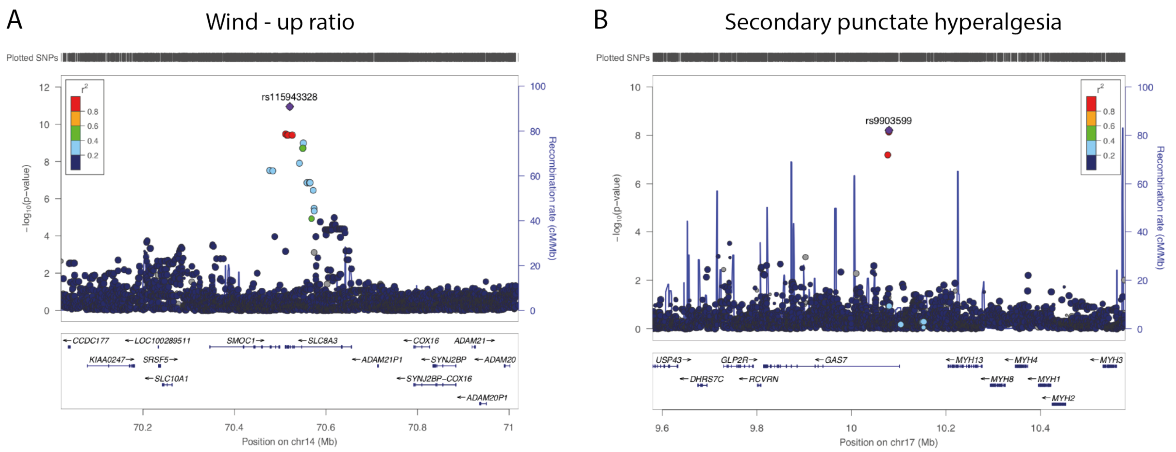


Fig. 1.7 GWAS in healthy participants - main findings.
A and C. Manhattan plots displaying all SNPs with p values exceeding thresholds for genome-wide suggestive (10^{-5}, blue line) or genome-wide significant (5×10^{-8}, red line) hits for each pain experiment. **B and D** Genomic regions showing genome-wide significant SNPs - Chromosome 14 (**B**, gene of interest *SLC8A3*); and Chromosome 17 (**D**, gene of interest *GAS7*). Data are unpublished. For methods and authors Schmid et al. (2019).

detailed description of the methods used in this GWAS can be found in Schmid et al. (2019). The results are yet unpublished but can be seen in (Figure 1.7). We found an association between *SLC8A3* (encoding the sodium-calcium exchanger NCX3) and wind-up, as well as – between *GAS7* (encoding the growth arrest-specific protein 7) and secondary punctate hyperalgesia after mustard oil application.

1.7 NCX3 – a novel target in spinal cord sensitisation and chronic pain

NCX3 is a sodium-calcium bidirectional transporter that effluxes or influxes Ca^{2+} in exchange for Na^{+} in a stoichiometry of 1:3, respectively (Michel et al., 2017). NCX1, 2 and 3 are the three known members of the NCX family of sodium-calcium exchangers, with NCX1 expressed universally, and NCX2 and 3 mainly found in neuronal tissue

and skeletal muscle (Khananshvili, 2014). More information about NCX3 specifically can be found in Chapters 2 and 3.

1.7.1 The domain structure of the NCX family of proteins

Prokaryotic and eukaryotic NCX proteins have been reported by some sources to contain 10 transmembrane helices (TM1-10) (Liao et al., 2012; Marinelli et al., 2014; Ren and Philipson, 2013) while others report 11 TM helices (Giladi et al., 2017)(Figure 1.8A). According to (Giladi et al., 2017), the protein starts with a Kosak-like sequence, which marks the beginning of the open reading frame. This is then followed by a signal peptide (M0) (Figure 1.8A) and 11 transmembrane regions. In addition, eukaryotic NCX proteins have a large cytosolic loop between TM5 and TM6, mainly composed of two Ca^{2+}-binding domains, CBD1 and CBD2 (Hilge et al., 2006). The two CBDs form a two-domain tandem, known as CBD12, with a short linker between the two domains (Figure 1.8B). X-ray crystallography has shown that CBD1 and 2 are very similar in structure, containing seven antiparallel β-strands (Hilge et al., 2006; Besserer et al., 2007; Nicoll et al., 2006). CBD1 has four Ca^{2+}-binding sites, important for Ca^{2+} sensing. In contrast, CBD2 varies in the number of Ca^{2+}-binding sites, depending on the specific ortholog and splice variant.

For example, NCX3 has six splice variants found in humans (Quednau et al., 1997; Lindgren et al., 2005) and two in mice (Michel et al., 2014). The two isoforms in mice (Figure 1.8C) are derived from the alternative splicing of the exons A, B and C, with A and B being mutually exclusive. All three exons code for residues within the regulatory intracellular loop. The alternative splicing leads to the production of **NCX3-AC** and **NCX3-B**(this topic will be revisited in Chapter 3). The first one is found mainly in skeletal muscle, whereas the second has been shown in the brain (Quednau et al., 1997;

Michel et al., 2014). NCX3-AC shows a higher capacity for Ca^{2+} transport and higher sensitivity to changes in intracellular [Ca^{2+}] in comparison to NCX3-B (Michel et al., 2014). The authors suggest that this is due to a high affinity Ca^{2+}-binding site in CBD2 of NCX3-AC, which "senses" Ca^{2+} at a lower concentration in comparison to the lower affinity binding sites of NCX3-B (Michel et al., 2014). Another CBD2-linked effect is the [Na^{+}]-dependent inactivation of the transporter, which is much more prominent in NCX3-B.

Importantly, the wide-range of Ca^{2+}-sensing machinery is modulated by alternative splicing of CBD12, which makes NCX proteins highly versatile sensors. In addition, small changes in the DNA sequence of different splice variants can lead to dramatic differences in function. For example, a point mutation in NCX3-B at position 580 (E580K) recapitulated the functional properties of NCX3-AC regarding Ca^{2+}-sensitivity, possibly through a structure stabilization of the Ca^{2+}-binding site. Interestingly, due to the splice variant specificity of the CBD, drugs can be designed to target the respective isoform and can also be designed to either enhance NCX activity (by domain stabilisation) or inhibit the protein (by disrupting specific interactions between the two CBDs) (Khananshvili, 2014; Giladi and Khananshvili, 2013).

1.7.2 Regulatory pathways affecting the function of the NCX family of proteins

ATP

ATP is usually not required for Ca^{2+} extrusion by NCX and Na+/Ca2+ exchange can be seen in ATP-depleted cells (Blaustein and Santiago, 1977; Blaustein and Hodgkin, 1969). Nevertheless, ATP can modify the exchanger kinetics (Blaustein and Santiago, 1977), most likely through a phosphorylation mechanism (Dipolo, 1974,

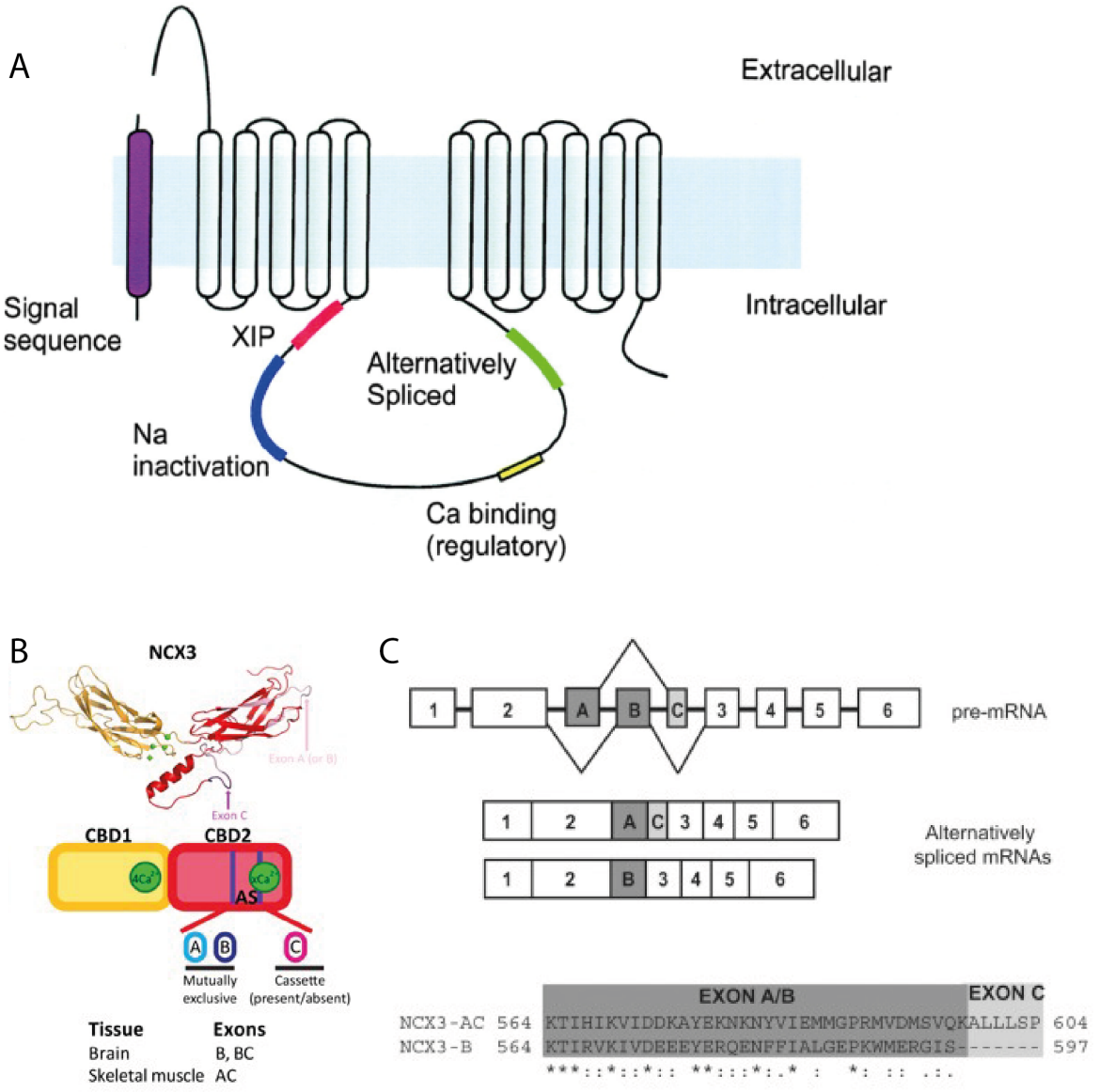


Fig. 1.8 Domain structure of NCX3.
A. Schematic describing the domain structure of the NCX protein – transmembrane domains are shown in light blue, as well as the XIP domain, the Na-inactivation region, the Ca^{2+} -binding site and the alternatively spliced region. **B**. Schematic showing the structure and alternative splicing of NCX3 – CBD12 and its calcium binding sites; C. Schematic describing NCX3 splice variants – NCX3-AC (expressed mainly in muscle tissue) and NCX3-B (expressed mainly in neuronal tissue). (adapted from (Michel et al., 2014; Giladi et al., 2017; Blaustein and Lederer, 1999; Nicoll et al., 1990).

1976). For example, studies like (Baker and Glitsch, 1973) showed that ATP promotes Na^+-dependent Ca^{2+} extrusion. This process was demonstrated to be mediated by a Ca^{2+}-dependent phosphorylation (DiPolo and Beauge, 1987).

MAPK-cascade and calmodulin

NCX proteins have been shown to interact with various kinases which could be another regulator pathway. For example, in experiments with NCX3-transfected PC12 cells both ERK1/2 and p38, activated by NGF, led to NCX3 upregulation and gain of function (Sirabella et al., 2012). In addition, other studies have demonstrated that calmodulin could also have an effect on NCX proteins. Pull-down experiments as well as mutations in the cytoplasmic loop of NCX1 have been used to show interaction and functional changes dependent on calmodulin (Chou et al., 2015).

Ion-transport systems – allosteric effect mediated by ions

In addition to this, kinetic modulation is mediated by Ca^{2+}, Na^+ and H^+ ions. For example, in cardiomyocytes, NCX-mediated ion-currents are elevated ~25-fold when the cytosolic Ca^{2+} level rises from 0.1 to 2 μM (Boyman et al., 2011). This effect is thought to be mediated by high-affinity Ca^{2+} sites on CBD1, which are the main Ca^{2+} sensor (Khananshvili, 2014).

The NCX protein is also very sensitive to cytosolic pH. One hypothesis with regards to cardiac function is that the CBDs may also sense proton concentration. Under acidosis/ischaemia, the interaction between H^+ ions and CBDs may lead to decreased Ca^{2+} affinity and therefore NCX inactivation (Boyman et al., 2011).

The role of NCX3, both in health and injury, as well as specifically in the context of pain, will be discussed in detail in Chapter 2 and 3.

1.8 Gas7 – a novel target in spinal cord sensitisation and chronic pain

Gas7 is a member of the Gas family of proteins which are functionally linked to growth arrest. It was first discovered in growth-arrested NIH3T3 cells (Brenner et al., 1989) where Gas7 was shown to induce the outgrowth of cellular processes via an F-actin-dependent mechanism. More, specific information about Gas7, as well as hypothesis for its possible link to structural changes with the central nervous system, can be found in Chapter 4.

1.8.1 The Gas family of proteins

The cell cycle concept was introduced in 1953 (Howard A, 1953). The state of cell resting, or quiescence is also known as growth arrest (GO phase). This phase is distinguished from the G1 phase of cell proliferation by the regulation of a variety of genes. For example, during G1, various growth factors, growth factor receptors and oncogenes (such as c-fos) are overexpressed. This prompted the realisation that there are specific genes that characterise the G0 phase and such genes are usually negatively regulated by culture serum and growth factors. These genes are termed Growth-arrest-specific (Gas) genes and are differentially expressed by quiescent cells that enter the G0 phase during serum deprivation or confluency (Schneider et al., 1988; Brenner et al., 1989). There are several different genes which belong to this family based on similarities in their function. For example, Gas1 blocks the transition from G0 to G1 in fibroblasts (Del Sal et al., 1995). Gas2 is associated with microfilaments and is involved in the rearrangement of the cytoskeleton during the G0-to-G1 transition (Brancolini et al., 1995). Another gene, Gas3, is also known as PMP22 and plays a

role in the proliferation and differentiation of Schwann cells (Zoidl et al., 1997). Point mutations in this gene have been linked to changes in the apoptotic behaviour of NIH-3T3 cells and a hereditary demyelinating neuropathy, known as Charcot-Marie-Tooth type 1A (Fabbretti et al., 1995). Another Gas gene, Gas6 has also been linked to cell survival and reduced apoptosis (Bellosta et al., 1997). Gas9, on the other hand, has been studied in relation to embryogenesis (Pledger et al., 1977; Schatteman et al., 1992), reviewed by (Lazakovitch et al., 1999).

1.9 Summary and aims

In summary, chronic pain is a significant source of suffering for patients and the existing treatments are insufficient, and in many cases, lead to serious adverse effects. We performed a GWAS using experimental pain protocols in a group of healthy volunteers. This work associated *SLC8A3*(encoding the sodium-calcium exchanger 3, NCX3) with temporal summation (wind-up ratio), and *GAS7*(encoding growth arrest-specific protein, GAS7) with secondary, punctate hyperalgesia after mustard oil application.

The aim of this thesis was to validate the targets, found through our GWAS, using a series of anatomical and behavioural experiments in global knock-out mice. The identified mouse phenotypes were then studied further and here, we report the possible mechanisms underlying our observations. Therefore, this work reveals the process of back-translating human genetics data and highlights the importance of combining GWAS and pre-clinical, animal testing in the search for novel therapeutic targets.

Chapter 2

Slc8a3 - anatomy and modulation of pain behaviour in the mouse

As discussed in Chapter 1, the peripheral information about noxious and innocuous stimulation travels from its detection point in the skin, through the dorsal root and trigeminal ganglia, to the central nervous system (spinal cord and brain). The brain then processes the signals it receives and relays them back to the spinal cord, creating a dynamic and adaptable circuit.

This chapter will discuss the first GWAS-identified target – *Slc8a3* (encoding the sodium-calcium exchanger 3, NCX3) and will provide evidence for its expression in the pain circuit. In addition, this chapter will provide data for the behavioural impact of the *Slc8a3* global knock-out (KO) in mice.

2.1 Introduction

2.1.1 Anatomy overview – approaches for studying *Slc8a3* expression in the DRG and dorsal horn of the spinal cord

The dorsal root ganglia

As discussed above, the simplest classification of DRG neuron sub-populations on physiological grounds is into LTMRs (broadly associated with detecting touch and proprioception), nociceptors (responsible for the transmission of noxious stimuli) and thermoceptors.

The Aβ fibers are light-touch mechanoreceptors and belong to the group of LTMRs, together with Aδ and C-LTMRs which also exhibit low activation thresholds. In this population of neurons, the myelinated ones (Aβ and some Aδ) are marked by neurofilament heavy chain 200 (NF200), while tyrosine hydroxylase (TH), in the rodent, is used to stain for C-LTMRs, associated with pleasant touch.

The group of nociceptors includes Aδ and C-fibers. They detect noxious stimuli and therefore are optimally activated by strong, threatening stimulation. Nociceptors are classified as peptidergic (often marked by calcitonin gene-related peptide CGRP) and non-peptidergic (expressing isolectin-B4, IB4) (Gascon and Moqrich, 2010; Willis W.D, 1991). As explained in Chapter 1 (Section 1.2.3), the peptidergic population is linked to mechanical and thermal sensations (Cavanaugh et al., 2009), while the IB4-positive, non-peptidergic neurons are mainly mechanical nociceptors (Zylka et al., 2005; Cavanaugh et al., 2009). It is important to highlight that the exact function of each neuron depends on its specific neurochemical make-up, as well as the environment surrounding it. Additionally, the markers that currently exist, do not select for homogeneous

populations and also mark overlapping populations. For example, the NF200-positive neurons can overlap with CGRP-positive ones to some extent – these are likely to be Aδ nociceptors. In addition, the IB4-positive neurons can also overlap with CGRP-positive cell bodies. This depends on species, as well as the differences between dorsal root and trigeminal ganglia (Price and Flores, 2007).

Spinal cord - interneurons

The neuronal sub-populations in the spinal cord are broadly classified into interneurons and projection neurons. The former form their synapses locally, usually within the lamina they reside in (Battaglia, 2016). They make up the majority of neurons in the superficial and deep laminae of the dorsal horn (Todd, 2010). Given the complexity of the region, this would mean that there are many sub-groups of interneurons, which are different neurochemically, morphologically and functionally. The main distinction so far is between inhibitory (with GABA and/or Glycine as major neurotransmitters) and excitatory interneurons (which use Glutamate). Common markers for the inhibitory population are GAD and the GlyT2 transporter. These neurons are mainly seen in laminae I-III, with GlyT2 expression largely in lamina III (Zeilhofer et al., 2012). Excitatory interneurons are marked mainly by VGLUT2, with some cells in lamina III expressing low levels of VGLUT3 (Todd et al., 2003; Battaglia, 2016). In this chapter we used mouse lines, carrying the fluorescent protein eGFP either in excitatory, glutamatergic neurons (VGLUT2-eGFP mice, (Gong et al., 2003)), inhibitory, GABAergic neurons (GAD67-EGFP mice (Tamamaki et al., 2003)) or inhibitory, glycinergic neurons (GlyT2-eGFP mice (Zeilhofer et al., 2005)). There are three types of VGLUT transporters – VGLUT1, 2 and 3. The first transporter is detected mainly in presynaptic terminals of myelinated LTMRs projecting into the deep laminae of the rat dorsal horn (Alvarez-Erviti et al., 2011). VGLUT3, on the other hand, appears to be expressed by C-LTMRs, terminating in lamina II (Larsson

and Broman, 2019). Of the three transporters, VGLUT2 is the one that shows strong neuronal expression and is considered to mark a large proportion of the excitatory interneurons in the spinal dorsal horn (Oliveira et al., 2003; Alvarez et al., 2004). The inhibitory markers GlyT2 and GAD67 are also very well established. GABA signals fast inhibition through chloride influx throughout the mammalian CNS, whereas Glycine is limited to the spinal cord and brainstem (Zeilhofer et al., 2005). Overall, these three mouse lines have been extensively used and have been found reliable in differentiating between inhibitory and excitatory interneurons.

Spinal cord - projection neurons

The second group of dorsal horn neurons, as described above, includes the spinal projection neurons which, broadly speaking, relay signals from the spinal cord to the brain. These neurons are found in lamina I of the dorsal horn, as well as deeper laminae III-V. One way to mark them is by staining for neurokinin 1 receptor (NK1R). As (Todd, 2002) has shown, this protein is expressed by roughly 80% of all projection neurons. Notably, the search for a strong projection neuron marker continues and other methods, such as *in-situ* hybridisation have been used. For example, the gene which codes for NK1R, *Tac1*, marks 57.3% of all spinoparabrachial (SPB) projection neurons. Another strong marker, *Gpr83*, was recently discovered (Choi et al., 2020) and the authors reported that in combination with *Tac1*, it labels almost 90% of all SPB projection neurons. In this study we used *Lypd1*, reported by (Haring et al., 2018),which has been shown to mark SPB projection neurons better than Tac1 alone.

As mentioned previously, this chapter aimed to study the expression of the *Slc8a3* mRNA in DRG and spinal cord, as well as to provide behavioural evidence for the role of NCX3 in pain. While there is little published data about NCX3 in the somatosensory system, there is a lot of general information on this particular exchanger, as well as the family to which it belongs(as discussed in Chapter 1, Section 1.7).

2.1.2 NCX3 - functional characteristics

NCX3 is a sodium-calcium bidirectional transporter that effluxes or influxes Ca^{2+} in exchange for Na^{+} in a stoichiometry of 1:3, respectively (Michel et al., 2017). NCX3 is one of three proteins that belong to the NCX family of sodium-calcium exchangers, together with NCX1 and NCX2. Their main role is to use the electrochemical gradient of Na^{+} to catalyse Ca^{2+} extrusion from the cytosol or organelle matrix (Blaustein and Lederer, 1999; Philipson and Nicoll, 2000; Khananshvili, 2013). However, depending on the electrochemical gradient, the transporter can change its directionality and instead of the usual Ca^{2+} efflux, it can function in reverse and transport Ca^{2+} into the cell. This effect can be important in both physiological and pathophysiological conditions (Blaustein and Lederer, 1999; Bers, 2002).

As mentioned in Chapter1, the expression of the three exchangers, from the NCX family, is tissue-specific with NCX1 being universally expressed, whereas NCX2 and 3 are mainly found in skeletal muscles and neuronal tissues (Khananshvili, 2014).

Functional characteristics of NCX3

NCX3 is involved in Ca^{2+} homeostasis and thus has a role in various systemic functions including neuronal development (Boscia et al., 2013), memory (Molinaro et al., 2011), immune response (Staiano et al., 2009) and stress handling (Pannaccione et al., 2012). NCX3 KO mice have normal gross cytoarchitecture of neurons, astrocytes and oligodendrocyte precursor cells (OPCs) (Molinaro et al., 2011). However, they show hypo-myelination, augmented OPC markers and a significant reduction in spinal cord size (Boscia et al., 2013).

In the context of pain, NCX3 is poorly studied. Its expression and role in the DRG is also debated with some authors (Verdru et al., 1997; Lu et al., 2006; Scheff et al., 2014) showing that general NCX activity is observed in the DRG, while others found

no NCX role in the cell bodies or their peripheral and central terminals (Werth and Thayer, 1994; Gover et al., 2007; Wan et al., 2012; Shutov et al., 2013).

2.1.3 Aims and hypotheses

Notably, NCX3 has not yet been studied in relation to pain sensitisation. Previous studies have only focused on peripheral sensory neurons and not considered a role in dorsal horn neurons. In fact, there is little published information about the expression of NCX3 in the spinal cord. However, given that our GWAS associated NCX3 with wind-up (a central phenomenon whose mechanism has been studied in depth and is linked to Ca^{2+} handling), we hypothesised that NCX3 would likely be expressed in the spinal cord, especially in regions and neurons linked to the processing of noxious stimuli. We also hypothesised that the deletion of NCX3 would cause a behavioural phenotype in KO mice, and that this phenotype might be related to sensitised pain.

2.2 Materials and Methods

2.2.1 Histology - Tissue preparation

For our immunohistochemistry and *in-situ* hybridisation experiments, we used both male and female naïve C57Bl/6J mice, aged between 8 and 16 weeks. Mice were overdosed with pentobarbital and perfused transcardially with room temperature sterile saline, followed by 10-15mL 4% paraformaldehyde (PFA). Once dissected, the DRGs were post-fixed in 4% PFA for 2 hours at room temperature, while the spinal cords were post-fixed for 24h at 4^{o}C. All tissue was dehydrated for cryoprotection in 30% sucrose at 4°C for 4-5 days. Optimal cutting temperature (OCT) medium (Tissue-Tek) was then used to embed the dissected tissue and allow for -80°C storage. Sections were

cut on a cryostat (14μm for DRG, 30μm for spinal cord) and stored at -80°C. Tissue preparation for *in-situ* hybridisation (multiplex) was different and is specified below.

2.2.2 Immunohistochemistry and *in-situ* hybridisation

Immunohistochemistry

For immunohistochemistry, DRG and spinal cord sections were washed in PBS and PBS Triton-X (0.3%), before being incubated overnight at room temperature with the respective primary antibodies diluted in PBS/Triton as stated in (Table 2.1). This was followed by washing in PBS/Triton and incubation for 2 hours at room temperature with the secondary antibodies, as stated in (Table 2.1). The tissue was then washed again and cover-slipped. Immunostaining was visualized using a confocal microscope (Axio LSM 700, Zeiss) and images were acquired using the Zen black software.

In-situ hybridisation

For *in-situ* hybridisation (singleplex), we used the RNA Scope 2.5 Red chromogenic assay kit (Biotechne, 322350) and followed manufacturer instructions. Briefly, after -80°C storage, tissue was allowed to reach room temperature and was then washed with PBS. Next, tissue was pre-treated with hydrogen peroxide at room temperature (10-minute pre-treatment for DRG, no pre-treatment for spinal cord) and protease at 40°C (10-minute protease treatment for DRG, 15minutes for spinal cord). Slides were then incubated with the respective probe for 2 hours at 40°C. mRNA probes used for this experiment are stated in (Table 2.1). Probe incubation was then followed by six amplification steps, with *Amplification 5* lasting 30 minutes for DRG samples and 15 minutes for spinal cord tissue. All other amplification steps were performed as per manufacturer's instructions. The development stage of the protocol involved a fast red reaction, which was also tissue-dependent: 7 minutes for DRGs and 10 minutes for

spinal cords. Any modifications to the protocol were optimised to reduce background staining and improve signal. ISH was followed by immunohistochemistry, where the standard protocol described above was used. Staining was visualised with the confocal microscope and images were acquired using the Zen black software.

For *in-situ* hybridisation (multiplex), we used RNA Scope Multiplex Kit V1 (Biotechne, cat number: 320851). This protocol was performed on fresh frozen tissue and the manufacturer's instructions were followed. For tissue preparation, the spinal cords were dissected using hydraulic extrusion as explained by (Richner et al., 2017). Tissue was then quickly placed on a frozen metal plate on dry ice. After freezing, the spinal cord was transferred to a cold Eppendorf tube and stored at -80°C. A cryostat was used for tissue cutting, where the spinal cords were left to equilibrate to -20°C and were then covered with OCT. We used 12-15μm section thickness and kept the tissue as cold as possible throughout the preparation procedure. Sections were then stored at -80°C on slides. Following tissue preparation and storage, the tissue was immediately post-fixed with 4% PFA for 15min at 4°C. Then the slices were dehydrated and treated with probes and amplification buffers as per manufacturer's instructions. Staining was visualised with confocal microscope and images were acquired using the Zen black software.

Image analysis

Analysis of the signal intensity for *in-situ* hybridisation studies on DRG was calculated using ImageJ. In a single image of a section of either L4 or L5 DRG, neurons were circled and the percentage coverage of red *Slc8a3* mRNA signal for that cell profile area was calculated. Each cell was subpopulation-defined by eye using the counterstain against NF200, IB4, CGRP or TH. For each marker at least 3 sections were imaged per animal. A background reading was performed for each image, using an unstained

area. The mean intensity per animal was calculated to account for any background measurement.

For spinal cord sections, mRNA positive cells were defined as those containing 3 or more red dots co-localising with each eGFP-marked cell (either GlyT2-eGFP, GAD67-eGFP or VGLUT2-eGFP). The total number of eGFP+ cells as well as the number of eGFP+/NCX3+ was counted. Double positive cells were expressed as a percentage of eGFP+ neurons.

2.2.3 Western blot

For Western blot analysis of mouse spinal cords (WT vs HOM), we performed tissue lysis in RIPA lysis buffer with added protease inhibitor (Roche). The protein concentration of the lysate was determined using a BCA Protein assay kit (Thermo Scientific). We used 10μg protein and separated it on a 10% Mini-PROTEAN TGX Precast Gels (Biorad) before transferring it onto a nitrocellulose membrane (Biorad). The membranes were then washed with PBS-Tween (0.1%) and blocked with 5% milk (non-fat milk powder diluted in PBS) for 1 hour at room temperature. This was followed by incubation with primary antibody (anti-NCX3, Swant) overnight at 4°C. Membranes were blocked with 5% milk and incubated with primary antibody overnight at 4°C. As described in (Table 2.1), primary antibody was used at 1:1000 and diluted in PBS-Tween (0.1%). After primary antibody incubation, the membrane was washed and incubated with an anti-rabbit horseradish peroxidase-conjugated secondary antibody (1:5000, Fisher Scientific) for 1 hour at room temperature. The membrane was then developed using an ECL-Plus Western Detection reagents (GE Healthcare). We used anti-GAPDH primary antibody (Abcam 1:1000) and anti-mouse secondary (1:10000, Fisher Scientific) as a loading control.

2.2.4 Mouse line and animal housing

All procedures were carried out in accordance with UK home office regulations. Animals were housed in IVCs and their welfare was continuously assessed throughout all procedures. The temperature and humidity of the rooms were monitored at all times and food and water were freely available. NCX3 KO mice, $Slc8a3^{tm1Sso}$, were generated and have been previously described by (Sokolow et al., 2004). Heterozygous mice were bred together to obtain NCX3 WT (control group), NCX3 HET (experimental group) and NCX3 HOM (experimental group) littermates. Both male and female adult mice were used for behaviour studies. No animals were excluded from the cohorts outlined below. Methods for statistical analyses are described below. We report this mouse line and our experiments according to the ARRIVE guidelines (Percie du Sert et al., 2020).

2.2.5 Behavioural procedures

At the start of each set of behavioural experiments, mice, aged 8-10weeks, were acclimatised to the testing equipment for 2-3 days prior to each test. For motor and acute sensitivity tests, baseline values were obtained by averaging data from 3 experimental sessions. For most behavioural experiments, we used the following two cohorts: **1st cohort**: 5WT ($n_{females}$=2, n_{males}=3), 9 HET ($n_{females}$=4, n_{males}=5) and 4 HOM ($n_{females}$=3, n_{males}=1); **2nd cohort**: 11 WT ($n_{females}$=5, n_{males}=6), 2 HET (n_{males}=2), 9 HOM ($n_{females}$=6, n_{males}=3) which brings the total of mice to 16 WT, 11 HET, 13 HOM. Hot plate at 50^{o}C was performed with a **3rd cohort** of mice – 5 WT ($n_{females}$=2, n_{males}=3), 5 HET ($n_{females}$=2, n_{males}=3),5 HOM ($n_{females}$=2, n_{males}=3) bringing the total number of animals for this experiment to 21 WT and 16 HET, 18 HOM. All tests were performed in the same room, at similar times of the day, by the same experimenter, who was blind to all animal genotypes and handled the mice in a

random order. Formalin experiments were performed last and therefore the animals were 20-25 weeks of age and very well acclimatised to the room and researcher.

Open field

For the open field test, a black box displaying a grid system on the floor was used. Mice were acclimatised to it the day before the experiment. Before the start of the test and after every animal, the open field box was wiped with a detergent to remove any scent clues left by previous mice. Each mouse was placed in the top left corner of the box and then allowed to explore the open field uninterrupted for 3 minutes. The number of boxes entered and the rearings performed by each mouse were recorded. The rearing behaviour consisted of animals standing on both hind paws in a vertical upright position. The open field test is usually used for a variety of complex behaviours, including anxiety and motor behaviour (Seibenhener and Wooten, 2015). The experiment was repeated three times, on three consecutive days.

RotaRod

Motor behaviour was assessed using a RotaRod, as described by (Dawes et al., 2018) and reviewed by (Deacon, 2013). Prior to the experiment, mice were trained on the treadmill by being placed on it three times the day before. Each mouse was placed on the rotating bar and the duration the mouse remained on it was measured. The cut-off time was 120seconds. A constant speed of 28rpm was used and the bar was wiped before each new mouse was placed on it.

Beam walk test

Proprioception was assessed using the beam walk test as previously described (Carter et al., 2001). We used a 1m long beam apparatus resting on two poles, 50cm above a tabletop. A black box with bedding material and food was placed at the end of it to attract the mouse. A light source at the beginning of the beam was used as an

aversive stimulus. The mice were placed on the beam three times the day prior to the experiment and were trained to walk to the black box. A video camera was set on a tripod to record the performance of each mouse. The experiment was repeated three times, on three separate days. The number of correct steps, as well as the number of slips and hops was recorded.

von Frey test

Mechanical sensitivity was assessed by applying calibrated von Frey hairs (Ugo Basile) to the plantar surface of the hind paw to calculate the 50% withdrawal threshold (Chaplan et al., 1994). The von Frey hairs are nylon monofilaments which apply different force to the stimulated skin. Mouse behaviour was scored using the up-down method which is a statistical tool to determine the 50% withdrawal threshold through a sequential array of experiments. Using a range of stimuli, we first applied the middle weight, 0.6g, where a negative response increased the next weight applied, and a positive one – decreased it. The resulting pattern of responses was used to select a constant k and determine the final 50% withdrawal threshold (Dixon, 1965). The same experiment was performed on 3 consecutive days and the mean value for each animal was reported.

Pin Prick test

Noxious mechanical stimulus response was assessed using the pin prick test as previously described (Arcourt et al., 2017). Briefly, a pin was attached to a 1g von Frey filament and then applied to the planter surface of the hind paw of each mouse. This test was done 3 times per paw, in three separate days. Videos were recorded with a Samsung mobile phone at 240 frames/sec and then analysed with the video editing programme Avidemux (details in Table 2.1). The latency of withdrawal from the second the pin touched the paw to the pain response was calculated.

Hargreaves test

Thermal sensitivity was assessed using the Hargreaves method (Hargreaves et al., 1988). The mice were acclimatised to small boxes with a glass floor for 2-3 days prior to experiment. On the day of the experiment, a radiant heat source was applied to the plantar surface of the hind paw and the latency to withdrawal was recorded. This was performed 3 times for each paw and was then repeated on three consecutive days.

Hot plate test

Response to a supra-threshold heat stimulus was measured using the hot plate test (Ugo Basile) where each mouse was placed on a metal surface maintained at a constant temperature (50^{o}C or 53^{o}C) as described by (Dawes et al., 2018). The time taken to elicit a nocifensive response (hind paw withdrawal or licking) was recorded. The cut-off time used to prevent tissue damage when no behaviour was observed, was 23 seconds.

Formalin test

The formalin test was performed by an intraplantar injection of 20μl formalin (5% v/v from 37% stock formaldehyde solution (Sigma). Mice were then placed in a Perspex cylinder and observed for nocifensive behaviour, such as biting, licking and paw lifting. The duration of pain behaviour was recorded over a 60-minute period, separated into 12, 5-minute bins. The behavioural response is biphasic and therefore further comparisons were made by pooling data in the first (0-20mins) and second (20-60mins) phases.

Data analysis for behavioural tests

Data are shown as means ± SEM. Statistical tests were carried out in GraphPad prism 9.0 (details in Table 2.1) and the tests used are specified in each legend. All data were tested for normality using visual inspection and the Kolmogorov-Smirnov test. When only two experimental groups were compared, independent t-tests were

performed. When more than two experimental groups were tested, we performed one-way ANOVA with Dunnett's multiple comparisons test. For our Formalin experiment, when analysing behaviour over time, we used two-way ANOVA with Dunnett's multiple comparisons test.

2.2.6 Materials

REAGENT	SOURCE	Dilution	IDENTIFICATION
Primary antibodies			
Sheep anti-CGRP	Enzo Life Sciences	1:400	Cat# BML-CA1137, RRID: AB_2050885
Rabbit anti-CGRP	Peninsula Laboratories	1:1000	Cat# T-4032, RRID: AB_2313775
Isolectin B4 (IB4), conjugated to biotin	Sigma-Aldrich	1:100	Cat# L2140, RRID: AB_2313663
Mouse anti-NF200	Sigma-Aldrich	1:250	Cat# N0142, RRID: AB_477257
Rabbit anti-PAX2	Thermo Fisher Scientific	1:200	Cat# 71-6000, RRID: AB_2533990
Rabbit anti-NCX3	Swant	1:1000	Cat# 95209
Chicken anti-NeuN	Millipore	1:500	Cat# ABN91, RRID: AB_11212808
Sheep anti-Tyrosine Hydroxylase	Millipore	1:200	Cat# AB1542, RRID: AB_90755
Rabbit anti-c-FOS	Synaptic Systems	1:1000	Cat# 226003
Chicken anti-GFP	Abcam	1:1000	Cat# ab13970, RRID:AB_300798
GAPDH	Abcam	1:1000	Cat# ab181602, RRID:AB
Secondary antibodies			
Donkey anti-rabbit IgG Alexa 488	Thermo Fisher Scientific	1:1000	Cat# A-21206, RRID:AB_2535792
Goat anti-rabbit IgG Pacific blue	Thermo Fisher Scientific	1:500	Cat# P-10994, RRID: AB_2539814
Streptavidin Pacific Blue	Thermo Fisher Scientific	1:500	Cat# S11222
Donkey anti-mouse IgG Alexa 488	Thermo Fisher Scientific	1:1000	Cat# A-21202, RRID: AB_141607
Goat anti-mouse IgG Pacific blue	Thermo Fisher Scientific	1:500	Cat# P31582, RRID: AB_10374586
Donkey anti-sheep IgG Alexa 488	Thermo Fisher Scientific	1:1000	Cat# A-11015, RRID: AB_2534082
Donkey anti-rabbit IgG Alexa 546	Thermo Fisher Scientific	1:1000	Cat# A10040 , RRID: AB_2534016
Goat anti-chicken Alexa 488	Thermo Fisher Scientific	1:1000	Cat# 11039, RRIDAB_2534096
Anti-rabbit HRP-conjugated	Fisher Scientific	1:5000	Cat# NA934VS
Anti-mouse HRP-conjugated	Fisher Scientific	1:10000	Cat# NA931VS
Chemicals, Peptides, and Recombinant Proteins			
Formaldehyde solution	Sigma-Aldrich	1:20	Cat#252549
Commercial kits and probes			
RNAscope 2.5 HD Reagent Kit-RED	Biotechne		Cat# 322350
RNAscope® Fluorescent Multiplex Detection Reagent kit	Biotechne		Cat# 320851
RNAscope® Probe- Mm-Slc8a3	Biotechne		Cat# 523681
Experimental Models: Organisms/Strains			
Slc8a3^{tm1Soo}	Sokolow *et al*, 2004		
Software and Algorithms			
ImageJ/Fiji	NIH		https://imagej.nih.gov/ij/index.html, https://fiji.sc/
Prism 9.0	GraphPad Software		https://www.graphpad.com/
Avidemux	Avidemux		https://avidemux.en.softonic.com/mac

Table 2.1 Reagents used in Chapter 2.

2.3 Results

2.3.1 Anatomical studies showed expression of NCX3 (*Slc8a3* mRNA) in the dorsal root ganglia and the spinal cord

We started this project by performing *in-situ* hybridisation staining for *Slc8a3* mRNA. This was then followed by immunofluorescence for the above-mentioned DRG markers (NF200, CGRP, IB4 and TH). We observed co-localisation with all 4 of them, but the intensity of the *Slc8a3* staining was much higher in the NF200-positive (intensity 54.6±10.3 units) and NF200/CGRP-positive populations (44.4±7.6 units), showing a much stronger co-localisation and more *Slc8a3*-positive punctae per cell. By contrast, the TH, IB4 and CGRP populations were weakly stained, showing fewer *Slc8a3*-positive punctae in each cell – 22.2±3 units, 21.9±1.3 units and 19.05±3 units, respectively (Figure 2.1A and B). These results use arbitrary units, where cells with a completely negative background showed intensity of 1.2±0.2. Therefore, the *Slc8a3* mRNA expression was present in all tested populations but was much more pronounced in large, myelinated LTMRs – A$\beta$and Aδ, stained with NF200 and NF200/CGRP. Interestingly, our immunohistochemistry results also pointed to membranous localisation of the NCX3 protein in the larger-diameter primary sensory neurons (Figure 2.1C).

The significant clinical association between wind-up and *Slc8a3*, and its reported expression in the human CNS, prompted us to investigate its anatomical expression using naïve C57Bl/6 mice. *In-situ* hybridisation of the spinal cord revealed that around 65% of all NeuN positive neurons co-localised with *Slc8a3* in the superficial laminae. This co-localisation was even stronger in the deeper laminae where around 80% of the neurons also expressed *Slc8a3* (Figure 2.1D and E).

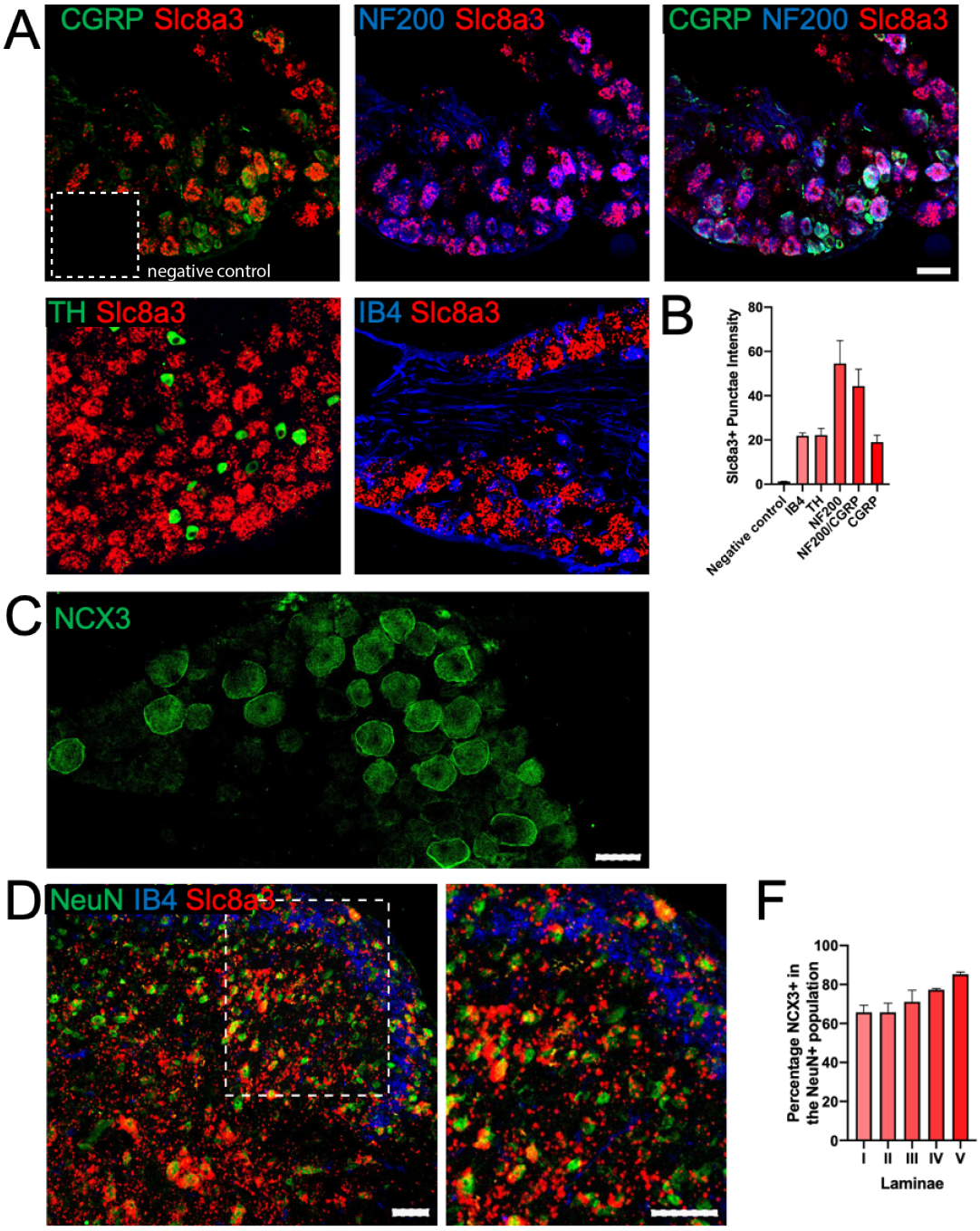


Fig. 2.1 *Slc8a3* is expressed in DRG neurons and the spinal cord.
A. Representative images of *Slc8a3* in-situ hybridisation combined with immunofluorescence for DRG neuronal markers (IB4, CGRP, NF200 and TH). **B**. Quantification of the images from **A** - data were quantified as average intensity (AU) of *Slc8a3* mRNA punctae in different populations of DRG neurons from WT L4 and L5 dorsal root ganglia (3 images per animal, n=5 animals). **C**. Representative image showing immunohistochemistry against the NCX3 protein **D**. Representative image of *Slc8a3 in-situ* hybridisation combined with immunofluorescence for NeuN (green) and IB4 (blue). **D**. Quantification of the data from **D** – percentage of *Slc8a3*-positive cells in the NeuN-positive neuronal population in laminae I to V in the spinal dorsal horn (3 images per animal, n=3 animals). Data are mean ± SEM. Scale bar = 50 μm.

2.3.2 *Slc8a3* mRNA expressed in all tested interneuronal populations and found in projection neurons

Next, we focused on the types of neurons that co-localise with *Slc8a3* mRNA. We used three mouse lines, carrying the fluorescent protein eGFP either in excitatory glutamatergic neurons (vGluT2-eGFP mice (Gong et al., 2003)), inhibitory GABAergic neurons (Gad67-EGFP mice (Tamamaki et al., 2003)) or inhibitory glycinergic neurons (GlyT2-eGFP mice (Zeilhofer et al., 2005) (gift from Prof H. Zeilhofer's laboratory, University of Zurich). There was no specific preference for *Slc8a3* expression in either excitatory or inhibitory neurons; *Slc8a3* expression was identified in 91.4±5% of the GlyT2 population; 68.8±7% of the Gad67 population, and 69.1±6% of the vGlut2 population (Figure 2.2A-C and E).

Another way to mark inhibitory interneurons in the spinal dorsal horn is staining for PAX2. This protein has been shown to be expressed by all inhibitory interneurons in laminae I-III (Foster et al., 2015; Larsson, 2017). Due to the *in-situ* hybridisation process prior to immunofluorescence, achieving high quality PAX2 staining was challenging. This might explain why a smaller overlap between antibody staining for PAX2 and *in-situ* hybridisation for *Slc8a3* was observed (40±9% for superficial laminae and 45±9% for deeper laminae, Figure 2.2D and E).

Next, we explored the expression of *Slc8a3* in *Lypd1* positive dorsal horn neurons (a marker of parabrachial projection neurons, as explained in Subsection 2.1.1). and reported by (Haring et al., 2018). We used multiplex *in-situ* hybridisation for *Slc8a3* and *Lypd1* mRNA. We observed co-localisation in both superficial and deep laminae, suggesting the presence of *Slc8a3* in projection neurons in the dorsal horn (Figure 2.3).

In summary, our DRG data suggested that *Slc8a3* was predominantly expressed in peripheral neurons representing low threshold mechanoreceptors and less so in

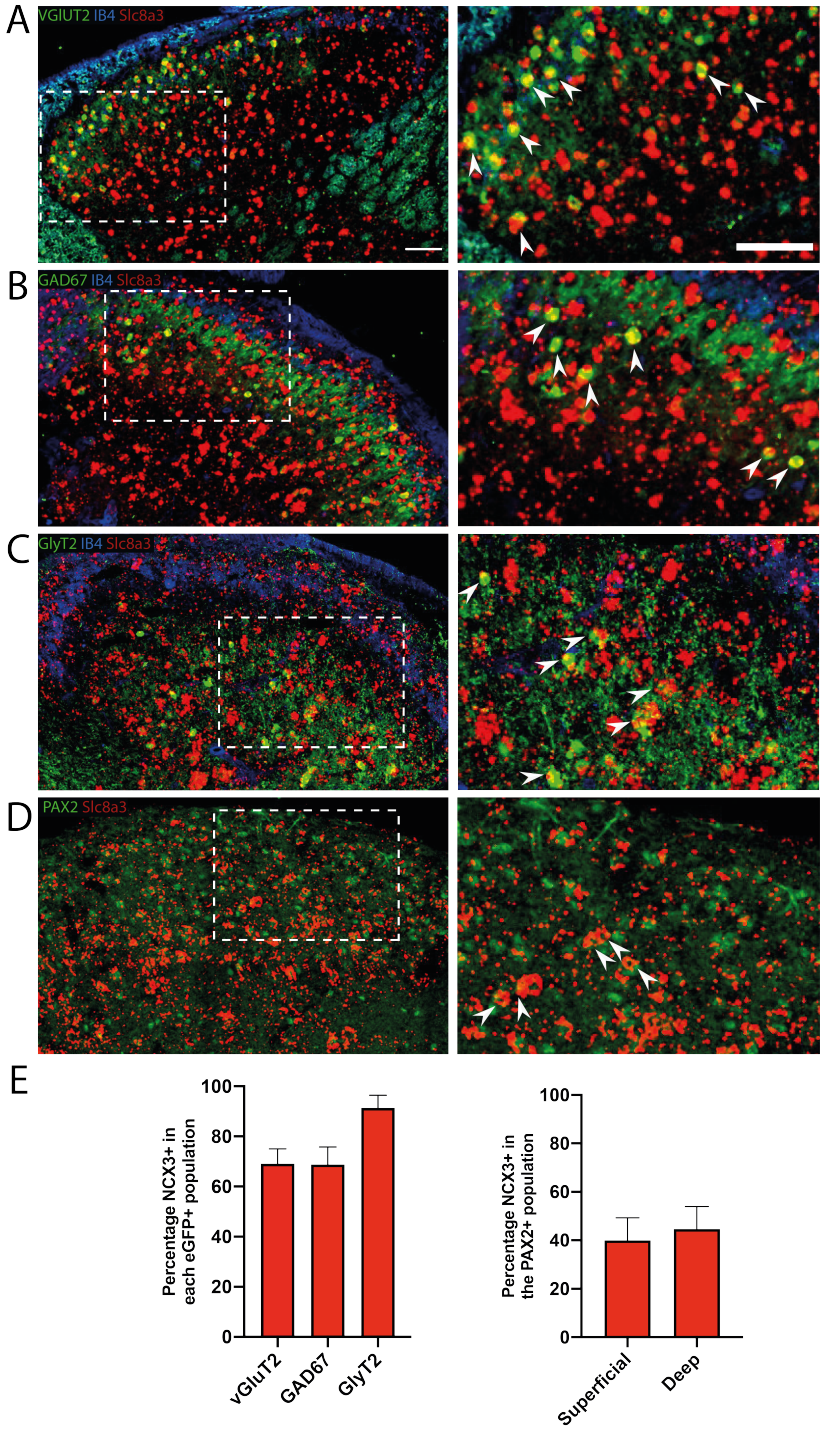


Fig. 2.2 *Slc8a3* mRNA co-localises with both excitatory and inhibitory spinal cord interneuron markers.
A-D. Representative images of *Slc8a3 in-situ* hybridisation (ISH) combined with immunofluorescence for interneuron markers in the spinal cord (GAD67-eGFP, GlyT2-eGFP, vGluT2-eGFP and PAX2). Left panels show magnified inserts **E.** Quantification of the images from **A** - data were quantified as percentage of *Slc8a3*-positive cells in the eGFP-positive or PAX2-positive populations (3 images per animal, n=3 animals). Data are mean ± SEM. Scale bar = 50 μm.

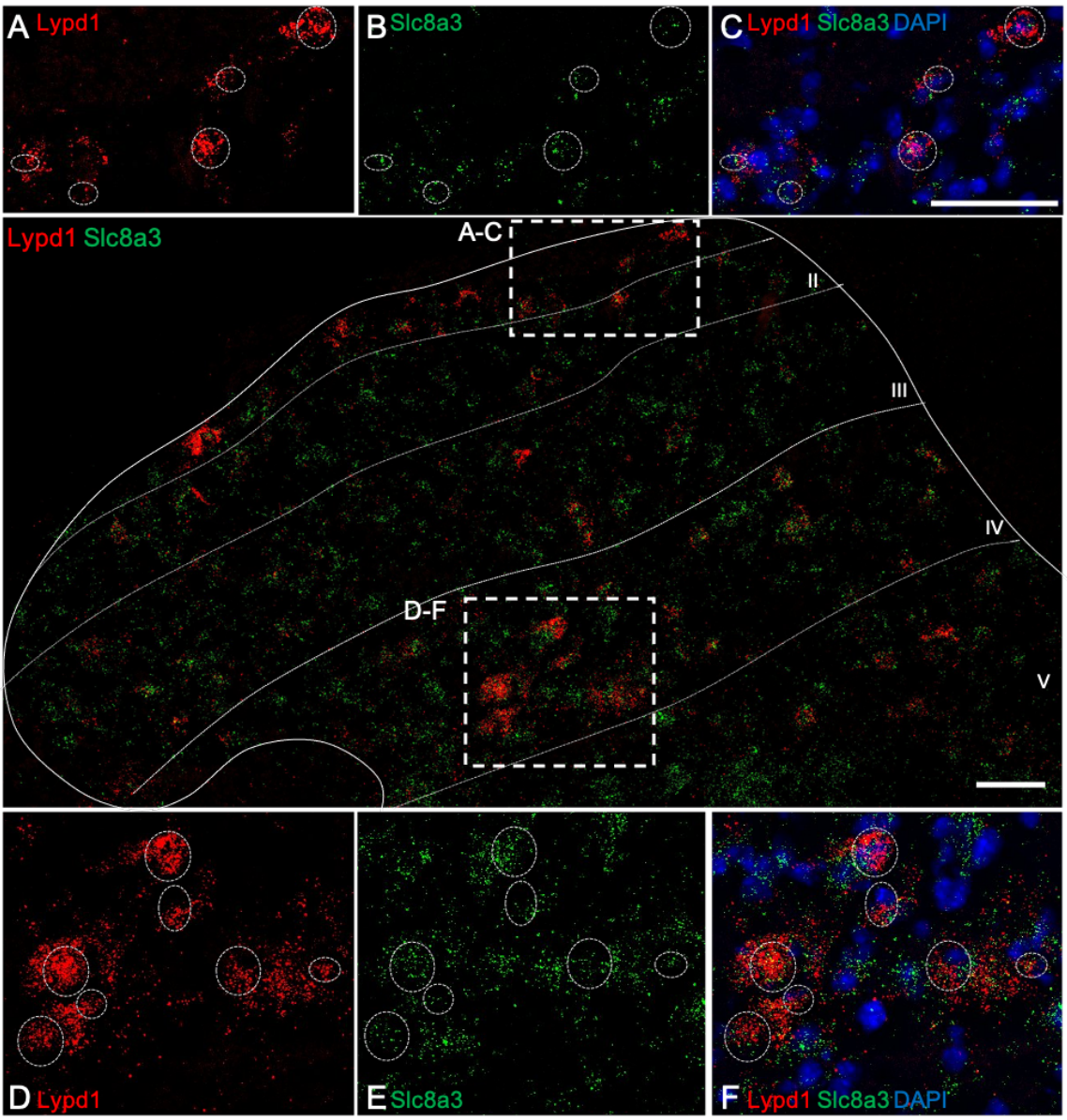


Fig. 2.3 *Slc8a3* mRNA co-localises with projection neuron marker *Lypd1*. **Central panel** – representative image showing multiplex ISH for *Slc8a3* and *Lypd1* mRNA in the spinal dorsal horn. **A-C.** Magnified panels showing co-localisation in the superficial laminae. **D-F.** Magnified panels showing co-localisation in the deep laminae. Scale bar = 50 μm.

nociceptive afferents. In contrast, the spinal cord showed significant expression in the superficial laminae, as well as the projection neurons of the anterolateral tract, which are linked to nociceptive transmission. This, together with the genome wide association of NCX3 with wind-up (a central phenomenon), led us to hypothesise that the target had its predominant action in the dorsal horn, and therefore would be involved in modulating pain behaviour.

2.3.3 NCX3 knock-out mice show normal motor and acute pain-related behaviour but hypersensitivity to the second phase of the formalin test

To test our hypothesis that NCX3 may modulate pain behaviour, we used a global knock-out mouse line (gift from A. Herchuelz's laboratory, University of Brussels). The mouse line was generated and previously validated by (Sokolow et al., 2004)). The KO was achieved by inserting a Neomycin cassette in exon2 of the *Slc8a3* gene. This part of the gene was identical in both known mouse splice variants and is also upstream to the sequence that differentiates them from each other. Therefore, the KO strategy is expected to disrupt both isoforms. In addition, the stop codon at the end of the Neo cassette is expected to terminate the production of mRNA and prevent functional mRNA and protein generation. This was confirmed by Western blot (Figure 2.4B) where the NCX3 band, at around 90kDa, was completely missing in the KO animals.

Next, we performed behavioural experiments in wild-type (WT) versus heterozygous (HET) and homozygous (HOM) NCX3 knock-out mice.

Experiments were performed for motor, mechanical, thermal as well as acute and sensitised pain behaviours. We did not observe significant differences in the open field (76.4±5.1 boxes entered by WT mice, 81.28±7.4 (HET), 95.2±5.2 (HOM)),

rotarod (46±9.14s (WT), 44.7±10.9 (HET) and 54.6±12.3 (HOM)) or beam walk test (86.4±3.2 for WT, 87.16±2.16 for HET and 93.6±1.5 for HOM) (Figure 2.4C-F). Acute mechanical behavioural tests were also not significantly different (Figure 2.4G and K); von Frey hairs showed 50% thresholds at 0.5±0.03g for WT, 0.51±0.03g for HET and 0.49±0.05g for HOM animals. We also saw no significant difference in the response to noxious pinprick (WT 228.1±19.2ms, HET 187.4±24,4ms, HOM 195.9±23.5). Similarly, thermal thresholds were comparable among groups (Figure 2.4H-J): Hargreaves (WT 9.9±0.6s, HET 9.1±0.7s, HOM 8.9±0.5s); hot plate at 50°C (WT 17.3±0.4s, HET 16.6±0.74s, HOM 18±0.42s), and 53°C (WT 9.8±0.63s WT, HET 9.61±0.9s, HOM 9.9±0.78s). These results suggested that NCX3 is unlikely to be linked to severe phenotypes in response to motor, innocuous or acute noxious stimulation.

Next, we evaluated the acute and sensitised phases of the formalin test. In line with our acute pain behaviour experiments, the first phase of the formalin test showed no significant group difference (WT 174.6±11.2s, HET 207.2±14.4s, HOM 198±12.1s). By contrast, the sensitised phase showed a pronounced phenotype in the HOM mice displaying higher sensitivity to formalin than WT mice, with the HET mice displaying an intermediate phenotype (WT 308.13±53.9s, HET 555.2±68.1s, HOM 634±92.2s), (Figure 2.4L-N)). These findings may reflect a gene dosage effect on the sensitised phase of the formalin test which is mediated by central mechanisms. Lastly, we counted the number of c-fos-positive dorsal horn neurons in the spinal dorsal horn but found no significant difference between the genotypes (Figure 2.4O).

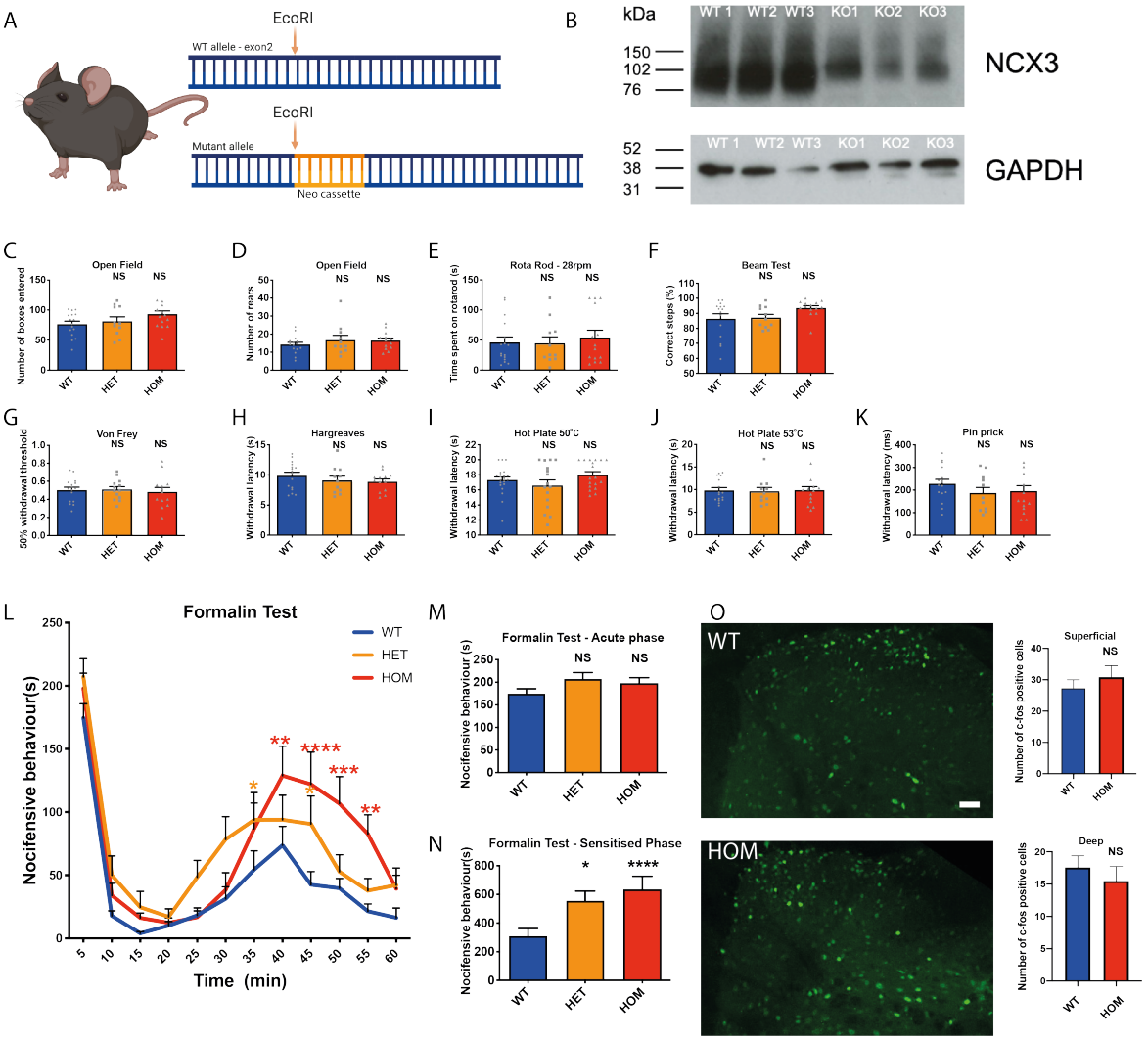


Fig. 2.4 NCX3 KO line – design and behavioural results.
A – Schematic explaining the generation of NCX3 KO line, designed and generated by (Sokolow et al., 2004). The line was initially generated by inserting a Neomycin cassette into the unique EcoRI site in exon II of the *Slc8a3* gene. **B** - In our hands, Western blot analysis confirmed the lack of NCX3 protein in three knock-out animals in comparison to WT. **C-F** – motor/balance/anxiety behavioural tests; **G-K** – acute tests for innocuous and noxious stimuli; **L-N** – formalin test; **M** - mean results from the first 5 minutes of the test; **N** - results from 20-60 min. Data are mean ± SEM, n=16 WT, n=11 NCX3 HET, n=13 NCX3 HOM; (except Hot plate at 50^{o}C, where n=21WT, n=16 NCX3 HET, n=18 NCX3 HOM). Significance shows comparison to WT (NS – p>0.05, * - p<0.05, **-p<0.01, ***- p<0.001, ****-p<0.0001). Data analysis – One-Way ANOVA, Dunnett's multiple comparisons test for all bar charts; Two-Way ANOVA, Dunnett's multiple comparisons test for formalin scatter plot. **O** – Representative images showing c-fos staining in WT and HOM spinal cord, ipsilateral to formalin injection. Quantification of data shows number of c-fos positive cells in superficial and deep laminae. Data are mean ± SEM, n = 11WT and 13HOM. Scale bar = 50 μm.

2.4 Discussion

Our initial approach to investigating the role of NCX3 in nociception was to combine *in-situ* hybridisation with immunohistochemistry to understand its localisation. We discovered that *Slc8a3* mRNA co-localises with all tested DRG markers, however the TH-, IB4- and the CGRP-positive populations showed lower expression of the mRNA of interest than the NF200-positive and NF200/CGRP groups of neurons. The co-localisation in the latter populations was more pronounced, with a larger number of positive punctae in each neuron. Our experiments in the spinal cord showed that *Slc8a3* was very highly expressed in the dorsal horn, with strong co-localisation with the neuronal marker NeuN, as well as strong co-localisation with markers of both inhibitory and excitatory interneurons. Interestingly, our data show evidence that *Slc8a3* is also expressed in projection neurons.

The expression of our protein of interest along the pain circuit is not well studied. This is likely due to the lack of good quality antibodies for this particular exchanger. There are few studies that show immunohistochemistry results, however most of the published work explores the NCX family of proteins in the DRG using functional assays.

2.4.1 Distribution of NCX3 in the DRG according to functional, molecular and anatomical studies

There is still a debate as to whether the NCX family is found and has a role in the DRG. Some authors (Verdru et al., 1997; Lu et al., 2006; Scheff et al., 2014) showed that general NCX activity is observed in the DRG, while others found no NCX role in the cell bodies or their peripheral and central terminals (Werth and Thayer, 1994; Gover et al.,

2007; Wan et al., 2012; Shutov et al., 2013). For example, Scheff et al. (2014) used Ca^{2+} imaging in retrogradely labelled neurons from the glabrous skin of rats and showed that NCX activity was only detected in small diameter (<30μm), capsaicin-sensitive, IB4+ fibres. In order to isolate the NCX activity, the authors replaced Na^{+} in the bath solution with Li^{+}. They also used a variety of NCX inhibitors and suggested that from the three members of the family, NCX3 had the most prominent role. Other authors (Verdru et al., 1997) also showed a role for the NCX family in cultured DRG neurons and this was done again through inhibition of NCX activity in a Na^{+}-free solution. Lu et al. (2006) also studied the NCX family using Ca^{2+} imaging and found a variety of channels and transporters which contribute to Ca^{2+} efflux in the DRG, depending on the specific population of neurons. They found that the NCX family plays a major role in the extrusion of Ca^{2+} in the IB4-positive, capsaicin-sensitive nociceptors, and a little role in the large-diameter, capsaicin-insensitive neurons.

We found expression of NCX3 mRNA in all DRG populations but as mentioned previously, the NF200-positive, large-diameter group of mechanoreceptors had much higher number of positive punctae. To my knowledge, our study is the first to use ISH to explore DRG expression of NCX3 on a population level. The functional assays, described by other authors, provide an indirect method for exploring this subject and come with limitations. For example, replacing the bath Na^{+} with Li^{+} can block other Na^{+}-dependent mechanisms and affect calcium handling through an NCX-independent mechanism. In addition, the only study that was able to selectively study NCX3, used an NCX3 inhibitor, known as KB-R7943. According to (Iwamoto and Shigekawa, 1998), this inhibitor is also capable of inhibiting NCX1 and 2, albeit with a lower potency. Therefore, there could be off-target mechanisms which could make pharmacological inhibition, as a means to study the specific role of NCX3, challenging.

Another study, by Persson et al. (2010), used staining methods to study the DRG expression of the NCX family. Antibody labelling showed pronounced NCX2 protein expression in primary sensory neurons, and minimal NCX1 and NCX3 expression. In the case of NCX3, the staining was dim, but the authors suggested its existence in all populations at the level of the DRG. This is in contrast with our antibody finding which pointed to membrane expression of NCX3 in large-diameter neurons. As mentioned previously, these results are dependent on the quality of the antibody used. In our case, it was reassuring that our ISH data corresponded well with our protein results.

There is much less literature regarding NCX3 expression in the spinal cord. For example Boscia et al. (2013) showed NCX3 antibody staining in the superficial dorsal horn, which agrees with our observation of mRNA in the same region.

Anatomy of NCX3 expression in the DRG and spinal cord – conclusions

Taken together, the research described above shows evidence for the expression and role of the NCX family in the DRG. The exact population of neurons that expresses NCX3 is still debatable, with functional studies showing role mainly in the IB4+ population; and staining results, including our ISH data, showing a much broader expression in all populations. Our data, together with data from Boscia et al. (2013) point to a strong expression of mRNA and NCX3 protein in the spinal cord. To my knowledge, we are the first to show the distribution of NCX3 mRNA within separate dorsal horn populations. We found the transcript in both inhibitory and excitatory interneurons, as well as in *Lypd1*-positive neurons projecting to the lateral parabrachial area. This finding pointed to a possible role of the exchanger in pain signalling due to the importance of projection neurons, as well as interneurons in the superficial laminae of the dorsal horn. These findings led us to hypothesise that our target of interest would be more important in spinal cord-mediated nociception and less so at the peripheral level.

2.4.2 Motor, tactile and acute pain phenotypes of the NCX KO mouse line

After studying the anatomy of NCX3 expression, we then focused on the possible behavioural effects of an NCX3 knock-out. We found no acute mechanical or thermal abnormalities, as well as no changes in motor activity. Interestingly,Sokolow et al. (2004), who first created the KO line, also studied motor abnormalities in the mouse. They found minor necrosis in skeletal muscles from NCX3 KO mice and explained the mildness of the phenotype with a possible low contribution of the exchanger in naïve states (i.e. when extreme physical exercise is not present). They suggested the exchanger may become crucial in conditions of sustained high [Ca^{2+}]i. In their rotarod test, the authors saw a significant phenotype where the KO mice performed worse than WTs. This is in contradiction with our results, but the discrepancy could be explained by a difference in the protocols used. Sokolow et al. (2004) performed three consecutive trials on one day for up to 300seconds, followed by rest and a 2000-second endurance test. By contrast, our test was much less strenuous (one trial per day for up to 120 seconds, for three consecutive days). As NCX3 is linked to endurance and fatiguing stimulation, the mild nature of our experiments could explain the discrepancy. In our hands, the motor experiments were designed to test the ability of the mice to perform successfully in paw-withdrawal sensory tests and were therefore not aimed at endurance or fatigue. Thus, we could conclude that the NCX3 KO mice were likely to perform well in the following sensory tests. This was supported by the lack of significant difference in the other motor, balance and anxiety tests we used. However, we cannot exclude a possible motor phenotype, especially in an experiment which requires endurance and can cause fatigue.

With regards to our sensory tests, we found no significant change in any of the acute motor or thermal experiments. This topic has not been studied in detail and the NCX3 KO mouse line has not been used in the context of pain. However, there is work from Scheff et al. (2014) showing a reduction in both thermal and mechanical pain thresholds in response to NCX3 knockdown in rats with sciatic nerve siRNA injection. This could be due to a significant difference between the methods used. Our genetic KO is complete, global and lasts for the lifetime of each animal. Therefore, there could be a variety of compensatory effects, associated with the DRG or any other part of the pain circuit. On the other hand, siRNA injections into the sciatic nerve can produce variable effects and genetic deletion is a more complete and stable method for the study of gene function. This points to the importance of creating inducible and cell-population selective KO models, which can study the phenomenon in more detail.

2.4.3 Sensitised pain phenotypes of the NCX KO mouse line

As our GWAS data pointed to a possible sensitisation phenotype, associating NCX3 with wind-up ratio in human participants, we next used the formalin test and found a significant, dose-dependent hypersensitivity in our KO mice. As mentioned previously the formalin test includes an injection of formalin into the hind paw of mice, which leads to bi-phasic response. The first phase is linked to direct activation of primary sensory neurons, while the second phase is thought to result from a combination of primary input and central sensitisation in the dorsal horn (Tjolsen et al., 1992). The exact mechanisms behind the two phases are still debatable but McNamara et al. (2007) have linked the first phase to the TRPA1 channel. Other authors such as Chisholm et al. (2018), contributed to the debate on whether the DRG affects the second phase – the authors show that during the second phase, weak firing from the periphery exists and could be generating the response of the spinal cord, which is heightened due to a

spinal-cord-based sensitisation. Pharmacological interventions have shown that indeed the two phases of the formalin test are different mechanistically. While the first phase is inhibited by local anaesthetics (such as lidocaine) (Abbadie et al., 1997), the second one responds to intrathecal nonsteroidal anti-inflammatory drugs, NMDA antagonists, morphine and gabapentin (Dubuisson and Dennis, 1977; Singh et al., 1996; Yoon et al., 2005) whose mode of action is linked to the spinal cord. This body of research supports our hypothesis that the phenotype we saw in the second phase of our experiment was likely linked to a central phenomenon. By contrast, the lack of significant changes in the first phase, together with our acute pain experiments point to the lower importance of the DRG. The possible peripheral effect, however, cannot be fully excluded.

As the formalin test is linked to inflammatory pain, the work of Scheff and Gold (2015) was also of interest to us. The authors focused on inflammation and reported that NCX3 activity in the central terminals of DRG neurons decreases during inflammation. They speculated that this could lead to higher $[Ca^{2+}]i$ and thus higher transmitter release. This notion, however, was not directly addressed and is controversial as Shutov et al. (2013) did not find a significant contribution of NCX3 at the central terminals of DRG neurons. This opens the discussion to the role of the spinal cord in the context of NCX3 and inflammation. The next chapter of this thesis will address this question in more detail.

Lastly, it is important to mention that the NCX3 KO line is global and therefore it has been associated with other phenotypes that can be relevant to our findings as well. For example, Boscia et al. (2013) found normal gross cytoarchitecture of neurons, astrocytes and oligodendrocyte precursor cells. However, they did discover defects in myelination and reduced expression of axonal markers in the spinal cord of NCX3 KO mice. Previous work has linked the genetic deletion of NCX3 to memory, learning

and hippocampal long-term potentiation (Molinaro et al., 2011). Whether any of our behavioural effects are linked to these phenotypes, is still to be elucidated.

The anatomical and behavioural data described above prompted us to study the biological mechanism responsible for our observation. This topic will be discussed in detail in Chapter 3.

Chapter 3

Slc8a3 - abnormalities in calcium handling and wind-up at the dorsal horn level

Chapter 2 of this thesis focused on the expression of NCX3 in the spinal cord, as well as the hyper-sensitivity of NCX3 knock-out mice in the second phase of the formalin test. We next examined the mechanisms underlying this observation. To do this, we conducted *in vitro* Ca^{2+} imaging and *in vivo* electrophysiology. Both techniques revealed phenotypic differences in the NCX3 mutants in comparison to WT. These phenotypes included increased intracellular Ca^{2+} during rest and neuronal stimulation of dorsal horn neurons, as well as enhanced wind-up. In addition, we designed an *Slc8a3*-containing adeno-associated virus (AAV) whose administration into the mouse spinal cord could inform future therapeutic strategies.

3.1 Introduction

3.1.1 The role of temporal summation in pain conditions

Our GWAS revealed an association between wind-up ratio (temporal summation) and the sodium-calcium exchanger NCX3. Temporal summation is the clinical manifestation of the electrophysiological phenomenon *wind-up*. This neuronal feature was discovered in 1965 by Mendell and Wall (1965) and it represents the ability of DH neurons to increase their response during a train of repetitive, identical, low-frequency C-fiber stimulations.

The role of temporal summation and wind-up has been explored in various different pain disorders and highlights the importance of expanding our knowledge of the mechanisms which underlie the phenomenon. For example, according to Maier et al. (2010), 33% of patients with neuropathic pain were found to have facilitated temporal summation. In another study, 5 out of 10 patients with chronic neuropathic pain also showed temporal summation (Felsby et al., 1996). In addition, 'wind-up like' pain in patients with spinal-cord injury was seen more commonly in painful than non-painful de-innervated skin areas (Eide et al., 1996). Similarly, facilitated wind-up pain was found in post-herpetic neuralgia (Eide et al., 1994) and in chronic post-surgical pain (Pud et al., 1998). Other experiments have shown increased wind-up after inflammation. For example, this effect was observed by Herrero and Cervero (1996) in an arthritis model in rats. Other conditions such as fibromyalgia Staud et al. (2003) and irritable bowel syndrome P. Rössel, A. M. Drewes, P. Peterse (1999) have also been linked to increased temporal summation. For example, in a cohort of fibromyalgia patients, temporal summation occurred at lower forces and frequency than in control subjects. In addition, painful after-sensations were greater in amplitude and duration in the fibromyalgia group (Staud et al., 2003). Lastly, the above-mentioned conditions are

not the only ones associated with increased temporal summation. This topic has been reviewed in greater detail in works by (Herrero et al., 2000; Arendt-Nielsen et al., 2018; Woolf, 2011).

Another important point is that wind-up represents a property of some spinal dorsal horn neurons and any change in their response to repeated stimulation could be a predisposition to the larger phenomenon known as central sensitisation (CS)(introduced in Chapter 1, Section 1.5). This phenomenon has been shown to be induced by injury to the peripheral tissues, but also after wind-up-inducing repetitive electrical stimulation (Cervero et al., 1984; Cook et al., 1987; Hylden et al., 1989b; Woolf and Thompson, 1991; Li et al., 1999). This observation led to the hypothesis that wind-up could be a prerequisite of central sensitisation, which is also supported by the fact that NMDA receptors are involved in both phenomena (Woolf and Thompson, 1991; Herrero et al., 2000). However, it is important to mention that central sensitisation can exist in neurons which do not show wind-up (Alarcon and Cervero, 1990; Laird et al., 1995).

3.1.2 Wind-up and central sensitisation

The similarity between CS and wind-up comes from the fact that in both cases intense stimulation causes an increased DH output. However, while the wind-up effect lasts during and only seconds after the stimulation, central sensitisation is longer-lasting, can affect areas around the stimulation point and is considered to be mechanistically more complex (reviewed by (Woolf, 2011)). Therefore, CS is an umbrella term, including **homosynaptic** (such as wind-up) and **heterosynaptic** mechanisms (Introduced in Chapter 1, Figure 1.5). In the former case, the conditioning stimulus is only able to strengthen the *conditioned synapses* (only those synapses, made by the pre-synaptic neuron, which were stimulated). This provides a limited and shorter

lasting facilitation. In the latter phenomenon, however, the conditioning stimulus can go beyond its *conditioned synapses*, spreading the heightened activity to adjacent synapses in the same neuron, ultimately affecting the full cell and providing conditions for complex and longer-lasting changes. Most injuries produce heterosynaptic plasticity, causing weaker, normally sub-threshold and even innocuous synaptic inputs to activate DH neurons and signal pain (reviewed by Latremoliere and Woolf (2009)).

The interconnection between wind-up and central sensitisation as well as the similarity between the mechanisms which develop and maintain them, is the reason why this thesis explores both phenomena, and most importantly – the potential of NCX3 to affect the development of both wind-up and the longer lasting CS.

3.1.3 Phases and maintenance of central sensitisation

The initial stages of central sensitisation are associated with functional plasticity where the conditioning stimulus leads to the voltage-dependent activation of NMDA receptors. Under normal conditions, NMDA receptors are blocked by Mg^{2+} and therefore require higher voltage to open and elicit Ca^{2+} entry. Once active, NMDA receptors are a major source of Ca^{2+} and play a key role in the initiation of central sensitisation (Mayer et al., 1984). This is complemented by AMPA receptors, voltage-gated Ca^{2+} channels, as well as intracellular stores. In addition, other neurotransmitters and receptors are also implicated. One such example is substance P which binds to the neurokinin 1 (NK1) G-protein-coupled receptor, expressed by most projection neurons (Mantyh et al., 1997; Khasabov et al., 2002; Willis, 2002). The binding of substance P to its receptor produces long-lasting depolarisation which allows for the temporal summation of incoming action potentials, thereby contributing to wind-up and CS (Henry, 1976; Dougherty and Willis, 1991; Xu et al., 1992). CGRP and BDNF have

similar functions when released by small-diameter DRG neurons (Zhou and Rush, 1996; Kerr et al., 1999; Thompson et al., 1999; Heppenstall and Lewin, 2001).

3.1.4 The importance of calcium as a second messenger

These initial events lead to increased intracellular Ca^{2+} . As a second messenger, Ca^{2+} is extremely important as it leads to a cascade of events which maintain and define the heightened sensitivity. Such events include the activation of kinases which change NMDA and AMPA receptors both functionally (by increasing their activity) and anatomically (by recruiting more receptors to the membrane). For example, high intracellular Ca^{2+} leads to the activation of protein kinase C (PKC) which phosphorylates NMDARs on Serine residues and leads to dramatic changes of their activation threshold, channel kinetics and voltage dependence properties. This ultimately leads to increased activity (Carvalho et al., 2000; Galan et al., 2004; Chen and Roche, 2007; Lau and Zukin, 2007). An example for structural changes in the synapse is the increase in trafficking of GluR1 AMPAR subunits. These subunits allow much more Ca^{2+} into the cells in comparison to the GluR2 subunits which are mainly expressed under normal conditions. This leads to an increase in synaptic strength (Banke et al., 2000; Esteban et al., 2003; Galan et al., 2004), (reviewed by (Battaglia, 2016)).

These initial changes usually lead to a short-lasting sensitisation. However, prolonged accumulation of intracellular Ca^{2+} can cause a more sustained facilitation of synapses. This second phase of CS involves transcriptional, translational and post-translational modifications through cascades including nuclear Ca^{2+} , the ERK1 and 2 kinases and the transcription factor CREB (Ji et al., 1999; Hu et al., 2003; Lever et al., 2003; Simonetti et al., 2013). There is also a growing body of evidence showing structural changes during prolonged CS, including increased dendritic and synaptic

density (Tan et al., 2012; Simonetti et al., 2013; Lu et al., 2015)(Reviewed by Kuner and Flor (2017a), (Diagram D.3.1).

3.1.5 Reorganisation of dorsal horn circuitry

As described above, central sensitisation includes many processes and affects the spinal cord on a circuitry level. Many studies have shown that large-diameter fibers, which do not normally transmit noxious signals, participate in the activation of projection neurons under pathological conditions. This can be linked to reduced activity of inhibitory interneurons, causing potentiation of normally weak circuit connections between Aβ terminals and projection neurons. An example of this was described in Chapter 1 with regards to parvalbumin-positive inhibitory interneurons Boyle et al. (2019)(Subsection 1.3.7. There have been numerous studies in the past predicting such circuitry reorganisation. For example, under physiological conditions, excitation of dorsal horn neurons evoked by Aβ-fiber input was observed mainly in the deep dorsal horn, whereas in slices taken from neuropathic mice, excitation was seen in the superficial dorsal horn as well (Schoffnegger et al., 2008).

Despite the knowledge that Ca^{2+} , as a second messenger, has a crucial role in the development of synaptic plasticity and CS (Fernyhough and Calcutt, 2010), little is published about the exact mechanisms that control its intracellular levels in the spinal dorsal horn. When it comes to the termination of Ca^{2+} signalling after periods of neuronal stimulation, the most common mechanisms involved are either Ca^{2+} extrusion by plasmalemmal systems (the plasma membrane calcium ATPase or Na^{+}/Ca^{2+} exchangers) or Ca^{2+} uptake into the ER and/or mitochondria (Fernyhough and Calcutt, 2010)(Diagram D.3.2).

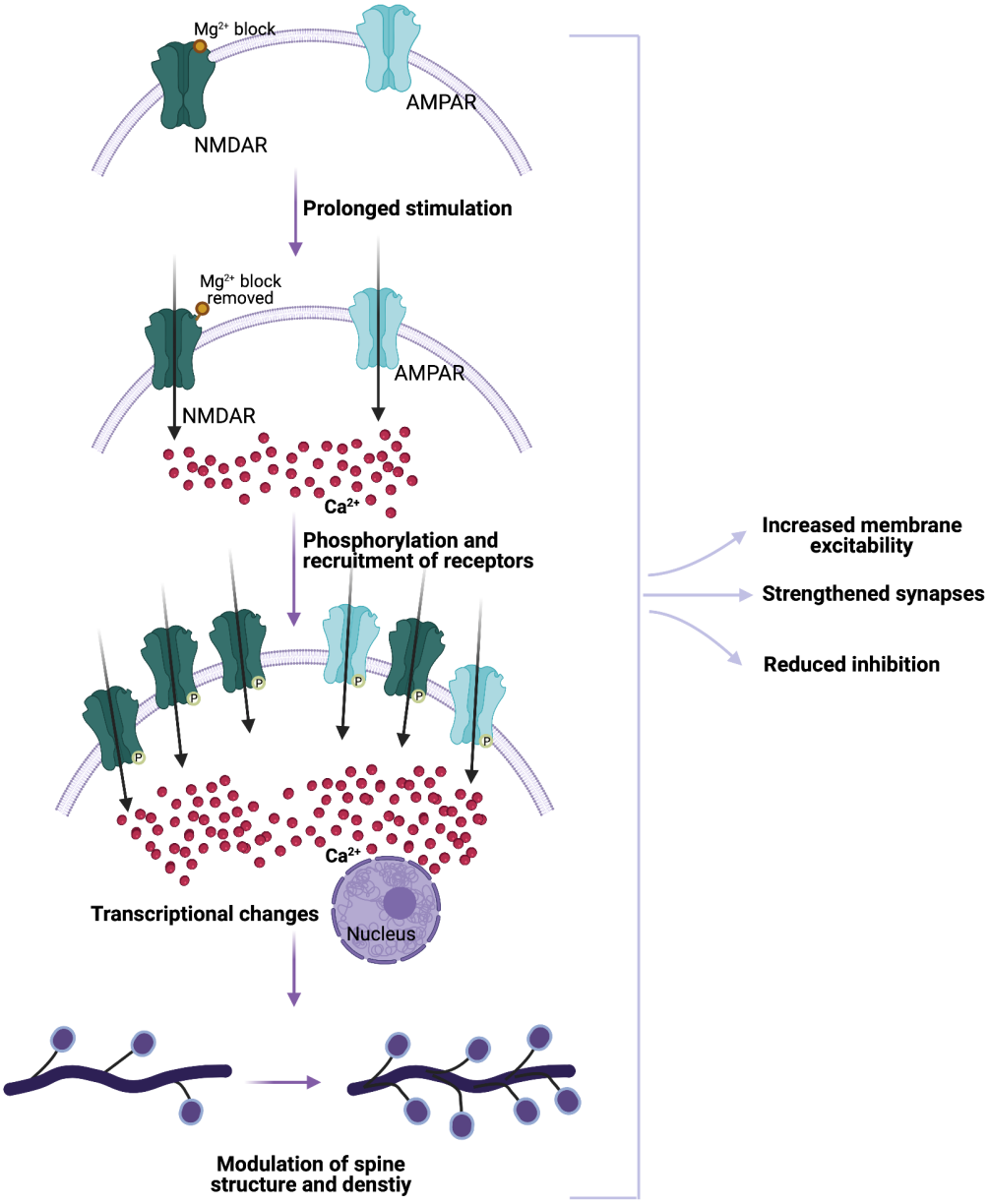


Diagram. D.3.1 The main neurobiological changes implicated in central sensitisation at the spinal cord level..
Legend: NMDA: N-methyl-D-aspartate, NMDAR: NMDA receptor, AMPA: α-amino-3-hydroxy-5-methyl-4-isoxazolepropionic acid, AMPAR: AMPA receptor, Ca^{2+} calcium.

For example, recent work by (Mirabelli et al., 2019) has shown the role of the plasma membrane calcium ATPase 2 (PMCA2) in maintaining resting calcium levels, as well as in clearing elevated calcium after neuronal activation. In addition, (Khariv et al., 2017) showed that healthy female PMCA2$^{+/-}$ mice showed increased evoked pain in the Von Frey test. In their later study from 2019, (Mirabelli et al., 2019), the group observed that PMCA2 was downregulated in an experimental autoimmune encephalomyelitis and this was correlated with a painful phenotype. Therefore, they hypothesised that the reduced expression of PMCA2 takes part in the development of inflammatory pain through perturbations in calcium handling. Interestingly, earlier studies also showed down-regulation of PMCA2 in chronic pain states (Tachibana et al., 2004) and during neuronal damage and cell loss (Kurnellas et al., 2005).

As mentioned previously, other mechanisms, important for monitoring the levels of intracellular calcium in dorsal horn neurons, are linked to the mitochondria. These organelles have been implicated in the central terminals of primary neurons (Medvedeva et al., 2008; Shutov et al., 2013), as well as in the second order neurons residing in the spinal cord. Interestingly, the uptake of excess calcium into the mitochondria has been linked to inflammatory and neuropathic pain due to changes in calcium dynamics within the mitochondria (such as the generation of reactive oxygen species) (Kim et al., 2011). Uptake of calcium into the nucleus has also been related to the development of chronic pain (Simonetti et al., 2013). Therefore, it can be inferred that the buffering of calcium into organelles comes with consequences. It can then be envisioned why the extrusion of this second messenger outside the cell must be of high importance. As mentioned previously, so far, little is known about the exact mechanism of this in dorsal horn neurons, with recent work showing the role of the PMCA2.

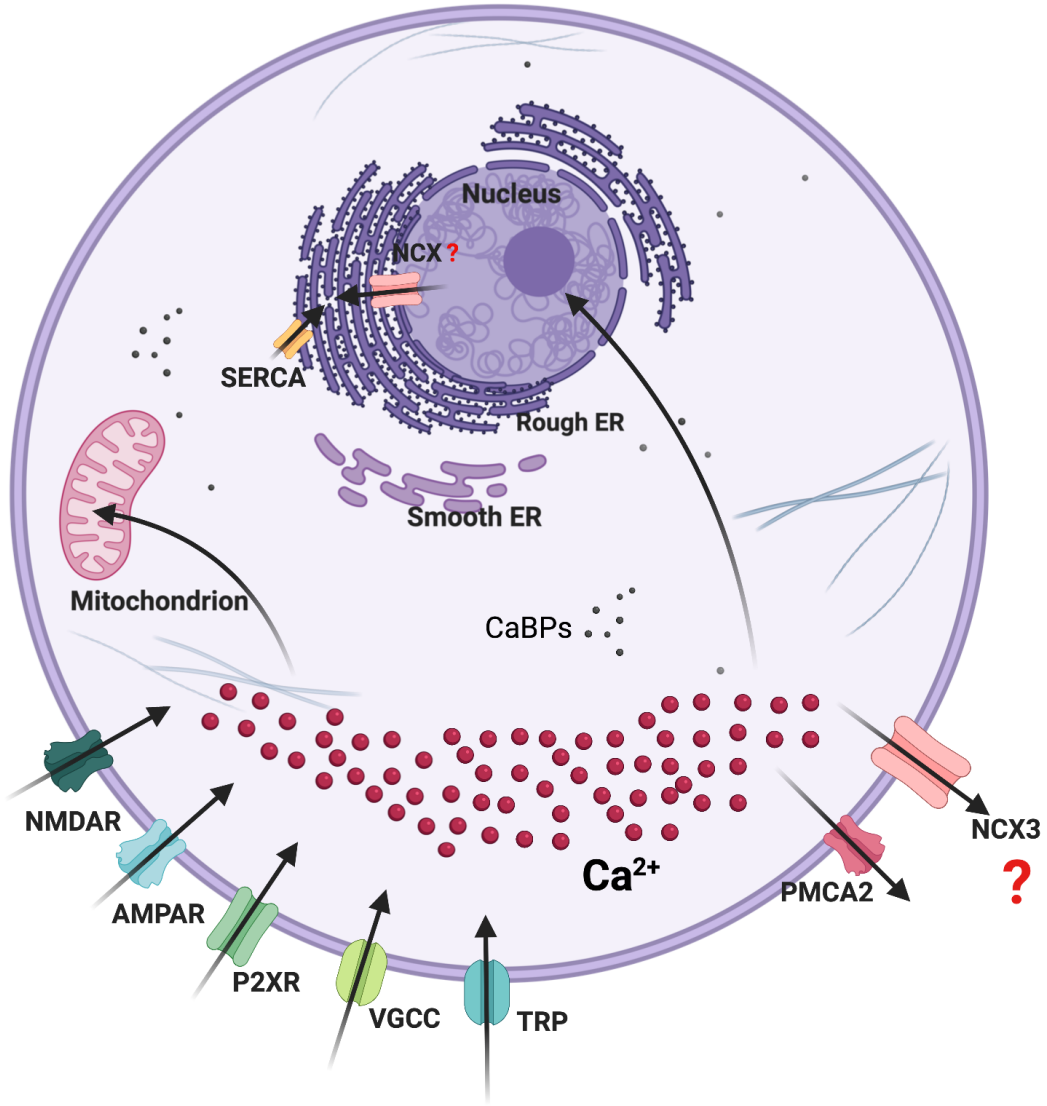


Diagram. D.3.2 calcium entry and exit mechanisms in neurons in the dorsal horn of the spinal cord.
Calcium entry through ligand-gated channels such as N-methyl-D-aspartate receptors (NMDARs), calcium-permeable α-amino-3-hydroxyl-5-methyl-4-isoxazolepropionate receptors (AMPARs), and ATP-responsive purinoreceptors (P2XRs); through transient receptor potential (TRP) channels; through voltage-gated calcium channels (VGCCs), activated in response to neuronal depolarization. Calcium sources are better studied but calcium extrusion mechanisms are also extremely important in the modulation of intracellular calcium. These include plasma membrane calcium ATPases (PMCA) and sodium/calcium exchangers (NCXs), which remove cytosolic calcium into the extracellular space; sarco/endoplasmic reticulum calcium ATPases (SERCA pumps), which pump calcium ions into the ER; nuclear NCXs, which move nuclear calcium into the nucleoplasmic reticulum; the mitochondrial uniporter (MCU), which mediates mitochondrial calcium uptake; and a wide range of calcium binding proteins (CaBPs). Schematic adapted from (Hagenston and Simonetti, 2014).

3.1.6 Aims and hypotheses

To my knowledge, the second major extrusion mechanism – the NCX family of proteins(discussed in more detail in Chapter 1, Section 1.7) – has not yet been studied in the context of dorsal horn-dependent pain and central sensitisation. As Ca^{2+} seems to serve as a major 'doorway' to synaptic plasticity in the spinal cord, it is likely that its intracellular concentration is closely monitored and regulated, both at its entry in the cell, and at its exit. This chapter will provide evidence for the role of NCX3 in calcium handling in the dorsal horn and for the development of wind-up.

3.2 Materials and Methods

3.2.1 Calcium imaging

Dorsal horn dissection and culture

For dissection of spinal dorsal horns, we euthanised NCX3 WT or NCX3 HOM KO mice at p6-p12 (male and female, n=5 from each genotype). Spinal cords were removed and placed into ice cold Hank's Balanced Salt Solution, HBSS (Invitrogen), as described by (Albuquerque et al., 2009). Once taken out, each spinal cord was placed with its dorsal side facing upward. Following a midline incision, the cord was spread open and only the outer (dorsal) one-third of each side was collected. This was followed by an enzymatic digestion for 75min in collagenase II (4mg/ml, Worthington) and dispase II (4.7mg/ml, Roche) at 37^{o}C. Then the tissue was mechanically dissociated using glass pipettes and spun down at 600xg for 6 minutes. The pelleted cells were resuspended into cell medium (Neurobasal medium supplemented with 2% (v/v) B27 supplement, 1% (v/v) N2 supplement, 1% (v/v) GlutaMAXTM and 1.5% antibiotic/antimycotic (ThermoFisher Scientific)) and plated on 13mm-coverslips pre-coated with laminin

(R&D Systems) and poly-D-lysin (BD biosciences). After allowing the cells to attach to the coverslips for 2 hours (at 37^{o}C), the wells were flooded with the above-mentioned cell medium. Following this procedure, the cultures contained both neurons and glial cells. They were maintained for 2-3 weeks at 37^{o}C, to allow time for recovery and maturation after the process of dissociation. This proved crucial for the ability of the neurons to respond to high . During the maintenance phase, the culture medium was replaced every 3-4 days.

Dorsal root ganglia dissection and culture

Mice aged between 4-8 weeks were euthanised using a CO_2 chamber(male and female, n=5 from each genotype). The spinal column was removed and cut in half through the midline. The cord was then removed to reveal the DRGs. The ganglia were taken out one by one, from all levels and placed into ice cold Hank's Balanced Salt Solution, HBSS (Invitrogen) as described by Dawes et al. (2018). This was followed by an enzymatic digestion for 90min in collagenase II (4mg/ml, Worthington) and dispase II (4.7mg/ml, Roche) at 37^{o}C. Then the tissue was mechanically dissociated using glass pipettes and spun down at 500xg for 5 minutes. The pelleted cells were then resuspended into cell medium (Neurobasal medium supplemented with 2% (v/v) B27 supplement, 1% (v/v) GlutaMAX^{TM} and 1% antibiotic/antimycotic (ThermoFisher Scientific)) and plated on 13mm-coverslips pre-coated with laminin (R&D Systems) and poly-D-lysin (BD biosciences). After allowing the cells to attach to the coverslips for 2 hours (at 37^{o}C), the wells were flooded with the above-mentioned cell medium, supplemented with mouse NGF (50ng/ml, Peprotech) and GDNF (10ng/ml, Peprotech). The prepared primary culture was then left at 37^{o}C overnight and calcium imaging was performed the next day (1DIV).

***In vitro* Ca^{2+} imaging**

An average of 87 dorsal horn neurons from each animal, of each genotype, were imaged. Similarly, for the DRG analysis, an average of 38 cells were used from each animal. Coverslips were incubated for 45-90 mins at 37^{o}C with 1μM Fura-2AM (Invitrogen) in Neurobasal medium supplemented as above. After incubation, coverslips were transferred to artificial extracellular fluid (140mM NaCl, 5mM KCl, 2mM $CaCl_2$, 1mM $MgCl_2$, 10mM D-Glucose, 10mM HEPES in distilled water). Coverslips were imaged every 1s with 4x4 binning for 340s on a Zeiss inverted fluorescence microscope with a 10x objective, dichroic LP 409 mirror, BP 340/30 and BP 387/15 excitation and 510/90 emission filters. ZEN Blue software was used for image acquisition and selection of regions of interest (ROIs). ECF was perfused continuously over the cells. After 60s of baseline recording, the cells were perfused with 50mM K^+ for 30s (100mM NaCl, 50mM KCl, 2mM $CaCl_2$, 1mM $MgCl_2$, 10mM D-Glucose, 10mM HEPES). This was followed by a 60s washout and then the high K^+ treatment/washout procedure was repeated two more times. Data were then analysed using GraphPad Prism (for AUC analysis) and a Matlab script (for quality control and decay kinetics analysis).

Quality control of neurons

Matlab was used for quality analysis. To this purpose we employed a function described by Sahani M, Linden J (2003). This function allowed the selection of neurons which respond reliably to the three consecutive K^+ pulses. Therefore, cells which showed three similar responses scored highly and were considered *of high reliability*. We chose the threshold of 1 and accepted only neurons whose signal-to-noise ratio was above that value. A threshold of 1 would mean that "signal power = noise power", and any neuron with a higher score is considered to respond above the noise level.

$$Signal-to-noise\ ratio = \frac{Signal\ power}{Noise\ power} = \frac{Explainable\ variance}{Total\ variance - Explainable\ variance}$$

This technique was used to refine the group of neurons we tested because: **1/** the DH cultures we generate contain both neurons and glia and it is difficult to select neurons based on cell morphology alone. Therefore, the initial data set was likely to contain glial cells, which would be non-responders skewing the final result; **2/** primary cultures are heterogeneous and therefore neurons can show different responses to the 3 consecutive high K^+ pulses. Although our exclusion criteria were generous and included neurons showing different patterns of Ca^{2+} transients, we attempted to exclude cells whose 3 pulses were grossly different. The most striking feature of the neurons our Matlab script selected as non-reliable, was the lack of second and third response. Biologically, this effect could be caused by neuronal death or it could be an innate feature of a subgroup of DH neurons. As we were interested in repetitive stimulation of live neurons, we considered both biological reasons for justified. **2/** the Ca^{2+} imaging protocol, as well as the high K^+ pulse can lead to some neuronal death, which would manifest itself as a lack of a second and/or third responses or continuous high Ca^{2+} levels. This type of cells was also considered of low reliability. From the original group of neurons (729 WT DH neurons and 789HOM DH neurons), 529 WT and 550 HOM remained (5 WT,5 HOM mice, male and female). We repeated the same protocol for DRG neurons. Of the original group of neurons (216 WT DRGs and 282 HOM DRGs), 179 WT and 197 HOM remained (5 WT,5 HOM mice, male and female). The same Matlab script and threshold (signal-to-noise ratio >1) was used for both DH and DRG neurons.

Data analysis on refined neurons

We calculated the following parameters: **1/** baseline at the start and end of experiment, as well as in between each peak; **2/** peak values at 90, 180 and 270 seconds; **3/** area under the curve (AUC), starting at the baseline for each genotype (which ensures that AUC differences are not baseline-dependent) **3/** tau (τ)– the time constant

describing how fast an exponential function decays. Baseline and peak values were detected using Excel and a Matlab script. Area under the curve for each individual cell was calculated using GraphPad prism. The tau value (τ) was calculated using a Matlab function for exponential decay and the following equation:

$$f(t) = A.e^{-\frac{t}{\tau}}$$

In the above equation, A is the 340/380 ratio at its peak, i.e. at time t=0. After a period of one time constant (t= τ, the function reaches e-1, which equals 37% of the initial value A. Both WT and HOM responses were normalised prior to analysis, so the final decay value was 0.

3.2.2 *In vivo* electrophysiology

Experiment performed by Ryan Patel, PhD at A. Dickenson's laboratory, University College London

In vivo electrophysiology was performed as previously described (Dawes et al., 2018). Both male and female NCX3 WT ($n_{males} = 9$, $n_{females} = 6$), NCX3 HET ($n_{males} = 7$, $n_{females} = 7$) and NCX3 HOM mice ($n_{males} = 6$, $n_{females} = 7$) were used between 8 and 12 weeks old; the experimenter was not blind to genotype. Mice were initially anaesthetised with 3.5% v/v isoflurane delivered in 3:2 ratio of nitrous oxide and oxygen. Once areflexic, mice were secured in a stereotaxic frame and subsequently maintained on 1.25% v/v isoflurane for the remainder of the experiment (approximately 3 hours in duration). Core body temperature was maintained with the use of a homeothermic blanket and respiratory rate was visually monitored throughout. A laminectomy was performed to expose the L3-L5 segments of the spinal cord; mineral oil was then applied to prevent dehydration. Extracellular recordings were made from deep dorsal horn wide

dynamic range (WDR) lamina V/VI neurons with receptive fields on the glabrous skin of the toes using 125μm 2 MΩ glass-coated tungsten electrodes (Microelectrodes Ltd, Cambridge, UK). Searching involved light tapping of the hind paw whilst manually moving the electrode. All recordings were made at depths delineating the deep dorsal horn laminae (Watson, Paxinos, Kayalioglu, 2009), and were classified as WDR on the basis of neuronal sensitivity to dynamic brushing (i.e. gentle stroking with a squirrel-hair brush), and noxious punctate mechanical (15 g) and heat (48^{o}C) stimulation of the receptive field.

The receptive field was then stimulated using a wide range of natural stimuli (brush, von Frey filaments - 1, 4, 8 and 15 g and heat - 32, 42, 45 and 48^{0}C) applied over a period of 10 s per stimulus and the evoked response quantified. The heat stimulus was applied with a constant water jet onto the centre of the receptive field. Ethyl chloride (25μl) was applied to the receptive field, described previously as an evaporative noxious cooling stimulus (Leith et al., 2010). Evoked responses to room temperature water (25^{o}C) were subtracted from ethyl chloride evoked responses to control for any concomitant mechanical stimulation during application. Natural stimuli were applied starting with the lowest intensity stimulus with approximately 40 s between stimuli in the following order: brush, von Frey, cold, heat. Receptive fields were determined using a 15 g von Frey. An area was considered part of the receptive field if a response of >30 action potentials over 5 s was obtained. A rest period of 30 s between applications was used to avoid sensitisation. Receptive field sizes are expressed as a percentage area of a standardised paw measured using ImageJ (NIH, Bethesda, MD). Electrical stimulation of WDR neurons was delivered transcutaneously via needles inserted into the receptive field after determining responses to natural stimuli. A train of 16 electrical stimuli (2 ms pulses, 0.2 Hz or 0.5 Hz) were applied at three times the threshold current for C-fibre activation. Responses evoked by A- (0-50 ms) and C-fibres (50-250 ms) were

separated and quantified on the basis of latency. Neuronal responses occurring after the C-fibre latency band were classed as post-discharge (PD). The input (I) and the wind-up (WU) were calculated as: Input = (action potentials evoked by first pulse) x total number of pulses (16), wind-up = (total action potentials after 16 train stimulus) - Input.

The signal was amplified (x6000), bandpass filtered (low/high frequency cut-off 150/2000 Hz) and digitised at rate of 20 kHz. Data were captured and analysed by a Cambridge Electronic Design 1401 interface coupled to a computer with Spike2 software v4 (CED, Cambridge, UK) with post-stimulus time histogram and rate functions. One to three neurons were characterised per mouse; in total, 21 neurons were characterised from 15 NCX3 WT mice, 20 neurons from 14 NCX3 HET mice, and 20 neurons from 15 NCX3 HOM mice. *In vivo* electrophysiological procedures were non-recovery; at the end of experiments mice were terminally anesthetised with isoflurane.

3.2.3 RNA extraction and Quantitative Real Time PCR

For RNA extraction, mice were sacrificed in a CO_2 chamber. Their DRGs, spinal cord and brain were dissected and snap-frozen on dry ice (or liquid nitrogen), followed by storage at -80^{o}C. On the day of extraction, tissue was mechanically homogenised in Tripure (Roche), treated with chloroform and then subjected to column purification, using a High Pure RNA Tissue kit (Roche). RNA was the eluted in RNAse-free water. cDNA was produced using Transcriptor reverse transcriptase (Roche), random hexamers (Invitrogen) and dNTPs (Roche).

mRNA expression of *Slc8a3* was achieved using SYBR green. DRG, spinal cord and brain cDNA (5ng) and primers (0.5mM) were added to LightCycler 480 SYBR Green Master mix (Roche) in a 1:1 ratio. 384 well plates (Roche) were then run on a 45 cycle

protocol as described by Dawes et al. (2018). Primer efficiency and specificity were validated before experimental use. Gene expression was validated against GAPDH as a housekeeping gene, using the delta delta CT method. Primer sequences are shown in Table 3.1.

3.2.4 Cloning

Cloning of *Slc8a3*-isoform B into an AAV vector was performed using the In Fusion® Cloning kit (Takara Bio). We used pAAV CAG-GFP viral vector (Addgene, see Table 3.1) as the host plasmid, as well as an insert amplified from *Slc8a3*-B vector (Origene, see Table 3.1). In short, we linearized the host plasmid using restriction enzymes BamHI and EcoRI (NEB). The resulting linearised vector was then gel purified. In parallel to this, the *Slc8a3* insert was amplified from its original plasmid using the primers listed in Table 3.1. The design of the primers was performed using Takara Bio online tool. We aimed to include a 15bp long overhangs, which were homologous to the ends of the linearized host vector, and to add a Kozak sequence (GCCACC) at the start of *Slc8a3*, before its original start codon. The resulting *Slc8a3*-B amplicon, containing the homologous overhangs and the Kozak sequence, was gel purified. The host plasmid and the insert were then mixed together into an In Fusion cloning reaction as described by the manufacturer. This allowed the recombination of the host and the insert using the homologous overhangs. The product of the cloning reaction was then used for bacterial transformation using the E coli provided by the manufacturer. After the initial screening of the bacterial colonies, their DNA was extracted using Mini prep kit (Quigen) and sequenced by Source Bioscience Oxford UK. The produced plasmid was then amplified further using MaxiPrep kit (Qiagen) and sent for virus production at the Viral Vector Facility of the Neuroscience centre in Zurich (University of Zurich, UZH).

3.2.5 Histology and Immunocytochemistry

Human embryonic kidney 293 (HEK293) cells were cultured in Dulbeccos's modified Eagles's medium with 10% fetal calf serum (TCS Cellworks Ltd) in 24-well plates at 37^{o}C.

For the AAV test experiment, either HEK cells or DRGs were incubated in medium containing 4μl/ml AAV (stock – 8.5x10^{12} vector genomes/mL), for 48h (HEK cells) or 7 days (DRGs).

On the day of collection, cells were washed with PBS and fixed with 4% PFA for 15 minutes. This was followed by immunocytochemistry, using the antibodies from Table 3.1 and following the immunohistochemistry method described in Chapter 2, (Subsection 2.2.2).

3.3 Results

3.3.1 *In vitro* calcium imaging of dorsal horn neurons shows significant differences in calcium handling of HOM vs WT neurons

In order to explore the mechanism behind the phenotype we observed in our NCX3 HET and HOM mice (Chapter 2), we first studied the calcium dynamics in WT vs mutant neurons in primary culture. To this purpose, we adapted a dorsal horn dissection technique Albuquerque et al. (2009) for use in our laboratory. The method involves dissecting the spinal cords of young mouse pups and collecting only the dorsal part of the tissue. After a series of mechanical and enzymatic dissociations, the neurons are collected and seeded on coverslips (as described in the Methods section

REAGENT	SOURCE	Dilution	IDENTIFICATION
Primary antibodies			
Mouse anti-c-Myc	Cell Signalling	1:1000	Cat# 2084, clone 9B11, RRID:AB_12813429B11
Rabbit anti-c-Myc	Abcam	1:500	Cat# ab9106, RRID:AB_307014
Chicken anti-GFP	Abcam	1:500	Cat# ab13970, RRID:AB_300798
Rabbit anti-Tubulin	Cell Signalling	1:500	Cat# 5568, RRID:AB_10694505
Secondary antibodies			
Donkey anti-rabbit IgG Alexa 488	Thermo Fisher Scientific	1:1000	Cat# A-21206, RRID:AB_2535792
Donkey anti-mouse IgG Alexa 488	Thermo Fisher Scientific	1:1000	Cat# A-21202, RRID: AB_141607
Donkey anti-rabbit IgG Alexa 546	Thermo Fisher Scientific	1:1000	Cat# A10040 , RRID: AB_2534016
Commercial kits			
In-Fusion® HD Cloning Plus	Takara Bio Inc		Cat# 638909
Oligos - cloning and qPCR			
Oligo 1 (BamHI) (Insert 1) Forward	Thermo Fisher Scientific		GCAAAGAATTGGATCCGCCACCATGGCGTGGTTA
Oligo 2 (Insert 1) (EcoRI) Reverse	Thermo Fisher Scientific		GCTTGATATCGAATTCTTAAACCTTATCGTCGTCATCCTTG
NCX3-AC Forward	Thermo Fisher Scientific - Michel *et al* , 2014		GGGCCCCCGCATGGTGGATA
NCX3-AC Reverse	Thermo Fisher Scientific - Michel *et al* , 2014		CAGCTTCCTGTCTGTCACTTCTGGA
NCX3-B Forward	Thermo Fisher Scientific - Michel *et al* , 2014		GCATATGGGGAGCTGGAGT
NCX3-B Reverse	Thermo Fisher Scientific - Michel *et al* , 2014		GTTCACCAAGGGCAATGAAG
Experimental Models: Organisms/Strains/Plasmids			
Slc8a3^{tm1Sso} mouse line	Sokolow *et al* , 2004		
pAAV CAG-GFP	Addgene		Cat# 37825
Slc8a3-B (Myc-DDK-tagged)	Origene		Cat# MR211189
ssAAV-1/2-shortCAG-mSlc8a3_myc_FLAG-WPRE-SV40p(A) (capsid 1)	VVF - custom		custom design
ssAAV-1/2-shortCAG-EGFP-WPRE-SV40p(A) (capsid 1)	VVF - repository		Cat# v587-1
Software and Algorithms			
Microsoft Excel	Microsoft		https://www.microsoft.com/en-gb/
Prism 9.0	GraphPad Software		https://www.graphpad.com/
Matlab	Mathworks		https://uk.mathworks.com/products/matlab.html
Biorender			https://biorender.com

Table 3.1 Reagents used in Chapter 3.

- Subsection 3.2.1. Through a series of pilot experiments with both Glutamate (not included) and 50mM KCl, we discovered that the primary neurons responded best to stimulation after 2-3 weeks in culture, and relatively few of them express β-Tubulin in the first days after seeding (Figure 3.1A and B). In addition, we saw a more robust and reliable response with KCl (in comparison to Glutamate) which informed our decision to proceed with an experimental design involving high K^+ activation. We also chose to apply three consecutive pulses in order to explore any differences between the genotypes after repetitive stimulation.

We collected the responses of 741 WT dorsal horn neurons and 784 HOM dorsal horn neurons from 8 and 5 mice, respectively. The activity of these neurons can be seen in (Figure 3.1C) (WT) and (Figure 3.1E) (HOM). During the process of calcium imaging, we noticed the difficulty in manually selecting neurons and ensuring the exclusion of glial cells, based on morphology alone. As seen from (Figure 3.1C) and (Figure 3.1E), the population of cells we measured included neurons which showed only one Ca^{2+} response, followed by silencing or continuous Ca^{2+} overload. In addition, there were cells which did not show a large Ca^{2+} increase from baseline throughout the experiment, and therefore did not respond to K^+ . In order to exclude these cells, while keeping the majority of neurons and their innate heterogeneity, we followed a quality control protocol (Subsection 3.2.1). We selected a lenient threshold of 1, which meant that in the selected population of neurons the signal power was equal or higher than the noise power. Using this technique, we selected 549 WT neurons from 7 mice (Figure 3.1D) and 550 HOM neurons from 5 mice (Figure 3.1E). In order to have a relatively equal contribution from each animal in our data set, we also excluded two mice from the WT group which only contributed 6 and 14 cells. This brought our final count of WT neurons to 529.

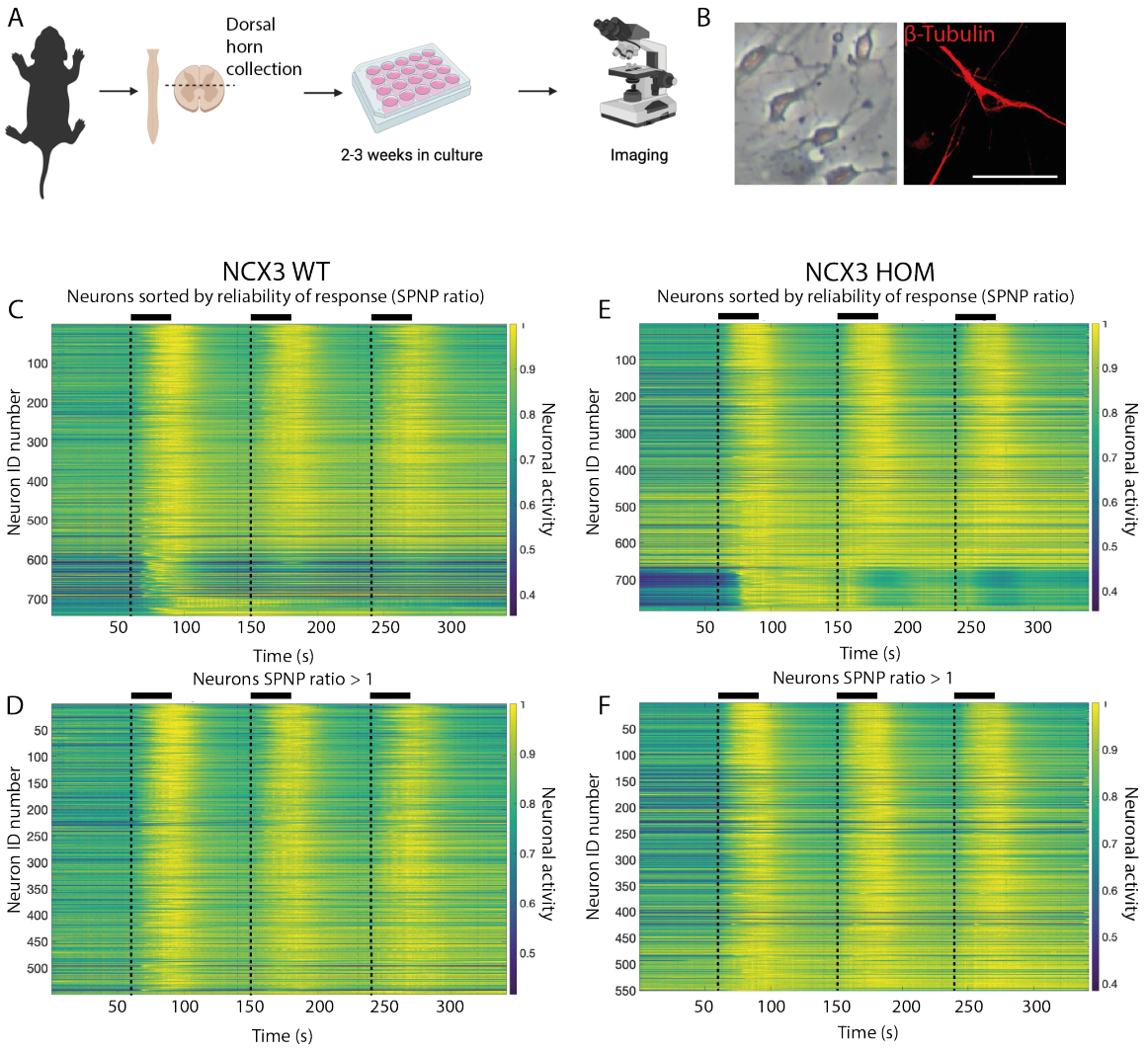


Figure. 3.1 Sorting of cultured dorsal horn neurons based on calcium imaging response reliability.
A - Schematic showing the design of the experiment from dissection to imaging; **B** - Images showing dorsal horn cultures at early stages of culture, β-tubulin shown in red; **C and E** - Raster plots showing the Ca^{2+} responses of DH neurons to 50mM K^+ pulses (each pulse starting at 60, 150 or 240 seconds and lasting for 30 seconds). Beginning and duration of each K^+ pulse are described with dashed vertical lines and black bars. Neurons were sorted based on similarity between their three Ca^{2+} responses (reliability, as measured by Signal power/Noise power ratio). Neurons at the top of the raster plots had the most reliable responses, while the ones at the bottom did not display high level of reliability. The raster plots show 741 WT dorsal horn neurons, **C** and 784 HOM dorsal horn neurons from 8 and 5 mice, respectively **C**; **D and F** - Raster plots showing the dorsal horn neurons from **C** (NCX3 WT) and **E** (NCX3 HOM), respectively, which displayed reliability of response (SPNP ratio) higher than 1 (549 cells from 7 mice and 550 neurons from 5 mice). Plot colour scheme – blue to yellow – low to high Ca^{2+} level. Scale bar = 50μm.

Next, we analysed our results by plotting the activity of the selected neurons as a Mean ± SEM for each second of the experiment. A strong difference in activity was observed both at baseline (0-60seconds), as well as at the peaks of Ca^{2+} response (90seconds, 180 seconds and 270 seconds) (Figure 3.2A). In Figure 3.2B, we normalised the baselines to zero and saw that the difference in peaks persisted, especially at peaks II (180 seconds) and III (270seconds). This presentation of the data also highlighted a possible phenotype in the decay kinetics of the mutant cells in comparison to WT. This was manifested in the time it took for the Ca^{2+} responses to decay, as well as the increased plateaus after each peak. The latter effect means that the mutants have a higher baseline from which to start the next response, and this could contribute to the risk of summation during repetitive stimulation. It is also an interesting observation, albeit not quantified, that the mutants show a small rise in activity at end of the experiment, which is spontaneous and in the absence of a new stimulation.

The data from Figure 3.2A was then used to compare the **baselines, peaks, AUC values (area under the curve) and tau values (exponential decay time constant)** of the selected neurons. We saw a significant difference for each of these parameters. For example, the **baselines** at 60s, 150s and 240s were as follows – 0.23 ± 0.001 for WT and 0.25 ± 0.003 for HOM; 0.25 ± 0.002 for WT and 0.27 ± 0.004 for HOM, 0.25 ± 0.002 for WT and 0.27 ± 0.004 for HOM, respectively (Figure 3.2C, C^{I} to C^{III}). The **peak** results at 90 seconds, 180 seconds and 270 seconds also showed a significant difference between the genotypes – 0.29±0.003 for WT and 0.31±0.005 for HOM; 0.28±0.003 for WT and 0.32±0.005 for HOM, 0.28±0.003 for WT and 0.31±0.005 for HOM, respectively (Figure 3.2D, D^{I} to D^{III}). We also measured **area under the curve (AUC)** for each of the three peaks, using each group's respective initial baseline. This would mean that the baseline recorded for the WT group at 60 seconds was used for all WT AUC calculations, while the HOM AUC calculations were

performed from the HOM baseline (illustrated in Figure 3.2D). The mean AUC values we recorded were as follows – 3.8±0.2 for WT and 7.2±0.3 for HOM; 3.9±0.2 for WT and 7.6±0.3 for HOM, 3.9±0.2 for WT and 7.5±0.3 for HOM (Figure 3.2D, D^{I} to D^{III}). Finally, we performed a single exponential decay fit to each cell of our data set, and each decaying response. Representative traces, showing this fit, can be seen in Figure 3.5A and B. Next, we calculated the **decay time constant (tau)** for each cell and each of the three pulses. Our results are reported in Figure 3.2E (E^{I} to E^{III}) and are as follows – 24.1 ± 0.03s for WT and 27 ± 0.5 for HOM; 25.6 ± 0.3 for WT and 26.2 ± 0.4 for HOM, 28.1 ± 0.4 for WT and 30.7 ± 0.5 for HOM, with significance observed only at the first pulse.

Therefore, dorsal horn neurons in primary culture, under the conditions we chose, showed significant differences on four different Ca^{2+} handling parameters, which all pointed to raised intracellular calcium and slowed calcium clearance following activity of the mutants in comparison to WT. This abnormal Ca^{2+} handling could lead to hyper-excitability in dorsal horn neurons, which we test with *in vivo* electrophysiology in Figure 3.7.

As NCX3 is expressed in DRG neurons, as well as in dorsal horn neurons (Chapter 2), we decided to perform the same tests in a population of primary sensory neurons. To this purpose, we cultured DRG neurons from our NCX3 WT and NCX3 HOM mice and imaged them on day 1 after isolation. We then subjected them to the same selection protocol described in (Figure 1.1) and used the same threshold (Th=1). As seen in (Figure 1.3), out of 216 WT DRG neurons, we selected 179, coming from 5 mice. In our HOM group, we selected 215 neurons (out of 282), coming from 6 mice. One mouse, contributing only 17 cells, was excluded from the HOM analysis, resulting in 197 neurons for this final group.

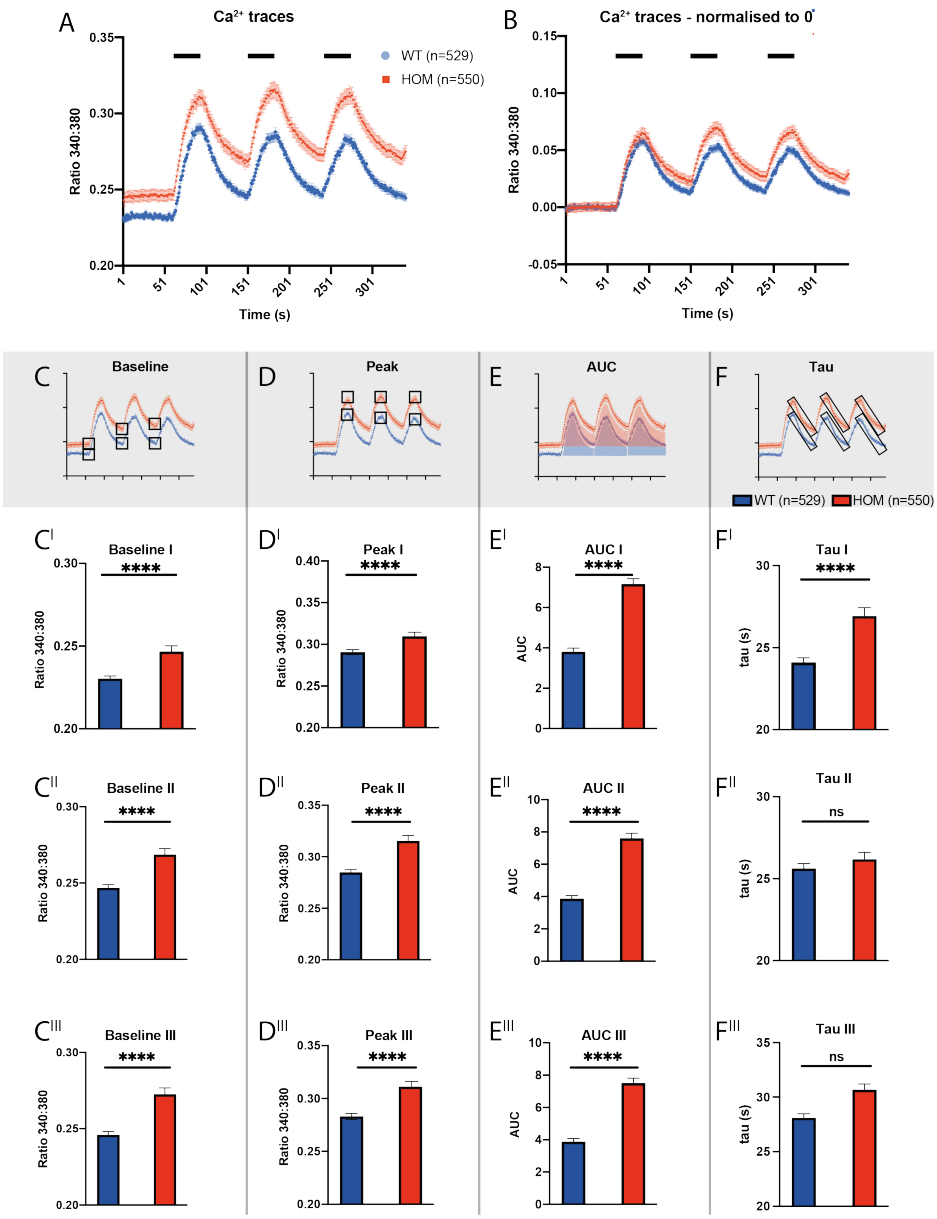


Figure. 3.2 Ca^{2+} maging properties of dorsal horn neurons from NCX3 HOM mice show significant differences to neurons from control NCX3 WT mice.

A - Scatter plots to show mean Ca^{2+} traces during the course of the experiment (NCX3 WT in blue, NCX3 HOM in red), n=529 WT and 550 HOM neurons, from 5 WT and 5 HOM mice. **B** - Scatter plots to show mean Ca^{2+} traces during the course of the experiment, normalised to 0 – shows difference between genotypes when baselines equal. **C-F** – assessed properties of the calcium imaging traces, top panels in grey are schematics explaining the properties compared in panels below, **C** – baselines at 60 seconds (baseline I - C^{I}), 150 seconds (baseline II - C^{II}) and 240 seconds (baseline III - C^{III}), **D** – peaks at 90 seconds (peak I - D^{I}), 180 seconds (peak II - D^{II}) and 270 seconds (peak III - D^{III}), **E** – Area under the curve (AUC) for 60 to 150 seconds (AUC I - E^{I}), 150-240 seconds (AUC II - E^{II}) and 240-330 seconds (AUC III - E^{III}), **F** - Exponential decay time constant (tau) for 90 -150 seconds – (decay I - F^{I}), 180 to 240 seconds (decay II - F^{II}) and 270 to 330 seconds (decay III - F^{III}). Data are mean ± SEM. Data are mean ± SEM. Significance was assessed with unpaired Students t-test and ****-$p<0.0001$.

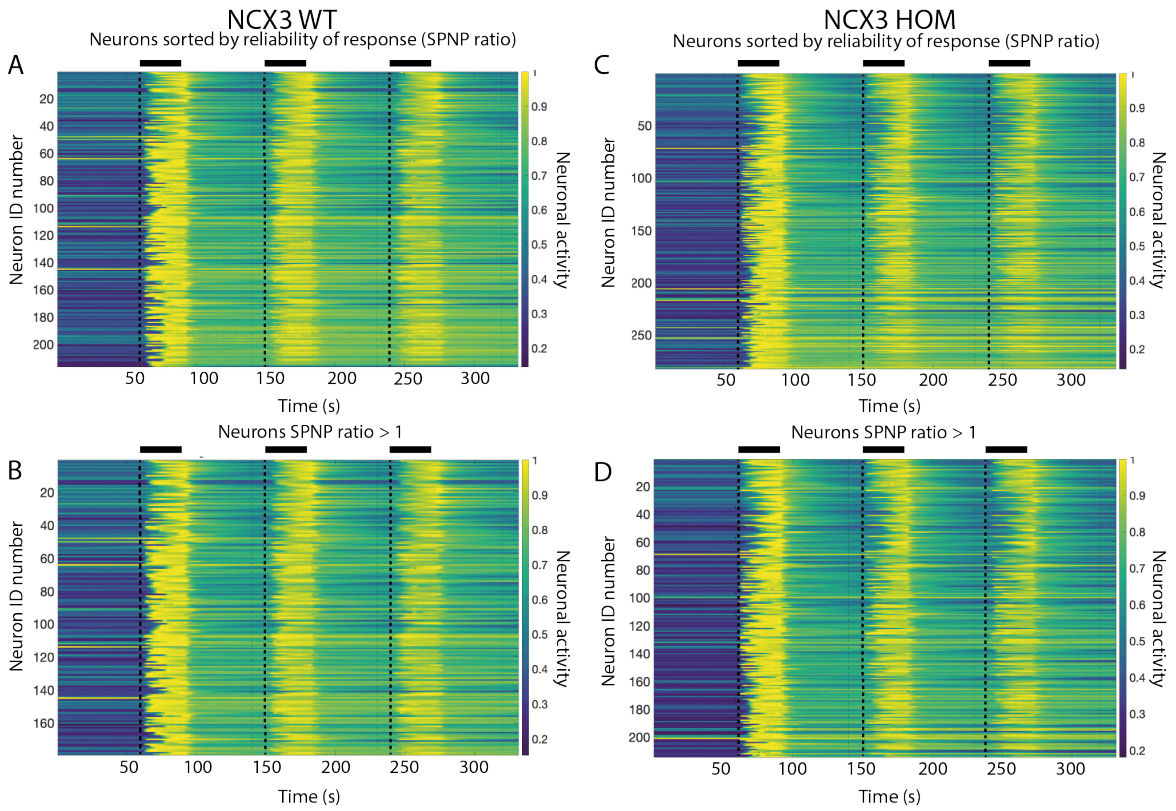


Figure. 3.3 Sorting of cultured DRG neurons based on calcium imaging response reliability.
A and C - Raster plots showing the Ca^{2+} responses of DRG neurons to 50mM K^+ pulses (each pulse starting at 60, 150 or 240 seconds and lasting for 30 seconds). Beginning and duration of each K^+ pulse showed with dashed vertical lines and black bars. Neurons were sorted based on similarity of their three Ca^{2+} responses (reliability, as in (Figure 1.1)). Neurons at the top of the raster plots had the most reliable responses, while the ones at the bottom did not display high level of reliability. The raster plots show 216 WT DRG neurons from 5 mice, **A** and 282 HOM DRG neurons from 6 mice, **C**; **B and D** - Raster plots showing the DRG neurons from **A** (NCX3 WT) and **C** (NCX3 HOM), respectively, which displayed reliability of response higher than 1 (179 cells from 5 mice and 215 neurons from 6 mice). Raster plot colour scheme – blue to yellow – low to high Ca^{2+} level.

Next, we performed the same tests as described for Figure 3.2 and reported the results in Figure 3.4. In contrast to our DH analysis, we saw no significant difference in our DRG group for any of the properties tested, in any of the K^+ pulses (the only exception was the first baseline in Figure 3.4C^I which showed a small but significant difference). This was visualised in Figure 3.4A and B, where we show the DRG scatter plots either as raw data, or after normalising the 0 to 60 seconds baseline to zero. The baselines at 60s, 150s and 240s were as follows – 0.29±0.008 for WT and 0.26±0.008 for HOM; 0.5±0.02 for WT and 0.5±0.01 for HOM, 0.5±0.02 for WT and 0.5±0.01 for HOM, respectively (Figure 3.4C, C^I to C^{III}). The peak results at 90 seconds, 180 seconds and 270 seconds also showed no significant difference between the genotypes – 0.74±0.03 for WT and 0.71±0.02 for HOM; 0.7±0.03 for WT and 0.7±0.02 for HOM, 0.7±0.02 for WT and 0.65±0.02 for HOM, respectively (Figure 3.4D, D^I to D^{III}). Next, the mean AUC values we recorded were also not significantly different and were as follows – 26.4±1.8 for WT and 26.12±1.3 for HOM; 27±1.8 for WT and 26.2±1.3 for HOM, 26.3±1.8 for WT and 25.6±1.3 for HOM (Figure 3.4D, D^I to D^{III}). Finally, we performed a single exponential decay fit to each cell of our data set, and each decaying response. Representative traces, showing this fit, can be seen in Figure 3.5C and D. We calculated the decay time constant (tau) for each cell and each of the three pulses. Our results are reported in Figure 3.4E (E^I to E^{III}) and are as follows – 14.8±1.1s for WT and 19±4s for HOM; 15.4±0.7s for WT and 16.1±0.6s for HOM, 16.5±1.1s for WT and 16.9±0.6s for HOM.

This negative result from the dorsal root ganglia supports our hypothesis that the mechanism of action of NCX3 is likely through altered nociceptive processing within the dorsal horn. This is consistent with our negative result for acute pain behaviour (Chapter 2) and strengthens the importance of the dorsal horn.

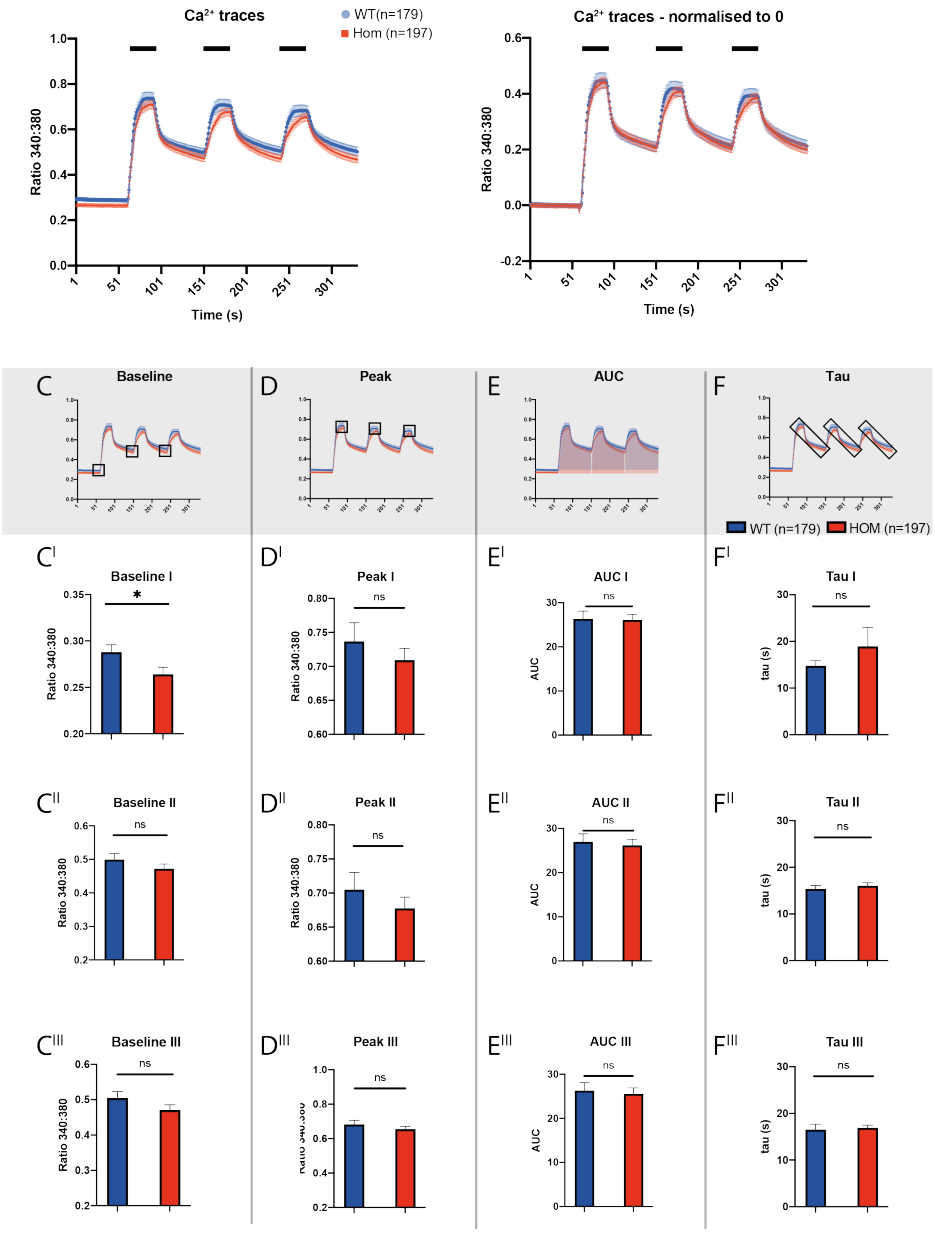


Figure. 3.4 Ca^{2+} maging properties of DRG neurons from NCX3 HOM mice show no significant differences to neurons from control NCX3 WT mice.

A - Scatter plots to show mean Ca^{2+} traces during the course of the experiment (NCX3 WT in blue, NCX3 HOM in red), n=179 WT and 197 HOM neurons, from 5 WT and 5 HOM mice. **B** - Scatter plots to show mean Ca^{2+} traces during the course of the experiment, normalised to 0 **C-F** - assessed properties of the calcium imaging traces, top panels in grey are schematics explaining the properties compared in panels below, **C** – baselines at 60 seconds (baseline I - C^I), 150 seconds (baseline II - C^{II}) and 240 seconds (baseline III - C^{III}), **D** – peaks at 90 seconds (peak I - D^I), 180 seconds (peak II - D^{II}) and 270 seconds (peak III - D^{III}), **E** – Area under the curve (AUC) for 60 to 150 seconds (AUC I - E^I), 150-240 seconds (AUC II - E^{II}) and 240-330 seconds (AUC III - E^{III}), **F** - Exponential decay time constant (tau) for 90 -150 seconds – (decay I - F^I), 180 to 240 seconds (decay II - F^{II}) and 270 to 330 seconds (decay III - F^{III}). Data are mean ± SEM. Significance was assessed with unpaired Students t-test and ns – $p>0.05$ and *-$p<0.05$.

3.3.2 Loss of NCX3 produces enhanced wind-up of deep dorsal horn neurons

Given the expression of NCX3 in the dorsal horn and the elevated second phase formalin response in NCX3 HET and NCX3 HOM mice (Chapter 2), as well as the evidence for changes in the Ca^{2+} qualities of dorsal horn neurons in culture, we next chose an *in vivo* method to investigate the role of NCX3 in the spinal cord processing of non-noxious and nociceptive stimuli. *in vivo* electrophysiology was performed to record from (wide-dynamic range) WDR neurons from depths delineating lamina V/VI (NCX3 WT 547 ± 22 μm; NCX3 HET 593 ± 15 μm; NCX3 HOM 598 ± 19 μm).

A range of natural stimuli were applied to the receptive field. Consistent with the behavioural observations (Chapter 2), there were no genotype differences in the evoked neuronal responses to punctate mechanical (Figure 3.6A and B) and heat stimuli (Figure 3.6C and D) across a range of stimulus intensities. In addition, there were no genotype differences in the neuronal responses to dynamic brushing (Figure 3.6E and F) and noxious evaporative cooling of the receptive field (Figure 3.6G and H). Receptive fields were mapped with a 15 g von Frey and were also comparable between genotypes (Figure 3.6I).

As explained above, wind-up has been interpreted as the capacity to amplify nociceptive signals and shares many features with central sensitisation. Wind-up of WDR neurons was calculated following a train of electrical stimuli delivered transcutaneously. Current thresholds for activation of A- and C- fibres did not differ between the genotypes (Figure 3.7A). Compared to NCX3 WT mice, however, the input (i.e. the non-potentiated response) was elevated in NCX3 HET and NCX3 HOM mice (Figure 3.7B). We observed an input of 428.2±26spikes in WT mice, in comparison to 580±42spikes in HETs and 592.4±40.5spikes in HOMs.

In response to a sub-optimal stimulation frequency (0.2 Hz) neurons from NCX3 WT mice exhibited minimal increases in neuronal excitability (Figure 3.7C, C^{I}-C^{III}), whereas neurons from NCX3 HET and NCX3 HOM mice exhibited higher levels of wind-up. This effect is visualised in Figure 3.7C^{I}, where the increased number of spikes at each consecutive stimulus is obvious for the mutants and missing in the WT controls. As a result, the cumulative number of spikes for WT was 135.2±20, while for the mutants it was almost tripled – 330.7±48 for HETs and 332.3±45 for HOMs (Figure 3.7B). These excess spikes were attributed to elevated neuronal activity in the A-, C- and post-discharge (PD) latency ranges (Figure 3.7C^{II}).

In contrast, at an optimal stimulation frequency (0.5 Hz) the degree of wind-up did not differ between genotypes (Figure 3.7D, D^{I} and D^{III}), though there were increased numbers of neuronal events in the A- and PD latencies (Figure 3.7D^{II}). We recorded 447.6±53 spikes for WT, 552.2±52 for HETs and 537.8±57.1 for HOMs (Figure 3.7B).

3.3.3 Generation of NCX3 AAV

Having explored the effect of NCX3 deficiency *in vitro*, *in vivo* and behaviourally, we next aimed at studying its therapeutic potential. Due to the current lack of NCX3 activators, we designed an NCX3 adeno-associated virus, which would allow us to overexpress the gene of interest in WT mice and test their formalin behaviour in comparison to controls. We hypothesise that the viral delivery of NCX3 would be able to improve the Ca^{2+} extrusion of DH neurons and therefore reduce the behavioural response in the second phase of the formalin test.

NCX3 has 2 known isoforms in mice – NCX3-AC, reported mainly in muscle tissue and NCX3-B, considered to be the neuronal isoform (Michel et al., 2014). In order to confirm this, we performed qPCR and found that, as expected, NCX3-AC

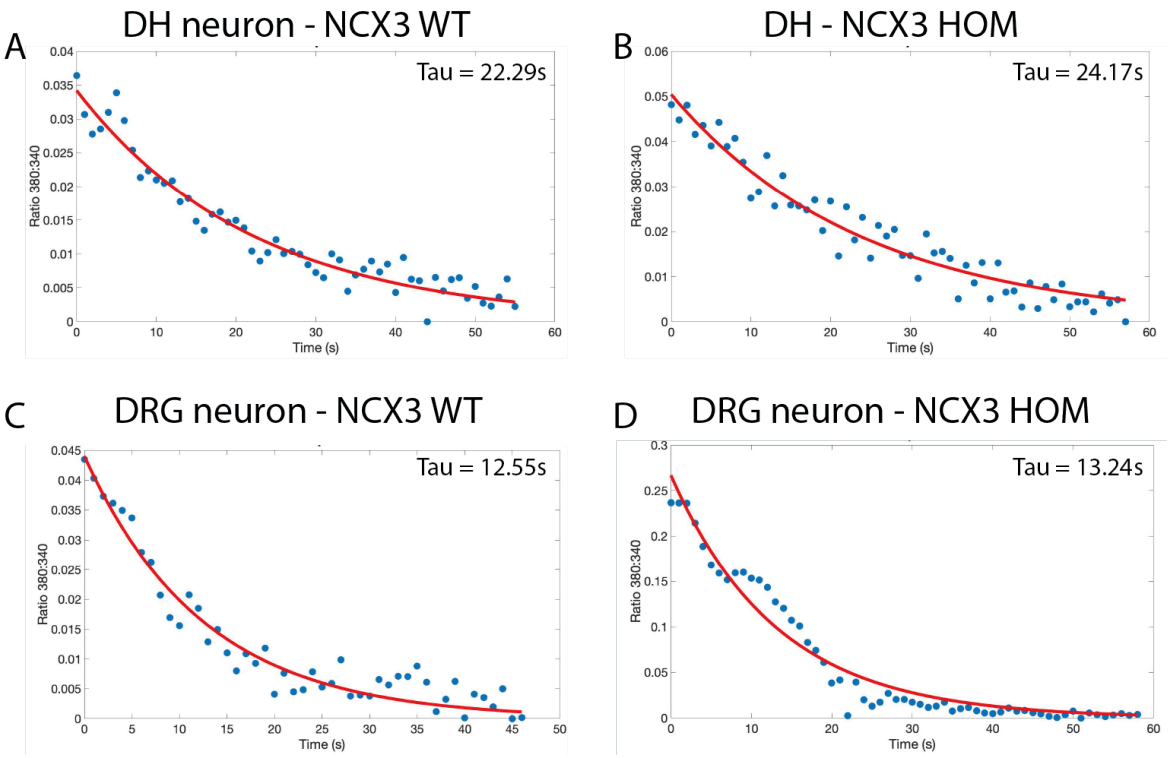


Figure. 3.5 Representative traces of single exponential decay fit of single cells from each of the four groups of neurons.
Results were presented in Figure 1.2 (dorsal horn neurons) and Figure 1.4 (DRG neurons). Single tau values reported in each panel.

mRNA had a low expression level in neuronal tissue. In comparison, NCX3-B was 323, 526 and 271 times more expressed in the brain, spinal cord and DRG, respectively (Figure 1.8A). Therefore, we cloned the NCX3-B isoform into an AAV vector as explained in Figure 1.8B. After production, the generated virus was added to the medium of cultured HEK cells and DRGs. The expression of the protein was then demonstrated via its c-Myc tag and it was, as expected, on the membrane of both types of cells (Figure 3.8C and D).

This experiment added another piece of evidence, this time from an *in vivo* model, showing the potential for hyper-sensitivity in NCX3 mutant mice. The animals in this experiment exhibited significant wind-up in response to what in WT is a sub-optimal

frequency, which normally does not induce wind-up. This allows us to suggest that NCX3 deficiency can lead to the accumulation of Ca^{2+} in dorsal horn neurons, which can then cause summation of responses and wind-up, in response to lower frequency stimulation.

3.4 Discussion

In Chapter 2, we explored the expression of NCX3 in the DRG and spinal cord, confirming its presence in pain circuits. We also investigated the behaviour of an NCX3 knock-out mouse and found a significant phenotype in the second phase of the formalin test. As NCX3 is a calcium-extrusion protein and the second phase of the formalin test has been linked to central sensitisation of spinal cord circuits, we hypothesised that mutant dorsal horn neurons in culture would exhibit abnormal Ca^{2+} extrusion after activation. Chapter 3 provides evidence in support of this hypothesis and shows enhanced wind-up in mutant dorsal horn neurons *in vivo*.

3.4.1 Abnormal calcium handling in cultured dorsal horn neurons

As mentioned previously, we first tested the Ca^{2+} handling properties of cultured dorsal horn neurons. During initial imaging experiments, I noted that differentiating between neurons and glial cells in culture, based on morphology alone, was difficult. Therefore, some glial cells, which are not expected to respond to K^+ , were included and their contribution to the final result was unavoidable. We also observed neurons which responded once and showed no return to baseline throughout the experiment. We suspected that these neurons might be unhealthy and dying. In order to optimise our

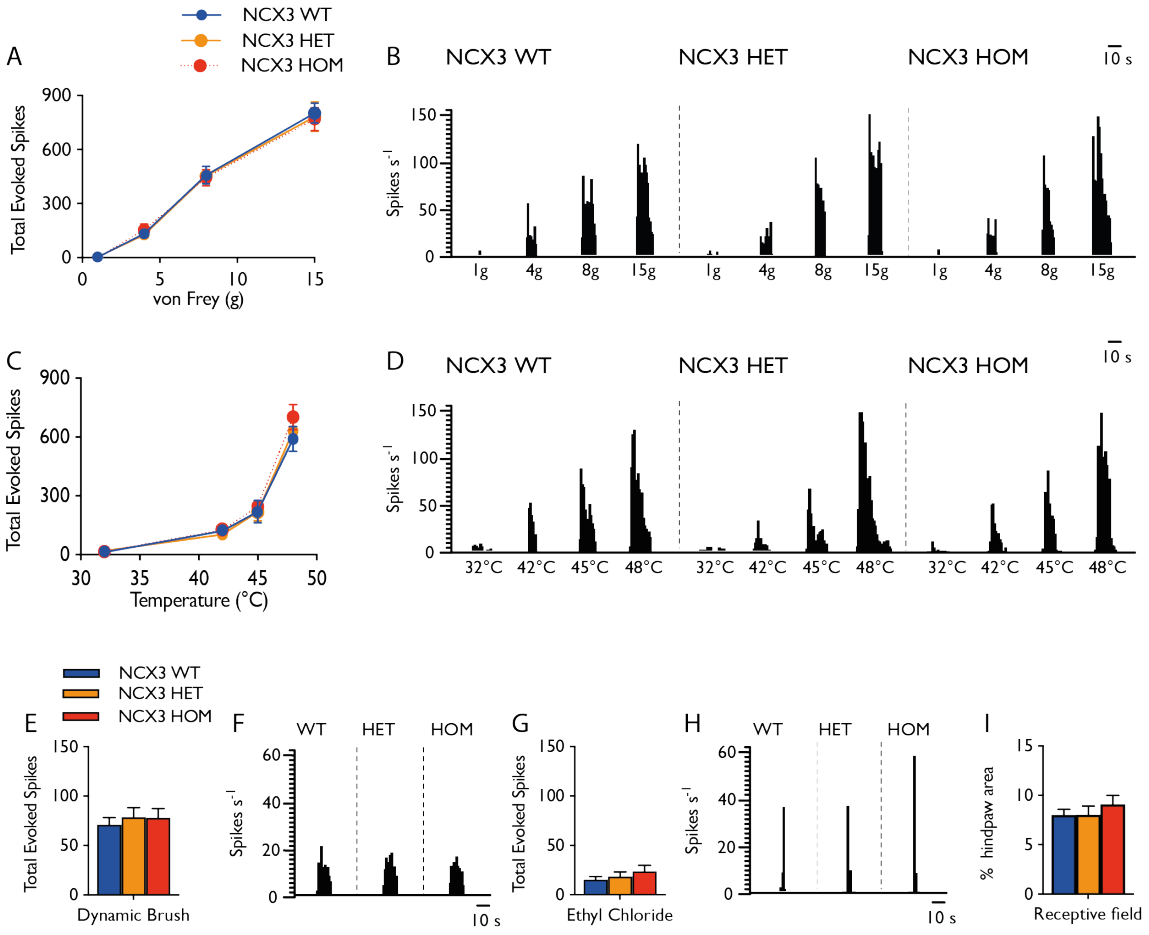


Figure. 3.6 Normal sensory coding of deep dorsal horn neurons in NCX3 WT, HET and HOM mice.

A, C, E and G - Evoked neuronal responses to punctate mechanical, **A**, heat, **C**, dynamic brush **E**, and noxious evaporative cooling **G** stimulation of the receptive field. **B, D, F and H** - Histogram traces depicting representative single unit responses. **I** - Receptive field size to a noxious punctate mechanical stimulus **E**. Data represents mean ± SEM. NCX3 WT n=21, NCX3 HET n=20, NCX3 HOM n=20. Two-way ANOVA (A and C) and One-way ANOVA (E, G and I), Bonferroni multiple comparisons test; No significant changes found.

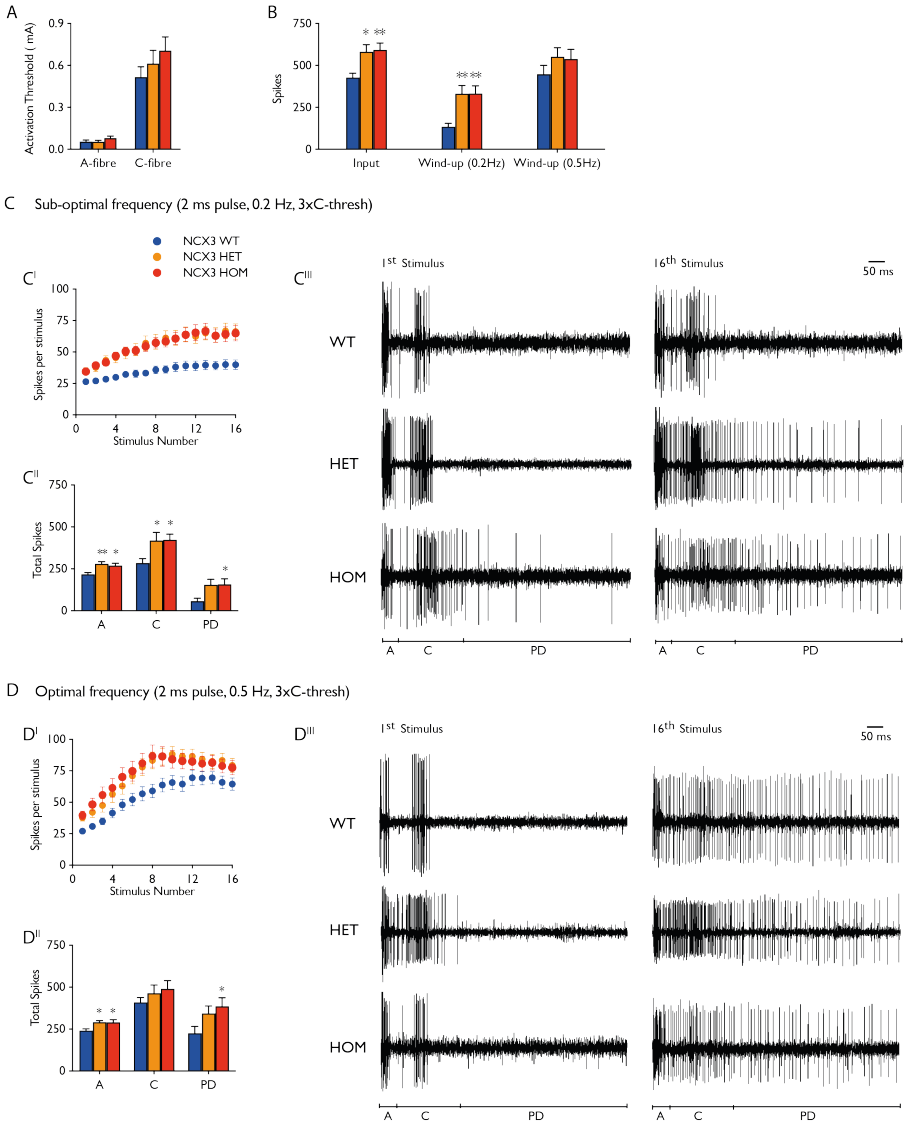


Figure. 3.7 Increased wind-up of deep dorsal horn neurons in NCX3 HET and NCX3 HOM mice vs NCX3 WT controls.
A. - Electrical thresholds for activation of A- and C-fibres; **B** - Input, and wind-up following 0.2 Hz and 0.5 Hz stimulation; **C** - Wind-up of deep dorsal horn neurons (0.2 Hz) expressed as mean number of spikes per stimulus number (C^{I}). Total spikes evoked separated according to latency: A: 0–50 ms, C: 50–250 ms, PD (post-discharge) >250 ms (C^{II}). Representative spike traces (C^{III}). **D** - Wind-up of deep dorsal horn neurons (0.5 Hz) expressed as mean number of spikes per stimulus number (D^{I}), total spikes evoked separated according to latency (D^{II}), representative spike traces (D^{III}). Data represents mean ± SEM, *P<0.05, **P<0.01. One-way ANOVA, Bonferroni multiple comparison test; NCX3 WT n=21, NCX3 HET n=20, NCX3 HOM n=20.

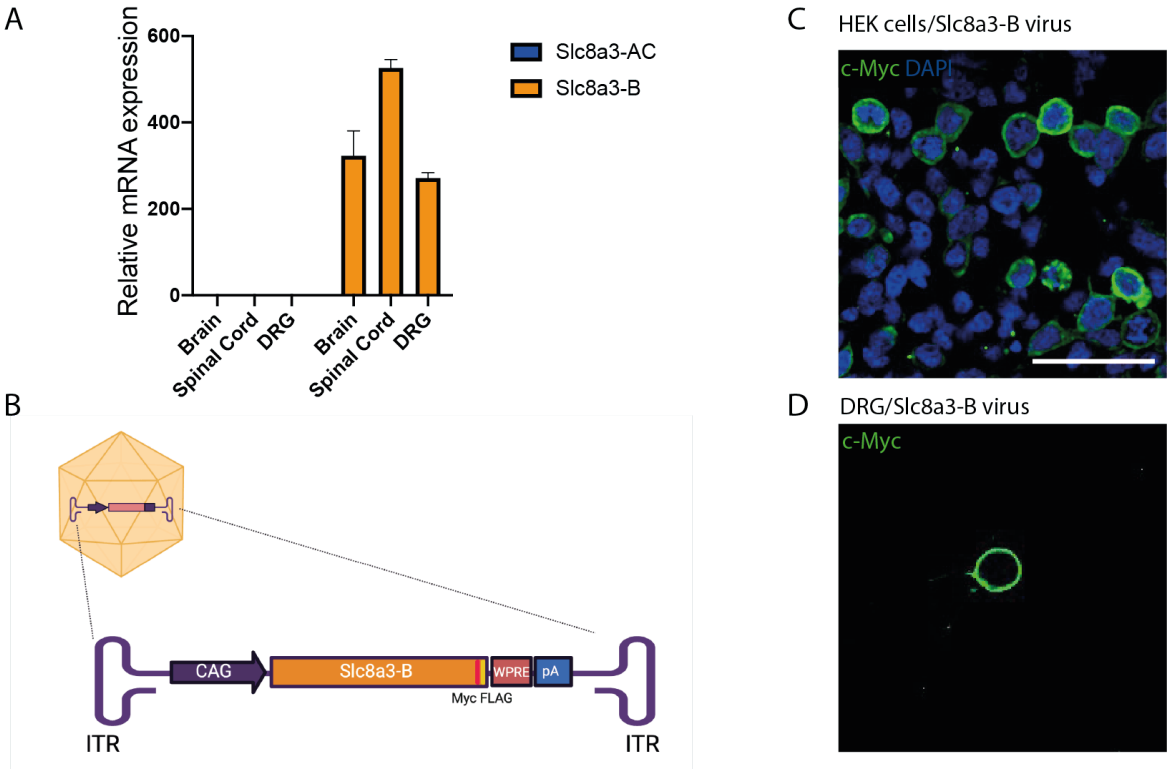


Figure. 3.8 Design of an adeno-associated virus (AAV) carrying the *Slc8a3*-isoform B.

A A - Quantitative Real Time PCR for *Slc8a3* isoform AC and B in brain, spinal cord and DRG; **B** – design of *Slc8a3*-B AAV, carrying the gene of interest tagged with Myc and FLAG tags at the C-terminus. Sequence also contains short CAG promoter, the post-transcriptional regulator element WPRE and a poly-A tail, packaged between two inverted terminal repeat (ITR) sites. **C** – Viral expression on the membrane of HEK cells and **D** – cultured DRG neurons. Scale bar = 50μm.

analysis of calcium imaging data, we developed a Matlab script, applying a previously published, unbiased method for assessing the ability of each neuron to respond to K^+ over the course of the experiment (Sahani M, Linden J, 2003). As a result, we selected a population of neurons, which is still heterogeneous but lacks some of the noise previously generated by non-neuronal cells or dying neurons. We cannot exclude the possibility that a small number of healthy neurons were also removed, but under the conditions and exclusion criteria we chose, we found significant and meaningful phenotypes and we applied exactly the same criteria to WT and HOM mice.

As seen in Figure 1.2, the dorsal horn neurons from NCX3 HOM mice, showed an increased baseline, suggesting that even under conditions of rest, these neurons retain more Ca^{2+} than WT neurons. This effect has been reported before in primary hippocampal neurons from NCX3 knock-out mice (Molinaro et al., 2011). This was a surprising observation, as NCX3 represents a high threshold calcium extrusion mechanism (Blaustein and Lederer, 1999; Scheff et al., 2014; Dipolo and Beaugé, 2006) and therefore it should clear calcium only at high intracellular concentrations. However, according to Boyman et al. (2011); Tal et al. (2016) NCX-mediated ion-currents are elevated ∼25-fold when the cytosolic [Ca^{2+}]i level rises from 0.1 to 2 μM and the exchanger has very dynamic and versatile Ca^{2+} -binding abilities. This means that NCX could have a small contribution to Ca^{2+} in resting states, and this could vary depending on the isoform. In addition, there are other reports which have shown baseline phenotype in selected populations of neurons, when the Na^+ in the bath solution was replaced with Li^+ (i.e. the activity of the NCX family of proteins was inhibited). Scheff et al. (2014) concluded that the NCX family of proteins had two modes of activity – one that affected resting [Ca^{2+}]i (active in resting states) and one that did not (only active during high neuronal activity).

Another report, from (Verdru et al., 1997), also found a baseline phenotype associated with the NCX group of proteins, but only in a sub-group of neurons in culture (discussed below). This observation points to the heterogeneity of neuronal populations. This is also true for our dorsal horn cultures and therefore, further analysis of our data, where we separate the sampled neurons into sub-populations according to their calcium dynamics, might be informative.

The other phenotypes that we observed in our mutant neurons were increased peak Ca^{2+} levels, increased AUCs and slowed Ca^{2+} clearance. All three changes are consistent with the lack of an important calcium extruder in the mutant cultures as well as with the previous phenotypes, observed in our study of NCX3. Interestingly, changes in decay kinetics have been previously observed by Molinaro et al. (2011) in hippocampal cultures from mice with an NCX3 deletion. In addition, similar decay phenotype has also been seen in DRG neurons, after replacing bath Na^{+} with Li^{+} Verdru et al. (1997); Scheff et al. (2014). Therefore, the published data from other neuronal populations supports our findings in the dorsal horn.

We also performed calcium imaging using DRG cultures and saw no significant differences. This was an encouraging result as it is consistent with: **1/** our anatomical data, pointing to strong NCX3 expression in non-nociceptive DRG neurons, and much less in the IB4+ and CGRP+ populations; **2/** the lack of phenotype in acute pain behaviour experiments and the first phase of the formalin test, which are mainly associated with the DRG. As mentioned in Chapter 2 (Subsection 2.4.1 and 2.4.2)., previous work by Scheff et al. (2014) showed NCX3 role in DRG nociceptors and found an acute pain phenotype linked to NCX3 deficiency. The caveats of this study were discussed in detail in Chapter 2 (Subsection 2.4.1 and 2.4.2). Interestingly, the same publication also showed that NCX3 was involved in the duration of high K+-evoked Ca^{2+} transients. Similar results were also observed previously by the same group (Lu

et al., 2006). Other authors (Verdru et al., 1997) had similar observations but only in sub-populations of DRG neurons. Interestingly, in the majority of their cells the decay of intracellular Ca^{2+} could be fitted with a single exponential, while a smaller group of neurons displayed biphasic Ca^{2+} extrusion. The decay phenotype was only observed in a sub-population of the monophasic group of neurons, after NCX family inhibition. This data points to the possibility that DRG neurons may exhibit NCX3-specific deficits, but only in selected neuronal populations.

It is important to note that all studies in the DRG used a non-specific method for NCX inhibition (replacement of the bath Na^+ with Li^+, or an NCX3 inhibitor with limited specificity (see Chapter 2 - Subsection 2.4.1, Iwamoto and Shigekawa (1998)). Therefore, the deficits found could be due to the other two isoforms of the NCX family or other Na^+-dependent membrane proteins, and not NCX3. Last but not least, the lack of phenotype seen in our DRG cultures could also be due to compensatory mechanisms, such as the sarco/endoplasmic reticulum calcium ATPase (SERCA), mitochondrial stores and other mechanisms (Lu et al., 2006). Nevertheless, as we performed the same procedure and analysis protocol in DH and DRG cultures and the difference between the two populations was striking, it is likely that the NCX3 protein has different roles in these two populations.

With regards to the analysis methodology we used, it is also important to note that both Verdru et al. (1997) and Scheff et al. (2014) chose to analyse their calcium imaging experiments by taking "the neuron" as a biological unit and observed population-specific differences. This is consistent with our approach and highlights the heterogeneity of different neuronal groups and therefore, the likelihood of losing important nuance when taking "the animal" as a biological unit.

In summary, based on the data we present in this thesis, the evidence points to a strong phenotype observed in DH neurons and a lack of such phenotype in the DRG.

This is consistent with our behavioural data, which showed a phenotype in the second phase of the formalin test (spinal cord-driven). By contrast, we saw no difference in the acute phase of the test or in experiments assessing evoked behavioural responses to noxious stumuli, which are, broadly speaking, linked to the DRG. Further study of the sub-populations in our cultures as well as the use of other methods, such as *in vivo* Ca^{2+} imaging, would be important future aims.

3.4.2 Loss of NCX3 produces exacerbated wind-up of deep dorsal horn neurons

After observing a difference in the intrinsic Ca^{2+} dynamics of DH neurons *in vitro*, we were interested in an *in vivo* method, that could show wind-up in a live animal. To this purpose, we employed *in vivo* electrophysiology and recorded from WDR neurons. We saw no differences in the evoked responses to punctate mechanical and heat stimuli (Figure 1.5C and D). We also observed a lack of phenotype to dynamic brush and evaporative cooling. This is consistent with our behavioural experiments, in which we saw no difference between the genotypes after von Frey, Hargreaves, hot plate or pinprick tests.

We next looked into the ability of WDR to wind-up and any differences caused by the lack or reduction of the NCX3 protein expression. We first looked at input(I), which measures the number of action potentials evoked by the first stimulus, i.e. the non-potentiated response. Interestingly, we saw a gene-dosage-dependent difference. This could be due to a **1/** pre-synaptic difference, where either the direct signal from the periphery is increased or the indirect, spinal cord signalling is amplified through circuit changes; **2/** post-synaptic effect caused by a hypersensitivity of the WDR neurons themselves. We cannot conclude which of these options is the most likely one,

but we can speculate that the lack of alteration in Ca^{2+} dynamics in DRG neurons (Figure 1.6) points to a more central mechanism.

We next looked at the response to repetitive stimulation and the ability of WDR neurons to wind up. We applied 16 stimuli at the optimal frequency of 0.5Hz and observed no striking phenotype (Figure 1.7D). As the responses evoked by A-fibers (0-50ms) and C-fibers (50-250ms) were separated and quantified on the basis of latency, we did see small but significant increase in the number of neuronal events at the A- and PD (post-discharge, later than 300ms) latencies. It is difficult to interpret this result, especially when the overall wind-up effect was not elevated, but it was promising to see an abnormality at a stimulation frequency of 0.5Hz.

Interestingly, the phenotype observed was much more striking when we applied the repetitive stimulation at a sub-optimal frequency (0.2Hz). Under these conditions, both the HET and HOM mice produced wind-up, while the WT controls did not. This striking effect means that in our mutant mice, lower frequency stimulation could cause summation of responses and an increased cumulative number of spikes. Therefore, events that should not "code for" wind-up, could lead to this form of plasticity and potentially an even longer-lasting sensitisation. This is consistent with our Ca^{2+} imaging data where we observed higher Ca^{2+} peaks and longer extrusion time in the mutant neurons, which could lead to summation of repetitive stimuli. Another important observation is that the phenotype of the heterozygotes is very similar (although in some cases less marked) to our homozygotes. These gene dosage effects suggest that a reduction in the NCX3 protein levels can have a physiologically relevant effect and therefore the phenotypes we observed were not limited to the complete absence of NCX3.

In conclusion, the observed wind-up effect is another piece of evidence supporting the mechanism underlying our formalin phenotype and even our GWAS result. Although

it is difficult to find direct correlations between mice and humans, it is interesting to note that temporal summation in patients with fibromyalgia occurred at lower forces and lower frequency stimulation than in control subjects (Staud et al., 2003). In addition, the painful after-sensations in these patients were greater in amplitude and more prolonged.

3.4.3 Generation of NCX3 AAV for overexpression in the mouse spinal cord

Next, we focused on the therapeutic potential of NCX3. To this purpose, we generated an AAV which carries the neuronal isoform of our gene of interest. Interestingly, the two isoforms of NCX3 found in mice, are derived from exons A, B and C, with A and B being mutually exclusive (Figure 1.7.1). Alternative splicing then leads to the production of NCX3-AC and NCX3-B. The first one is found mainly in skeletal muscle, whereas the second has been shown in the brain (Quednau et al., 1997; Michel et al., 2014). Consistent with these previous findings, we show a much higher expression of NCX3 in neuronal tissues along the pain axis (DRG, spinal cord and brain). Therefore, we used isoform B to generate our AAV and saw a promising expression in HEK cells and DRGs. Our future aims now include the overexpression of the generated AAV in the spinal cord of mice, followed by observation of their formalin response. We hypothesise that WT mice which received our NCX3 virus will show less pain behaviour in the sensitised phase of the experiment than WT mice overexpressing GFP alone.

3.5 Conclusion

In conclusion, Chapter 3 of this thesis focused on exploring the mechanisms behind our behavioural observations in Chapter 2. We used *in vitro* calcium imaging and in-vivo electrophysiology, both of which showed phenotypes in our mutants in comparison to WT. Based on these data, we propose that the reduction of NCX3 expression is associated with abnormal Ca^{2+} handling during rest and neuronal stimulation. This would render the affected neurons more susceptible to summation of action potentials and wind-up. Looking forward, we have generated an NCX3-containing adeno-associated virus (AAV) whose administration into the mouse spinal cord may show a therapeutic use for NCX3.

Chapter 4

Gas7 - anatomy and modulation of pain behaviour in the mouse

As discussed in the General Introduction of this thesis (Chapter 1), our GWAS discovered significant associations in two separate genes – *Slc8a3* (NCX3), associated with wind-up ratio, and *Gas7* (growth arrest specific protein 7), which showed an association with secondary punctate hyperalgesia after mustard oil (which can be described as enhanced pain perception in response to von Frey hair application in the area surrounding the site of mustard oil application). This chapter will focus on the second GWAS-identified target *Gas7*, and will provide evidence for its expression in the pain circuit. In addition, this chapter will provide data for the behavioural impact of the *Gas7* global knock-out (KO) in mice and finally, it will describe our hypotheses, experimental search for mechanistic explanation of the observed phenotypes, and possible future aims.

4.1 Introduction

4.1.1 Mustard oil as an irritant

Inflammation is a well-known phenomenon which produces pain, swelling and redness of the affected area. It is a part of the body's response to injury and irritation, and therefore many models have been developed to study it. One such model is the application of mustard oil. The active component of this chemical irritant is AITC, allyl isothiocyanate, and is thought to activate TRPA1 channels, producing flare and nociceptive sensitisation (Koltzenburg et al., 1992; Schmid et al., 2019). The inflammatory response to mustard oil also involves sensitisation to heat in the primary area of injury, as well as dynamic mechanical allodynia and punctate hyperalgesia in the secondary zone (a halo of undamaged tissue surrounding the injury (Koltzenburg et al., 1992; Harding, 2013). Interestingly, while some of the components of the injury response are driven by afferent input, the *secondary* punctate hyperalgesia appears independent of the peripheral sensitisation and may remain for a long period of time, linking its mechanism to central sensitisation (Harding, 2013). This is in line with the large amount of evidence pointing towards the central origin of secondary mechanical hyperalgesia (discussed in Chapter 1, Section 1.5) (Torebjork et al., 1992; Klede et al., 2003) .Therefore, our GWAS study pointed to a second target with potential to affect central sensitisation, with the important distinction that while wind-up ratio represents temporal summation (increasing response to repetitive nociceptive stimiluation within the primary affected area), *Gas7* was linked to spatial summation (heightened pain sensitivity experienced with stimulation of wider areas, surrounding the injury).

4.1.2 Overview of Gas7

As a member of the Gas family, the *Gas7* gene is functionally linked to growth arrest. It was first discovered in growth-arrested NIH3T3 cells (Brenner et al., 1989) where Gas7 was shown to induce the outgrowth of cellular processes by an F-actin-dependent mechanism. The authors showed that Gas7 was localised close to the plasma membrane and co-localised with microfilaments. Later studies showed that Gas7 is expressed well in the CNS, and more specifically in the cerebral cortex, cerebellum and hippocampus (Ju et al., 1998; Meyer, 2018). Its function was confirmed in NGF-stimulated PC12 cells (Chao et al., 2003) as well as in cultured cerebellar neurons (Ju et al., 1998). Downregulation of Gas7 in primary cerebellar neurons showed inhibition of neurite outgrowth, while upregulation in neuroblastoma cells led to an increase in the length of processes (Ju et al., 1998). Therefore, Gas7 has an important role in the maturation of neuronal cells.

Domain structure of Gas7

Gas7 is a functional member of the Gas family. However, structurally it has been allocated to the PCH (Pombe Cdc15 homology) protein family (You and Lin-Chao, 2010). Most PCH proteins have an N-terminal FCH domain, a coiled-coil (CC) region and one or two C-terminal Src homology domains (Chitu and Stanley, 2007). In addition, the FCH domain and the CC-region have been represented as a single, extended domain known as F-BAR. FCH-containing proteins have been implicated in the regulation of the cytoskeleton and the interactions with the submembrane region (You and Lin-Chao, 2010). Interestingly, the function of Gas7 has been linked both to its F-BAR domain and an additional region known as WW (Liu et al., 2015). You and Lin-Chao (2010) reported that Gas7 co-localises and physically interacts with N-WASP, a regulator of the Arp2/3 complex, through the WW domain (Diagram D.4.1).

Both Wiskott-Aldrich syndrome protein (WASP) and WASP-family verprolin-homologous protein (WAVE) play an important role in the activation of the ARP2/3 complex which, in turn, activates actin polymerization, as illustrated in (Diagram D.4.1). The formation of actin filaments in sub-membrane regions leads to the generation of cellular protrusions, known as filopodia, and therefore plays an important role in the neurite outgrowth process (reviewed by Takenawa and Suetsugu (2007)). Interestingly, this intracellular cascade has been previously linked to chronic pain and central sensitisation (Kuner, 2017).

Gas7 interaction with N-WASP – functional implications

N-WASP is an important player in the regulation of actin polymerisation. It is usually activated/modulated by Cdc42 and PIP2, but also by a variety of proteins, including Gas7. After activation, N-WASP unwinds, and this leads to the exposure of the VCA domain which then recruits the Arp2/3 complex and initiates actin polymerization (Diagram D.4.1). The formation of actin filaments is then followed by the generation of spike-like cell protrusions, known as filopodia (Fawcett, 2000; Takenawa and Suetsugu, 2007). N-WASP is usually activated by proteins that contain an SH3 domain, which is lacking in mouse Gas7. However, the WW domain of Gas7 has been shown to interact with the Proline-rich regions on N-WASP. This process regulates actin polymerisation and the production of cellular protrusions (You and Lin-Chao, 2010). In addition, the human Gas7-C has an SH3 domain as well as a WW domain, pointing to its importance in modulating N-WASP and the cytoskeleton (Chao et al., 2005; Tsujita et al., 2006; You and Lin-Chao, 2010). The C-terminal domains (FCH and CC) of Gas7 have also been linked to N-WASP interaction, as selective deletions reduce the Gas7-driven actin production (You and Lin-Chao, 2010).

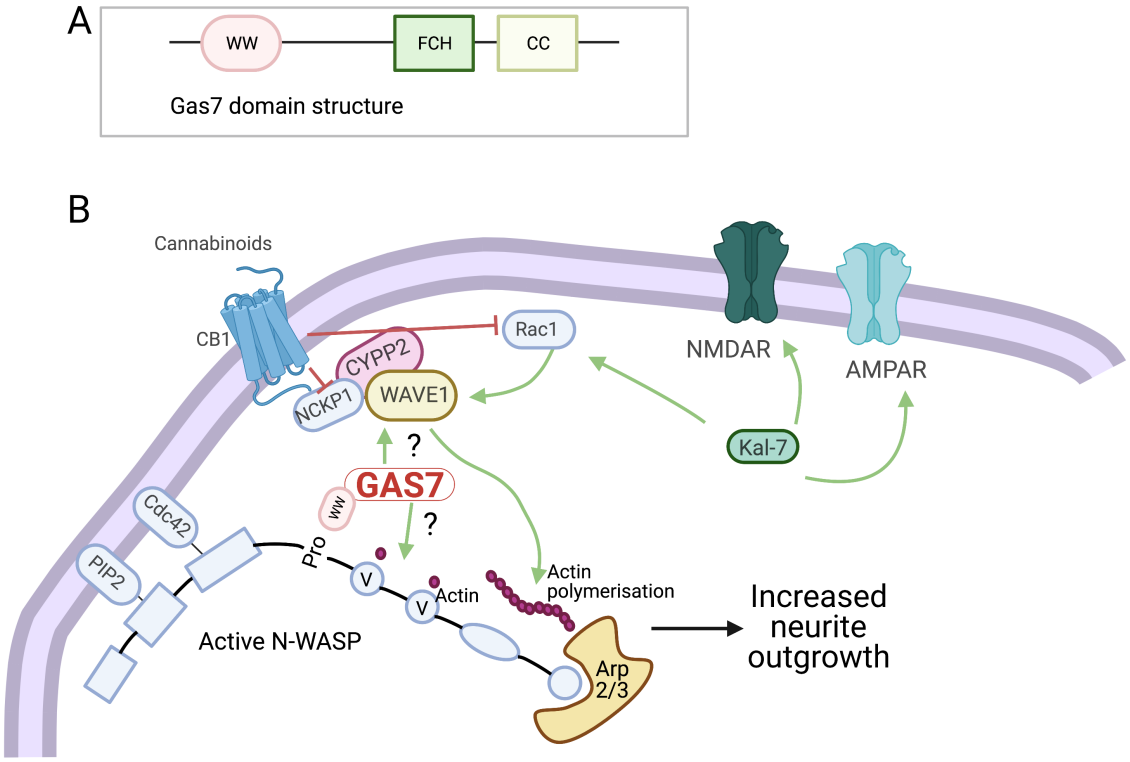


Diagram. D.4.1 Schematic describing the possible role of Gas7 in neurite outgrowth..
A Domain structure of Gas7: WW region – short, conserved region, found in a variety of proteins, with signature repeats of tryptophan residues; FCH and coiled-coil region which are known as the F-Bar domain. **B**. Actin polymerisation signalling: NMDA receptor activation is stimulated by Kal7-Rac1 signalling. This then causes the activation of the WAVE1 complex and Arp2/3-dependent actin polymerisation, which eventually leads to increased spine density. Cannabinoids have been shown to inhibit this pathway. Gas7 regulates N-WASP (and possibly the WAVE complex) through its WW domain. Actin monomers bind to the V region of N-WASP, the Arp2/3 complex is activated, and actin assembly is initiated. This pathway may be a useful link between Gas7 and chronic pain. Schematic is a compilation of figures from (Fawcett, 2000; You and Lin-Chao, 2010; Kuner, 2017). Green arrows show activation of pathways, red arrows – inhibition.

4.1.3 Dendritic spine formation in the spinal cord – implication in chronic pain

The density of synaptic spines on dendrites has been associated with a variety of chronic pain models (both inflammatory and neuropathic) (Tan et al., 2012; Lu et al., 2015). RHO GTPases serve as molecular switches in the actin polymerisation pathway, with Rac1 working as an actin stabiliser. Lu et al. (2015) showed kalirin 7 (kal 7) as one of the upstream regulators of this pathway. Disrupting the kal 7 pathway abrogated activity-dependent spine remodelling and CFA-induced inflammatory pain. This showed a direct link between structural changes and central sensitisation. This process most likely involves not only actin polymerisation but a series of second messengers (such as PKA and ERKs, as well as calcium signalling coming from activated synapses and reaching the nucleus).

As mentioned previously, actin polymerisation leads to filopodia protrusions, which then contribute to the generation of dendritic spines. These structures take part in synaptic and circuit formations (Segev and Rall, 1988; Tan et al., 2009) as they act as bioelectrical transducers (Benson et al., 2020). Therefore, even small changes in their size, location and content (receptors and synaptic vesicles) can significantly alter the propagation of action potentials. For example, mushroom-shaped dendritic spines are linked to the expression of glutamatergic receptors, such as AMPA and NMDA, and therefore an increase in these structures is a signal for increased excitatory neurotransmission (Bourne and Harris, 2008; Benson et al., 2020). Therefore, mushroom-shaped spines can affect input summation and neuronal hyperexcitability associated with central sensitisation (Araya et al., 2006; Tan et al., 2009).

There is a growing body of evidence showing structural changes during prolonged CS, including inflammatory and neuropathic states. For example, Benson et al. (2020)

observed more stable mushroom spines associated with nerve injury-induced chronic pain. Similar results were seen by (Tan et al., 2009), who linked the transition from thin to mushroom spines with the generation of pain after spinal cord injury. Another study by Tan et al. (2011), explored chronic constriction injury and saw that 10 days post-injury the same increase of mushroom-shaped spines occurred, which was also accompanied by increased spine density closer to the cell body. When it comes to inflammatory pain, Lu et al. (2015) discovered that Kal-7 KO from dorsal horn neurons led to a significant reduction of nocifensive behaviour in the second phase of the formalin test, which was correlated with a decrease in spine density in the spinal cord.

4.1.4 Aims and hypotheses

In summary, the importance of neurite outgrowth and spine generation in central sensitisation and pain, is becoming clearer. The evidence in both neuropathic and inflammatory models is growing and pointing more to a dynamic process of remodelling after injury. Many reports show the change in shape, size and number of dendritic spines in response to injuries and disease insults (Halpain et al., 2005). This, therefore, puts the GWAS-identification of *Gas7* into context and provides us with the hypothesis that this gene might have a role in secondary hyperalgesia following an inflammatory stimulus. To test this we examined its expression along the nociceptive pathway, the possible behavioural outcomes of its genetic deletion and its impact on the morphology of spinal neurons.

4.2 Materials and Methods

4.2.1 Histology

Tissue preparation

For our immunohistochemistry and *in situ* hybridisation experiments, we followed the protocol from Chapter 2, Subsection 2.2.2. Briefly, mice were perfused transcardially and DRG and spinal cords were dissected, post-fixed and dehydrated in sucrose. This was followed by freezing and cryostat cutting.

Immunohistochemistry and *in situ* hybridisation

The process followed for immunohistochemistry and *in situ* hybridisation was similar to the one in Chapter 2, Subsection 2.2.2. The primary and secondary antibodies are stated in Table 4.1. Immunostaining was visualized using a confocal microscope (Zeiss) and images were acquired using the Zen black software.

For *in situ* hybridisation (singleplex), we used the RNA Scope 2.5 Red chromogenic assay kit (Biotechne, 322350) and followed the manufacturer's instructions. The protocol used is similar to the one described in Chapter 2, Subsection 2.2.2. Briefly, after -80°C storage, tissue was allowed to reach room temperature and was then washed with PBS. Next, tissue was pre-treated with hydrogen peroxide at RT (for DRG - 2-minute pre-treatment, for spinal cords – no pre-treatment) and protease at 40^{o}C (for DRG – 20-minute protease treatment, for spinal cord – 15 minutes). Slides were then incubated with the *Gas7* probe for 2 hours at 40^{o}C in the supplied RNAscope oven (Table 4.1 for probe details). This was then followed by six amplification steps, with Amplification 5 lasting 30 minutes for DRG samples and reduced to 15 minutes for spinal cord tissue. All other amplification steps were performed as per manufacturer's instructions. The development stage of the protocol involved a fast red reaction, which

lasted 10 minutes for both DRG and spinal cords. Any modifications to the protocol were optimised to reduce background staining and improve signal. ISH was followed by immunohistochemistry, where the standard protocol described in Chapter 2 was used. Staining was visualised with a confocal microscope and images were acquired using the Zen black software.

Image analysis

Analysis of the signal intensity for *in situ* hybridisation studies was performed on spinal cord tissue only. The cells positive for *Gas7* mRNA were defined as those containing 3 or more red dots co-localising with each NeuN, eGFP (either GlyT2-eGFP, Gad67- eGFP or vGLUT2-eGFP) or PAX2-marked cell. The total number of NeuN, eGFP and PAX2-positive cells as well as the number of NeuN+/*Gas7*+, eGFP+/*Gas7*+ and PAX2+/*Gas7*+ was counted. Then the double positive cells were calculated as percentage of the NeuN, eGFP, or PAX2-postive neurons.

Multiplex *in situ* hybridisation and analysis (performed by Dr Andrew Bell, Professor A. Todd's laboratory)

For *in situ* hybridisation (multiplex), we used RNA Scope Multiplex Kit V1 (Biotechne, cat number: 320851). This protocol was performed on fresh frozen tissue and the manufacturer's instructions were followed. The protocol for tissue preparation is identical to Chapter 2, Subsection 2.2.2. Following this procedure, the slides were treated with probes and amplification buffers as per manufacturer's instructions (see Table 4.1) for probe details). They were then mounted in prolong-glass anti-fade medium with NucBlue (Hoechst 3342S, ThermoFisher Scientific, Paisley, UK). Staining was visualised with a confocal microscope LSM710, with a 40x oil objective.

Analysis was conducted on a single representative optical section from the centre of the image stack using the cell detection and sub-cellular objects features of Qupath software (Bankhead et al., 2017).

Recognition and segmentation of individual nuclei was performed based on NucBlue staining and an additional 1μm perimeter was added to each nucleus to allow detection of perinuclear transcripts. Single RNA transcripts for each target gene appeared as individual puncta and detection thresholds were adjusted manually until the mark-up accurately reflected the transcript distribution. Cells were defined as positive for a marker if they contained >3 transcripts.

4.2.2 Behavioural studies

Mouse line and animal housing

All procedures were carried out in accordance with UK home office regulations. Animals were housed in IVCs and their welfare was continuously assessed throughout all procedures. The temperature and humidity of the rooms were monitored at all times and food and water were freely available.

Behavioural procedures

Gas7 KO mice, $Gas7^{em1}$, were generated at UC Davis/The Jackson Laboratory for the Knockout Mouse Phenotyping Program (KOMP). The production strategy involved the deletion of 320 base pairs of the *Gas7* gene. This included exon 4 and 234 base pairs of flanking intronic sequence. The mutation is predicted to lead to a premature truncation of the protein at residue 91. The mice were generated and bred on a C57Bl/6NJ background. To date, there are no published studies using this mouse line.

We used heterozygous breeding strategy to obtain *Gas7* WT, HET and HOM littermates. Both male and female adult mice were used for behaviour studies. As explained in Chapter 2, at the start of each set of behavioural experiments, mice, aged 8-10 weeks, were acclimatised to the testing equipment for 2-3 days prior to each test. For motor and acute sensitivity tests, baseline values were obtained by averaging data from 3 experimental sessions. For most behavioural experiments, we used the following cohort of mice: 6WT ($n_{females}$=4, n_{males}=2), 8 HET ($n_{females}$=4, n_{males}=4) and 8 HOM ($n_{females}$=4, n_{males}=4). The hot plate and rotarod tests were performed on a second cohort as well, bringing the total of mice used to 14WT ($n_{females}$=8, n_{males}=6), 16HET ($n_{females}$=8, n_{males}=8), 16HOM ($n_{females}$=8, n_{males}=8). The Capsaicin test was performed on a separate cohort of 5 WT ($n_{females}$=3, n_{males}=2), 8 HET ($n_{females}$=4, n_{males}=4) and 8 HOM ($n_{females}$=3, n_{males}=5) mice. All tests were carried out in the same room, at similar times of the day, by the same experimenter, who was blind to all animal genotypes and handled the mice in a random order. No animals were excluded from the above-mentioned cohorts. The method for statistical analysis is outlined below. We report this mouse line and experiments according to (Percie du Sert et al., 2020).

For behavioural testing, we followed the same experimental procedures as in Chapter 2, Subsection 2.2.5. Therefore, we performed tests assessing motor ability (Open Field, RotaRod and Beam Walk Test) as well as behavioural response to thermal and mechanical stimuli (von Frey, Pin Prick, Hargreaves and Hot Plate). We finished our behavioural study with two sensitising tests, namely formalin (described previously, Subsection 2.2.5) and capsaicin (described below).

Capsaicin test

For our capsaicin test, we used 3μg of capsaicin (Sigma) diluted in sterile saline with 1% ethanol and 0.5% tween in a volume of 10μl. We injected our cohort subcutaneously,

in the ankle area (lateral side of the ankle, in close proximity to the heel). This experiment was designed to test both the acute sensitivity to capsaicin but also the sensitisation effect in the secondary area of the injury – the plantar surface of the paw. To this purpose, we first recorded the duration of the pain behaviour in the first 5 minutes after capsaicin administration (licking, shaking, biting, repetitive lifting of the paw). This was followed by von Frey assessment of the ipsi- and contralateral paws (method described in Chapter 2, Subsection 2.2.5) at 15min, 30min, 1h and 24h post-injection.

Data analysis

Data are shown as the mean ± SEM. Statistical tests were carried out in GraphPad prism 9.0 and the tests used, are specified in each legend. Briefly, all experimental groups were tested for normality, using the Kolmogorov-Smirnov test. When more than two experimental groups were tested, we performed one-way ANOVA with Dunnett's multiple comparisons test. For our formalin and capsaicin tests, we analysed behaviour results over time and therefore, we used two-way ANOVA with Dunnett's multiple comparisons test.

4.2.3 Electrophysiology

Collaboration with Dr. Ryan Patel, A. Dickenson's laboratory

In vivo electrophysiology of spinal cord wide dynamic range neurons was performed following the protocol from Chapter 3, Subsection 3.2.2 and as previously described by Dawes et al. (2018). Both male and female *Gas7* mutant mice - 6 mice in the WT group ($n_{females}$=4, n_{males}=2) and 9 in the *Gas7* HOM group ($n_{females}$=3, n_{males}=6) - were used at age 7-8 months. Of these mice, we recorded from a total of 6 neurons in

each group. *In vivo* electrophysiological procedures were non-recovery; at the end of experiments mice were terminally anesthetised with isoflurane.

4.2.4 Assessment of dendritic spine morphology in *Gas7*-KO mice

Collaboration with Dr Andrew Bell and Dr Allen Dickie, at Professor A. Todd's laboratory

To study the dendritic spines of spinal dorsal horn neurons in *Gas7* KO mice, we crossed our mouse line with a *Tac1*^{Cre} knock-in mouse line (*Tac1*-IRES2-Cre-D; The Jackson Laboratory, Bar Harbor, ME, USA; Stock number 021877). The resulting offspring mice were injected with an AAV Brainbow vector (Cai et al., 2013), which codes for Cre-dependent, membrane-targeted teal fluorescent protein (TFP) and mCherry (AAV9-EF1a-BbChT, referred to as AAV-BB2).

The labelled *Tac1* neurons are excitatory and express substance-P. Structurally, they are part of the lamina II radial cell population. Lamina II has been previously studied in the context of spinal cord changes in neuropathic injury Cao et al. (2017). As mentioned previously, we performed multiplex ISH hybridisation to confirm the co-localisation of *Gas7* and *Tac1*, prior to this experiment.

Two *Tac1*^{Cre}/*Gas7* WT and two *Tac1*^{Cre}/*Gas7* HOM ($n_{females}$=2, n_{males}=2) mice, aged 6 - 8 weeks were anaesthetised with isoflurane, in addition to perioperative analgesia (buprenorphine 0.3 mg/kg and carprofen 5 mg/kg) and placed in a stereotaxic frame. Each mouse was subjected to surgery, where the vertebral column was exposed and an intraspinal injection of 500 nl of the Brainbow virus (Table 4.1) was administered, at a rate of 30 nl/min. This was done on the right side, 400 μm lateral to the midline and at a depth of 300 μm below the pial surface. In addition, the injection was targeted

to the L5 spinal segment. The incision was closed, and mice were allowed to recover. 2 weeks post-surgery, the mice were anaesthesised with pentobarbitone (30mg, ip) and perfused transcardially with 4% fresh PFA. The spinal cords were then dissected out and post-fixed for 2h in PFA. The fixed tissue was then placed in 30% sucrose for 2-3 days and stored at -80^{o}C.

To investigate the dendritic spine morphology in the spinal cord of WT vs HOM mice, we then cut the tissue into 60μm thick parasagittal sections, focusing on the L5 segment. This was followed by immunohistochemistry against mTFP. Briefly, the sections were incubated for 72 hours at 4^{o}C with mTFP primary antibody (Table 4.1). After washing, the tissue was incubated with a biotinylated secondary antibody (Table 4.1) for 24 hours at 4^{o}C, followed by a an Streptavidin-Pacific blue (1:1000) for 4 hours at room temperature. All antibodies were diluted in PBS with 0.3% Triton-X and 5% normal donkey serum. As the procedure was performed on free-floating sections, they were then mounted in antifade mounting medium and stored until imaging. The resulting slides were scanned with a Zeiss LSM710 confocal microscope equipped with Argon multi-line, 405 nm diode, 561 nm solid state, and 633 nm HeNe lasers.

Analysis of dendritic spines

The produced scans were analysed with Neurolucida for Confocal software (MBF Bioscience, Williston, VT, USA). The investigator was blind to the genotype of the neurons studied. The cell bodies, dendritic trees and dendritic spines were reconstructed in 3 dimensions and the type of dendritic spines (thin vs mushroom) was recorded. A protrusion from a dendrite branch was considered a spine when a clear neck structure was present. Spines with head-like enlargements, with diameter less than the neck of the spine, were considered “thin”. If the head diameters were larger than the neck length, the recorded spines were considered “mushroom”. This was done following instructions from Kim et al. (2006); Cao et al. (2017). The data extracted from

the reconstructions included the following parameters: spine length, spine number (mushroom vs thin), dendrite length. The spine density and the ratio of mushroom to thin spines was then calculated. We also performed Scholl analysis to study the location of the above-mentioned structures – $<25\mu$m or $>25\mu$m from the cell body.

REAGENT	SOURCE	Dilution	IDENTIFICATION
Primary antibodies			
Sheep anti-CGRP	Enzo Life Sciences	1:400	Cat# BML-CA1137, RRID: AB_2050885
Rabbit anti-CGRP	Peninsula Laboratories	1:1000	Cat# T-4032, RRID: AB_2313775
Isolectin B4 (IB4), conjugated to biotin	Sigma-Aldrich	1:100	Cat# L2140, RRID: AB_2313663
Mouse anti-NF200	Sigma-Aldrich	1:250	Cat# N0142, RRID: AB_477257
Rabbit anti-PAX2	Thermo Fisher Scientific	1:200	Cat# 71-6000, RRID: AB_2533990
Chicken anti-NeuN	Millipore	1:500	Cat# ABN91, RRID: AB_11212808
Chicken anti-GFP	Abcam	1:1000	Cat# ab13970, RRID:AB_300798
Rat anti-mTFP	Kerafast	1:500	Cat# EMU103
Secondary antibodies			
Donkey anti-rabbit IgG Alexa 488	Thermo Fisher Scientific	1:1000	Cat# A-21206, RRID:AB_2535792
Goat anti-rabbit IgG Pacific blue	Thermo Fisher Scientific	1:500	Cat# P-10994, RRID: AB_2539814
Streptavidin Pacific Blue	Thermo Fisher Scientific	1:500	Cat# S11222
Donkey anti-mouse IgG Alexa 488	Thermo Fisher Scientific	1:1000	Cat# A-21202, RRID: AB_141607
Goat anti-mouse IgG Pacific blue	Thermo Fisher Scientific	1:500	Cat# P31582, RRID: AB_10374586
Donkey anti-sheep IgG Alexa 488	Thermo Fisher Scientific	1:1000	Cat# A-11015, RRID: AB_2534082
Donkey anti-rabbit IgG Alexa 546	Thermo Fisher Scientific	1:1000	Cat# A10040 , RRID: AB_2534016
Goat anti-chicken Alexa 488	Thermo Fisher Scientific	1:1000	Cat# 11039, RRIDAB_2534096
Anti-rat Biotin	JacksonImmunoResearch	1:500	Cat# 712-065-150
Chemicals, Peptides, Recombinant and Viruses			
Formaldehyde solution	Sigma-Aldrich	1:20	Cat#252549
Capsaicin	Sigma-Aldrich		Cat#M2028
AAV-EF1a-BbChT(AAV-BB2)	Addgene		Cat#45186
Commercial kits and probes			
RNAscope 2.5 HD Reagent Kit-RED	Biotechne		Cat# 322350
RNAscope® Fluorescent Multiplex Detection Reagent kit	Biotechne		Cat# 320851
RNAscope® Probe- Mm-Gas7	Biotechne		Cat# 518561
Experimental Models: Organisms/Strains			
Gas7em1(IMPC)J	The Jackson Laboratory/UCD		Stock number 047805-UCD
Tac1-IRES2-Cre-D	The Jackson Laboratory		Stock number 021877
Genotyping primers Gas7em1(IMPC)J			
Gas7_F	Life Technologies		CTCAGGAGATGGTGGAGGAG
Gas7_R	Life Technologies		GATGGTCACATTCCTAAATTCCA
Software and Algorithms			
ImageJ/Fiji	NIH		https://imagej.nih.gov/ij/index.html, https://fiji.sc/
Prism 9.0	GraphPad Software		https://www.graphpad.com/
Avidemux	Avidemux		https://avidemux.en.softonic.com/mac
Neurolucida	MBFBioscience		https://www.mbfbioscience.com/neurolucida
QuPath	QuPath		https://qupath.github.io

Table 4.1 Reagents used in Chapter 4.

4.3 Results

4.3.1 Anatomical studies show expression of *Gas7* mRNA in the dorsal root ganglia and the spinal cord

Our first aim was to study the expression of the *Gas7* mRNA in the DRG and spinal cord. As with our NCX3 work, we carried out *in situ* hybridisation experiments in combination with immunohistochemistry. We found very little expression of *Gas7* mRNA in the cell bodies of primary sensory neurons, with the major expression observed in the space between neurons, likely in glial cells (Figure 4.1A-C). Therefore, we focused on the expression of this gene in the spinal cord. This time, the signal was much stronger in neuronal cell bodies and *Gas7* mRNA co-localised with NeuN. Our quantification showed that around 50% of the neurons in the more superficial laminae of the spinal cord expressed *Gas7* (44.6 ± 4% in lamina I and 64.3 ± 4.1% in lamina II and 66.7 ± 4% in lamina III). The gene was less expressed in the deeper laminae – around 30 ± 3.2% in lamina IV and 15.7 ± 1.7% in lamina V (Figure 4.1D-F). This was encouraging as we observed the majority of *Gas7* mRNA punctae in the area of the dorsal horn associated with nociception.

4.3.2 Anatomical studies show all interneuronal populations express *Gas7* mRNA.

Next, we focused on the expression of *Gas7* in the excitatory and inhibitory neurons in the spinal dorsal horn. As in Chapter 2, we used three mouse lines - vGluT2-eGFP mice (Gong et al., 2003), marking excitatory interneurons, Gad67-EGFP mice (Tamamaki et al., 2003), labelling GABAergic inhibitory neurons or GlyT2-eGFP mice (Zeilhofer et al., 2005) used to mark inhibitory, glycinergic neurons (tissue was a gift

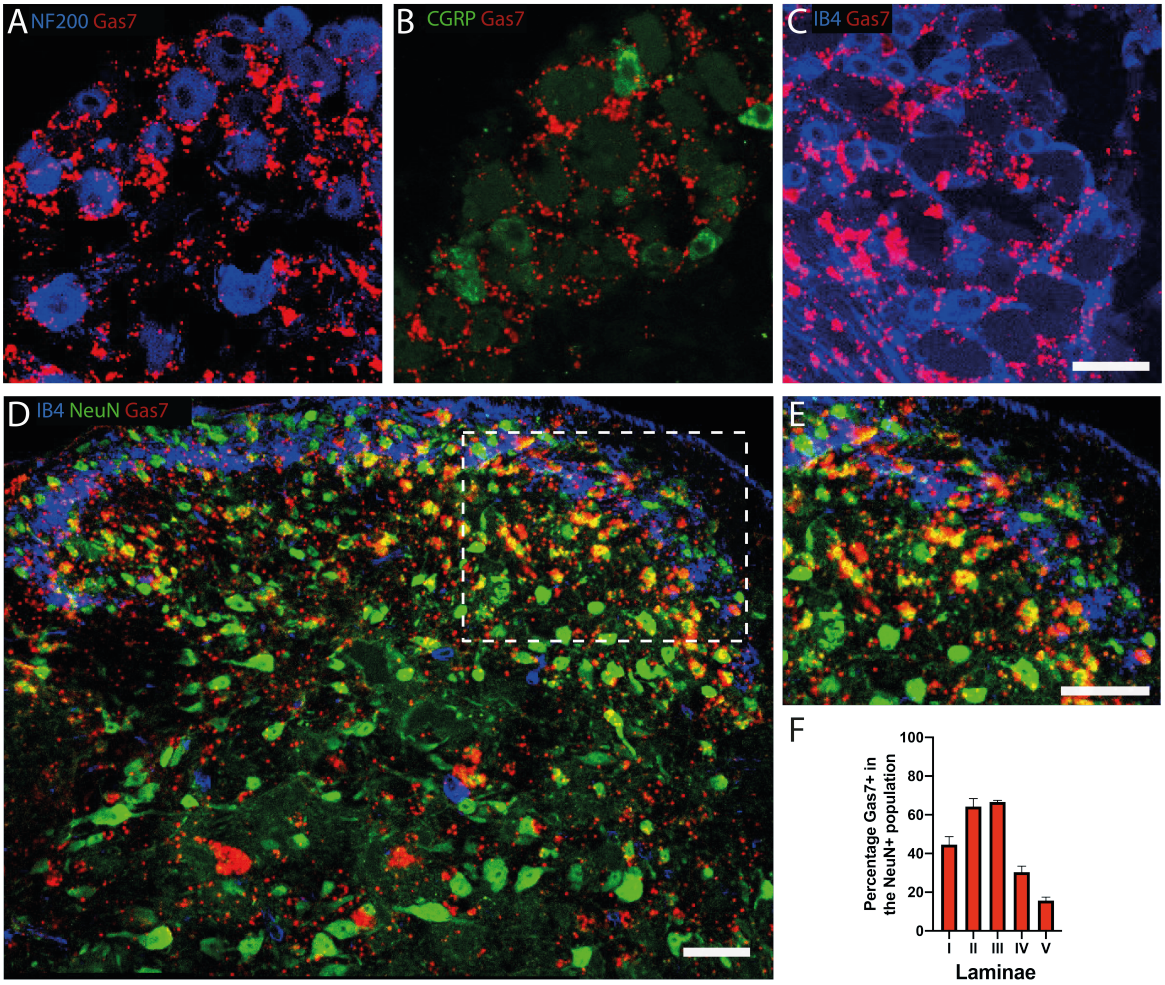


Figure. 4.1 *Gas7* is likely expressed in DRG glia and co-localises with NeuN in the spinal dorsal horn.
textbfA-C. Representative images of *Gas7* in-situ hybridisation (ISH) combined with immunofluorescence for DRG neuronal markers (NF200, CGRP, IB4). textbfD. Representative image of *Gas7* in-situ hybridisation (ISH) combined with immunofluorescence for NeuN (green) and IB4 (blue). textbfE. Magnified image corresponding to the image in D. textbfF. Quantification of the data from D – percentage of *Gas7*-positive cells in the NeuN-positive neuronal population in laminae I to V in the spinal dorsal horn (3 images per animal, n=3 animals). Data are mean ± SEM. Scale bar = 50 μm.

from Prof H. Zeilhofer's laboratory, University of Zurich). We saw that the *Gas7* mRNA was expressed in all three populations, although to differing proportions – 26.2 ± 1.7% in the vGluT2 population, 41 ± 3.7% for Gad67 and 24 ± 2% for GlyT2. As with our Slc8a3 target, we saw no preference for inhibitory or excitatory interneurons (Figure 4.2A-C, E).

This observation was also confirmed in our next experiment, where we used another marker for inhibitory interneurons in the spinal dorsal horn - PAX2. This protein has been shown to be expressed by all inhibitory interneurons in laminae I-III (Foster et al., 2015; Larsson, 2017). The overlap between antibody staining for PAX2 and in-situ hybridisation for *Gas7* was 42.7 ± 4% for superficial laminae and 32 ± 6.4% for deeper laminae, showing a parallel with the above-mentioned results in GABA- and glycinergic population (Figure 4.2D and E). The lack of preference for a specific interneuronal population was also confirmed in other experiments, independent to this one, which will be described below ((Figure 4.6).

4.3.3 Behavioural assays in a Gas7 knock-out mouse line show hyposensitivity to hot plate, capsaicin and the second phase of formalin.

To test our hypothesis that Gas7 may modulate pain behaviour, we used a global knock-out mouse line. We designed our behavioural experiments looking for motor, mechanical, thermal and acute pain behaviours, as well as sensitised pain phenotypes.

To test motor and anxiety levels, we performed open field, rotarod and beam walk test (Figure 4.3F-J). We observed no significant differences in any of these tests. The results in the open field test were as follows: 88 ± 8.6 boxes entered by WT mice, 88.28 ± 8 (HET), 77 ± 9.3 (HOM), showing a lack of phenotype in our mutants in comparison

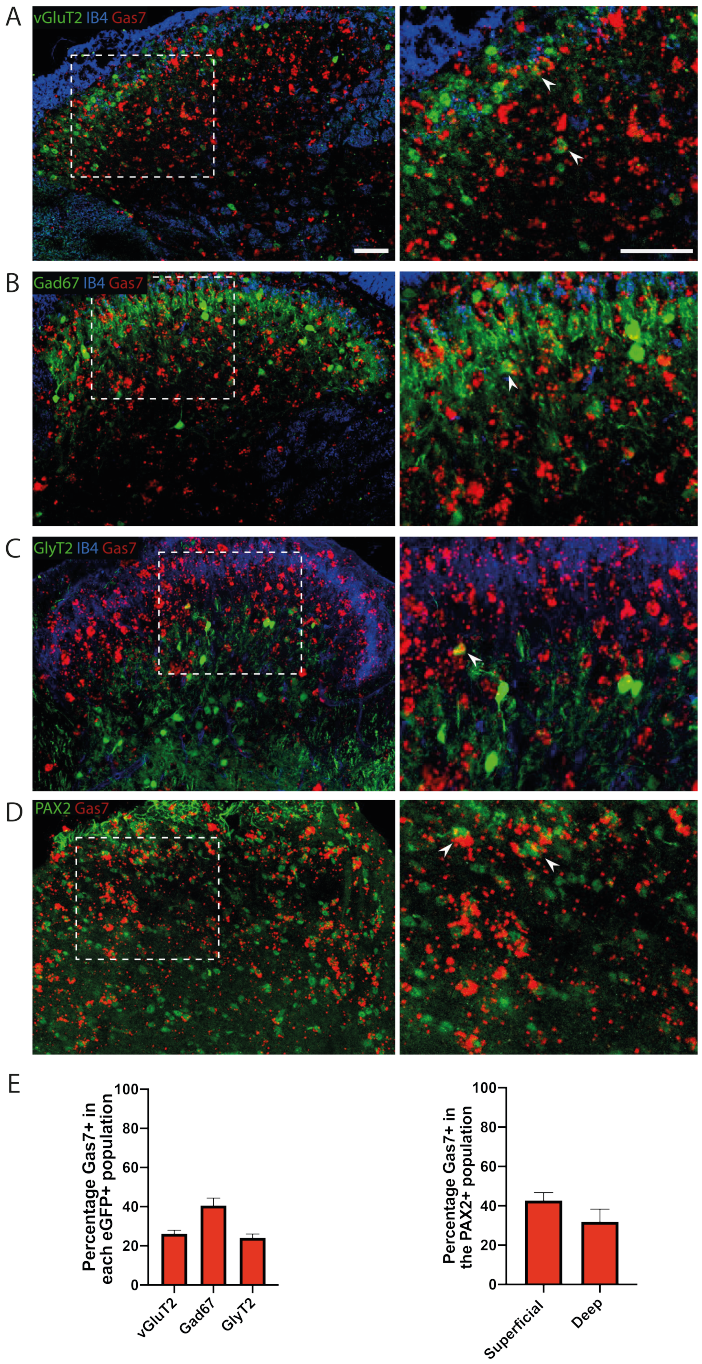


Figure. 4.2 *Gas7* mRNA co-localises with both excitatory and inhibitory spinal cord interneuron markers.
textbfA-D. Representative images of *Gas7* in-situ hybridisation (ISH) combined with immunofluorescence for interneuron markers in the spinal cord (vGluT2-eGFP, GAD67-eGFP, GlyT2-eGFP and PAX2). Right panels show zoomed-in images. E. Quantification of the images from A-D - data were quantified as percentage of *Gas7*-positive cells in the eGFP-positive or PAX2-positive populations (3 images per animal, n=3 animals). Data are mean ± SEM. Scale bar = 50 μm.

to controls. In addition, there was no significant difference in the rearing behaviour of our mice – 17.3 ± 1.3 (WT), 20.3 ± 2.6 (HET) and 16.3 ± 2.4 (HOM). Another test we performed was rotarod, with results also showing a lack of phenotype – 31 ± 7.6s (WT), 32.8 ± 7.3 (HET) and 46.5 ± 9.2 (HOM), when we used a 28rounds/minute protocol. Similar non-significance was observed at a faster rotation speed of 32rpm – 25.4 ± 7.11s (WT), 24.8 ± 4s (HET) and 31 ± 6s (HOM). On the beam walk test, used to assess balance and co-ordination, there was once again no significant change – 93% ± 1.8 for WT, 83% ± 5.2 for HET and 88% ± 2.8 for HOM.

This result was encouraging as, similarly to our NCX3 KO line, it points towards preserved motor function. In our next tests, we observed lack of phenotypic differences, with the exception of hot plate. For example, our von Frey tests showed similar thresholds - 0.55±0.06 for WT, 0.58±0.04 for HET and 0.53±0.03 for HOM animals. We also saw no significant difference in the response to noxious pinprick, where the withdrawal latencies were: 156.4 ± 7.5ms for WT, 166.8 ± 17.8ms for HET and 165.4 ± 7.9 for HOM. Similarly, non-significant changes were observed with most thermal thresholds: Hargreaves (11.7 ± 0.75s WT, 10.5 ± 0.5s HET and 11.7 ± 0.8s HOM); hot plate at 53^{o}C (10.6 ± 0.5s WT, 10.9s ± 0.6s HET and 10.3s ± 0.6s HOM), (Figure 4.3A,B,D and E). Interestingly, we observed significant hyposensitivity in our homozygote GAS7 KO mice on the hot plate test at 50^{o}C, which was a consistent result in the two cohorts we tested. The results were as follows: 18.3 ± 0.8s WT, 17.7s ± 0.8s HET and 21s ± 0.7s HOM.

These results showed that Gas7 is unlikely to be linked to severe phenotypes in response to motor, innocuous or acute noxious stimulation in the mouse, but also directed us to a possible heat-related hyposensitivity. Next, we used the formalin test to explore the acute and sensitised response of our mutants. We saw a subtle hyposensitivity phenotype in the second phase of the experiment, pointing us once

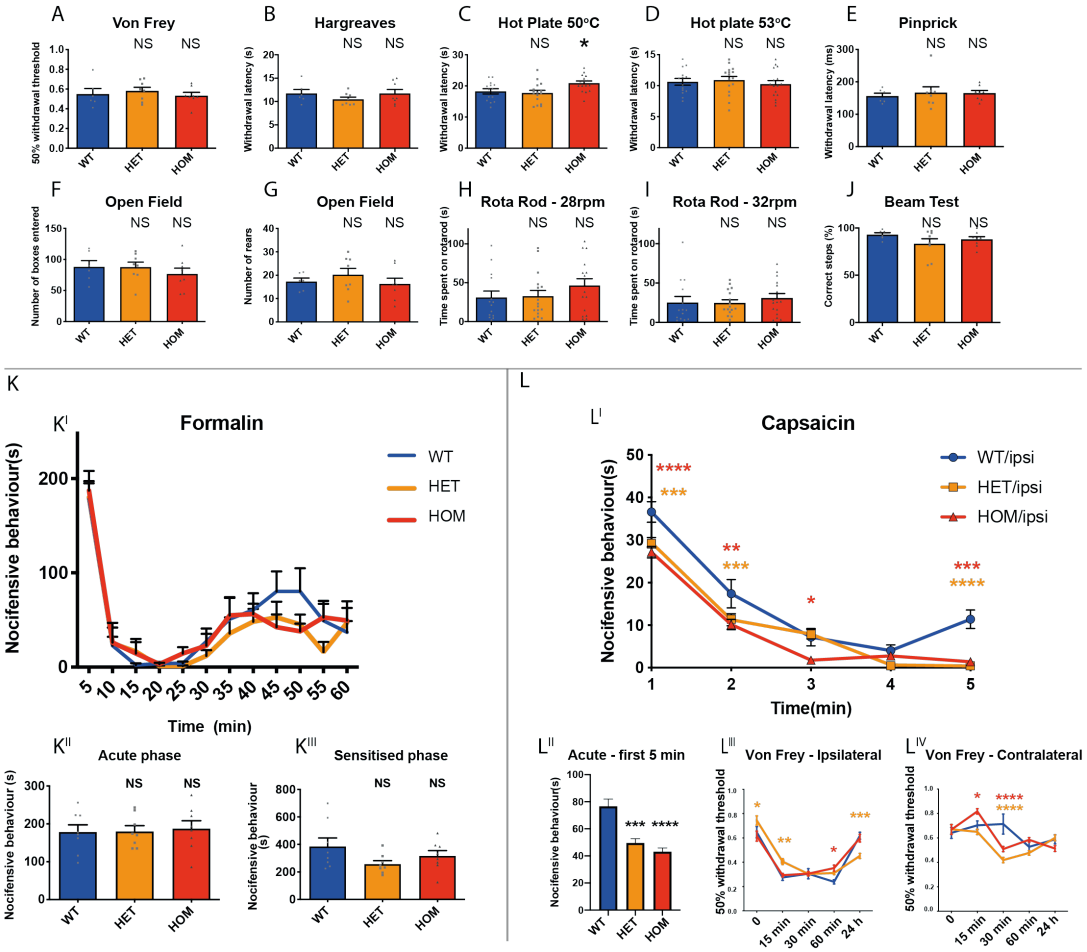


Figure. 4.3 Gas7 KO line – behavioural results.
A-E. Acute tests for innocuous and noxious stimuli; **F-J.** Motor/balance/anxiety behavioural tests; **K.** Formalin test; $\mathbf{K}^{II}$ - mean results from the first 5 minutes of the test; $\mathbf{K}^{III}$ - results from 20-60 min. **L** – Ankle capsaicin test; $\mathbf{L}^{II}$ – acute response, $\mathbf{L}^{III}$ – von Frey at the ipsilateral paw 15, 30, 60min and 24h post-injection, $\mathbf{L}^{IV}$ - von Frey at the contralateral paw 15, 30, 60min and 24h post-injection. Data are mean ± SEM, n=6 WT, n=8 HET, n=8 HOM; (except Rotarod and Hot plate at 50^{o}C and 53^{o}C, where n=14WT, n=16 HET, n=16 HOM; and the Capsaicin test, where n=8 WT, n=8 HET, n=8 HOM). Significance shows comparison to WT (NS – $p>0.05$, * - $p<0.05$, **-$p<0.01$, ***- $p<0.001$, ****-$p<0.0001$). Data analysis – One-Way ANOVA, Dunnett's multiple comparisons test for all bar charts; Two-Way ANOVA, Dunnett's multiple comparisons test for scatter plots.

again towards the spinal cord as a possible mechanistic explanation. The results at 50 minutes post-injection were 80.4 ± 25s for WT and about two times lower for the mutants 45.3 ± 10s HET and 38 ± 8s HOM (Figure 4.3K). This difference, however, did not reach significance when tested with 2-way ANOVA (p=0.07). When we calculated the acute response (first 5 minutes post-formalin) and the sensitised response (minute 20 to 60, post injection) we also did not find significant differences. Results were as follows: 178 ± 19s (WT), 180 ± 15s (HET) and 187 ± 21 (HOM) for acute formalin; and 393 ± 61s (WT), 241 ± 30 (HET) and 334 ± 38.2 (HOM) for the sensitised phase of the test. This result was promising, though not significant, and further investigation into the possible formalin phenotype of these mice should be considered.

Given that we saw a significant hyposensitivity in our hot plate test and a promising result in our formalin test, we decided to study another pain behaviour test, associated with heat - the Capsaicin test. Additionally, we chose this test for its ability to cause central sensitisation (Torebjork et al., 1992; Woolf, 2011) and designed the experiment in order to study the area, secondary to the injury. This was an attempt to mirror the mustard oil experiment we carried out during our GWAS. Therefore, we injected capsaicin subcutaneously, in the ankle area of mice, observed their acute pain response, and recorded their mechanical withdrawal thresholds from a region, secondary to the injury – the plantar surface of the paw.

Interestingly, we observed a striking phenotype with both heterozygote and homozygote mutants showing hyposensitivity in the first 5 minutes of acute response - 76.6 ± 12s WT, 49.5 ± 8.3s HET and 43.1 ± 7.8s HOM (Figure 4.3L). We next performed von Frey on both ipsi- and contralateral paws to test for sensitisation of the secondary area. This experiment was much more challenging and would require a larger cohort of mice for conclusive results. We observed a level of hyposensitivity in the inpsilateral paw of heterozygous Gas7 KO mice at 15 minutes post-capsaicin

(thresholds at 0.27 ± 0.05 for WT and 0.41 ± 0.07 for HET) and homozygotes, at 60 minutes (thresholds at 0.24 ± 0.04 for WT and 0.35 ± 0.07 for HOM). Interestingly, the most striking difference, which was true for both genotypes was the increased sensitivity in both HET and HOM Gas7 mutants at the contralateral paw, 30 minutes post-injection (thresholds at 0.7 ± 0.18 for WT, 0.42 ± 0.03 for HET and 0.51 ± 0.06 for HOM). These results, though not conclusive and difficult to interpret, could inform future experiments about a possible hyposensitivity in the ipsilateral paw, combined with hypersensitivity on the contralateral side. Explanation of this kind of phenotype is difficult and could be linked to circuit-based differences in the spinal cord of our mutants, or even supra-spinal changes.

In summary, our anatomical and behavioural experiments, taken together, showed a possible role for Gas7 in the spinal cord of mice, in the context of pain regulation.

4.3.4 Loss of Gas7 does not change sensory coding properties or wind-up of dorsal horn neurons.

Next, we chose to explore the spinal cord excitability of deep, wide dynamic range dorsal horn neurons. *In vivo* electrophysiology was performed to record from WDR neurons from depths delineating lamina V/VI.

A range of natural stimuli were applied to the receptive field. However, there were no genotype differences in the evoked neuronal responses to punctate mechanical and heat stimuli (Figure 4.4A and B) across a range of stimulus intensities. In addition, there were no genotype differences in the neuronal responses to dynamic brush (104.83 ± 12.4 spikes WT and 113 ± 17.7 spikes HOM) and noxious evaporative cooling of the receptive field (29.83 ± 12.6 spikes for WT and 24.33 ± 12.8 spikes for HOM) (Figure 4.4C and D). As described above, the receptive fields were mapped with a 15 g

von Frey and were also similar between the control and mutant mice (7.7 ± 1.5 for WT and 8.8 ± 1.7 for HOM) (Figure 4.4E). The majority of these results are consistent with our mechanical and heat behavioural phenotypes. In Figure 4.3C, we observed a subtle heat phenotype at 50^{o}C hot plate. This was not seen in our *in vivo* recordings, suggesting that the underlying mechanism for this phenotype might be outside the population of WDR neurons we probed.

Next, we tested the wind-up properties of WDR neurons. To this purpose we recorded the spiking of WDR neurons in response to a train of electrical stimuli delivered transcutaneously. Current thresholds for activation of A- and C- fibres did not differ between the genotypes (Figure 4.4F).

In response to a train of 16 electrical stimuli at a frequency of 0.5 Hz, neurons from Gas7 WT, HET and HOM mice responded with the generation of wind-up (a progressive increase in the number of spikes during a train of identical stimuli). We found no difference in the input (the non-potentiated response) or the wind-up result in the mutant vs WT mice. The results were as follows: Input - 457 ± 48 spikes for WT and 394 ± 59 for HOM and Wind-up – 363 ± 70 spikes for WT and 420 ± 52 for HOM (Figure 4.4G and H).

4.3.5 Loss of Gas7 does not affect dendritic morphology of *Tac1* excitatory interneurons in the dorsal horn.

Next, we studied the dendritic spine architecture of Gas7 WT vs KO neurons. As Gas7 has been linked to actin polymerisation and neurite outgrowth, we hypothesised that the hyposensitivity in our behavioural experiments could be linked to fewer dendritic spines in excitatory interneurons from the KO mice in comparison to the WT. To test this hypothesis, we chose the *Tac1*-positive population of excitatory

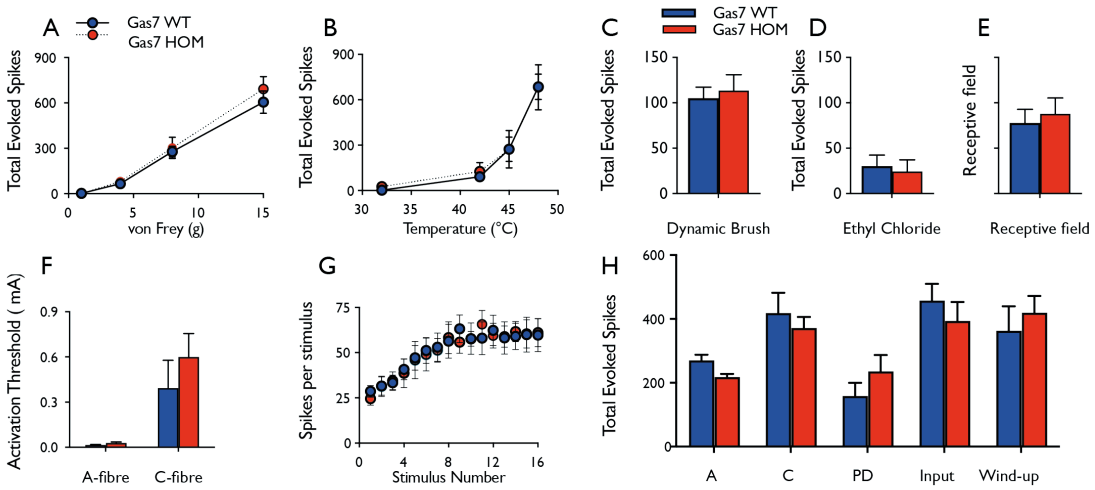


Figure. 4.4 No change in wind-up of deep dorsal horn neurons in Gas7 HET, Gas7 HOM mice and Gas7 WT controls.
A. Evoked neuronal responses to punctate mechanical stimuli, **B.** heat stimuli, **C.** dynamic brush, and **D.** noxious evaporative cooling. **E.** Receptive field size. **F.** Electrical thresholds for activation of A- and C-fibres, **G.** Wind-up of deep dorsal horn neurons (0.5 Hz) expressed as mean number of spikes per stimulus number. **H.** Total spikes evoked separated according to latency: A: 0–50 ms, C: 50–250 ms, PD (post-discharge) >250 ms. Input (number of spikes at the first stimulus, multiplied by 16, non-potentiated response) and wind-up (potentiated response – total number of spikes minus the input). Data represents mean ± SEM, Two-way ANOVA (A and B) and One-way ANOVA (C-H), Bonferroni multiple comparison test; no significance was found. Gas7 WT, n=6 neurons, Gas7 HOM, n=6.

interneurons in lamina II. This choice was informed by previous research showing significant structural changes at the same laminar level after injury (Cao et al., 2017). Therefore, we first performed multiplex in-situ hybridisation to check the expression of *Gas7* in the *Tac1*+ population (Figure 4.5).

We started with a wider exploration of *Gas7* expression in Hoechst-positive cells, followed by co-localisation with the excitatory interneuron marker *Slc17a6*, and finally focusing on the *Slc17a6*/*Tac1*-positive sub-population. The quantified results in Figure 4.5B show the overlap between *Gas7* and the nuclear dye Hoechst. We saw a strong expression of *Gas7* in laminae I to III (51.5% of all Hoechst+ cells in lamina I also expressed *Gas7*, 61.3% in lamina II and 52.6% in lamina III). This expression was slightly lower in the deeper laminae – 39.9%. Although slightly different mechanistically, this experiment confirmed our data from Figure 4.1F, where we show stronger neuronal expression in the superficial laminae (between 45% and 67%) in comparison to the deeper (between 16% and 30%).

Next, we focused on the expression of *Gas7* in the vGlut2 population of interneurons, marked by *Slc17a6*. Similarly, we saw higher expression in lamina I to III – 61.7% in lamina I, 64.1% in lamina II and 54.2% in lamina III; and slightly lower in the deeper laminae – 44% (Figure 4.5C). Next, we checked the overlap between *Gas7*+ and the *Tac1*/*Slc17a6*+ population. We observed 65% of all *Tac1*/ *Slc17a6*+ cells also expressing *Gas7* in lamina I, 48.3% in lamina II, 70% in lamina III, and 67% in deeper laminae (Figure 4.4D). On one side, the percentage of *Tac1*/*Slc17a6*/*Gas7*+ cells, especially in lamina II was only 48%, which would mean that any experiment trying to target specifically the *Tac1* population and compare it in Gas7 WT vs KO mice, would have the caveat of only 1 in 2 cells affected by the knock-out. On the other side, however, the percentage of *Gas7* expressing *Tac1*/*Slc17a6* cells was similar to the overall percentage of *Gas7*+ neurons in the excitatory *Slc17a6*+ population.

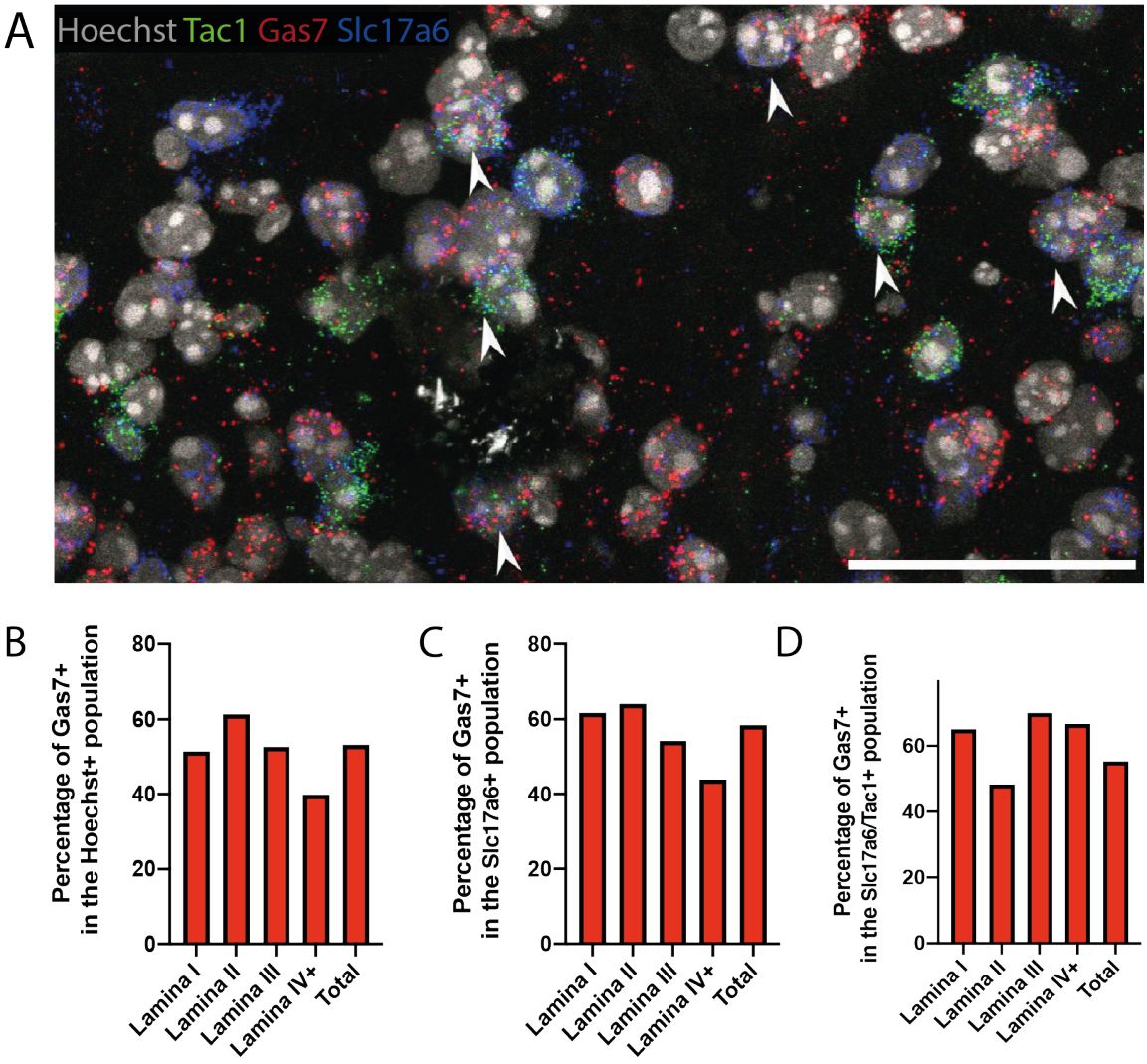


Figure. 4.5 Expression of *Gas7* in the *Tac1* population in the spinal dorsal horn.

A. Representative images showing co-localisation of *Gas7* with *Tac1* and Slc17a. **B.** Percentage of *Gas7*+ cells in the Hoechst+ population depending on laminar level (total of 1266 cells analysed). **C.** Percentage of *Gas7*+ cells in the *Slc17a6*+(vGlut2) population in each dorsal horn lamina (total of 637 cells analysed); **D.** Percentage of *Gas7*+ cells in the *Slc17a6*/*Tac1*+ population (total of 141 cells analysed). Data are from 2 mice per genotype (1 section each). Scale bar = 50 μm.

This could suggest that the *Tac1* population is likely representative of the rest of the excitatory sub-populations and the caveat mentioned above would be true independent of whether we chose to study the *Tac1* population, another excitatory sub-population or the whole excitatory group of interneurons. Another point for consideration would be the developmental expression of Gas7, which could also significantly affect the dendritic morphology of adult neurons. Nevertheless, lamina II (containing the majority of *Tac1*+ neurons) has been linked to significant changes in spine architecture post-injury (Cao et al., 2017) and we chose to focus on the *Tac1* population for our next experiment.

Next, we crossed our Gas7 mutant mice with a $Tac1^{Cre}$ mouse line and then injected the offspring mice with a virus containing the Brainbow construct. This resulted in sparse labelling of *Tac1*+ positive neurons with the membrane-targeted teal fluorescent protein (TFP) or mCherry. We then used an anti-mTFP antibody and scanned the *Tac1*-positive, lamina II excitatory interneurons. Neurolucida was then used to reconstruct the dendritic tree and spine architecture of the selected neurons. These reconstructions were then used to study several different parameters – total spine number, total length, spine density and thin/mushroom shape ratio. We found no significant difference in any of these parameters, and this was also independent of how far the spines were from the cell body (Scholl's analysis). We also studied dendritic length (not included) and did not find a significant difference between the genotypes (Figure 4.6).

4.4 Discussion

This chapter focused on studying the expression of *Gas7* in DRG and spinal cord, validating its functional role through pre-clinical experiments, and understanding more about the possible mechanism underlying the discovered phenotypes.

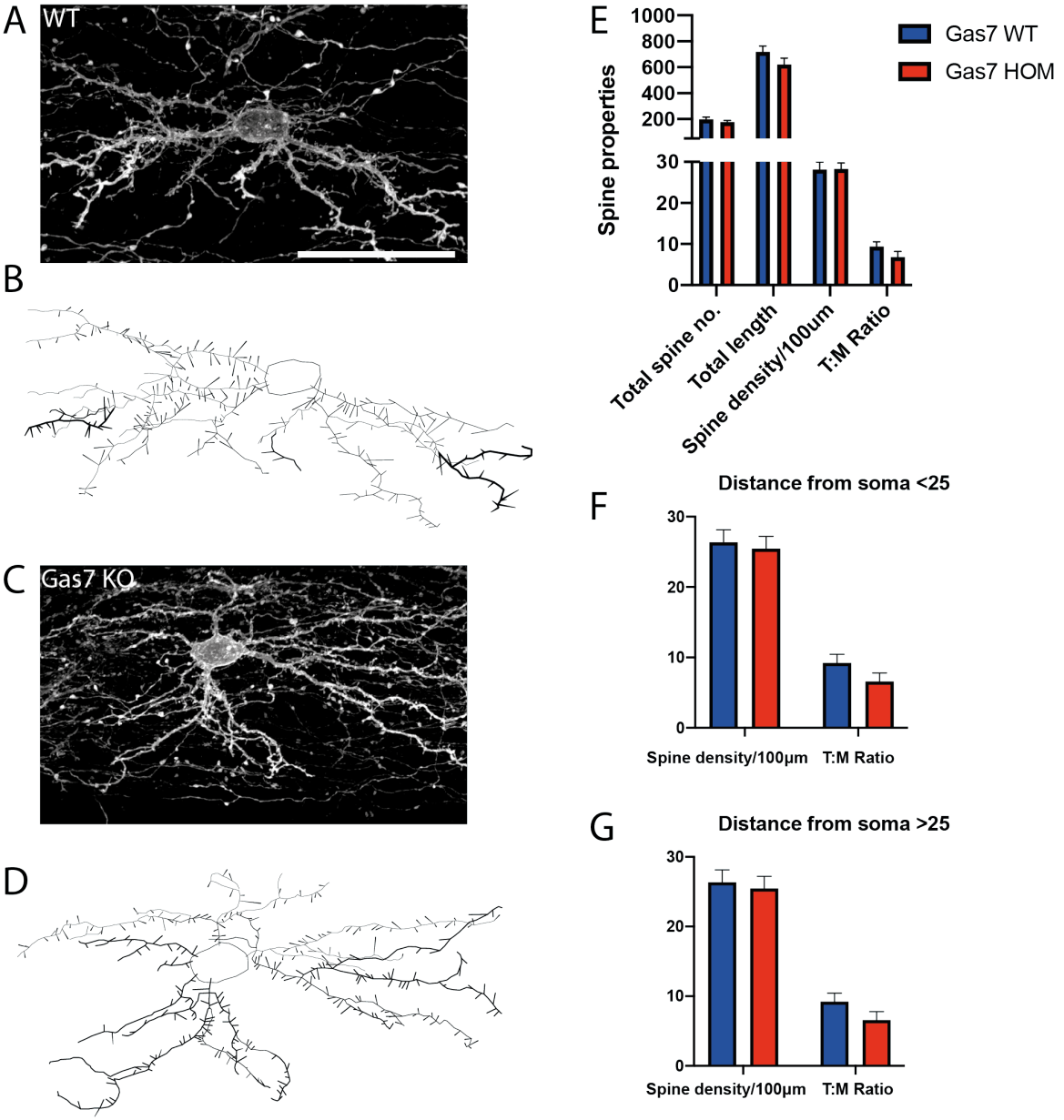


Figure. 4.6 Dendritic spine properties in Gas7 WT vs mutant HOM neurons in the *Tac1* population of excitatory interneurons.
A-D. Representative images showing *Tac1*+ interneurons in lamina II of WT **A** or Gas7 KO **C** neurons. Reconstructions of the respective neurons shown in **B** and **D**. **E-G.** Quantification of the images from **A-D** – total spine number, total length of spines, spine density and T:M ratio (number of thin versus mushroom spines) were tested. Scholl's analysis was performed showing dendritic spine parameters according to spine location (less or more than 25μm from the cell body), **F,G**. Data are Mean ± SEM, Student's t-test, unpaired - no significance was found. Gas7 WT, n=12 neurons, Gas7 HOM, n=12, 2 mice per genotype. Scale bar = 50 μm.

Our initial anatomical studies showed low, or even lacking, expression of *Gas7* in the DRG. Interestingly, the gene was found in structures around the neuronal soma which are likely satellite glia. We did not focus on examining this phenomenon further. However, a recently published database of RNA sequencing results from FACS-sorted satellite glial cells (SGC) shows high expression of *Gas7* in SGC from naïve mice, which appeared downregulated 14 days after full sciatic nerve ligation. The database also shows that *Gas7* expression was higher (more concentrated) after purification of SGC, in comparison to samples containing all cell types in the DRG (Jager et al., 2020). These data support our results and therefore further investigation into the role of *Gas7* in the satellite glial population might be of interest.

We focused our research mainly on the spinal cord. Two independent experiments (Figure 4.1 and Figure 4.5), using different staining techniques and methods for analysis, showed that *Gas7* is highly expressed in the superficial laminae of the spinal dorsal horn and less so in the deeper laminae. Our data from Figure 4.1 shows strong neuronal co-localisation between *Gas7* mRNA and NeuN, with between 45% and 67% of all neurons in the superficial laminae expressing the gene of interest. To my knowledge, this is the first report of *Gas7* expression in the spinal dorsal horn as even existing RNA-sequencing data bases did not show reliable expression data (Haring et al., 2018). We also studied the expression of *Gas7* within different interneuronal populations. As with NCX3, we did not find striking differences between excitatory and inhibitory interneurons, as all three populations we tested (vGLuT2, Gad67 and GlyT2) showed relatively similar expression levels (Figure 4.2). As mentioned previously, this is the first report of *Gas7* expression in the spinal dorsal horn, especially when it comes to interneuron distribution. Most published research points to high expression in the brain, and more specifically in the cerebral cortex, cerebellum and hippocampus (Ju et al., 1998; Meyer, 2018).

The result from our anatomical search encouraged us to perform a number of behavioural tests in our Gas7 KO mice, looking for motor and pain phenotypes. Very little of this work has been performed in previous studies. For example, (Huang et al., 2012) reported a mouse model expressing reduced levels of functional Gas7, whose performance on the rotarod test was impaired only at older age (12 months), while younger, adult mice were healthy. This result is in line with our lack of phenotype in adult mice, but also points to possible neuromuscular impairment in aged animals.

Our behavioural tests showed a suggestive, but not significant, trend towards hyposensitivity in both heterozygous and homozygous mutant mice following intraplanar injection of formalin. In addition, we saw significant hyposensitivity in our Hot plate test at 50^{o}C (in homozygous animals) and capsaicin in the first 5 minutes after injection (in both HET and HOM animals). Therefore, there appears to be a significant trend towards hyposensitivity in heat-related tests. Interestingly, both mustard oil and formalin tests, as well as heat sensitivity have been associated with TRPA1 channels (Koltzenburg et al., 1992; McNamara et al., 2007; Moparthi et al., 2016), while the capsaicin test is well-known to be linked to another heat sensor and member of the TRP family – TRPV1 (reviewed by Basbaum et al. (2009)). Whether this family of channels can explain the Gas7 phenotype is yet to be explored and would require bigger cohorts of mice and different experimental paradigms. However, the hyposensitivity phenotype appears to be persistent among the different tests we used. In addition, it is interesting that differences were seen in both acute tests (hot plate and acute capsaicin) as well as in experiments linked to sensitised pain (mustard oil in our human GWAS, formalin and the von-Frey analysis post-capsaicin injection). Given the phenotypes we identified in our Gas7 mutant mice, we aimed to investigate any abnormalities, both structural and functional, that could explain the observed hyposensitivity.

We did not find a phenotype in the neuronal responses of WDR neurons in the deep laminae of the dorsal horn. This was the case when we tested both mechanical and heat stimuli, as well as the wind-up properties of the neurons (Figure 4.3). While slightly discouraging, these data could be explained by the relatively low expression of *Gas7* in deep spinal cord laminae (Figure 4.1(F) – between 15 to 30% of NeuN+ cells expressed *Gas7*). Therefore, this could mean that our experiment was underpowered, as we tested only 6 neurons per genotype in a pilot study. This points to the importance of targeting the *Gas7*+ population more specifically. Unlike our NCX3 target, which was very strongly expressed in the spinal dorsal horn, the *Gas7* expression seems to be sparse. Therefore, future experiments should focus on targeting the *Gas7*+ cells more specifically. This could involve the generation of a Gas7^{Cre} line, which would allow the better labelling of *Gas7*+ neurons. In addition, an interesting approach is the work done by Lu et al. (2015). The authors prepared acute lumbar spinal cord slices with attached dorsal roots and performed patch clamp recordings on retrogradely labelled projection neurons from the periaqueductal grey. This method targets more superficial neurons and is therefore more likely to explore the *Gas7*-specific population. The authors used this method to study another player in the actin polymerisation cascade – kal-7, which is linked to central sensitisation and structural changes in the spinal cord. They applied a conditioning stimulus of C-fiber stimulation to the dorsal roots and found that WT but not Kal-7 KO neurons produced long-term potentiation. This experiment is of particular interest as Kal-7, like Gas7, is part of the actin-polymerisation pathway and is involved in dendritic spine regulation and activity-dependent structure-function modulation of spinal nociceptive synapses. However, Kal-7 is thought to be at a convergent point where it can modulate a number of mechanisms, including the recruitment and function of AMPA and NMDA receptors

Xie et al. (2007) which makes it different to our gene of interest. Nevertheless, using the parallel between Kal-7 and Gas7 could be of use for the design of future experiments.

Our final experiment focused on the investigation of Gas7 in dendritic spine remodelling. As described in Chapter 1, (Section 1.8, Gas7 has a well-studied role in actin polymerisation and neurite outgrowth. Therefore, we hypothesised that Gas7 mutant mice might have a gross dendritic spine deficiency, especially in excitatory interneurons, which could explain the hyposensitivity observed in our behavioural tests. While we found evidence that gross abnormality in the Gas7 KO mice is unlikely (Figure 4.6), it is possible that more targeted experiments can be designed in future studies. For example, we chose to study the *Tac1* population of excitatory interneurons due to its importance for pain signalling and the previous reports of significant dendritic spine remodelling in lamina II of the spinal dorsal horn (Cao et al., 2017). However, we also found that at this laminar level only 48% of the neurons express Gas7 and therefore using a relatively small sample size (n=12) might miss a more subtle phenotype. Therefore, increasing the sample size, targeting other populations of excitatory interneurons, or dual labelling techniques for excitatory interneurons and Gas7, could be possible future aims. In addition, as our KO mouse model is global and non-inducible, it is likely that many compensatory mechanisms occur during development and this could explain the lack of gross abnormalities in naïve mice. Therefore, exploring expression of Gas7 during development might also be an important future aim.

Other interesting experiments could involve the culture of spinal dorsal horn neurons from Gas7 WT and mutant mice, following by comparison of the dendritic trees and spines they from *de novo*. As dendritic spine remodelling during central sensitisation is a dynamic process, the formation of these structures *de novo* might be more indicative of the mechanism underlying Gas7-related hyposensitivity.

In this context, it would be interesting to explore the spine architecture of lamina II *Tac1* neurons post-injury, especially if dual labelling for Gas7 is also possible. This is because, with the exception of our hot plate result, the experiments that showed Gas7 hyposensitivity involved an injury and possible central sensitisation. Therefore, any Gas7-induced phenotypes might become much more prominent under injury conditions, when novel dendritic spines are generated.

Last but not least, Gas7 has been found to be highly expressed in the brain. Therefore, there is a possibility of brain-associated mechanisms that can make the understanding of the above-mentioned phenotypes even more challenging. In order to simplify the interpretation of our experiments, the generation of tissue-specific knock-out mice would be ideal.

4.5 Conclusion

In conclusion, this chapter reports the validation of the GWAS-identified target *Gas7* in pre-clinical models of pain, especially in the capsaicin test where the ablation of *Gas7* led to strong hyposensitivity. Although our attempts to understand the mechanism behind this phenotype returned negative data, they gave us ideas for future experiments which could lead to better understanding not only of *Gas7* but also of the structural remodelling of the spinal cord during central sensitisation.

Chapter 5

General Discussion

5.1 From Human to Mouse and back

The work, presented in this thesis, shows our effort to cross the bridge between human genetic studies and basic science. As mentioned in Chapter 1(Subsection 1.6.1 and 1.6.2), GWAS results come with a dose of scepticism. This is because variants, found through GWAS-s, represent common single nucleotide polymorphisms (SNPs), which usually have low penetrance (effect size) and a relatively small contribution to the traits studied. Therefore, understanding their role in complex conditions, such as chronic pain, is challenging. As mentioned in Chapter 1 (Subsection 1.6.2), few studies have achieved the goal of providing a mechanistic explanation of the genetic associations they found (Smemo et al., 2014; Claussnitzer et al., 2015). This thesis is an example of achieving this goal and providing converging evidence from human, mouse and cellular models in support of our GWAS-identified targets. The challenge in studies like ours comes from the small effect sizes the discovered SNPs have, the chance for false positives, as well as the risk, time and skills, linked to translating GWAS results into basic biology. In addition, difficulties with GWAS studies in the pain field specifically,

include the phenotyping paradigms used when evaluating a subjective perception like pain (Schmid et al., 2019; Zorina-Lichtenwalter et al., 2016). Nevertheless, there have been published GWAS-s in the field, most of which focused on pain-related conditions (Zorina-Lichtenwalter et al., 2016). With regards to experimental pain in healthy individuals, there is evidence that greater sensitivity to temporal summation, for example, predicts the development of post-operative pain (Weissman-Fogel et al., 2009). This study is an example of a publication which highlights the link between experimental pain in healthy participants (pre-operative), and clinically relevant pain. In addition, studying healthy volunteers has the advantage of reduced bias coming from medication, disease severity or aging which are all caveats in GWAS-s with chronic pain patients. This approach, which is also the paradigm we chose for our study, allows for control of pain modality, location, intensity and temporal profile.

The challenges and caveats of GWAS studies, however, should not hinder the development of this technology. Currently, drug development for analgesics shows a high level of failure with only 2% of candidate molecules progressing from Phase I to Phase II clinical trials. This is especially alarming as in other therapeutic areas the success rate is 10% at the same stage (Thomas D, Wessel C., 2018). Interestingly, pipeline drug targets, supported by evidence from human genetic studies, have been shown to be two times more likely to lead to drug approval (Nelson et al., 2015; King et al., 2019). Therefore, GWAS studies provide an important advantage in drug development outcome and the methods currently used are aiming at overcoming the existing challenges. One future goal is the automation of the existing "one-locus-at-a-time" approach in GWAS studies and providing a systematic workflow in order to study the functionality of the discovered SNPs (Claussnitzer et al., 2020). Understanding the genotype-phenotype relationship in GWAS-s is a strong point for future development

and will allow for better translation of human genetics into basic biology and drug discovery (discussed in more detail in Chapter 1, Subsection 1.6.2).

5.2 Central sensitisation - physiology meets anatomy

5.2.1 Calcium signalling and *NCX3*

Our GWAS work showed significant associations between two genes (*NCX3* and *Gas7*) and two traits - temporal and spatial summation - both linked to central sensitisation in humans. This phenomenon represents a state of heightened sensitivity which spinal circuits reach in response to continuous, intense stimulation. Like many processes in the body, central sensitisation is the result of a variety of converging mechanisms which continuously interact through feedback loops and across different neuronal circuits. Therefore, heightened sensitivity in the spinal cord represents the attempt of this integrated network to establish a dynamic equilibrium in a state of continuous stimulation. Knowing that calcium serves as a second messenger, activating many downstream processes in the spinal cord (discussed in Chapter 3, Subsection 3.1.4), it is not surprising that neurons would keep the intracellular levels of this ion under strict control. As explored in Chapter 3 (Diagram D.3.2), "the sources" of Ca^{2+} in dorsal horn neurons have been studied extensively, while the extrusion proteins ("the sinks") have been largely overlooked (Hagenston and Simonetti, 2014). The PMCA2 was recently identified as an important Ca^{2+} clearance mechanism in the dorsal horn and its downregulation following inflammation was linked to enhanced pain behaviour (Mirabelli et al., 2019). Therefore, the discovery of *NCX3* as another Ca^{2+} sink is not surprising, and it should represent the beginning of deeper analysis of Ca^{2+} regulatory mechanisms in dorsal horn neurons.

In this thesis we report that variants in the *NCX3* gene locus were found to be significantly associated with temporal summation in humans. The identified target was highly expressed in dorsal horn neurons which included interneuronal populations and projection neurons. In addition, we observed enhanced pain responses in the second phase of the formalin test. This phase, like wind-up ratio, has been linked to central alterations. Studying the mechanism, underlying this phenotype, we found that neurons lacking *NCX3* had higher basal levels, increased peak concentration and slower clearance of Ca^{2+}. In addition, *in vivo* recordings showed that electrophysiological wind-up was increased and achieved by a lower frequency stimulation. All of these results, taken together, provide molecular, cellular and behavioural evidence in support of our GWAS-identified target, showing that *NCX3* is one of the important mechanisms for calcium extrusion in the spinal dorsal horn.

Therefore, the exploration of the polymorphisms in the *NCX3* gene in relation to pain conditions, their possible phenotypic manifestations, as well as any changes in expression levels after injury and inflammation, should be considered. While NCX3 activators have not yet been developed, targeting of the isoform-specific calcium-binding domains may provide a route to the discovery of selective small molecules (Khananshvili, 2014). In this context, many questions could be asked and more research should be carried out to bring answers. For example, one such question could be what kind of pain conditions would be best affected by NCX3 activators. While difficult to answer, this question can be partially addressed by our data as the observed strong phenotype in the second phase of the formalin test has been linked to inflammatory pain (Hunskaar and Hole, 1987). In addition, we observed no differences after acute mechanical and thermal stimulation. Therefore, we would expect that NCX3 would have an important role in pain conditions and not so much in nociceptive pain, after a noxious stimulus. This would mean that testing the impact of an *NCX3* genetic

deletion in other models, such as chronic inflammatory models (Carrageenan injection and Complete Freund's adjuvant), neuropathic pain models (spared nerve injury, chronic constriction injury) or even visceral, cancer, and postoperative pain, could be very informative with regards to any future therapeutic strategy (Gregory et al., 2013). In addition, there are pain conditions whose origins have not yet been explained and which can be linked to heightened central sensitivity. Such conditions include fibromyalgia, tension-type headache, irritable bowel syndrome and more (Woolf, 2011). As mentioned in Chapter 3, both fibromyalgia and irritable bowel syndrome, have been associated with higher temporal summation in patients (Staud et al., 2003; P. Rössel, A. M. Drewes, P. Peterse, 1999), which makes NCX3 an interesting target to explore in the context of these diseases as well. Notably, there are existing mouse models which could be used to investigate this hypothesis further (DeSantana et al., 2013; Maria Vannucchi and Stefano Evangelista, 2018). Another question would be whether NCX3 activators should be used pre-emptively to reduce the risk of chronic pain development after surgery, amputation or chemotherapy. This is interesting, as although we observed some basal phenotypes in our NCX3 mutant mice, the most striking changes were seen after strong stimulation. This could imply that mutant neurons are more susceptible to Ca^{2+} accumulation and the following downstream effects. Although many of these effects are reversible (Chapter 1, Figure 1.6), it is tempting to speculate that pre-emptive treatment, protecting from initial Ca^{2+} accumulation, might be an effective strategy. One opportunity to test this would be our future NCX3 over-expression experiment, using our designed AAV, described in Chapter 3. It is important, however, to highlight that studies on pre-emptive analgesia in post-operative pain have not shown great clinical advantage over full analgesia during surgery and recovery (Woolf, 2011).

5.2.2 Structural changes and *Gas7*

If NCX3 and Ca^{2+} levels in the cell represent a link to the functional changes during central sensitisation in the dorsal horn, then Gas7 could be a protein associated with structural adaptations, occurring in the spinal cord. In fact, the anatomical changes during central sensitisation are a relatively new topic of research and are therefore underexplored. As mentioned in Chapter 4, Subsection 4.1.3, a variety of structural changes post-injury in the superficial dorsal horn have already been reported. Such changes include dorsal horn re-modelling processes such as **1/** an increase in spine density, **2/** transition to a larger number of mushroom-shaped dendritic spines (linked to excitatory synaptic signalling), in comparison to thinly-shaped ones, and **3/** an increased number of spines closer to the neuronal soma which have a higher impact on cell excitability (Subsection 4.1.3). This fascinating plasticity and structure-function relationship is also not surprising, as the link between anatomy and physiology, as well as the adaptivity of the human body to change in order to maintain homeostasis, are key principles in biology.

Despite the evidence that *Gas7* is linked to neurite outgrowth (Ju et al., 1998), we did not find a direct structural or functional explanation for the role of this gene in the spinal cord of naïve animals. Therefore, it would be beneficial to study the response of our mutant mouse line to injury, when *de novo* spines are formed (Chapter 4, Section 4.4). In addition, we found evidence for *Gas7* expression in satellite cells in the DRG and this points to the importance of exploring its role in glial cells. This is especially interesting as there is research pointing to the role of satellite glial cells after injury (Hanani, 2015). Expression levels in the skin, nerve and brain, as well as the function-structure relationship in these tissues should also be investigated. Last but not least, our GWAS found a significant association between *Gas7* and spatial summation after mustard oil. We also found a promising, albeit non-significant, decrease in pain

behaviour after formalin, a significant hyposensitivity to hot plate at 50^{o}C, and a strong decrease in the response to capsaicin. As these changes seem to be linked to the TRP family of proteins (explored in more details in Chapter 4, Section 4.4), it would be interesting to explore this topic further. Questions on how this knowledge can be translated into future therapies are very difficult at this stage, mainly because *Gas7* is not a membrane protein and the mechanisms of the observed behavioural phenotypes are yet to be explored. However, our research points once again to the variety of proteins likely contributing to structural adaptations as part of the development of pain sensitisation.

5.2.3 Central sensitisation - translational potential and challenges

The paragraphs above discussed *NCX3* and *Gas7* as possible targets linked to central sensitisation. However, it is important to highlight that at the clinical level, this phenomenon still represents a major challenge. Historically, heightened central sensitivity, especially when occurring without clear pathology, was considered "psychosomatic" and difficult to address (Woolf, 2011). Today, although central sensitisation is a well studied neurobiological phenomenon, there are still challenges arising from the variety of central adaptations that occur and the difficulties in diagnosis and treatment. For example, in a recent invited viewpoint article, my colleagues and I discussed the importance of making a distinction between central sensitisation and psychological conditions (such as depression and anxiety)van Griensven et al. (2020b). This is challenging as the two can influence each other but, as described in detail in this thesis, the former phenomenon has its own physiological causes which can be identified and addressed using existing or yet to be developed approaches.

For example, methods for diagnosing possible central components in patient pain conditions were also described by van Griensven et al. (2020b). Ongoing, spontaneous, and widespread pain as well as severe, long-lasting pain following usually innocuous stimuli, can raise the suspicion of a central contribution to a patient condition. In these cases, diagnostic methods currently include using quantitative sensory testing for cold/heat and mechanical hyperalgesia in areas which are secondary (ipsilateral but innervated by a different segmental level) or even tertiary (contralateral) to the primary site (Zhu et al., 2019). In addition, other methods include dynamic mechanical hyperalgesia (painful sensation in response to light touch); temporal summation (exacerbated pain ratings during and after a train of repetitive stimulation); spatial summation (heightened pain sensation when using, for example, an increasing area of simultaneous pinprick stimulation); and conditioned pain modulation which tests to what extent one noxious stimulus causes the inhibition of another (van Griensven et al., 2020b) . While quantitative sensory testing provides a surrogate technique for diagnosis of central sensitisation, van Griensven et al. (2020b) note that direct biomarkers, such as methods for functional neuroimaging, are also under development.

Interestingly, a recent comprehensive review of the neuroimaging literature in five central sensitivity syndromes (fibromyalgia, chronic fatigue syndrome, irritable bowel syndrome, temporomandibular joint disorder, and vulvodynia syndrome) shows that evoked sensory paradigms reveal augmentation to painful and non-painful stimulation in different brain regions, but the heterogeneity between and within these syndromes makes the identification of a clear central sensitisation signature challenging (Walitt et al., 2016). The authors also stress the importance of improving the existing spinal cord neuroimaging techniques which currently show greater technical complexity than brain imaging. Nevertheless, there are published spinal cord studies, such as (Rempe et al., 2015), who performed spinal fMRI in healthy subjects. Their work shows

increased spinal cord grey matter activation after capsaicin sensitisation, in comparison to non-sensitised, innocuous or noxious heat application. Moreover, the authors report that capsaicin sensitisation led to activation of more segments, both ipsi- and contralateral to the site of stimulation (Rempe et al., 2015). Another similar study performed fMRI in groups of control subjects and fibromyalgia patients. A temporal summation paradigm showed enhanced dorsal horn activity and after-sensations in the latter group of volunteers (Bosma et al., 2016). These advances in neuroimaging point to a possible future biomarker for central sensitisation, which would be a significant step towards the diagnosis and treatment of this phenomenon. Such achievement in clinical neuroscience may also coincide with the development of our fundamental biological knowledge, including deeper understanding of the underlying spinal cord mechanisms, the calcium dynamics in dorsal horn neurons and possibly - the development of small molecules, such as NCX3 activators.

In conclusion, the current thesis presented the results of a GWAS study using experimental pain paradigms on healthy participants and successfully validated its two genome-wide significant associations. This study provides ideas for crossing the gap between GWAS and basic biology, as well as for the better understanding of the functional and structural alterations occurring during central sensitisation. Although there is much more to be explored and discovered, I am proud to have added this knowledge and future aim to the field of pain research.

Bibliography

C. Abbadie, B. K. Taylor, M. A. Peterson, and A. I. Basbaum. Differential contribution of the two phases of the formalin test to the pattern of c-fos expression in the rat spinal cord: studies with remifentanil and lidocaine. *Pain*, 69(1-2):101–10, January 1997. ISSN 0304-3959 (Print) 0304-3959 (Linking). doi: 10.1016/s0304-3959(96)03285-x. URL https://www.ncbi.nlm.nih.gov/pubmed/9060019. Edition: 1997/01/01.

V. E. Abraira and D. D. Ginty. The Sensory Neurons of Touch. *Neuron*, 79(4): 618–639, August 2013. ISSN 0896-6273. doi: 10.1016/j.neuron.2013.07.051. URL ://WOS:000323587000004.

V. E. Abraira, E. D. Kuehn, A. M. Chirila, M. W. Springel, A. A. Toliver, A. L. Zimmerman, L. L. Orefice, K. A. Boyle, L. Bai, B. J. Song, K. A. Bashista, T. G. O'Neill, J. Zhuo, C. Tsan, J. Hoynoski, M. Rutlin, L. Kus, V. Niederkofler, M. Watanabe, S. M. Dymecki, S. B. Nelson, N. Heintz, D. I. Hughes, and D. D. Ginty. The Cellular and Synaptic Architecture of the Mechanosensory Dorsal Horn. *Cell*, 168(1-2): 295–310 e19, January 2017. ISSN 1097-4172 (Electronic) 0092-8674 (Linking). doi: 10.1016/j.cell.2016.12.010. URL https://www.ncbi.nlm.nih.gov/pubmed/28041852. Edition: 2017/01/04.

G. Alarcon and F. Cervero. The effects of electrical stimulation of A and C visceral afferent fibres on the excitability of viscerosomatic neurones in the thoracic spinal cord of the cat. *Brain Research*, 509(1):24–30, February 1990. ISSN 00068993. doi: 10.1016/0006-8993(90)90304-T. URL https://linkinghub.elsevier.com/retrieve/pii/000689939090304T.

C. Albuquerque, D. J. Joseph, P. Choudhury, and A. B. MacDermott. Dissection, Plating, and Maintenance of Dorsal Horn Neuron Cultures. *Cold Spring Harbor Protocols*, 2009(8):pdb.prot5274–pdb.prot5274, August 2009. ISSN 1559-6095. doi: 10.1101/pdb.prot5274. URL http://www.cshprotocols.org/cgi/doi/10.1101/pdb.prot5274.

F. J. Alvarez, R. M. Villalba, R. Zerda, and S. P. Schneider. Vesicular glutamate transporters in the spinal cord, with special reference to sensory primary afferent synapses. *J Comp Neurol*, 472(3):257–80, May 2004. ISSN 0021-9967 (Print) 0021-9967 (Linking). doi: 10.1002/cne.20012. URL https://www.ncbi.nlm.nih.gov/pubmed/15065123. Edition: 2004/04/06.

L. Alvarez-Erviti, Y. Seow, A. H. Schapira, C. Gardiner, I. L. Sargent, M. J. A. Wood, and J. M. Cooper. Lysosomal dysfunction increases exosome-mediated alpha-

synuclein release and transmission. *Neurobiology of Disease*, 42(3):360–367, June 2011. ISSN 0969-9961. doi: 10.1016/j.nbd.2011.01.029. URL ://WOS:000290081700016.

D. Andrew. Sensitization of lamina I spinoparabrachial neurons parallels heat hyperalgesia in the chronic constriction injury model of neuropathic pain. *J Physiol*, 587(Pt 9):2005–17, May 2009. ISSN 1469-7793 (Electronic) 0022-3751 (Linking). doi: 10.1113/jphysiol.2009.170290. URL https://www.ncbi.nlm.nih.gov/pubmed/19289544. Edition: 2009/03/18.

R. Araya, K. B. Eisenthal, and R. Yuste. Dendritic spines linearize the summation of excitatory potentials. *Proceedings of the National Academy of Sciences*, 103(49):18799–18804, December 2006. ISSN 0027-8424, 1091-6490. doi: 10.1073/pnas.0609225103. URL http://www.pnas.org/cgi/doi/10.1073/pnas.0609225103.

A. Arcourt, L. Gorham, R. Dhandapani, V. Prato, F. J. Taberner, H. Wende, V. Gangadharan, C. Birchmeier, P. A. Heppenstall, and S. G. Lechner. Touch Receptor-Derived Sensory Information Alleviates Acute Pain Signaling and Fine-Tunes Nociceptive Reflex Coordination. *Neuron*, 93(1):179–193, January 2017. ISSN 0896-6273. doi: 10.1016/j.neuron.2016.11.027. URL ://WOS:000396427800017.

L. Arendt-Nielsen, B. Morlion, S. Perrot, A. Dahan, A. Dickenson, H. G. Kress, C. Wells, D. Bouhassira, and A. M. Drewes. Assessment and manifestation of central sensitisation across different chronic pain conditions. *European Journal of Pain*, 22(2):216–241, February 2018. ISSN 1090-3801. doi: 10.1002/ejp.1140. URL ://WOS:000425824100003.

L. Bai, B. P. Lehnert, J. Liu, N. L. Neubarth, T. L. Dickendesher, P. H. Nwe, C. Cassidy, C. J. Woodbury, and D. D. Ginty. Genetic Identification of an Expansive Mechanoreceptor Sensitive to Skin Stroking. *Cell*, 163(7):1783–1795, December 2015. ISSN 1097-4172 (Electronic) 0092-8674 (Linking). doi: 10.1016/j.cell.2015.11.060. URL https://www.ncbi.nlm.nih.gov/pubmed/26687362. Edition: 2015/12/22.

P. F. Baker and H. G. Glitsch. Does metabolic energy participate directly in the Na+-dependent extrusion of Ca2+ -Ca2+ ions from squid giant axons? *J Physiol*, 233(1):44P–46P, August 1973. ISSN 0022-3751 (Print) 0022-3751 (Linking). URL https://www.ncbi.nlm.nih.gov/pubmed/4759120. Edition: 1973/08/01.

M. Bandell, G. M. Story, S. W. Hwang, V. Viswanath, S. R. Eid, M. J. Petrus, T. J. Earley, and A. Patapoutian. Noxious cold ion channel TRPA1 is activated by pungent compounds and bradykinin. *Neuron*, 41(6):849–57, March 2004. ISSN 0896-6273 (Print) 0896-6273 (Linking). doi: 10.1016/s0896-6273(04)00150-3. URL https://www.ncbi.nlm.nih.gov/pubmed/15046718. Edition: 2004/03/30.

T. G. Banke, D. Bowie, H. Lee, R. L. Huganir, A. Schousboe, and S. F. Traynelis. Control of GluR1 AMPA receptor function by cAMP-dependent protein kinase. *J Neurosci*, 20(1):89–102, January 2000. ISSN 1529-2401 (Electronic) 0270-6474 (Linking). URL https://www.ncbi.nlm.nih.gov/pubmed/10627585. Edition: 2000/01/11.

Peter Bankhead, Maurice B. Loughrey, José A. Fernández, Yvonne Dombrowski, Darragh G. McArt, Philip D. Dunne, Stephen McQuaid, Ronan T. Gray, Liam J. Murray, Helen G. Coleman, Jacqueline A. James, Manuel Salto-Tellez, and Peter W. Hamilton. QuPath: Open source software for digital pathology image analysis.

Scientific Reports, 7(1):16878, December 2017. ISSN 2045-2322. doi: 10.1038/s41598-017-17204-5. URL http://www.nature.com/articles/s41598-017-17204-5.

Allan I. Basbaum, Diana M. Bautista, Grégory Scherrer, and David Julius. Cellular and Molecular Mechanisms of Pain. *Cell*, 139(2):267–284, October 2009. ISSN 00928674. doi: 10.1016/j.cell.2009.09.028. URL https://linkinghub.elsevier.com/retrieve/pii/S0092867409012434.

Anna A. Battaglia. An Introduction to Pain and Its Relation to Nervous System Disorders. 2016.

M. C. Battie, T. Videman, E. Levalahti, K. Gill, and J. Kaprio. Heritability of low back pain and the role of disc degeneration. *Pain*, 131(3):272–80, October 2007. ISSN 1872-6623 (Electronic) 0304-3959 (Linking). doi: 10.1016/j.pain.2007.01.010. URL https://www.ncbi.nlm.nih.gov/pubmed/17335977. Edition: 2007/03/06.

D. M. Bautista and E. A. Lumpkin. Perspectives on: information and coding in mammalian sensory physiology: probing mammalian touch transduction. *J Gen Physiol*, 138(3):291–301, September 2011. ISSN 1540-7748 (Electronic) 0022-1295 (Linking). doi: 10.1085/jgp.201110637. URL https://www.ncbi.nlm.nih.gov/pubmed/21875978. Edition: 2011/08/31.

Diatchenko L. Belfer I. Pain Genetics: Basic to Translational Science. 2013.

P. Bellosta, Q. Zhang, S. P. Goff, and C. Basilico. Signaling through the ARK tyrosine kinase receptor protects from apoptosis in the absence of growth stimulation. *Oncogene*, 15(20):2387–97, November 1997. ISSN 0950-9232 (Print) 0950-9232 (Linking). doi: 10.1038/sj.onc.1201419. URL https://www.ncbi.nlm.nih.gov/pubmed/9395235. Edition: 1997/12/12.

Curtis A. Benson, Keith K. Fenrich, Kai-Lan Olson, Siraj Patwa, Lakshmi Bangalore, Stephen G. Waxman, and Andrew M. Tan. Dendritic Spine Dynamics after Peripheral Nerve Injury: An Intravital Structural Study. *The Journal of Neuroscience*, 40 (22):4297–4308, May 2020. ISSN 0270-6474, 1529-2401. doi: 10.1523/JNEUROSCI.2858-19.2020. URL http://www.jneurosci.org/lookup/doi/10.1523/JNEUROSCI.2858-19.2020.

Cacioppo Berntson. Handbook of neuroscience for the behavioural sciences. 2009.

D. M. Bers. Cardiac excitation-contraction coupling. *Nature*, 415(6868):198–205, January 2002. ISSN 0028-0836 (Print) 0028-0836 (Linking). doi: 10.1038/415198a. URL https://www.ncbi.nlm.nih.gov/pubmed/11805843. Edition: 2002/01/24.

G. M. Besserer, M. Ottolia, D. A. Nicoll, V. Chaptal, D. Cascio, K. D. Philipson, and J. Abramson. The second Ca2+-binding domain of the Na+ Ca2+ exchanger is essential for regulation: crystal structures and mutational analysis. *Proc Natl Acad Sci U S A*, 104(47):18467–72, November 2007. ISSN 1091-6490 (Electronic) 0027-8424 (Linking). doi: 10.1073/pnas.0707417104. URL https://www.ncbi.nlm.nih.gov/pubmed/17962412. Edition: 2007/10/27.

P. Bessou and E. R. Perl. Response of cutaneous sensory units with unmyelinated fibers to noxious stimuli. *J Neurophysiol*, 32(6):1025–43, November 1969. ISSN 0022-3077 (Print) 0022-3077 (Linking). doi: 10.1152/jn.1969.32.6.1025. URL https://www.ncbi.nlm.nih.gov/pubmed/5347705. Edition: 1969/11/01.

H. Bester, V. Chapman, J. M. Besson, and J. F. Bernard. Physiological properties of the lamina I spinoparabrachial neurons in the rat. *J Neurophysiol*, 83(4):2239–59, April 2000. ISSN 0022-3077 (Print) 0022-3077 (Linking). doi: 10.1152/jn.2000.83.4.2239. URL https://www.ncbi.nlm.nih.gov/pubmed/10758132. Edition: 2000/04/12.

M. P. Blaustein and A. L. Hodgkin. The effect of cyanide on the efflux of calcium from squid axons. *J Physiol*, 200(2):497–527, February 1969. ISSN 0022-3751 (Print) 0022-3751 (Linking). doi: 10.1113/jphysiol.1969.sp008704. URL https://www.ncbi.nlm.nih.gov/pubmed/5764408. Edition: 1969/02/01.

M. P. Blaustein and W. J. Lederer. Sodium/calcium exchange: its physiological implications. *Physiol Rev*, 79(3):763–854, July 1999. ISSN 0031-9333 (Print) 0031-9333 (Linking). doi: 10.1152/physrev.1999.79.3.763. URL https://www.ncbi.nlm.nih.gov/pubmed/10390518. Edition: 1999/07/03.

M. P. Blaustein and E. M. Santiago. Effects of internal and external cations and of ATP on sodium-calcium and calcium-calcium exchange in squid axons. *Biophys J*, 20(1):79–111, October 1977. ISSN 0006-3495 (Print) 0006-3495 (Linking). doi: 10.1016/S0006-3495(77)85538-0. URL https://www.ncbi.nlm.nih.gov/pubmed/901903. Edition: 1977/10/01.

F. Boscia, C. D'Avanzo, A. Pannaccione, A. Secondo, A. Casamassa, L. Formisano, N. Guida, and L. Annunziato. SILENCING OR KNOCKING-OUT OF THE NA(+)/CA(2+) EXCHANGER 3 (NCX3) IMPAIRS OLIGODENDROCYTE DIFFERENTIATION. *Glia*, 61:S135–S135, July 2013. ISSN 0894-1491. URL ://WOS:000320408400428.

Rachael L. Bosma, Elham Ameli Mojarad, Lawrence Leung, Caroline Pukall, Roland Staud, and Patrick W. Stroman. FMRI of spinal and supra-spinal correlates of temporal pain summation in fibromyalgia patients. *Human Brain Mapping*, 37(4):1349–1360, April 2016. ISSN 1097-0193. doi: 10.1002/hbm.23106.

Jennifer N Bourne and Kristen M Harris. Balancing Structure and Function at Hippocampal Dendritic Spines. *Annual Review of Neuroscience*, 31(1):47–67, July 2008. ISSN 0147-006X, 1545-4126. doi: 10.1146/annurev.neuro.31.060407.125646. URL http://www.annualreviews.org/doi/10.1146/annurev.neuro.31.060407.125646.

K. A. Boyle, M. A. Gradwell, T. Yasaka, A. C. Dickie, E. Polgar, R. P. Ganley, D. P. H. Orr, M. Watanabe, V. E. Abraira, E. D. Kuehn, A. L. Zimmerman, D. D. Ginty, R. J. Callister, B. A. Graham, and D. I. Hughes. Defining a Spinal Microcircuit that Gates Myelinated Afferent Input: Implications for Tactile Allodynia. *Cell Rep*, 28(2):526–540 e6, July 2019. ISSN 2211-1247 (Electronic). doi: 10.1016/j.celrep.2019.06.040. URL https://www.ncbi.nlm.nih.gov/pubmed/31291586. Edition: 2019/07/11.

L. Boyman, B. M. Hagen, M. Giladi, R. Hiller, W. J. Lederer, and D. Khananshvili. Proton-sensing Ca2+ binding domains regulate the cardiac Na+/Ca2+ exchanger. *J Biol Chem*, 286(33):28811–20, August 2011. ISSN 1083-351X (Electronic) 0021-9258 (Linking). doi: 10.1074/jbc.M110.214106. URL https://www.ncbi.nlm.nih.gov/pubmed/21680748. Edition: 2011/06/18.

C. Brancolini, M. Benedetti, and C. Schneider. Microfilament reorganization during apoptosis: the role of Gas2, a possible substrate for ICE-like proteases. *EMBO J*, 14

(21):5179–90, November 1995. ISSN 0261-4189 (Print) 0261-4189 (Linking). URL https://www.ncbi.nlm.nih.gov/pubmed/7489707. Edition: 1995/11/01.

H. Breivik, B. Collett, V. Ventafridda, R. Cohen, and D. Gallacher. Survey of chronic pain in Europe: prevalence, impact on daily life, and treatment. *Eur J Pain*, 10(4):287–333, May 2006. ISSN 1090-3801 (Print) 1090-3801 (Linking). doi: 10.1016/j.ejpain.2005.06.009. URL https://www.ncbi.nlm.nih.gov/pubmed/16095934. Edition: 2005/08/13.

D. G. Brenner, S. Lin-Chao, and S. N. Cohen. Analysis of mammalian cell genetic regulation in situ by using retrovirus-derived "portable exons" carrying the Escherichia coli lacZ gene. *Proc Natl Acad Sci U S A*, 86(14):5517–21, July 1989. ISSN 0027-8424 (Print) 0027-8424 (Linking). doi: 10.1073/pnas.86.14.5517. URL https://www.ncbi.nlm.nih.gov/pubmed/2501787. Edition: 1989/07/01.

A. G. Brown. Neuronal organization in the dorsal horn of the spinal cord. *Acta Morphol Hung*, 31(1-3):87–99, 1983. ISSN 0236-5391 (Print) 0236-5391 (Linking). URL https://www.ncbi.nlm.nih.gov/pubmed/6312776. Edition: 1983/01/01.

A. G. Brown and A. Iggo. A quantitative study of cutaneous receptors and afferent fibres in the cat and rabbit. *J Physiol*, 193(3):707–33, December 1967. ISSN 0022-3751 (Print) 0022-3751 (Linking). doi: 10.1113/jphysiol.1967.sp008390. URL https://www.ncbi.nlm.nih.gov/pubmed/16992307. Edition: 1967/12/01.

A. G. Brown, R. E. Fyffe, P. K. Rose, and P. J. Snow. Spinal cord collaterals from axons of type II slowly adapting units in the cat. *J Physiol*, 316:469–80, July 1981. ISSN 0022-3751 (Print) 0022-3751 (Linking). doi: 10.1113/jphysiol.1981.sp013801. URL https://www.ncbi.nlm.nih.gov/pubmed/7320876. Edition: 1981/07/01.

P. R. Burgess and E. R. Perl. Myelinated afferent fibres responding specifically to noxious stimulation of the skin. *J Physiol*, 190(3):541–62, June 1967. ISSN 0022-3751 (Print) 0022-3751 (Linking). doi: 10.1113/jphysiol.1967.sp008227. URL https://www.ncbi.nlm.nih.gov/pubmed/6051786. Edition: 1967/06/01.

S. E. Burgess, L. R. Gardell, M. H. Ossipov, T. P. Malan, Jr., T. W. Vanderah, J. Lai, and F. Porreca. Time-dependent descending facilitation from the rostral ventromedial medulla maintains, but does not initiate, neuropathic pain. *J Neurosci*, 22(12):5129–36, June 2002. ISSN 1529-2401 (Electronic) 0270-6474 (Linking). URL https://www.ncbi.nlm.nih.gov/pubmed/12077208. Edition: 2002/06/22.

W. S. Bush and J. H. Moore. Chapter 11: Genome-wide association studies. *PLoS Comput Biol*, 8(12):e1002822, 2012. ISSN 1553-7358 (Electronic) 1553-734X (Linking). doi: 10.1371/journal.pcbi.1002822. URL https://www.ncbi.nlm.nih.gov/pubmed/23300413. Edition: 2013/01/10.

Dawen Cai, Kimberly B Cohen, Tuanlian Luo, Jeff W Lichtman, and Joshua R Sanes. Improved tools for the Brainbow toolbox. *Nature Methods*, 10(6):540–547, June 2013. ISSN 1548-7091, 1548-7105. doi: 10.1038/nmeth.2450. URL http://www.nature.com/articles/nmeth.2450.

Xiaoyu C Cao, Laura W Pappalardo, Stephen G Waxman, and Andrew M Tan. Dendritic spine dysgenesis in superficial dorsal horn sensory neurons after spinal cord injury. *Molecular Pain*, 13:174480691668801, January 2017. ISSN 1744-8069,

1744-8069. doi: 10.1177/1744806916688016. URL http://journals.sagepub.com/doi/10.1177/1744806916688016.

R. J. Carter, J. Morton, and S. B. Dunnett. Motor coordination and balance in rodents. *Curr Protoc Neurosci*, Chapter 8:Unit 8 12, August 2001. ISSN 1934-8576 (Electronic) 1934-8576 (Linking). doi: 10.1002/0471142301.ns0812s15. URL https://www.ncbi.nlm.nih.gov/pubmed/18428540. Edition: 2008/04/23.

A. L. Carvalho, C. B. Duarte, and A. P. Carvalho. Regulation of AMPA receptors by phosphorylation. *Neurochemical Research*, 25(9-10):1245–1255, October 2000. ISSN 0364-3190. doi: 10.1023/a:1007644128886. URL ://WOS:000090143900011.

M. J. Caterina. Transient receptor potential ion channels as participants in thermosensation and thermoregulation. *Am J Physiol Regul Integr Comp Physiol*, 292(1):R64–76, January 2007. ISSN 0363-6119 (Print) 0363-6119 (Linking). doi: 10.1152/ajpregu.00446.2006. URL https://www.ncbi.nlm.nih.gov/pubmed/16973931. Edition: 2006/09/16.

N. Cauna. Nerve supply and nerve endings in Meissner's corpuscles. *Am J Anat*, 99(2):315–50, September 1956. ISSN 0002-9106 (Print) 0002-9106 (Linking). doi: 10.1002/aja.1000990206. URL https://www.ncbi.nlm.nih.gov/pubmed/13372495. Edition: 1956/09/01.

D. J. Cavanaugh, H. Lee, L. Lo, S. D. Shields, M. J. Zylka, A. I. Basbaum, and D. J. Anderson. Distinct subsets of unmyelinated primary sensory fibers mediate behavioral responses to noxious thermal and mechanical stimuli. *Proc Natl Acad Sci U S A*, 106(22):9075–80, June 2009. ISSN 1091-6490 (Electronic) 0027-8424 (Linking). doi: 10.1073/pnas.0901507106. URL https://www.ncbi.nlm.nih.gov/pubmed/19451647. Edition: 2009/05/20.

F. Cervero, J. Shouenborg, B.H. Sjo¨lund, and Pamela J. Waddell. Cutaneous inputs to dorsal horn neurones in adult rats treated at birth with capsaicin. *Brain Research*, 301(1):47–57, May 1984. ISSN 00068993. doi: 10.1016/0006-8993(84)90401-3. URL https://linkinghub.elsevier.com/retrieve/pii/0006899384904013.

C. C. Chao, L. J. Su, N. K. Sun, Y. T. Ju, J. C. Lih, and S. Lin-Chao. Involvement of Gas7 in nerve growth factor-independent and dependent cell processes in PC12 cells. *J Neurosci Res*, 74(2):248–54, October 2003. ISSN 0360-4012 (Print) 0360-4012 (Linking). doi: 10.1002/jnr.10763. URL https://www.ncbi.nlm.nih.gov/pubmed/14515354. Edition: 2003/09/30.

Chuck C.-K. Chao, P.-Y. Chang, and Henry H.-P. Lu. Human Gas7 isoforms homologous to mouse transcripts differentially induce neurite outgrowth. *Journal of Neuroscience Research*, 81(2):153–162, July 2005. ISSN 0360-4012, 1097-4547. doi: 10.1002/jnr.20552. URL http://doi.wiley.com/10.1002/jnr.20552.

S. R. Chaplan, F. W. Bach, J. W. Pogrel, J. M. Chung, and T. L. Yaksh. QUANTITATIVE ASSESSMENT OF TACTILE ALLODYNIA IN THE RAT PAW. *Journal of Neuroscience Methods*, 53(1):55–63, July 1994. ISSN 0165-0270. doi: 10.1016/0165-0270(94)90144-9. URL ://WOS:A1994PA94400008.

B. S. Chen and K. W. Roche. Regulation of NMDA receptors by phosphorylation. *Neuropharmacology*, 53(3):362–368, September 2007. ISSN 0028-3908. doi: 10.1016/

j.neuropharm.2007.05.018. URL ://WOS:000249512300002.

K. I. Chisholm, N. Khovanov, D. M. Lopes, F. La Russa, and S. B. McMahon. Large Scale In Vivo Recording of Sensory Neuron Activity with GCaMP6. *Eneuro*, 5 (1), January 2018. ISSN 2373-2822. doi: 10.1523/eneuro.0417-17.2018. URL ://WOS:000429409900060.

V. Chitu and E. R. Stanley. Pombe Cdc15 homology (PCH) proteins: coordinators of membrane-cytoskeletal interactions. *Trends Cell Biol*, 17(3):145–56, March 2007. ISSN 1879-3088 (Electronic) 0962-8924 (Linking). doi: 10.1016/j.tcb.2007.01.003. URL https://www.ncbi.nlm.nih.gov/pubmed/17296299. Edition: 2007/02/14.

Seungwon Choi, Junichi Hachisuka, Matthew A. Brett, Alexandra R. Magee, Yu Omori, Noor-ul-Aine Iqbal, Dawei Zhang, Michelle M. DeLisle, Rachel L. Wolfson, Ling Bai, Celine Santiago, Shiaoching Gong, Martyn Goulding, Nathaniel Heintz, H. Richard Koerber, Sarah E. Ross, and David D. Ginty. Parallel ascending spinal pathways for affective touch and pain. *Nature*, 587(7833):258–263, November 2020. ISSN 0028-0836, 1476-4687. doi: 10.1038/s41586-020-2860-1. URL http://www.nature.com/articles/s41586-020-2860-1.

A. C. Chou, Y. T. Ju, and C. Y. Pan. Calmodulin Interacts with the Sodium/Calcium Exchanger NCX1 to Regulate Activity. *PLoS One*, 10(9):e0138856, 2015. ISSN 1932-6203 (Electronic) 1932-6203 (Linking). doi: 10.1371/journal.pone.0138856. URL https://www.ncbi.nlm.nih.gov/pubmed/26421717. Edition: 2015/10/01.

M. Claussnitzer, S. N. Dankel, K. H. Kim, G. Quon, W. Meuleman, C. Haugen, V. Glunk, I. S. Sousa, J. L. Beaudry, V. Puviindran, N. A. Abdennur, J. Liu, P. A. Svensson, Y. H. Hsu, D. J. Drucker, G. Mellgren, C. C. Hui, H. Hauner, and M. Kellis. FTO Obesity Variant Circuitry and Adipocyte Browning in Humans. *N Engl J Med*, 373(10):895–907, September 2015. ISSN 1533-4406 (Electronic) 0028-4793 (Linking). doi: 10.1056/NEJMoa1502214. URL https://www.ncbi.nlm.nih.gov/pubmed/26287746. Edition: 2015/08/20.

M. Claussnitzer, J. H. Cho, R. Collins, N. J. Cox, E. T. Dermitzakis, M. E. Hurles, S. Kathiresan, E. E. Kenny, C. M. Lindgren, D. G. MacArthur, K. N. North, S. E. Plon, H. L. Rehm, N. Risch, C. N. Rotimi, J. Shendure, N. Soranzo, and M. I. McCarthy. A brief history of human disease genetics. *Nature*, 577(7789): 179–189, January 2020. ISSN 1476-4687 (Electronic) 0028-0836 (Linking). doi: 10.1038/s41586-019-1879-7. URL https://www.ncbi.nlm.nih.gov/pubmed/31915397. Edition: 2020/01/10.

G. TEx Consortium, Data Analysis Laboratory, Group Coordinating Center Analysis Working, Group Statistical Methods groups Analysis Working, GTEx groups Enhancing, N. I. H. Common Fund, Nih/Nci, Nih/Nhgri, Nih/Nimh, Nih/Nida, Ndri Biospecimen Collection Source Site, Rpci Biospecimen Collection Source Site, Vari Biospecimen Core Resource, Bank Brain Bank Repository-University of Miami Brain Endowment, Management Leidos Biomedical-Project, Elsi Study, Integration Genome Browser Data, E. B. I. Visualization, Integration Genome Browser Data, University of California Santa Cruz Visualization-Ucsc Genomics Institute, analysts Lead, Data Analysis Laboratory, Center Coordinating, N. I. H. program manage-

ment, collection Biospecimen, Pathology, Q. T. L. manuscript working group e, A. Battle, C. D. Brown, B. E. Engelhardt, and S. B. Montgomery. Genetic effects on gene expression across human tissues. *Nature*, 550(7675):204–213, October 2017. ISSN 1476-4687 (Electronic) 0028-0836 (Linking). doi: 10.1038/nature24277. URL https://www.ncbi.nlm.nih.gov/pubmed/29022597. Edition: 2017/10/13.

Alison J. Cook, Clifford J. Woolf, Patrick D. Wall, and Stephen B. McMahon. Dynamic receptive field plasticity in rat spinal cord dorsal horn following C-primary afferent input. *Nature*, 325(6100):151–153, January 1987. ISSN 0028-0836, 1476-4687. doi: 10.1038/325151a0. URL http://www.nature.com/articles/325151a0.

J. M. Dawes, G. A. Weir, S. J. Middleton, R. Patel, K. I. Chisholm, P. Pettingill, L. J. Peck, J. Sheridan, A. Shakir, L. Jacobson, M. Gutierrez-Mecinas, J. Galino, J. Walcher, J. Kuhnemund, H. Kuehn, M. D. Sanna, B. Lang, A. J. Clark, A. C. Themistocleous, N. Iwagaki, S. J. West, K. Werynska, L. Carroll, T. Trendafilova, D. A. Menassa, M. P. Giannoccaro, E. Coutinho, I. Cervellini, D. Tewari, C. Buckley, M. I. Leite, H. Wildner, H. U. Zeilhofer, E. Peles, A. J. Todd, S. B. McMahon, A. H. Dickenson, G. R. Lewin, A. Vincent, and D. L. Bennett. Immune or Genetic-Mediated Disruption of CASPR2 Causes Pain Hypersensitivity Due to Enhanced Primary Afferent Excitability. *Neuron*, 97(4):806–+, February 2018. ISSN 0896-6273. doi: 10.1016/j.neuron.2018.01.033. URL ://WOS:000425713200010.

Robert M.J. Deacon. Measuring Motor Coordination in Mice. *Journal of Visualized Experiments*, (75):2609, May 2013. ISSN 1940-087X. doi: 10.3791/2609. URL http://www.jove.com/video/2609/measuring-motor-coordination-in-mice.

G. Del Sal, E. M. Ruaro, R. Utrera, C. N. Cole, A. J. Levine, and C. Schneider. Gas1-induced growth suppression requires a transactivation-independent p53 function. *Mol Cell Biol*, 15(12):7152–60, December 1995. ISSN 0270-7306 (Print) 0270-7306 (Linking). doi: 10.1128/mcb.15.12.7152. URL https://www.ncbi.nlm.nih.gov/pubmed/8524283. Edition: 1995/12/01.

Josimari M. DeSantana, Kamilla M. L. da Cruz, and Kathleen A. Sluka. Animal models of fibromyalgia. *Arthritis Research & Therapy*, 15(6):222, 2013. ISSN 1478-6362. doi: 10.1186/ar4402.

A. H. Dickenson, V. Chapman, and G. M. Green. The pharmacology of excitatory and inhibitory amino acid-mediated events in the transmission and modulation of pain in the spinal cord. *General Pharmacology-the Vascular System*, 28(5): 633–638, May 1997. ISSN 0306-3623. doi: 10.1016/s0306-3623(96)00359-x. URL ://WOS:A1997WZ41700001.

Allen C. Dickie, Andrew M. Bell, Noboru Iwagaki, Erika Polgár, Maria Gutierrez-Mecinas, Rosalind Kelly, Heather Lyon, Kirsten Turnbull, Steven J. West, Alexander Etlin, Joao Braz, Masahiko Watanabe, David L.H. Bennett, Allan I. Basbaum, John S. Riddell, and Andrew J. Todd. Morphological and functional properties distinguish the substance P and gastrin-releasing peptide subsets of excitatory interneuron in the spinal cord dorsal horn. *Pain*, 160(2):442–462, February 2019. ISSN 0304-3959, 1872-6623. doi: 10.1097/j.pain.0000000000001406. URL https://journals.lww.com/00006396-201902000-00018.

R. Dipolo. Effect of ATP on the calcium efflux in dialyzed squid giant axons. *J Gen Physiol*, 64(4):503–17, October 1974. ISSN 0022-1295 (Print) 0022-1295 (Linking). doi: 10.1085/jgp.64.4.503. URL https://www.ncbi.nlm.nih.gov/pubmed/4418552. Edition: 1974/10/01.

R. Dipolo. The influence of nucleotides on calcium fluxes. *Fed Proc*, 35(14):2579–82, December 1976. ISSN 0014-9446 (Print) 0014-9446 (Linking). URL https://www.ncbi.nlm.nih.gov/pubmed/992109. Edition: 1976/12/01.

R. DiPolo and L. Beauge. In squid axons, ATP modulates Na+-Ca2+ exchange by a Ca2+i-dependent phosphorylation. *Biochim Biophys Acta*, 897(3):347–54, March 1987. ISSN 0006-3002 (Print) 0006-3002 (Linking). doi: 10.1016/0005-2736(87)90432-9. URL https://www.ncbi.nlm.nih.gov/pubmed/3814592. Edition: 1987/03/12.

Reinaldo Dipolo and Luis Beaugé. Sodium/Calcium Exchanger: Influence of Metabolic Regulation on Ion Carrier Interactions. *Physiological Reviews*, 86(1):155–203, January 2006. ISSN 0031-9333, 1522-1210. doi: 10.1152/physrev.00018.2005. URL https://www.physiology.org/doi/10.1152/physrev.00018.2005.

W. J Dixon. The Up-and-Down Method for Small Samples. *Journal of American Statistical Association*, 1965.

R. D'Mello and A. H. Dickenson. Spinal cord mechanisms of pain. *British Journal of Anaesthesia*, 101(1):8–16, July 2008. ISSN 0007-0912. doi: 10.1093/bja/aen088. URL ://WOS:000256757700003.

P. M. Dougherty and W. D. Willis. Enhancement of spinothalamic neuron responses to chemical and mechanical stimuli following combined micro-iontophoretic application of N-methyl-D-aspartic acid and substance P. *Pain*, 47(1):85–93, October 1991. ISSN 0304-3959 (Print) 0304-3959 (Linking). doi: 10.1016/0304-3959(91)90015-p. URL https://www.ncbi.nlm.nih.gov/pubmed/1722895. Edition: 1991/10/01.

C. A. Doyle and S. P. Hunt. Substance P receptor (neurokinin-1)-expressing neurons in lamina I of the spinal cord encode for the intensity of noxious stimulation: a c-Fos study in rat. *Neuroscience*, 89(1):17–28, March 1999. ISSN 0306-4522 (Print) 0306-4522 (Linking). doi: 10.1016/s0306-4522(98)00276-0. URL https://www.ncbi.nlm.nih.gov/pubmed/10051214. Edition: 1999/03/02.

A. E. Dubin and A. Patapoutian. Nociceptors: the sensors of the pain pathway. *J Clin Invest*, 120(11):3760–72, November 2010. ISSN 1558-8238 (Electronic) 0021-9738 (Linking). doi: 10.1172/JCI42843. URL https://www.ncbi.nlm.nih.gov/pubmed/21041958. Edition: 2010/11/03.

D. Dubuisson and S. G. Dennis. The formalin test: a quantitative study of the analgesic effects of morphine, meperidine, and brain stem stimulation in rats and cats. *Pain*, 4(2):161–74, December 1977. ISSN 0304-3959 (Print) 0304-3959 (Linking). doi: 10.1016/0304-3959(77)90130-0. URL https://www.ncbi.nlm.nih.gov/pubmed/564014. Edition: 1977/12/01.

R. H. Duerr, K. D. Taylor, S. R. Brant, J. D. Rioux, M. S. Silverberg, M. J. Daly, A. H. Steinhart, C. Abraham, M. Regueiro, A. Griffiths, T. Dassopoulos, A. Bitton, H. Yang, S. Targan, L. W. Datta, E. O. Kistner, L. P. Schumm, A. T. Lee, P. K.

Gregersen, M. M. Barmada, J. I. Rotter, D. L. Nicolae, and J. H. Cho. A genome-wide association study identifies IL23R as an inflammatory bowel disease gene. *Science*, 314 (5804):1461–3, December 2006. ISSN 1095-9203 (Electronic) 0036-8075 (Linking). doi: 10.1126/science.1135245. URL https://www.ncbi.nlm.nih.gov/pubmed/17068223. Edition: 2006/10/28.

P K Eide, E Jorum, and A E Stenehjem. Somatosensory findings in patients with spinal cord injury and central dysaesthesia pain. *Journal of Neurology, Neurosurgery & Psychiatry*, 60(4):411–415, April 1996. ISSN 0022-3050. doi: 10.1136/jnnp.60.4.411. URL https://jnnp.bmj.com/lookup/doi/10.1136/jnnp.60.4.411.

Per Kristian Eide, Ellen Jørum, Audun Stubhaug, Jørn Bremnes, and Harald Breivik. Relief of post-herpetic neuralgia with the Symbol receptor antagonist ketamine: A double-blind, cross-over comparison with morphine and placebo. *Pain*, 58(3): 347–354, September 1994. ISSN 0304-3959. doi: 10.1016/0304-3959(94)90129-5. URL https://journals.lww.com/00006396-199409000-00007.

J. A. Esteban, S. H. Shi, C. Wilson, M. Nuriya, R. L. Huganir, and R. Malinow. PKA phosphorylation of AMPA receptor subunits controls synaptic trafficking underlying plasticity. *Nat Neurosci*, 6(2):136–43, February 2003. ISSN 1097-6256 (Print) 1097-6256 (Linking). doi: 10.1038/nn997. URL https://www.ncbi.nlm.nih.gov/pubmed/12536214. Edition: 2003/01/22.

E. Fabbretti, P. Edomi, C. Brancolini, and C. Schneider. Apoptotic phenotype induced by overexpression of wild-type gas3/PMP22: its relation to the demyelinating peripheral neuropathy CMT1A. *Genes Dev*, 9(15):1846–56, August 1995. ISSN 0890-9369 (Print) 0890-9369 (Linking). doi: 10.1101/gad.9.15.1846. URL https://www.ncbi.nlm.nih.gov/pubmed/7649472. Edition: 1995/08/01.

J. Fawcett. SIGNAL TRANSDUCTION: N-WASP Regulation–the Sting in the Tail. *Science*, 290(5492):725–726, October 2000. ISSN 00368075, 10959203. doi: 10.1126/science.290.5492.725. URL https://www.sciencemag.org/lookup/doi/10.1126/science.290.5492.725.

S. Felsby, J. Nielsen, L. Arendt-Nielsen, and T. S. Jensen. NMDA receptor blockade in chronic neuropathic pain: a comparison of ketamine and magnesium chloride. *Pain*, 64(2):283–291, February 1996. ISSN 0304-3959. doi: 10.1016/0304-3959(95)00113-1. URL https://journals.lww.com/00006396-199602000-00010.

Paul Fernyhough and Nigel A. Calcutt. Abnormal calcium homeostasis in peripheral neuropathies. *Cell Calcium*, 47(2):130–139, February 2010. ISSN 01434160. doi: 10.1016/j.ceca.2009.11.008. URL https://linkinghub.elsevier.com/retrieve/pii/S0143416009001894.

T. Z. Fischer and S. G. Waxman. Familial pain syndromes from mutations of the NaV1.7 sodium channel. *Ann N Y Acad Sci*, 1184:196–207, January 2010. ISSN 1749-6632 (Electronic) 0077-8923 (Linking). doi: 10.1111/j.1749-6632.2009.05110.x. URL https://www.ncbi.nlm.nih.gov/pubmed/20146699. Edition: 2010/02/12.

E. Foster, H. Wildner, L. Tudeau, S. Haueter, W. T. Ralvenius, M. Jegen, H. Johannssen, L. Hosli, K. Haenraets, A. Ghanem, K. K. Conzelmann, M. Bosl, and H. U. Zeilhofer. Targeted ablation, silencing, and activation establish glycinergic dorsal horn neurons

as key components of a spinal gate for pain and itch. *Neuron*, 85(6):1289–304, March 2015. ISSN 1097-4199 (Electronic) 0896-6273 (Linking). doi: 10.1016/j.neuron.2015.02.028. URL https://www.ncbi.nlm.nih.gov/pubmed/25789756. Edition: 2015/03/20.

A. Galan, J. M. A. Laird, and F. Cervero. In vivo recruitment by painful stimuli of AMPA receptor subunits to the plasma membrane of spinal cord neurons. *Pain*, 112 (3):315–323, December 2004. ISSN 0304-3959. doi: 10.1016/j.pain.2004.09.011. URL ://WOS:000225601500012.

E. L. Garland. Pain processing in the human nervous system: a selective review of nociceptive and biobehavioral pathways. *Prim Care*, 39(3):561–71, September 2012. ISSN 1558-299X (Electronic) 0095-4543 (Linking). doi: 10.1016/j.pop.2012.06.013. URL https://www.ncbi.nlm.nih.gov/pubmed/22958566. Edition: 2012/09/11.

E. Gascon and A. Moqrich. Heterogeneity in primary nociceptive neurons: from molecules to pathology. *Arch Pharm Res*, 33(10):1489–507, October 2010. ISSN 0253-6269 (Print) 0253-6269 (Linking). doi: 10.1007/s12272-010-1003-x. URL https://www.ncbi.nlm.nih.gov/pubmed/21052929. Edition: 2010/11/06.

M. Giladi and D. Khananshvili. Molecular determinants of allosteric regulation in NCX proteins. *Adv Exp Med Biol*, 961:35–48, 2013. ISSN 0065-2598 (Print) 0065-2598 (Linking). doi: 10.1007/978-1-4614-4756-6_4. URL https://www.ncbi.nlm.nih.gov/pubmed/23224868. Edition: 2012/12/12.

M. Giladi, S. Y. Lee, Y. Ariely, Y. Teldan, R. Granit, R. Strulovich, Y. Haitin, K. Y. Chung, and D. Khananshvili. Structure-based dynamic arrays in regulatory domains of sodium-calcium exchanger (NCX) isoforms. *Sci Rep*, 7(1):993, April 2017. ISSN 2045-2322 (Electronic) 2045-2322 (Linking). doi: 10.1038/s41598-017-01102-x. URL https://www.ncbi.nlm.nih.gov/pubmed/28428550. Edition: 2017/04/22.

M. S. Gold and G. F. Gebhart. Nociceptor sensitization in pain pathogenesis. *Nat Med*, 16(11):1248–57, November 2010. ISSN 1546-170X (Electronic) 1078-8956 (Linking). doi: 10.1038/nm.2235. URL https://www.ncbi.nlm.nih.gov/pubmed/20948530. Edition: 2010/10/16.

S. Gong, C. Zheng, M. L. Doughty, K. Losos, N. Didkovsky, U. B. Schambra, N. J. Nowak, A. Joyner, G. Leblanc, M. E. Hatten, and N. Heintz. A gene expression atlas of the central nervous system based on bacterial artificial chromosomes. *Nature*, 425(6961):917–25, October 2003. ISSN 1476-4687 (Electronic) 0028-0836 (Linking). doi: 10.1038/nature02033. URL https://www.ncbi.nlm.nih.gov/pubmed/14586460. Edition: 2003/10/31.

T. D. Gover, T. H. Moreira, J. P. Kao, and D. Weinreich. Calcium regulation in individual peripheral sensory nerve terminals of the rat. *J Physiol*, 578(Pt 2): 481–90, January 2007. ISSN 0022-3751 (Print) 0022-3751 (Linking). doi: 10.1113/jphysiol.2006.119008. URL https://www.ncbi.nlm.nih.gov/pubmed/17095566. Edition: 2006/11/11.

Nicholas S. Gregory, Amber L. Harris, Caleb R. Robinson, Patrick M. Dougherty, Perry N. Fuchs, and Kathleen A. Sluka. An Overview of Animal Models of Pain: Disease Models and Outcome Measures. *The Journal of Pain*, 14(11):1255–1269,

November 2013. ISSN 15265900. doi: 10.1016/j.jpain.2013.06.008. URL https://linkinghub.elsevier.com/retrieve/pii/S1526590013010985.

T. J. Grudt and E. R. Perl. Correlations between neuronal morphology and electrophysiological features in the rodent superficial dorsal horn. *J Physiol*, 540(Pt 1):189–207, April 2002. ISSN 0022-3751 (Print) 0022-3751 (Linking). doi: 10.1113/jphysiol.2001.012890. URL https://www.ncbi.nlm.nih.gov/pubmed/11927679. Edition: 2002/04/03.

M. Gutierrez-Mecinas, T. Furuta, M. Watanabe, and A. J. Todd. A quantitative study of neurochemically defined excitatory interneuron populations in laminae I-III of the mouse spinal cord. *Mol Pain*, 12, 2016. ISSN 1744-8069 (Electronic) 1744-8069 (Linking). doi: 10.1177/1744806916629065. URL https://www.ncbi.nlm.nih.gov/pubmed/27030714. Edition: 2016/04/01.

M. Gutierrez-Mecinas, A. Bell, E. Polgar, M. Watanabe, and A. J. Todd. Expression of Neuropeptide FF Defines a Population of Excitatory Interneurons in the Superficial Dorsal Horn of the Mouse Spinal Cord that Respond to Noxious and Pruritic Stimuli. *Neuroscience*, 416:281–293, September 2019a. ISSN 1873-7544 (Electronic) 0306-4522 (Linking). doi: 10.1016/j.neuroscience.2019.08.013. URL https://www.ncbi.nlm.nih.gov/pubmed/31421202. Edition: 2019/08/20.

M. Gutierrez-Mecinas, A. M. Bell, F. Shepherd, E. Polgar, M. Watanabe, T. Furuta, and A. J. Todd. Expression of cholecystokinin by neurons in mouse spinal dorsal horn. *J Comp Neurol*, 527(11):1857–1871, August 2019b. ISSN 1096-9861 (Electronic) 0021-9967 (Linking). doi: 10.1002/cne.24657. URL https://www.ncbi.nlm.nih.gov/pubmed/30734936. Edition: 2019/02/09.

H. Haeberle and E. A. Lumpkin. Merkel Cells in Somatosensation. *Chemosens Percept*, 1(2):110–118, June 2008. ISSN 1936-5802 (Print) 1936-5802 (Linking). doi: 10.1007/s12078-008-9012-6. URL https://www.ncbi.nlm.nih.gov/pubmed/19834574. Edition: 2008/06/01.

Anna M. Hagenston and Manuela Simonetti. Neuronal calcium signaling in chronic pain. *Cell and Tissue Research*, 357(2):407–426, August 2014. ISSN 0302-766X, 1432-0878. doi: 10.1007/s00441-014-1942-5. URL http://link.springer.com/10.1007/s00441-014-1942-5.

Shelley Halpain, Kathy Spencer, and Simone Graber. Dynamics and pathology of dendritic spines. In *Progress in Brain Research*, volume 147, pages 29–37. Elsevier, 2005. ISBN 978-0-444-51663-3. doi: 10.1016/S0079-6123(04)47003-4. URL https://linkinghub.elsevier.com/retrieve/pii/S0079612304470034.

Menachem Hanani. Role of satellite glial cells in gastrointestinal pain. *Frontiers in Cellular Neuroscience*, 9:412, 2015. ISSN 1662-5102. doi: 10.3389/fncel.2015.00412.

Louise Harding. Human Models of Inflammatory Pain. In Gerald F. Gebhart and Robert F. Schmidt, editors, *Encyclopedia of Pain*, pages 1500–1503. Springer Berlin Heidelberg, Berlin, Heidelberg, 2013. ISBN 978-3-642-28752-7 978-3-642-28753-4. doi: 10.1007/978-3-642-28753-4_1790. URL http://link.springer.com/10.1007/978-3-642-28753-4_1790.

K. Hargreaves, R. Dubner, F. Brown, C. Flores, and J. Joris. A NEW AND SENSITIVE METHOD FOR MEASURING THERMAL NOCICEPTION IN CUTANEOUS HYPERALGESIA. *Pain*, 32(1):77–88, January 1988. ISSN 0304-3959. doi: 10.1016/0304-3959(88)90026-7. URL ://WOS:A1988L777300011.

M. Haring, A. Zeisel, H. Hochgerner, P. Rinwa, J. E. T. Jakobsson, P. Lonnerberg, G. La Manno, N. Sharma, L. Borgius, O. Kiehn, M. C. Lagerstrom, S. Linnarsson, and P. Ernfors. Neuronal atlas of the dorsal horn defines its architecture and links sensory input to transcriptional cell types. *Nat Neurosci*, 21(6):869–880, June 2018. ISSN 1546-1726 (Electronic) 1097-6256 (Linking). doi: 10.1038/s41593-018-0141-1. URL https://www.ncbi.nlm.nih.gov/pubmed/29686262. Edition: 2018/04/25.

J. L. Henry. Effects of substance P on functionally identified units in cat spinal cord. *Brain Res*, 114(3):439–51, September 1976. ISSN 0006-8993 (Print) 0006-8993 (Linking). doi: 10.1016/0006-8993(76)90965-3. URL https://www.ncbi.nlm.nih.gov/pubmed/953765. Edition: 1976/09/24.

P. A. Heppenstall and G. R. Lewin. BDNF but not NT-4 is required for normal flexion reflex plasticity and function. *Proc Natl Acad Sci U S A*, 98(14):8107–12, July 2001. ISSN 0027-8424 (Print) 0027-8424 (Linking). doi: 10.1073/pnas.141015098. URL https://www.ncbi.nlm.nih.gov/pubmed/11438749. Edition: 2001/07/05.

J. F. Herrero, J. M. A. Laird, and J. A. Lopez-Garcia. Wind-up of spinal cord neurones and pain sensation: much ado about something? *Progress in Neurobiology*, 61(2):169–203, June 2000. ISSN 0301-0082. doi: 10.1016/s0301-0082(99)00051-9. URL ://WOS:000086078200003.

Juan F. Herrero and Fernando Cervero. Changes in nociceptive reflex facilitation during carrageenan-induced arthritis. *Brain Research*, 717(1-2):62–68, April 1996. ISSN 00068993. doi: 10.1016/0006-8993(95)01585-X. URL https://linkinghub.elsevier.com/retrieve/pii/000689939501585X.

M. Hilge, J. Aelen, and G. W. Vuister. Ca2+ regulation in the Na+/Ca2+ exchanger involves two markedly different Ca2+ sensors. *Mol Cell*, 22(1):15–25, April 2006. ISSN 1097-2765 (Print) 1097-2765 (Linking). doi: 10.1016/j.molcel.2006.03.008. URL https://www.ncbi.nlm.nih.gov/pubmed/16600866. Edition: 2006/04/08.

K. W. Horch, R. P. Tuckett, and P. R. Burgess. A key to the classification of cutaneous mechanoreceptors. *J Invest Dermatol*, 69(1):75–82, July 1977. ISSN 0022-202X (Print) 0022-202X (Linking). doi: 10.1111/1523-1747.ep12497887. URL https://www.ncbi.nlm.nih.gov/pubmed/874346. Edition: 1977/07/01.

Pelc S. P. Howard A. Synthesis of deoxyribonucleic acid in normal and irradiated cells and its relation to chromosome breakage. 1953.

H. J. Hu, K. S. Glauner, and R. W. Gereau. ERK integrates PKA and PKC signaling in superficial dorsal horn neurons. I. Modulation of A-type K+ currents. *Journal of Neurophysiology*, 90(3):1671–1679, September 2003. ISSN 0022-3077. doi: 10.1152/jn.00340.2003. URL ://WOS:000185217700030.

Bo-Tsang Huang, Pu-Yuan Chang, Ching-Hua Su, Chuck C.-K. Chao, and Sue Lin-Chao. Gas7-Deficient Mouse Reveals Roles in Motor Function and Muscle Fiber Composition during Aging. *PLoS ONE*, 7(5):e37702, May 2012. ISSN 1932-6203.

doi: 10.1371/journal.pone.0037702. URL https://dx.plos.org/10.1371/journal.pone.0037702.

D. I. Hughes, S. Sikander, C. M. Kinnon, K. A. Boyle, M. Watanabe, R. J. Callister, and B. A. Graham. Morphological, neurochemical and electrophysiological features of parvalbumin-expressing cells: a likely source of axo-axonic inputs in the mouse spinal dorsal horn. *J Physiol*, 590(16):3927–51, August 2012. ISSN 1469-7793 (Electronic) 0022-3751 (Linking). doi: 10.1113/jphysiol.2012.235655. URL https://www.ncbi.nlm.nih.gov/pubmed/22674718. Edition: 2012/06/08.

Steinar Hunskaar and Kjell Hole. The formalin test in mice: dissociation between inflammatory and non-inflammatory pain. *Pain*, 30(1):103–114, July 1987. ISSN 0304-3959. doi: 10.1016/0304-3959(87)90088-1.

J. L. Hylden, F. Anton, and R. L. Nahin. Spinal lamina I projection neurons in the rat: collateral innervation of parabrachial area and thalamus. *Neuroscience*, 28(1):27–37, 1989a. ISSN 0306-4522 (Print) 0306-4522 (Linking). doi: 10.1016/0306-4522(89)90229-7. URL https://www.ncbi.nlm.nih.gov/pubmed/2548118. Edition: 1989/01/01.

Janice L.K. Hylden, Richard L. Nahin, Richard J. Traub, and Ronald Dubner. Expansion of receptive fields of spinal lamina I projection neurons in rats with unilateral adjuvant-induced inflammation: the contribution of dorsal horn mechanisms. *Pain*, 37(2):229–243, May 1989b. ISSN 0304-3959. doi: 10.1016/0304-3959(89)90135-8. URL https://journals.lww.com/00006396-198905000-00011.

C. Ide. The fine structure of the digital corpuscle of the mouse toe pad, with special reference to nerve fibers. *Am J Anat*, 147(3):329–55, November 1976. ISSN 0002-9106 (Print) 0002-9106 (Linking). doi: 10.1002/aja.1001470307. URL https://www.ncbi.nlm.nih.gov/pubmed/983972. Edition: 1976/11/01.

A. Iggo and A. R. Muir. The structure and function of a slowly adapting touch corpuscle in hairy skin. *J Physiol*, 200(3):763–96, February 1969. ISSN 0022-3751 (Print) 0022-3751 (Linking). doi: 10.1113/jphysiol.1969.sp008721. URL https://www.ncbi.nlm.nih.gov/pubmed/4974746. Edition: 1969/02/01.

A. Iggo and H. Ogawa. Correlative physiological and morphological studies of rapidly adapting mechanoreceptors in cat's glabrous skin. *J Physiol*, 266(2):275–96, April 1977. ISSN 0022-3751 (Print) 0022-3751 (Linking). doi: 10.1113/jphysiol.1977.sp011768. URL https://www.ncbi.nlm.nih.gov/pubmed/853451. Edition: 1977/04/01.

H. Ikeda, J. Stark, H. Fischer, M. Wagner, R. Drdla, T. Jager, and J. Sandkuhler. Synaptic amplifier of inflammatory pain in the spinal dorsal horn. *Science*, 312(5780):1659–62, June 2006. ISSN 1095-9203 (Electronic) 0036-8075 (Linking). doi: 10.1126/science.1127233. URL https://www.ncbi.nlm.nih.gov/pubmed/16778058. Edition: 2006/06/17.

S. Ikegawa. A short history of the genome-wide association study: where we were and where we are going. *Genomics Inform*, 10(4):220–5, December 2012. ISSN 1598-866X (Print) 1598-866X (Linking). doi: 10.5808/GI.2012.10.4.220. URL https://www.ncbi.nlm.nih.gov/pubmed/23346033. Edition: 2013/01/25.

Consortium International HapMap. A haplotype map of the human genome. *Nature*, 437(7063):1299–320, October 2005. ISSN 1476-4687 (Electronic) 0028-0836 (Linking). doi: 10.1038/nature04226. URL https://www.ncbi.nlm.nih.gov/pubmed/16255080. Edition: 2005/10/29.

Consortium International Human Genome Sequencing. Finishing the euchromatic sequence of the human genome. *Nature*, 431(7011):931–45, October 2004. ISSN 1476-4687 (Electronic) 0028-0836 (Linking). doi: 10.1038/nature03001. URL https://www.ncbi.nlm.nih.gov/pubmed/15496913. Edition: 2004/10/22.

T. Iwamoto and M. Shigekawa. Differential inhibition of Na+/Ca2+ exchanger isoforms by divalent cations and isothiourea derivative. *Am J Physiol*, 275(2):C423–30, August 1998. ISSN 0002-9513 (Print) 0002-9513 (Linking). doi: 10.1152/ajpcell.1998.275.2.C423. URL https://www.ncbi.nlm.nih.gov/pubmed/9688596. Edition: 1998/08/04.

Sara E. Jager, Lone T. Pallesen, Mette Richner, Peter Harley, Zoe Hore, Stephen McMahon, Franziska Denk, and Christian B. Vægter. Changes in the transcriptional fingerprint of satellite glial cells following peripheral nerve injury. *Glia*, 68(7):1375–1395, July 2020. ISSN 0894-1491, 1098-1136. doi: 10.1002/glia.23785. URL https://onlinelibrary.wiley.com/doi/abs/10.1002/glia.23785.

R. R. Ji, H. Baba, G. J. Brenner, and C. J. Woolf. Nociceptive-specific activation of ERK in spinal neurons contributes to pain hypersensitivity. *Nature Neuroscience*, 2(12):1114–1119, December 1999. ISSN 1097-6256. doi: 10.1038/16040. URL ://WOS:000085810100016.

K. O. Johnson. The roles and functions of cutaneous mechanoreceptors. *Curr Opin Neurobiol*, 11(4):455–61, August 2001. ISSN 0959-4388 (Print) 0959-4388 (Linking). doi: 10.1016/s0959-4388(00)00234-8. URL https://www.ncbi.nlm.nih.gov/pubmed/11502392. Edition: 2001/08/15.

K. O. Johnson, T. Yoshioka, and F. Vega-Bermudez. Tactile functions of mechanoreceptive afferents innervating the hand. *J Clin Neurophysiol*, 17(6):539–58, November 2000. ISSN 0736-0258 (Print) 0736-0258 (Linking). doi: 10.1097/00004691-200011000-00002. URL https://www.ncbi.nlm.nih.gov/pubmed/11151974. Edition: 2001/01/11.

Y. T. Ju, A. C. Chang, B. R. She, M. L. Tsaur, H. M. Hwang, C. C. Chao, S. N. Cohen, and S. Lin-Chao. gas7: A gene expressed preferentially in growth-arrested fibroblasts and terminally differentiated Purkinje neurons affects neurite formation. *Proc Natl Acad Sci U S A*, 95(19):11423–8, September 1998. ISSN 0027-8424 (Print) 0027-8424 (Linking). doi: 10.1073/pnas.95.19.11423. URL https://www.ncbi.nlm.nih.gov/pubmed/9736752. Edition: 1998/09/16.

B. J. Kerr, E. J. Bradbury, D. L. Bennett, P. M. Trivedi, P. Dassan, J. French, D. B. Shelton, S. B. McMahon, and S. W. Thompson. Brain-derived neurotrophic factor modulates nociceptive sensory inputs and NMDA-evoked responses in the rat spinal cord. *J Neurosci*, 19(12):5138–48, June 1999. ISSN 1529-2401 (Electronic) 0270-6474 (Linking). URL https://www.ncbi.nlm.nih.gov/pubmed/10366647. Edition: 1999/06/15.

W. Kessler, C. Kirchhoff, P. W. Reeh, and H. O. Handwerker. Excitation of cutaneous afferent nerve endings in vitro by a combination of inflammatory mediators and conditioning effect of substance P. *Exp Brain Res*, 91(3):467–76, 1992. ISSN 0014-4819 (Print) 0014-4819 (Linking). doi: 10.1007/bf00227842. URL https://www.ncbi.nlm.nih.gov/pubmed/1282891. Edition: 1992/01/01.

D. Khananshvili. The SLC8 gene family of sodium-calcium exchangers (NCX) - structure, function, and regulation in health and disease. *Mol Aspects Med*, 34 (2-3):220–35, April 2013. ISSN 1872-9452 (Electronic) 0098-2997 (Linking). doi: 10.1016/j.mam.2012.07.003. URL https://www.ncbi.nlm.nih.gov/pubmed/23506867. Edition: 2013/03/20.

D. Khananshvili. Sodium-calcium exchangers (NCX): molecular hallmarks underlying the tissue-specific and systemic functions. *Pflugers Arch*, 466(1):43–60, January 2014. ISSN 1432-2013 (Electronic) 0031-6768 (Linking). doi: 10.1007/s00424-013-1405-y. URL https://www.ncbi.nlm.nih.gov/pubmed/24281864. Edition: 2013/11/28.

Veronika Khariv, Li Ni, Ayomi Ratnayake, Sujitha Sampath, Brianna M. Lutz, Xuan-Xiang Tao, Robert F. Heary, and Stella Elkabes. Impaired sensitivity to pain stimuli in plasma membrane calcium ATPase 2 (PMCA2) heterozygous mice: a possible modality- and sex-specific role for PMCA2 in nociception. *The FASEB Journal*, 31 (1):224–237, January 2017. ISSN 0892-6638, 1530-6860. doi: 10.1096/fj.201600541r. URL https://onlinelibrary.wiley.com/doi/abs/10.1096/fj.201600541r.

S. G. Khasabov, S. D. Rogers, J. R. Ghilardi, C. M. Peters, P. W. Mantyh, and D. A. Simone. Spinal neurons that possess the substance P receptor are required for the development of central sensitization. *J Neurosci*, 22(20):9086–98, October 2002. ISSN 1529-2401 (Electronic) 0270-6474 (Linking). URL https://www.ncbi.nlm.nih.gov/pubmed/12388616. Edition: 2002/10/22.

Byung G. Kim, Hai-Ning Dai, Marietta McAtee, Stefano Vicini, and Barbara S. Bregman. Remodeling of synaptic structures in the motor cortex following spinal cord injury. *Experimental Neurology*, 198(2):401–415, April 2006. ISSN 00144886. doi: 10.1016/j.expneurol.2005.12.010. URL https://linkinghub.elsevier.com/retrieve/pii/S001448860500467X.

H. Y. Kim, K. Y. Lee, Y. Lu, J. Wang, L. Cui, S. J. Kim, J. M. Chung, and K. Chung. Mitochondrial Ca2+ Uptake Is Essential for Synaptic Plasticity in Pain. *Journal of Neuroscience*, 31(36):12982–12991, September 2011. ISSN 0270-6474, 1529-2401. doi: 10.1523/JNEUROSCI.3093-11.2011. URL http://www.jneurosci.org/cgi/doi/10.1523/JNEUROSCI.3093-11.2011.

Emily A. King, J. Wade Davis, and Jacob F. Degner. Are drug targets with genetic support twice as likely to be approved? Revised estimates of the impact of genetic support for drug mechanisms on the probability of drug approval. *PLOS Genetics*, 15 (12):e1008489, December 2019. ISSN 1553-7404. doi: 10.1371/journal.pgen.1008489. URL https://dx.plos.org/10.1371/journal.pgen.1008489.

Monika Klede, Hermann O. Handwerker, and Martin Schmelz. Central Origin of Secondary Mechanical Hyperalgesia. *Journal of Neurophysiology*, 90(1):353–359, July 2003. ISSN 0022-3077, 1522-1598. doi: 10.1152/jn.01136.2002. URL https:

//www.physiology.org/doi/10.1152/jn.01136.2002.

R. J. Klein, C. Zeiss, E. Y. Chew, J. Y. Tsai, R. S. Sackler, C. Haynes, A. K. Henning, J. P. SanGiovanni, S. M. Mane, S. T. Mayne, M. B. Bracken, F. L. Ferris, J. Ott, C. Barnstable, and J. Hoh. Complement factor H polymorphism in age-related macular degeneration. *Science*, 308(5720):385–9, April 2005. ISSN 1095-9203 (Electronic) 0036-8075 (Linking). doi: 10.1126/science.1109557. URL https://www.ncbi.nlm.nih.gov/pubmed/15761122. Edition: 2005/03/12.

S. C. Koch, D. Acton, and M. Goulding. Spinal Circuits for Touch, Pain, and Itch. *Annu Rev Physiol*, 80:189–217, February 2018. ISSN 1545-1585 (Electronic) 0066-4278 (Linking). doi: 10.1146/annurev-physiol-022516-034303. URL https://www.ncbi.nlm.nih.gov/pubmed/28961064. Edition: 2017/09/30.

Martin Koltzenburg, Lars E.R. Lundberg, and Erik H. Torebjörk. Dynamic and static components of mechanical hyperalgesia in human hairy skin. *Pain*, 51(2): 207–219, November 1992. ISSN 0304-3959. doi: 10.1016/0304-3959(92)90262-A. URL https://journals.lww.com/00006396-199211000-00010.

M. T. Kronschlager, R. Drdla-Schutting, M. Gassner, S. D. Honsek, H. L. Teuchmann, and J. Sandkuhler. Gliogenic LTP spreads widely in nociceptive pathways. *Science*, 354(6316):1144–1148, December 2016. ISSN 1095-9203 (Electronic) 0036-8075 (Linking). doi: 10.1126/science.aah5715. URL https://www.ncbi.nlm.nih.gov/pubmed/27934764. Edition: 2016/12/10.

R. Kuner. The plastic spinal cord: functional and structural plasticity in the transition from acute to chronic pain. 2017.

R. Kuner and H. Flor. Structural plasticity and reorganisation in chronic pain (vol 18, pg 20, 2017). *Nature Reviews Neuroscience*, 18(2), February 2017a. ISSN 1471-003X. URL ://WOS:000415269600001.

R. Kuner and H. Flor. Structural plasticity and reorganisation in chronic pain. *Nature Reviews Neuroscience*, 18(1):20–30, January 2017b. ISSN 1471-003X. doi: 10.1038/nrn.2016.162. URL ://WOS:000390744200006.

Michael P. Kurnellas, Arnaud Nicot, Gary E. Shull, and Stella Elkabes. Plasma membrane calcium ATPase deficiency causes neuronal pathology in the spinal cord: a potential mechanism for neurodegeneration in multiple sclerosis and spinal cord injury. *The FASEB Journal*, 19(2):1–19, February 2005. ISSN 0892-6638, 1530-6860. doi: 10.1096/fj.04-2549fje. URL https://onlinelibrary.wiley.com/doi/abs/10.1096/fj.04-2549fje.

J M Laird, P G de la Rubia, and F Cervero. Excitability changes of somatic and viscero-somatic nociceptive reflexes in the decerebrate-spinal rabbit: role of NMDA receptors. *The Journal of Physiology*, 489(2):545–555, December 1995. ISSN 00223751. doi: 10.1113/jphysiol.1995.sp021071. URL http://doi.wiley.com/10.1113/jphysiol.1995.sp021071.

C. C. LaMotte, S. E. Kapadia, and C. M. Shapiro. Central projections of the sciatic, saphenous, median, and ulnar nerves of the rat demonstrated by transganglionic transport of choleragenoid-HRP (B-HRP) and wheat germ agglutinin-HRP (WGA-HRP). *J Comp Neurol*, 311(4):546–62, September 1991. ISSN 0021-9967 (Print)

0021-9967 (Linking). doi: 10.1002/cne.903110409. URL https://www.ncbi.nlm.nih.gov/pubmed/1721924. Edition: 1991/09/22.

M. Larsson. Pax2 is persistently expressed by GABAergic neurons throughout the adult rat dorsal horn. *Neurosci Lett*, 638:96–101, January 2017. ISSN 1872-7972 (Electronic) 0304-3940 (Linking). doi: 10.1016/j.neulet.2016.12.015. URL https://www.ncbi.nlm.nih.gov/pubmed/27939388. Edition: 2016/12/13.

M. Larsson and J. Broman. Synaptic Organization of VGLUT3 Expressing Low-Threshold Mechanosensitive C Fiber Terminals in the Rodent Spinal Cord. *eNeuro*, 6(1), January 2019. ISSN 2373-2822 (Electronic) 2373-2822 (Linking). doi: 10.1523/ENEURO.0007-19.2019. URL https://www.ncbi.nlm.nih.gov/pubmed/30783617. Edition: 2019/02/21.

A. Latremoliere and C. J. Woolf. Central Sensitization: A Generator of Pain Hypersensitivity by Central Neural Plasticity. *Journal of Pain*, 10(9):895–926, September 2009. ISSN 1526-5900. doi: 10.1016/j.jpain.2009.06.012. URL ://WOS:000269759500001.

C. G. Lau and R. S. Zukin. NMDA receptor trafficking in synaptic plasticity and neuropsychiatric disorders. *Nature Reviews Neuroscience*, 8(6):413–426, June 2007. ISSN 1471-0048. doi: 10.1038/nrn2153. URL ://WOS:000246658800011.

E. M. Lazakovitch, B. R. She, C. L. Lien, W. M. Woo, Y. T. Ju, and S. Lin-Chao. The Gas7 gene encodes two protein isoforms differentially expressed within the brain. *Genomics*, 61(3):298–306, November 1999. ISSN 0888-7543 (Print) 0888-7543 (Linking). doi: 10.1006/geno.1999.5964. URL https://www.ncbi.nlm.nih.gov/pubmed/10552931. Edition: 1999/11/24.

C. E. Le Pichon and A. T. Chesler. The functional and anatomical dissection of somatosensory subpopulations using mouse genetics. *Front Neuroanat*, 8:21, 2014. ISSN 1662-5129 (Print) 1662-5129 (Linking). doi: 10.3389/fnana.2014.00021. URL https://www.ncbi.nlm.nih.gov/pubmed/24795573. Edition: 2014/05/06.

J. Lianne Leith, Stella Koutsikou, Bridget M. Lumb, and Richard Apps. Spinal processing of noxious and innocuous cold information: differential modulation by the periaqueductal gray. *The Journal of Neuroscience: The Official Journal of the Society for Neuroscience*, 30(14):4933–4942, April 2010. ISSN 1529-2401. doi: 10.1523/JNEUROSCI.0122-10.2010.

I. J. Lever, S. Pezet, S. B. McMahon, and M. Malcangio. The signaling components of sensory fiber transmission involved in the activation of ERK MAP kinase in the mouse dorsal horn. *Molecular and Cellular Neuroscience*, 24(2):259–270, October 2003. ISSN 1044-7431. doi: 10.1016/s1044-7431(03)00200-8. URL ://WOS:000186164400001.

Jun Li, Donald A Simone, and Alice A Larson. Windup leads to characteristics of central sensitization. *Pain*, 79(1):75–82, January 1999. ISSN 0304-3959. doi: 10.1016/S0304-3959(98)00154-7. URL https://journals.lww.com/00006396-199901010-00010.

L. Li, M. Rutlin, V. E. Abraira, C. Cassidy, L. Kus, S. Gong, M. P. Jankowski, W. Luo, N. Heintz, H. R. Koerber, C. J. Woodbury, and D. D. Ginty. The functional organization of cutaneous low-threshold mechanosensory neurons. *Cell*, 147(7):1615–27, December 2011. ISSN 1097-4172 (Electronic) 0092-8674 (Linking). doi: 10.1016/j.cell.2011.11.027. URL https://www.ncbi.nlm.nih.gov/pubmed/22196735.

Edition: 2011/12/27.

J. Liao, H. Li, W. Zeng, D. B. Sauer, R. Belmares, and Y. Jiang. Structural insight into the ion-exchange mechanism of the sodium/calcium exchanger. *Science*, 335 (6069):686–90, February 2012. ISSN 1095-9203 (Electronic) 0036-8075 (Linking). doi: 10.1126/science.1215759. URL https://www.ncbi.nlm.nih.gov/pubmed/22323814. Edition: 2012/02/11.

A. R. Light and E. R. Perl. Spinal termination of functionally identified primary afferent neurons with slowly conducting myelinated fibers. *J Comp Neurol*, 186(2):133–50, July 1979. ISSN 0021-9967 (Print) 0021-9967 (Linking). doi: 10.1002/cne.901860203. URL https://www.ncbi.nlm.nih.gov/pubmed/109477. Edition: 1979/07/15.

R. M. Lindgren, J. Zhao, S. Heller, H. Berglind, and M. Nister. Molecular cloning and characterization of two novel truncated isoforms of human Na+/Ca2+ exchanger 3, expressed in fetal brain. *Gene*, 348:143–55, March 2005. ISSN 0378-1119 (Print) 0378-1119 (Linking). doi: 10.1016/j.gene.2005.01.003. URL https://www.ncbi.nlm.nih.gov/pubmed/15777725. Edition: 2005/03/22.

Q. Liu, S. Vrontou, F. L. Rice, M. J. Zylka, X. Dong, and D. J. Anderson. Molecular genetic visualization of a rare subset of unmyelinated sensory neurons that may detect gentle touch. *Nat Neurosci*, 10(8):946–8, August 2007. ISSN 1097-6256 (Print) 1097-6256 (Linking). doi: 10.1038/nn1937. URL https://www.ncbi.nlm.nih.gov/pubmed/17618277. Edition: 2007/07/10.

S. Liu, X. Xiong, X. Zhao, X. Yang, and H. Wang. F-BAR family proteins, emerging regulators for cell membrane dynamic changes-from structure to human diseases. *J Hematol Oncol*, 8:47, May 2015. ISSN 1756-8722 (Electronic) 1756-8722 (Linking). doi: 10.1186/s13045-015-0144-2. URL https://www.ncbi.nlm.nih.gov/pubmed/25956236. Edition: 2015/05/10.

L. E. Lorenzo, M. Ramien, M. St Louis, Y. De Koninck, and A. Ribeiro-da Silva. Postnatal changes in the Rexed lamination and markers of nociceptive afferents in the superficial dorsal horn of the rat. *J Comp Neurol*, 508(4):592–604, June 2008. ISSN 1096-9861 (Electronic) 0021-9967 (Linking). doi: 10.1002/cne.21691. URL https://www.ncbi.nlm.nih.gov/pubmed/18383051. Edition: 2008/04/03.

J. N. Lu, C. Luo, K. K. Bali, R. G. Xie, R. E. Mains, B. A. Eipper, and R. Kuner. A role for Kalirin-7 in nociceptive sensitization via activity-dependent modulation of spinal synapses. *Nature Communications*, 6, April 2015. ISSN 2041-1723. doi: 10.1038/ncomms7820. URL ://WOS:000353703000003.

S. G. Lu, X. Zhang, and M. S. Gold. Intracellular calcium regulation among subpopulations of rat dorsal root ganglion neurons. *J Physiol*, 577(Pt 1):169–90, November 2006. ISSN 0022-3751 (Print) 0022-3751 (Linking). doi: 10.1113/jphysiol.2006.116418. URL https://www.ncbi.nlm.nih.gov/pubmed/16945973. Edition: 2006/09/02.

B. Lynn and S. E. Carpenter. Primary afferent units from the hairy skin of the rat hind limb. *Brain Res*, 238(1):29–43, April 1982. ISSN 0006-8993 (Print) 0006-8993 (Linking). doi: 10.1016/0006-8993(82)90768-5. URL https://www.ncbi.nlm.nih.gov/pubmed/6282398. Edition: 1982/04/22.

Q. Ma. Labeled lines meet and talk: population coding of somatic sensations. *J Clin Invest*, 120(11):3773–8, November 2010. ISSN 1558-8238 (Electronic) 0021-9738 (Linking). doi: 10.1172/JCI43426. URL https://www.ncbi.nlm.nih.gov/pubmed/21041959. Edition: 2010/11/03.

Q. P. Ma and L. Tian. Cholera toxin B subunit labeling in lamina II of spinal cord dorsal horn following chronic inflammation in rats. *Neurosci Lett*, 327(3):161–4, July 2002. ISSN 0304-3940 (Print) 0304-3940 (Linking). doi: 10.1016/s0304-3940(02)00416-0. URL https://www.ncbi.nlm.nih.gov/pubmed/12113902. Edition: 2002/07/13.

A. J. MacGregor, T. Andrew, P. N. Sambrook, and T. D. Spector. Structural, psychological, and genetic influences on low back and neck pain: a study of adult female twins. *Arthritis Rheum*, 51(2):160–7, April 2004. ISSN 0004-3591 (Print) 0004-3591 (Linking). doi: 10.1002/art.20236. URL https://www.ncbi.nlm.nih.gov/pubmed/15077255. Edition: 2004/04/13.

C. Maier, R. Baron, T. R. Tölle, A. Binder, N. Birbaumer, F. Birklein, J. Gierthmühlen, H. Flor, C. Geber, V. Huge, E. K. Krumova, G. B. Landwehrmeyer, W. Magerl, C. Maihöfner, H. Richter, R. Rolke, A. Scherens, A. Schwarz, C. Sommer, V. Tronnier, N. Üçeyler, M. Valet, G. Wasner, and D.-R. Treede. Quantitative sensory testing in the German Research Network on Neuropathic Pain (DFNS): somatosensory abnormalities in 1236 patients with different neuropathic pain syndromes. *Pain*, 150 (3):439–450, September 2010. ISSN 1872-6623. doi: 10.1016/j.pain.2010.05.002.

Teri A. Manolio, Lisa D. Brooks, and Francis S. Collins. A HapMap harvest of insights into the genetics of common disease. *Journal of Clinical Investigation*, 118(5):1590–1605, May 2008. ISSN 0021-9738. doi: 10.1172/JCI34772. URL http://www.jci.org/articles/view/34772.

P. W. Mantyh, S. D. Rogers, P. Honore, B. J. Allen, J. R. Ghilardi, J. Li, R. S. Daughters, D. A. Lappi, R. G. Wiley, and D. A. Simone. Inhibition of hyperalgesia by ablation of lamina I spinal neurons expressing the substance P receptor. *Science*, 278(5336):275–9, October 1997. ISSN 0036-8075 (Print) 0036-8075 (Linking). doi: 10.1126/science.278.5336.275. URL https://www.ncbi.nlm.nih.gov/pubmed/9323204. Edition: 1997/10/10.

Maria Vannucchi and Stefano Evangelista. Experimental Models of Irritable Bowel Syndrome and the Role of the Enteric Neurotransmission. *Journal of Clinical Medicine*, 7(1):4, January 2018. ISSN 2077-0383. doi: 10.3390/jcm7010004. URL http://www.mdpi.com/2077-0383/7/1/4.

S. M. Maricich, K. M. Morrison, E. L. Mathes, and B. M. Brewer. Rodents rely on Merkel cells for texture discrimination tasks. *J Neurosci*, 32(10):3296–300, March 2012. ISSN 1529-2401 (Electronic) 0270-6474 (Linking). doi: 10.1523/JNEUROSCI.5307-11.2012. URL https://www.ncbi.nlm.nih.gov/pubmed/22399751. Edition: 2012/03/09.

F. Marinelli, L. Almagor, R. Hiller, M. Giladi, D. Khananshvili, and J. D. Faraldo-Gomez. Sodium recognition by the Na+/Ca2+ exchanger in the outward-facing conformation. *Proc Natl Acad Sci U S A*, 111(50):E5354–62, December 2014. ISSN 1091-6490 (Electronic) 0027-8424 (Linking). doi: 10.1073/pnas.1415751111. URL https://www.ncbi.nlm.nih.gov/pubmed/25468964. Edition: 2014/12/04.

A. R. Martin, M. Kanai, Y. Kamatani, Y. Okada, B. M. Neale, and M. J. Daly. Clinical use of current polygenic risk scores may exacerbate health disparities. *Nat Genet*, 51(4):584–591, April 2019. ISSN 1546-1718 (Electronic) 1061-4036 (Linking). doi: 10.1038/s41588-019-0379-x. URL https://www.ncbi.nlm.nih.gov/pubmed/30926966. Edition: 2019/03/31.

M. L. Mayer, G. L. Westbrook, and P. B. Guthrie. VOLTAGE-DEPENDENT BLOCK BY MG-2+ OF NMDA RESPONSES IN SPINAL-CORD NEURONS. *Nature*, 309(5965):261–263, 1984. ISSN 0028-0836. doi: 10.1038/309261a0. URL ://WOS:A1984SR70900050.

W. D. McCall, K. D. Tanner, and J. D. Levine. Formalin induces biphasic activity in C-fibers in the rat. *Neuroscience Letters*, 208(1):45–48, April 1996. ISSN 0304-3940. doi: 10.1016/0304-3940(96)12552-0. URL ://WOS:A1996UG33000012.

C. R. McNamara, J. Mandel-Brehm, D. M. Bautista, J. Siemens, K. L. Deranian, M. Zhao, N. J. Hayward, J. A. Chong, D. Julius, M. M. Moran, and C. M. Fanger. TRPA1 mediates formalin-induced pain. *Proc Natl Acad Sci U S A*, 104(33):13525–30, August 2007. ISSN 0027-8424 (Print) 0027-8424 (Linking). doi: 10.1073/pnas.0705924104. URL https://www.ncbi.nlm.nih.gov/pubmed/17686976. Edition: 2007/08/10.

Y. V. Medvedeva, M.-S. Kim, and Y. M. Usachev. Mechanisms of Prolonged Presynaptic Ca2+ Signaling and Glutamate Release Induced by TRPV1 Activation in Rat Sensory Neurons. *Journal of Neuroscience*, 28(20):5295–5311, May 2008. ISSN 0270-6474, 1529-2401. doi: 10.1523/JNEUROSCI.4810-07.2008. URL http://www.jneurosci.org/cgi/doi/10.1523/JNEUROSCI.4810-07.2008.

R. Melzack and P. D. Wall. PAIN MECHANISMS - A NEW THEORY. *Science*, 150(3699):971–+, 1965. ISSN 0036-8075. doi: 10.1126/science.150.3699.971. URL ://WOS:A19657000600005.

L. M. Mendell. Constructing and deconstructing the gate theory of pain. *Pain*, 155 (2):210–6, February 2014. ISSN 1872-6623 (Electronic) 0304-3959 (Linking). doi: 10.1016/j.pain.2013.12.010. URL https://www.ncbi.nlm.nih.gov/pubmed/24334188. Edition: 2013/12/18.

L. M. Mendell and P. D. Wall. RESPONSES OF SINGLE DORSAL CORD CELLS TO PERIPHERAL CUTANEOUS UNMYELINATED FIBRES. *Nature*, 206(4979):97–&, 1965. ISSN 0028-0836. doi: 10.1038/206097a0. URL ://WOS:A19656294700107.

Fr Merkel. Tastzellen und Tastkörperchen bei den Hausthieren und beim Menschen. *Archiv f. mikrosk. Anat. 11, 636–652 (1875).*, 1875. doi: 10.1007/BF02933819.

M. A. Meyer. Neuronal localization of GAS7 within human brain tissue: Implications for schizophrenia research. *Neurol Int*, 10(4):7563, December 2018. ISSN 2035-8385 (Print) 2035-8385 (Linking). doi: 10.4081/ni.2018.7563. URL https://www.ncbi.nlm.nih.gov/pubmed/30687465. Edition: 2019/01/29.

L. Y. Michel, S. Verkaart, W. J. Koopman, P. H. Willems, J. G. Hoenderop, and R. J. Bindels. Function and regulation of the Na+-Ca2+ exchanger NCX3 splice variants in brain and skeletal muscle. *J Biol Chem*, 289(16):11293–303, April 2014. ISSN 1083-351X (Electronic) 0021-9258 (Linking). doi: 10.1074/jbc.M113.529388. URL

https://www.ncbi.nlm.nih.gov/pubmed/24616101. Edition: 2014/03/13.

L. Y. M. Michel, S. Verkaart, F. Latta, J. G. J. Hoenderop, and R. J. M. Bindels. Differential regulation of the Na+-Ca2+ exchanger 3 (NCX3) by protein kinase PKC and PKA. *Cell Calcium*, 65:52–62, July 2017. ISSN 0143-4160. doi: 10.1016/j.ceca.2017.02.005. URL ://WOS:000403992700007.

Ersilia Mirabelli, Li Ni, Lun Li, Cigdem Acioglu, Robert F. Heary, and Stella Elkabes. Pathological pain processing in mouse models of multiple sclerosis and spinal cord injury: contribution of plasma membrane calcium ATPase 2 (PMCA2). *Journal of Neuroinflammation*, 16(1):207, December 2019. ISSN 1742-2094. doi: 10.1186/s12974-019-1585-2. URL https://jneuroinflammation.biomedcentral.com/articles/10.1186/s12974-019-1585-2.

S. K. Mishra and M. A. Hoon. The cells and circuitry for itch responses in mice. *Science*, 340(6135):968–71, May 2013. ISSN 1095-9203 (Electronic) 0036-8075 (Linking). doi: 10.1126/science.1233765. URL https://www.ncbi.nlm.nih.gov/pubmed/23704570. Edition: 2013/05/25.

J. S. Mogil, F. Miermeister, F. Seifert, K. Strasburg, K. Zimmermann, H. Reinold, J.-S. Austin, N. Bernardini, E. J. Chesler, H. A. Hofmann, C. Hordo, K. Messlinger, K. V. S. Nemmani, A. L. Rankin, J. Ritchie, A. Siegling, S. B. Smith, S. Sotocinal, A. Vater, S. G. Lehto, S. Klussmann, R. Quirion, M. Michaelis, M. Devor, and P. W. Reeh. Variable sensitivity to noxious heat is mediated by differential expression of the CGRP gene. *Proceedings of the National Academy of Sciences*, 102(36):12938–12943, September 2005. ISSN 0027-8424, 1091-6490. doi: 10.1073/pnas.0503264102. URL http://www.pnas.org/cgi/doi/10.1073/pnas.0503264102.

P. Molinaro, D. Viggiano, R. Nistico, R. Sirabella, A. Secondo, F. Boscia, A. Pannaccione, A. Scorziello, B. Mehdawy, S. Sokolow, A. Herchuelz, G. F. Di Renzo, and L. Annunziato. Na+-Ca2+ Exchanger (NCX3) Knock-Out Mice Display an Impairment in Hippocampal Long-Term Potentiation and Spatial Learning and Memory. *Journal of Neuroscience*, 31(20):7312–7321, May 2011. ISSN 0270-6474. doi: 10.1523/jneurosci.6296-10.2011. URL ://WOS:000290716600010.

Lavanya Moparthi, Tatjana I. Kichko, Mirjam Eberhardt, Edward D. Högestätt, Per Kjellbom, Urban Johanson, Peter W. Reeh, Andreas Leffler, Milos R. Filipovic, and Peter M. Zygmunt. Human TRPA1 is a heat sensor displaying intrinsic U-shaped thermosensitivity. *Scientific Reports*, 6(1):28763, September 2016. ISSN 2045-2322. doi: 10.1038/srep28763. URL http://www.nature.com/articles/srep28763.

Matthew R. Nelson, Hannah Tipney, Jeffery L. Painter, Judong Shen, Paola Nicoletti, Yufeng Shen, Aris Floratos, Pak Chung Sham, Mulin Jun Li, Junwen Wang, Lon R. Cardon, John C. Whittaker, and Philippe Sanseau. The support of human genetic evidence for approved drug indications. *Nature Genetics*, 47(8):856–860, August 2015. ISSN 1546-1718. doi: 10.1038/ng.3314.

Nicole L. Neubarth, Alan J. Emanuel, Yin Liu, Mark W. Springel, Annie Handler, Qiyu Zhang, Brendan P. Lehnert, Chong Guo, Lauren L. Orefice, Amira Abdelaziz, Michelle M. DeLisle, Michael Iskols, Julia Rhyins, Soo J. Kim, Stuart J. Cattel, Wade Regehr, Christopher D. Harvey, Jan Drugowitsch, and David D. Ginty. Meissner

corpuscles and their spatially intermingled afferents underlie gentle touch perception. *Science*, 368(6497):eabb2751, June 2020. ISSN 0036-8075, 1095-9203. doi: 10.1126/science.abb2751. URL https://www.sciencemag.org/lookup/doi/10.1126/science.abb2751.

D. A. Nicoll, S. Longoni, and K. D. Philipson. Molecular cloning and functional expression of the cardiac sarcolemmal Na(+)-Ca2+ exchanger. *Science*, 250(4980): 562–5, October 1990. ISSN 0036-8075 (Print) 0036-8075 (Linking). doi: 10.1126/science.1700476. URL https://www.ncbi.nlm.nih.gov/pubmed/1700476. Edition: 1990/10/26.

D. A. Nicoll, M. R. Sawaya, S. Kwon, D. Cascio, K. D. Philipson, and J. Abramson. The crystal structure of the primary Ca2+ sensor of the Na+/Ca2+ exchanger reveals a novel Ca2+ binding motif. *J Biol Chem*, 281(31):21577–81, August 2006. ISSN 0021-9258 (Print) 0021-9258 (Linking). doi: 10.1074/jbc.C600117200. URL https://www.ncbi.nlm.nih.gov/pubmed/16774926. Edition: 2006/06/16.

C. S. Nielsen, G. P. Knudsen, and O. A. Steingrimsdottir. Twin studies of pain. *Clin Genet*, 82(4):331–40, October 2012. ISSN 1399-0004 (Electronic) 0009-9163 (Linking). doi: 10.1111/j.1399-0004.2012.01938.x. URL https://www.ncbi.nlm.nih.gov/pubmed/22823509. Edition: 2012/07/25.

Timothy A. Norbury, Alex J. MacGregor, Jane Urwin, Tim D. Spector, and Stephen B. McMahon. Heritability of responses to painful stimuli in women: a classical twin study. *Brain*, 130(11):3041–3049, November 2007. ISSN 1460-2156, 0006-8950. doi: 10.1093/brain/awm233. URL https://academic.oup.com/brain/article-lookup/doi/10.1093/brain/awm233.

A. L. Oliveira, F. Hydling, E. Olsson, T. Shi, R. H. Edwards, F. Fujiyama, T. Kaneko, T. Hokfelt, S. Cullheim, and B. Meister. Cellular localization of three vesicular glutamate transporter mRNAs and proteins in rat spinal cord and dorsal root ganglia. *Synapse*, 50(2):117–29, November 2003. ISSN 0887-4476 (Print) 0887-4476 (Linking). doi: 10.1002/syn.10249. URL https://www.ncbi.nlm.nih.gov/pubmed/12923814. Edition: 2003/08/19.

K. Ozaki, Y. Ohnishi, A. Iida, A. Sekine, R. Yamada, T. Tsunoda, H. Sato, H. Sato, M. Hori, Y. Nakamura, and T. Tanaka. Functional SNPs in the lymphotoxin-alpha gene that are associated with susceptibility to myocardial infarction. *Nat Genet*, 32(4):650–4, December 2002. ISSN 1061-4036 (Print) 1061-4036 (Linking). doi: 10.1038/ng1047. URL https://www.ncbi.nlm.nih.gov/pubmed/12426569. Edition: 2002/11/12.

P. Rössel, A. M. Drewes, P. Peterse. Pain Produced by Electric Stimulation of the Rectum in Patients with Irritable Bowel Syndrome: Further Evidence of Visceral Hyperalgesia. *Scandinavian Journal of Gastroenterology*, 34(10):1001–1006, January 1999. ISSN 0036-5521, 1502-7708. doi: 10.1080/003655299750025101. URL http://www.tandfonline.com/doi/full/10.1080/003655299750025101.

A. Pannaccione, A. Secondo, P. Molinaro, C. D'Avanzo, M. Cantile, A. Esposito, F. Boscia, A. Scorziello, R. Sirabella, G. Di Renzo, and L. Annunziato. A New Concept: A beta(1-42) Generates a Hyperfunctional Proteolytic NCX3 Fragment

That Delays Caspase-12 Activation and Neuronal Death. *Journal of Neuroscience*, 32 (31):10609–10617, August 2012. ISSN 0270-6474. doi: 10.1523/jneurosci.6429-11.2012. URL ://WOS:000307125900018.

M. Pare, A. M. Smith, and F. L. Rice. Distribution and terminal arborizations of cutaneous mechanoreceptors in the glabrous finger pads of the monkey. *J Comp Neurol*, 445(4):347–59, April 2002. ISSN 0021-9967 (Print) 0021-9967 (Linking). doi: 10.1002/cne.10196. URL https://www.ncbi.nlm.nih.gov/pubmed/11920712. Edition: 2002/03/29.

Nathalie Percie du Sert, Viki Hurst, Amrita Ahluwalia, Sabina Alam, Marc T. Avey, Monya Baker, William J. Browne, Alejandra Clark, Innes C. Cuthill, Ulrich Dirnagl, Michael Emerson, Paul Garner, Stephen T. Holgate, David W. Howells, Natasha A. Karp, Stanley E. Lazic, Katie Lidster, Catriona J. MacCallum, Malcolm Macleod, Esther J. Pearl, Ole H. Petersen, Frances Rawle, Penny Reynolds, Kieron Rooney, Emily S. Sena, Shai D. Silberberg, Thomas Steckler, and Hanno Würbel. The ARRIVE guidelines 2.0: Updated guidelines for reporting animal research. *PLOS Biology*, 18(7):e3000410, July 2020. ISSN 1545-7885. doi: 10.1371/journal.pbio.3000410. URL https://dx.plos.org/10.1371/journal.pbio.3000410.

A. K. Persson, J. A. Black, A. Gasser, X. Cheng, T. Z. Fischer, and S. G. Waxman. Sodium-calcium exchanger and multiple sodium channel isoforms in intra-epidermal nerve terminals. *Mol Pain*, 6:84, November 2010. ISSN 1744-8069 (Electronic) 1744-8069 (Linking). doi: 10.1186/1744-8069-6-84. URL https://www.ncbi.nlm.nih.gov/pubmed/21118538. Edition: 2010/12/02.

H. Petitjean, S. A. Pawlowski, S. L. Fraine, B. Sharif, D. Hamad, T. Fatima, J. Berg, C. M. Brown, L. Y. Jan, A. Ribeiro-da Silva, J. M. Braz, A. I. Basbaum, and R. Sharif-Naeini. Dorsal Horn Parvalbumin Neurons Are Gate-Keepers of Touch-Evoked Pain after Nerve Injury. *Cell Rep*, 13(6):1246–1257, November 2015. ISSN 2211-1247 (Electronic). doi: 10.1016/j.celrep.2015.09.080. URL https://www.ncbi.nlm.nih.gov/pubmed/26527000. Edition: 2015/11/04.

K. D. Philipson and D. A. Nicoll. Sodium-calcium exchange: a molecular perspective. *Annu Rev Physiol*, 62:111–33, 2000. ISSN 0066-4278 (Print) 0066-4278 (Linking). doi: 10.1146/annurev.physiol.62.1.111. URL https://www.ncbi.nlm.nih.gov/pubmed/10845086. Edition: 2000/06/09.

W. J. Pledger, C. D. Stiles, H. N. Antoniades, and C. D. Scher. Induction of DNA synthesis in BALB/c 3T3 cells by serum components: reevaluation of the commitment process. *Proc Natl Acad Sci U S A*, 74(10):4481–5, October 1977. ISSN 0027-8424 (Print) 0027-8424 (Linking). doi: 10.1073/pnas.74.10.4481. URL https://www.ncbi.nlm.nih.gov/pubmed/270695. Edition: 1977/10/01.

E. Polgar, C. Durrieux, D. I. Hughes, and A. J. Todd. A quantitative study of inhibitory interneurons in laminae I-III of the mouse spinal dorsal horn. *PLoS One*, 8(10):e78309, 2013a. ISSN 1932-6203 (Electronic) 1932-6203 (Linking). doi: 10.1371/journal.pone.0078309. URL https://www.ncbi.nlm.nih.gov/pubmed/24205193. Edition: 2013/11/10.

E. Polgar, T. C. Sardella, S. Y. Tiong, S. Locke, M. Watanabe, and A. J. Todd. Functional differences between neurochemically defined populations of inhibitory interneurons in the rat spinal dorsal horn. *Pain*, 154(12):2606–15, December 2013b. ISSN 1872-6623 (Electronic) 0304-3959 (Linking). doi: 10.1016/j.pain.2013.05.001. URL https://www.ncbi.nlm.nih.gov/pubmed/23707280. Edition: 2013/05/28.

S. A. Prescott, Q. Ma, and Y. De Koninck. Normal and abnormal coding of somatosensory stimuli causing pain. *Nat Neurosci*, 17(2):183–91, February 2014. ISSN 1546-1726 (Electronic) 1097-6256 (Linking). doi: 10.1038/nn.3629. URL https://www.ncbi.nlm.nih.gov/pubmed/24473266. Edition: 2014/01/30.

T. J. Price and C. M. Flores. Critical evaluation of the colocalization between calcitonin gene-related peptide, substance P, transient receptor potential vanilloid subfamily type 1 immunoreactivities, and isolectin B4 binding in primary afferent neurons of the rat and mouse. *J Pain*, 8(3):263–72, March 2007. ISSN 1526-5900 (Print) 1526-5900 (Linking). doi: 10.1016/j.jpain.2006.09.005. URL https://www.ncbi.nlm.nih.gov/pubmed/17113352. Edition: 2006/11/23.

F. Proudlock, R. C. Spike, and A. J. Todd. Immunocytochemical study of somatostatin, neurotensin, GABA, and glycine in rat spinal dorsal horn. *J Comp Neurol*, 327 (2):289–97, January 1993. ISSN 0021-9967 (Print) 0021-9967 (Linking). doi: 10.1002/cne.903270210. URL https://www.ncbi.nlm.nih.gov/pubmed/7678841. Edition: 1993/01/08.

Dorit Pud, Elon Eisenberg, Ada Spitzer, Rivka Adler, Georgetta Fried, and David Yarnitsky. The NMDA receptor antagonist amantadine reduces surgical neuropathic pain in cancer patients: a double blind, randomized, placebo controlled trial:. *Pain*, 75(2):349–354, January 1998. ISSN 0304-3959. doi: 10.1016/S0304-3959(98)00014-1. URL http://journals.lww.com/00006396-199801020-00021.

B. D. Quednau, D. A. Nicoll, and K. D. Philipson. Tissue specificity and alternative splicing of the Na+/Ca2+ exchanger isoforms NCX1, NCX2, and NCX3 in rat. *Am J Physiol*, 272(4 Pt 1):C1250–61, April 1997. ISSN 0002-9513 (Print) 0002-9513 (Linking). doi: 10.1152/ajpcell.1997.272.4.C1250. URL https://www.ncbi.nlm.nih.gov/pubmed/9142850. Edition: 1997/04/01.

I. S. Ramsey, M. Delling, and D. E. Clapham. An introduction to TRP channels. *Annu Rev Physiol*, 68:619–47, 2006. ISSN 0066-4278 (Print) 0066-4278 (Linking). doi: 10.1146/annurev.physiol.68.040204.100431. URL https://www.ncbi.nlm.nih.gov/pubmed/16460286. Edition: 2006/02/08.

M. Randic, M. C. Jiang, and R. Cerne. Long-term potentiation and long-term depression of primary afferent neurotransmission in the rat spinal cord. *J Neurosci*, 13(12): 5228–41, December 1993. ISSN 0270-6474 (Print) 0270-6474 (Linking). URL https://www.ncbi.nlm.nih.gov/pubmed/8254370. Edition: 1993/12/01.

F. Reimann, J. J. Cox, I. Belfer, L. Diatchenko, D. V. Zaykin, D. P. McHale, J. P. Drenth, F. Dai, J. Wheeler, F. Sanders, L. Wood, T. X. Wu, J. Karppinen, L. Nikolajsen, M. Mannikko, M. B. Max, C. Kiselycznyk, M. Poddar, R. H. Te Morsche, S. Smith, D. Gibson, A. Kelempisioti, W. Maixner, F. M. Gribble, and C. G. Woods. Pain perception is altered by a nucleotide polymorphism in SCN9A. *Proc Natl Acad*

Sci U S A, 107(11):5148–53, March 2010. ISSN 1091-6490 (Electronic) 0027-8424 (Linking). doi: 10.1073/pnas.0913181107. URL https://www.ncbi.nlm.nih.gov/pubmed/20212137. Edition: 2010/03/10.

Torge Rempe, Stephan Wolff, Christian Riedel, Ralf Baron, Patrick W. Stroman, Olav Jansen, and Janne Gierthmühlen. Spinal and supraspinal processing of thermal stimuli: an fMRI study. *Journal of magnetic resonance imaging: JMRI*, 41(4): 1046–1055, April 2015. ISSN 1522-2586. doi: 10.1002/jmri.24627.

X. Ren and K. D. Philipson. The topology of the cardiac Na(+)/Ca(2)(+) exchanger, NCX1. *J Mol Cell Cardiol*, 57:68–71, April 2013. ISSN 1095-8584 (Electronic) 0022-2828 (Linking). doi: 10.1016/j.yjmcc.2013.01.010. URL https://www.ncbi.nlm.nih.gov/pubmed/23376057. Edition: 2013/02/05.

B. Rexed. The cytoarchitectonic organization of the spinal cord in the cat. *J Comp Neurol*, 96(3):414–95, June 1952. ISSN 0021-9967 (Print) 0021-9967 (Linking). doi: 10.1002/cne.900960303. URL https://www.ncbi.nlm.nih.gov/pubmed/14946260. Edition: 1952/06/01.

D. V. Reynolds. Surgery in the rat during electrical analgesia induced by focal brain stimulation. *Science*, 164(3878):444–5, April 1969. ISSN 0036-8075 (Print) 0036-8075 (Linking). doi: 10.1126/science.164.3878.444. URL https://www.ncbi.nlm.nih.gov/pubmed/4887743. Edition: 1969/04/25.

M. Richner, S. B. Jager, P. Siupka, and C. B. Vaegter. Hydraulic Extrusion of the Spinal Cord and Isolation of Dorsal Root Ganglia in Rodents. *J Vis Exp*, (119), January 2017. ISSN 1940-087X (Electronic) 1940-087X (Linking). doi: 10.3791/55226. URL https://www.ncbi.nlm.nih.gov/pubmed/28190031. Edition: 2017/02/13.

Ruffini. Di un novo organo nervoso terminale, e sulla presenza dei corpuscoli Golgi-Mazzoni nel connettivo sottocutaneo dei polpastrelli delle dita dell-uomo. Attl Dell Accademia Nazionale dei Lincet.; 7:398–410. 1894.

M. Rutlin, C. Y. Ho, V. E. Abraira, C. Cassidy, L. Bai, C. J. Woodbury, and D. D. Ginty. The cellular and molecular basis of direction selectivity of Adelta-LTMRs. *Cell*, 159 (7):1640–51, December 2014. ISSN 1097-4172 (Electronic) 0092-8674 (Linking). doi: 10.1016/j.cell.2014.11.038. URL https://www.ncbi.nlm.nih.gov/pubmed/25525881. Edition: 2014/12/20.

Sahani M, Linden J. How linear are auditory cortical responses? In *Advances in neural information processing systems*, pages 125–132. MIT Press, 2003.

T. A. Samad, K. A. Moore, A. Sapirstein, S. Billet, A. Allchorne, S. Poole, J. V. Bonventre, and C. J. Woolf. Interleukin-1 beta-mediated induction of Cox-2 in the CNS contributes to inflammatory pain hypersensitivity. *Nature*, 410(6827): 471–475, March 2001. ISSN 0028-0836. doi: 10.1038/35068566. URL ://WOS:000167583800042.

J. Sandkuhler. Understanding LTP in pain pathways. *Mol Pain*, 3:9, April 2007. ISSN 1744-8069 (Electronic) 1744-8069 (Linking). doi: 10.1186/1744-8069-3-9. URL https://www.ncbi.nlm.nih.gov/pubmed/17407590. Edition: 2007/04/05.

G. C. Schatteman, K. Morrison-Graham, A. van Koppen, J. A. Weston, and D. F. Bowen-Pope. Regulation and role of PDGF receptor alpha-subunit expression during

embryogenesis. *Development*, 115(1):123–31, May 1992. ISSN 0950-1991 (Print) 0950-1991 (Linking). URL https://www.ncbi.nlm.nih.gov/pubmed/1322269. Edition: 1992/05/01.

N. N. Scheff and M. S. Gold. Trafficking of Na+/Ca2+ Exchanger to the Site of Persistent Inflammation in Nociceptive Afferents. *Journal of Neuroscience*, 35(22): 8423–8432, June 2015. ISSN 0270-6474. doi: 10.1523/jneurosci.3597-14.2015. URL ://WOS:000358247900006.

N. N. Scheff, E. Yilmaz, and M. S. Gold. The properties, distribution and function of Na+-Ca2+ exchanger isoforms in rat cutaneous sensory neurons. *Journal of Physiology-London*, 592(22):4969–4993, November 2014. ISSN 0022-3751. doi: 10.1113/jphysiol.2014.278036. URL ://WOS:000345773100013.

Annina B. Schmid, Kaustubh Adhikari, Luis Miguel Ramirez-Aristeguieta, Juan-Camilo Chacón-Duque, Giovanni Poletti, Carla Gallo, Francisco Rothhammer, Gabriel Bedoya, Andres Ruiz-Linares, and David L. Bennett. Genetic components of human pain sensitivity: a protocol for a genome-wide association study of experimental pain in healthy volunteers. *BMJ open*, 9(4):e025530, April 2019. ISSN 2044-6055. doi: 10.1136/bmjopen-2018-025530.

C. Schneider, R. M. King, and L. Philipson. Genes specifically expressed at growth arrest of mammalian cells. *Cell*, 54(6):787–93, September 1988. ISSN 0092-8674 (Print) 0092-8674 (Linking). doi: 10.1016/s0092-8674(88)91065-3. URL https://www.ncbi.nlm.nih.gov/pubmed/3409319. Edition: 1988/09/09.

D. Schoffnegger, R. Ruscheweyh, and J. Sandkuhler. Spread of excitation across modality borders in spinal dorsal horn of neuropathic rats. *Pain*, 135(3):300–10, April 2008. ISSN 1872-6623 (Electronic) 0304-3959 (Linking). doi: 10.1016/j.pain.2007.12.016. URL https://www.ncbi.nlm.nih.gov/pubmed/18262362. Edition: 2008/02/12.

I. Segev and W. Rall. Computational study of an excitable dendritic spine. *Journal of Neurophysiology*, 60(2):499–523, August 1988. ISSN 0022-3077, 1522-1598. doi: 10.1152/jn.1988.60.2.499. URL https://www.physiology.org/doi/10.1152/jn.1988.60.2.499.

Michael L. Seibenhener and Michael C. Wooten. Use of the Open Field Maze to Measure Locomotor and Anxiety-like Behavior in Mice. *Journal of Visualized Experiments*, (96):52434, February 2015. ISSN 1940-087X. doi: 10.3791/52434. URL http://www.jove.com/video/52434/use-open-field-maze-to-measure-locomotor-anxiety-like-behavior.

Leonid P. Shutov, Man-Su Kim, Patrick R. Houlihan, Yuliya V. Medvedeva, and Yuriy M. Usachev. Mitochondria and plasma membrane Ca $^{2+}$ -ATPase control presynaptic Ca $^{2+}$ clearance in capsaicin-sensitive rat sensory neurons: Mitochondria and PMCA control presynaptic Ca $^{2+}$ in nociceptors. *The Journal of Physiology*, 591(10):2443–2462, May 2013. ISSN 00223751. doi: 10.1113/jphysiol.2012.249219. URL http://doi.wiley.com/10.1113/jphysiol.2012.249219.

M. Simonetti, A. M. Hagenston, D. Vardeh, H. E. Freitag, D. Mauceri, J. N. Lu, V. P. Satagopam, R. Schneider, M. Costigan, H. Bading, and R. Kuner. Nuclear Calcium

Signaling in Spinal Neurons Drives a Genomic Program Required for Persistent Inflammatory Pain. *Neuron*, 77(1):43–57, January 2013. ISSN 0896-6273. doi: 10.1016/j.neuron.2012.10.037. URL ://WOS:000313404600007.

L. Singh, M. J. Field, P. Ferris, J. C. Hunter, R. J. Oles, R. G. Williams, and G. N. Woodruff. The antiepileptic agent gabapentin (Neurontin) possesses anxiolytic-like and antinociceptive actions that are reversed by D-serine. *Psychopharmacology (Berl)*, 127(1):1–9, September 1996. ISSN 0033-3158 (Print) 0033-3158 (Linking). doi: 10.1007/BF02805968. URL https://www.ncbi.nlm.nih.gov/pubmed/8880937. Edition: 1996/09/01.

R. Sirabella, A. Secondo, A. Pannaccione, P. Molinaro, L. Formisano, N. Guida, G. Di Renzo, L. Annunziato, and M. Cataldi. ERK1/2, p38, and JNK regulate the expression and the activity of the three isoforms of the Na+ /Ca2+ exchanger, NCX1, NCX2, and NCX3, in neuronal PC12 cells. *J Neurochem*, 122(5):911–22, September 2012. ISSN 1471-4159 (Electronic) 0022-3042 (Linking). doi: 10.1111/j.1471-4159.2012.07838.x. URL https://www.ncbi.nlm.nih.gov/pubmed/22708976. Edition: 2012/06/20.

S. Smemo, J. J. Tena, K. H. Kim, E. R. Gamazon, N. J. Sakabe, C. Gomez-Marin, I. Aneas, F. L. Credidio, D. R. Sobreira, N. F. Wasserman, J. H. Lee, V. Puviindran, D. Tam, M. Shen, J. E. Son, N. A. Vakili, H. K. Sung, S. Naranjo, R. D. Acemel, M. Manzanares, A. Nagy, N. J. Cox, C. C. Hui, J. L. Gomez-Skarmeta, and M. A. Nobrega. Obesity-associated variants within FTO form long-range functional connections with IRX3. *Nature*, 507(7492):371–5, March 2014. ISSN 1476-4687 (Electronic) 0028-0836 (Linking). doi: 10.1038/nature13138. URL https://www.ncbi.nlm.nih.gov/pubmed/24646999. Edition: 2014/03/22.

S. Sokolow, M. Manto, P. Gailly, J. Molgo, C. Vandebrouck, J. M. Vanderwinden, A. Herchuelz, and S. Schurmans. Impaired neuromuscular transmission and skeletal muscle fiber necrosis in mice lacking Na/Ca exchanger 3. *Journal of Clinical Investigation*, 113(2):265–273, January 2004. ISSN 0021-9738. doi: 10.1172/jci200418688. URL ://WOS:000188195600016.

R. C. Spike, Z. Puskar, D. Andrew, and A. J. Todd. A quantitative and morphological study of projection neurons in lamina I of the rat lumbar spinal cord. *Eur J Neurosci*, 18(9):2433–48, November 2003. ISSN 0953-816X (Print) 0953-816X (Linking). doi: 10.1046/j.1460-9568.2003.02981.x. URL https://www.ncbi.nlm.nih.gov/pubmed/14622144. Edition: 2003/11/19.

R. L. Staiano, F. Granata, A. Secondo, A. Petraroli, S. Loffredo, A. Frattini, L. Annunziato, G. Marone, and M. Triggiani. Expression and function of Na+/Ca2+ exchangers 1 and 3 in human macrophages and monocytes. *European Journal of Immunology*, 39(5):1405–1418, May 2009. ISSN 0014-2980. doi: 10.1002/eji.200838792. URL ://WOS:000266137700023.

R. Staud. The important role of CNS facilitation and inhibition for chronic pain. 2013. doi: 10.2217/ijr.13.57.

Roland Staud, Richard C Cannon, Andre P Mauderli, Michael E Robinson, Donald D Price, and Charles J Vierck. Temporal summation of pain from mechanical stimula-

tion of muscle tissue in normal controls and subjects with fibromyalgia syndrome. *Pain*, 102(1):87–95, March 2003. ISSN 0304-3959. doi: 10.1016/s0304-3959(02)00344-5. URL https://journals.lww.com/00006396-200303000-00010.

T. N. Stitt, G. Conn, M. Gore, C. Lai, J. Bruno, C. Radziejewski, K. Mattsson, J. Fisher, D. R. Gies, P. F. Jones, and et al. The anticoagulation factor protein S and its relative, Gas6, are ligands for the Tyro 3/Axl family of receptor tyrosine kinases. *Cell*, 80(4):661–70, February 1995. ISSN 0092-8674 (Print) 0092-8674 (Linking). doi: 10.1016/0092-8674(95)90520-0. URL https://www.ncbi.nlm.nih.gov/pubmed/7867073. Edition: 1995/02/24.

Y. Sugiura, C. L. Lee, and E. R. Perl. Central projections of identified, unmyelinated (C) afferent fibers innervating mammalian skin. *Science*, 234(4774):358–61, October 1986. ISSN 0036-8075 (Print) 0036-8075 (Linking). doi: 10.1126/science.3764416. URL https://www.ncbi.nlm.nih.gov/pubmed/3764416. Edition: 1986/10/17.

Toshiya Tachibana, Hiroyuki Ogura, Atsushi Tokunaga, Yi Dai, Hiroki Yamanaka, Daisuke Seino, and Koichi Noguchi. Plasma membrane calcium ATPase expression in the rat spinal cord. *Molecular Brain Research*, 131(1-2):26–32, November 2004. ISSN 0169328X. doi: 10.1016/j.molbrainres.2004.08.001. URL https://linkinghub.elsevier.com/retrieve/pii/S0169328X04003833.

T. Takenawa and S. Suetsugu. The WASP-WAVE protein network: connecting the membrane to the cytoskeleton. *Nat Rev Mol Cell Biol*, 8(1):37–48, January 2007. ISSN 1471-0072 (Print) 1471-0072 (Linking). doi: 10.1038/nrm2069. URL https://www.ncbi.nlm.nih.gov/pubmed/17183359. Edition: 2006/12/22.

I. Tal, T. Kozlovsky, D. Brisker, M. Giladi, and D. Khananshvili. Kinetic and equilibrium properties of regulatory Ca(2+)-binding domains in sodium-calcium exchangers 2 and 3. *Cell Calcium*, 59(4):181–8, April 2016. ISSN 1532-1991 (Electronic) 0143-4160 (Linking). doi: 10.1016/j.ceca.2016.01.008. URL https://www.ncbi.nlm.nih.gov/pubmed/26924806. Edition: 2016/03/01.

N. Tamamaki, Y. Yanagawa, R. Tomioka, J. Miyazaki, K. Obata, and T. Kaneko. Green fluorescent protein expression and colocalization with calretinin, parvalbumin, and somatostatin in the GAD67-GFP knock-in mouse. *J Comp Neurol*, 467(1):60–79, December 2003. ISSN 0021-9967 (Print) 0021-9967 (Linking). doi: 10.1002/cne.10905. URL https://www.ncbi.nlm.nih.gov/pubmed/14574680. Edition: 2003/10/24.

A. M. Tan, O. A. Samad, T. Z. Fischer, P. Zhao, A. K. Persson, and S. G. Waxman. Maladaptive Dendritic Spine Remodeling Contributes to Diabetic Neuropathic Pain. *Journal of Neuroscience*, 32(20):6795–6807, May 2012. ISSN 0270-6474. doi: 10.1523/jneurosci.1017-12.2012. URL ://WOS:000304419700006.

Andrew M. Tan, Jin-Sung Choi, Stephen G. Waxman, and Bryan C. Hains. Dendritic Spine Remodeling After Spinal Cord Injury Alters Neuronal Signal Processing. *Journal of Neurophysiology*, 102(4):2396–2409, October 2009. ISSN 0022-3077, 1522-1598. doi: 10.1152/jn.00095.2009. URL https://www.physiology.org/doi/10.1152/jn.00095.2009.

Andrew M. Tan, Yu-Wen Chang, Peng Zhao, Bryan C. Hains, and Stephen G. Waxman. Rac1-regulated dendritic spine remodeling contributes to neuropathic pain after

peripheral nerve injury. *Experimental Neurology*, 232(2):222–233, December 2011. ISSN 00144886. doi: 10.1016/j.expneurol.2011.08.028. URL https://linkinghub.elsevier.com/retrieve/pii/S0014488611003153.

B. K. Taylor, M. A. Peterson, and A. I. Basbaum. Persistent cardiovascular and behavioral nociceptive responses to subcutaneous formalin require peripheral nerve input. *J Neurosci*, 15(11):7575–84, November 1995. ISSN 0270-6474 (Print) 0270-6474 (Linking). URL https://www.ncbi.nlm.nih.gov/pubmed/7472508. Edition: 1995/11/01.

Thomas D, Wessel C. The State of Innovation in Highly Prevalent Chronic Diseases Volume II: Pain and Addiction Therapeutics. 2018.

S. W. Thompson, D. L. Bennett, B. J. Kerr, E. J. Bradbury, and S. B. McMahon. Brain-derived neurotrophic factor is an endogenous modulator of nociceptive responses in the spinal cord. *Proc Natl Acad Sci U S A*, 96(14):7714–8, July 1999. ISSN 0027-8424 (Print) 0027-8424 (Linking). doi: 10.1073/pnas.96.14.7714. URL https://www.ncbi.nlm.nih.gov/pubmed/10393886. Edition: 1999/07/08.

A. Tjolsen, O. G. Berge, S. Hunskaar, J. H. Rosland, and K. Hole. THE FORMALIN TEST - AN EVALUATION OF THE METHOD. *Pain*, 51(1):5–17, October 1992. ISSN 0304-3959. doi: 10.1016/0304-3959(92)90003-t. URL ://WOS:A1992JU95600002.

A. J. Todd. Anatomy of primary afferents and projection neurones in the rat spinal dorsal horn with particular emphasis on substance P and the neurokinin 1 receptor. *Exp Physiol*, 87(2):245–9, March 2002. ISSN 0958-0670 (Print) 0958-0670 (Linking). doi: 10.1113/eph8702351. URL https://www.ncbi.nlm.nih.gov/pubmed/11856970. Edition: 2002/02/22.

A. J. Todd. Neuronal circuitry for pain processing in the dorsal horn. *Nat Rev Neurosci*, 11(12):823–36, December 2010. ISSN 1471-0048 (Electronic) 1471-003X (Linking). doi: 10.1038/nrn2947. URL https://www.ncbi.nlm.nih.gov/pubmed/21068766. Edition: 2010/11/12.

A. J. Todd. Identifying functional populations among the interneurons in laminae I-III of the spinal dorsal horn. *Molecular Pain*, 13:1–19, February 2017. ISSN 1744-8069. doi: 10.1177/1744806917693003. URL ://WOS:000399901700001.

A. J. Todd, D. I. Hughes, E. Polgar, G. G. Nagy, M. Mackie, O. P. Ottersen, and D. J. Maxwell. The expression of vesicular glutamate transporters VGLUT1 and VGLUT2 in neurochemically defined axonal populations in the rat spinal cord with emphasis on the dorsal horn. *Eur J Neurosci*, 17(1):13–27, January 2003. ISSN 0953-816X (Print) 0953-816X (Linking). doi: 10.1046/j.1460-9568.2003.02406.x. URL https://www.ncbi.nlm.nih.gov/pubmed/12534965. Edition: 2003/01/22.

H. E. Torebjork, L. E. Lundberg, and R. H. LaMotte. Central changes in processing of mechanoreceptive input in capsaicin-induced secondary hyperalgesia in humans. *J Physiol*, 448:765–80, March 1992. ISSN 0022-3751 (Print) 0022-3751 (Linking). doi: 10.1113/jphysiol.1992.sp019069. URL https://www.ncbi.nlm.nih.gov/pubmed/1593489. Edition: 1992/03/01.

C. Torsney and A. B. MacDermott. Disinhibition opens the gate to pathological pain signaling in superficial neurokinin 1 receptor-expressing neurons in rat spinal cord. *J Neurosci*, 26(6):1833–43, February 2006. ISSN 1529-2401 (Electronic) 0270-6474 (Linking). doi: 10.1523/JNEUROSCI.4584-05.2006. URL https://www.ncbi.nlm.nih.gov/pubmed/16467532. Edition: 2006/02/10.

I. Tracey and P. W. Mantyh. The cerebral signature for pain perception and its modulation. *Neuron*, 55(3):377–91, August 2007. ISSN 0896-6273 (Print) 0896-6273 (Linking). doi: 10.1016/j.neuron.2007.07.012. URL https://www.ncbi.nlm.nih.gov/pubmed/17678852. Edition: 2007/08/07.

Kazuya Tsujita, Shiro Suetsugu, Nobunari Sasaki, Masahiro Furutani, Tsukasa Oikawa, and Tadaomi Takenawa. Coordination between the actin cytoskeleton and membrane deformation by a novel membrane tubulation domain of PCH proteins is involved in endocytosis. *Journal of Cell Biology*, 172(2):269–279, January 2006. ISSN 1540-8140, 0021-9525. doi: 10.1083/jcb.200508091. URL https://rupress.org/jcb/article/172/2/269/52309/Coordination-between-the-actin-cytoskeleton-and.

D. Usoskin, A. Furlan, S. Islam, H. Abdo, P. Lonnerberg, D. Lou, J. Hjerling-Leffler, J. Haeggstrom, O. Kharchenko, P. V. Kharchenko, S. Linnarsson, and P. Ernfors. Unbiased classification of sensory neuron types by large-scale single-cell RNA sequencing. *Nature Neuroscience*, 18(1):145–+, January 2015. ISSN 1097-6256. doi: 10.1038/nn.3881. URL ://WOS:000346995000022.

A. B. Vallbo, K. A. Olsson, K. G. Westberg, and F. J. Clark. Microstimulation of single tactile afferents from the human hand. Sensory attributes related to unit type and properties of receptive fields. *Brain*, 107 (Pt 3):727–49, September 1984. ISSN 0006-8950 (Print) 0006-8950 (Linking). doi: 10.1093/brain/107.3.727. URL https://www.ncbi.nlm.nih.gov/pubmed/6478176. Edition: 1984/09/01.

Hubert van Griensven, Annina Schmid, Teodora Trendafilova, and Matthew Low. Central Sensitization in Musculoskeletal Pain: Lost in Translation? *Journal of Orthopaedic & Sports Physical Therapy*, 50(11):592–596, November 2020a. ISSN 0190-6011, 1938-1344. doi: 10.2519/jospt.2020.0610. URL https://www.jospt.org/doi/10.2519/jospt.2020.0610.

Hubert van Griensven, Annina Schmid, Teodora Trendafilova, and Matthew Low. Central Sensitization in Musculoskeletal Pain: Lost in Translation? *Journal of Orthopaedic & Sports Physical Therapy*, 50(11):592–596, November 2020b. ISSN 0190-6011, 1938-1344. doi: 10.2519/jospt.2020.0610. URL https://www.jospt.org/doi/10.2519/jospt.2020.0610.

P. Verdru, C. De Greef, L. Mertens, E. Carmeliet, and G. Callewaert. Na(+)-Ca2+ exchange in rat dorsal root ganglion neurons. *J Neurophysiol*, 77(1):484–90, January 1997. ISSN 0022-3077 (Print) 0022-3077 (Linking). doi: 10.1152/jn.1997.77.1.484. URL https://www.ncbi.nlm.nih.gov/pubmed/9120589. Edition: 1997/01/01.

S. Vrontou, A. M. Wong, K. K. Rau, H. R. Koerber, and D. J. Anderson. Genetic identification of C fibres that detect massage-like stroking of hairy skin in vivo. *Nature*, 493(7434):669–73, January 2013. ISSN 1476-4687 (Electronic) 0028-0836 (Linking). doi: 10.1038/nature11810. URL https://www.ncbi.nlm.nih.gov/pubmed/23364746.

Edition: 2013/02/01.

Brian Walitt, Marta Ceko, John L. Gracely, and Richard H. Gracely. Neuroimaging of Central Sensitivity Syndromes: Key Insights from the Scientific Literature. *Current Rheumatology Reviews*, 12(1):55–87, 2016. ISSN 1875-6360. doi: 10.2174/1573397112666151231111104.

Q. F. Wan, E. Nixon, and R. Heidelberger. Regulation of presynaptic calcium in a mammalian synaptic terminal. *J Neurophysiol*, 108(11):3059–67, December 2012. ISSN 1522-1598 (Electronic) 0022-3077 (Linking). doi: 10.1152/jn.00213.2012. URL https://www.ncbi.nlm.nih.gov/pubmed/22972962. Edition: 2012/09/14.

Watson, Paxinos, Kayalioglu. *The spinal cord: a Christopher and Dana Reeve Foundation text and atlas*. Academic press, November 2009.

I. Weissman-Fogel, Y. Granovsky, Y. Crispel, A. Ben-Nun, L. A. Best, D. Yarnitsky, and M. Granot. Enhanced presurgical pain temporal summation response predicts post-thoracotomy pain intensity during the acute postoperative phase. *J Pain*, 10(6):628–36, June 2009. ISSN 1528-8447 (Electronic) 1526-5900 (Linking). doi: 10.1016/j.jpain.2008.12.009. URL https://www.ncbi.nlm.nih.gov/pubmed/19398382. Edition: 2009/04/29.

J. L. Werth and S. A. Thayer. Mitochondria buffer physiological calcium loads in cultured rat dorsal root ganglion neurons. *J Neurosci*, 14(1):348–56, January 1994. ISSN 0270-6474 (Print) 0270-6474 (Linking). URL https://www.ncbi.nlm.nih.gov/pubmed/8283242. Edition: 1994/01/01.

W. D. Willis. Long-term potentiation in spinothalamic neurons. *Brain Res Brain Res Rev*, 40(1-3):202–14, October 2002. doi: 10.1016/s0165-0173(02)00202-3. URL https://www.ncbi.nlm.nih.gov/pubmed/12589918. Edition: 2003/02/19.

Coggeshall R. E. Willis W.D. Sensory Mechanisms of the Spinal Cord. 1991.

C. J. Woolf. EVIDENCE FOR A CENTRAL COMPONENT OF POST-INJURY PAIN HYPERSENSITIVITY. *Nature*, 306(5944):686–688, 1983. ISSN 0028-0836. doi: 10.1038/306686a0. URL ://WOS:A1983RU75800046.

C. J. Woolf. Central sensitization: Implications for the diagnosis and treatment of pain. *Pain*, 152(3):S2–S15, March 2011. ISSN 0304-3959. doi: 10.1016/j.pain.2010.09.030. URL ://WOS:000287307200002.

C. J. Woolf and Q. Ma. Nociceptors–noxious stimulus detectors. *Neuron*, 55(3): 353–64, August 2007. ISSN 0896-6273 (Print) 0896-6273 (Linking). doi: 10.1016/j.neuron.2007.07.016. URL https://www.ncbi.nlm.nih.gov/pubmed/17678850. Edition: 2007/08/07.

Clifford J. Woolf and Stephen W.N. Thompson. The induction and maintenance of central sensitization is dependent on N -methyl-d-aspartic acid receptor activation; implications for the treatment of post-injury pain hypersensitivity states. *Pain*, 44 (3):293–299, March 1991. ISSN 0304-3959. doi: 10.1016/0304-3959(91)90100-C. URL https://journals.lww.com/00006396-199103000-00014.

Zhong Xie, Deepak P. Srivastava, Huzefa Photowala, Li Kai, Michael E. Cahill, Kevin M. Woolfrey, Cassandra Y. Shum, D. James Surmeier, and Peter Penzes. Kalirin-7 Controls Activity-Dependent Structural and Functional Plasticity of Dendritic Spines.

Neuron, 56(4):640–656, November 2007. ISSN 08966273. doi: 10.1016/j.neuron.2007.10.005. URL https://linkinghub.elsevier.com/retrieve/pii/S0896627307007611.

X. J. Xu, C. J. Dalsgaard, and Z. Wiesenfeld-Hallin. Spinal substance P and N-methyl-D-aspartate receptors are coactivated in the induction of central sensitization of the nociceptive flexor reflex. *Neuroscience*, 51(3):641–8, December 1992. ISSN 0306-4522 (Print) 0306-4522 (Linking). doi: 10.1016/0306-4522(92)90303-j. URL https://www.ncbi.nlm.nih.gov/pubmed/1283208. Edition: 1992/12/01.

T. Yasaka, S. Y. Tiong, D. I. Hughes, J. S. Riddell, and A. J. Todd. Populations of inhibitory and excitatory interneurons in lamina II of the adult rat spinal dorsal horn revealed by a combined electrophysiological and anatomical approach. *Pain*, 151 (2):475–88, November 2010. ISSN 1872-6623 (Electronic) 0304-3959 (Linking). doi: 10.1016/j.pain.2010.08.008. URL https://www.ncbi.nlm.nih.gov/pubmed/20817353. Edition: 2010/09/08.

M. H. Yoon, H. B. Bae, J. I. Choi, S. W. Jeong, S. S. Chung, K. Y. Yoo, C. Y. Jeong, S. J. Kim, S. T. Chung, C. M. Kim, and T. H. An. Evaluation of interaction between intrathecal adenosine and MK801 or NBQX in a rat formalin pain model. *Pharmacology*, 75(3):157–64, November 2005. ISSN 0031-7012 (Print) 0031-7012 (Linking). doi: 10.1159/000088345. URL https://www.ncbi.nlm.nih.gov/pubmed/16166819. Edition: 2005/09/17.

J. J. You and S. Lin-Chao. Gas7 Functions with N-WASP to Regulate the Neurite Outgrowth of Hippocampal Neurons. *Journal of Biological Chemistry*, 285(15): 11652–11666, April 2010. ISSN 0021-9258. doi: 10.1074/jbc.M109.051094. URL ://WOS:000276286200070.

H. U. Zeilhofer, B. Studler, D. Arabadzisz, C. Schweizer, S. Ahmadi, B. Layh, M. R. Bosl, and J. M. Fritschy. Glycinergic neurons expressing enhanced green fluorescent protein in bacterial artificial chromosome transgenic mice. *J Comp Neurol*, 482(2):123–41, February 2005. ISSN 0021-9967 (Print) 0021-9967 (Linking). doi: 10.1002/cne.20349. URL https://www.ncbi.nlm.nih.gov/pubmed/15611994. Edition: 2004/12/22.

H. U. Zeilhofer, H. Wildner, and G. E. Yevenes. Fast synaptic inhibition in spinal sensory processing and pain control. *Physiol Rev*, 92(1):193–235, January 2012. ISSN 1522-1210 (Electronic) 0031-9333 (Linking). doi: 10.1152/physrev.00043.2010. URL https://www.ncbi.nlm.nih.gov/pubmed/22298656. Edition: 2012/02/03.

Hanns Ulrich Zeilhofer and Robert Ganley. The Oxford Handbook of the Neurobiology of Pain. 2019.

A. Zeisel, H. Hochgerner, P. Lonnerberg, A. Johnsson, F. Memic, J. van der Zwan, M. Haring, E. Braun, L. E. Borm, G. La Manno, S. Codeluppi, A. Furlan, K. Lee, N. Skene, K. D. Harris, J. Hjerling-Leffler, E. Arenas, P. Ernfors, U. Marklund, and S. Linnarsson. Molecular Architecture of the Mouse Nervous System. *Cell*, 174(4): 999–1014 e22, August 2018. ISSN 1097-4172 (Electronic) 0092-8674 (Linking). doi: 10.1016/j.cell.2018.06.021. URL https://www.ncbi.nlm.nih.gov/pubmed/30096314. Edition: 2018/08/11.

X. Zhang, J. Wu, Y. Z. Lei, L. Fang, and W. D. Willis. Protein phosphatase modulates the phosphorylation of spinal cord NMDA receptors in rats following intradermal

injection of capsaicin. *Molecular Brain Research*, 138(2):264–272, August 2005. ISSN 0169-328X. doi: 10.1016/j.molbrainres.2005.05.001. URL ://WOS:000231475800018.

X. Zhang, J. Wu, L. Fang, and W. D. Willis. The effects of protein phosphatase inhibitors on the duration of central sensitization of rat dorsal horn neurons following injection of capsaicin. *Molecular Pain*, 2, July 2006a. ISSN 1744-8069. doi: 10.1186/1744-8069-2-23. URL ://WOS:000246278300001.

X. Zhang, J. Wu, Y. Z. Lei, L. Fang, and W. D. Willis. Protein phosphatase 2A regulates central sensitization in the spinal cord of rats following intradermal injection of capsaicin. *Molecular Pain*, 2, March 2006b. ISSN 1744-8069. doi: 10.1186/1744-8069-2-9. URL ://WOS:000246219400001.

X. F. Zhou and R. A. Rush. Endogenous brain-derived neurotrophic factor is anterogradely transported in primary sensory neurons. *Neuroscience*, 74(4):945–53, October 1996. ISSN 0306-4522 (Print) 0306-4522 (Linking). doi: 10.1016/0306-4522(96)00237-0. URL https://www.ncbi.nlm.nih.gov/pubmed/8895863. Edition: 1996/10/01.

Guan Cheng Zhu, Karina Böttger, Helen Slater, Chad Cook, Scott F. Farrell, Louise Hailey, Brigitte Tampin, and Annina B. Schmid. Concurrent validity of a low-cost and time-efficient clinical sensory test battery to evaluate somatosensory dysfunction. *European Journal of Pain (London, England)*, 23(10):1826–1838, November 2019. ISSN 1532-2149. doi: 10.1002/ejp.1456.

G. Zoidl, D. D'Urso, S. Blass-Kampmann, C. Schmalenbach, R. Kuhn, and H. W. Muller. Influence of elevated expression of rat wild-type PMP22 and its mutant PMP22Trembler on cell growth of NIH3T3 fibroblasts. *Cell Tissue Res*, 287(3):459–70, February 1997. ISSN 0302-766X (Print) 0302-766X (Linking). doi: 10.1007/s004410050770. URL https://www.ncbi.nlm.nih.gov/pubmed/9023077. Edition: 1997/03/01.

K. Zorina-Lichtenwalter, C. B. Meloto, S. Khoury, and L. Diatchenko. Genetic predictors of human chronic pain conditions. *Neuroscience*, 338:36–62, December 2016. ISSN 1873-7544 (Electronic) 0306-4522 (Linking). doi: 10.1016/j.neuroscience.2016.04.041. URL https://www.ncbi.nlm.nih.gov/pubmed/27143481. Edition: 2016/10/27.

M. J. Zylka, F. L. Rice, and D. J. Anderson. Topographically distinct epidermal nociceptive circuits revealed by axonal tracers targeted to Mrgprd. *Neuron*, 45(1):17–25, January 2005. ISSN 0896-6273. doi: 10.1016/j.neuron.2004.12.015. URL ://WOS:000226217100006.